ISTANBUL TECHNICAL UNIVERSITY ★ GRADUATE SCHOOL

PLANT-WIDE PROCESS ANALYSIS TARGETING RELIABLE ESTIMATION OF BIOGAS PRODUCTION FROM ANAEROBIC SLUDGE DIGESTION

Ph.D. THESIS

Gökşin ÖZYILDIZ

Department of Environmental Engineering

Environmental Sciences Engineering and Management Programme

MAY 2024

ISTANBUL TECHNICAL UNIVERSITY ★ GRADUATE SCHOOL

PLANT-WIDE PROCESS ANALYSIS TARGETING RELIABLE ESTIMATION OF BIOGAS PRODUCTION FROM ANAEROBIC SLUDGE DIGESTION

Ph.D. THESIS

Gökşin ÖZYILDIZ
(501172714)

Department of Environmental Engineering

Environmental Sciences Engineering and Management Programme

Thesis Advisor: Prof. Dr. H. Güçlü İNSEL

MAY 2024

ISTANBUL TEKNİK ÜNİVERSİTESİ ★ LİSANSÜSTÜ EĞİTİM ENSTİTÜSÜ

ANAEROBİK ÇAMUR ÇÜRÜTME PROSESİNDEN BİYOGAZ ÜRETİMİNİN GÜVENİLİR TAHMİNİNE YÖNELİK TESİS GENELİ PROSES ANALİZİ

DOKTORA TEZİ

Gökşin ÖZYILDIZ
(501172714)

Çevre Mühendisliği Anabilim Dalı

Çevre Bilimleri Mühendisliği ve Yönetimi Programı

Tez Danışmanı: Prof. Dr. H. Güçlü İNSEL

MAYIS 2024

Gökşin ÖZYILDIZ, a Ph.D. student of ITU Graduate School student ID 501172714 successfully defended the thesis/dissertation entitled "PLANT-WIDE PROCESS ANALYSIS TARGETING RELIABLE ESTIMATION OF BIOGAS PRODUCTION FROM ANAEROBIC SLUDGE DIGESTION", which she prepared after fulfilling the requirements specified in the associated legislations, before the jury whose signatures are below.

Thesis Advisor :	**Prof. Dr. H. Güçlü İNSEL** Istanbul Technical University	.....
Jury Members :	**Prof. Dr. Emine ÇOKGÖR** Istanbul Technical University	.....
	Prof. Dr. Ayşen ERDİNÇLER Boğaziçi University	.....
	Assoc. Prof. Dr. Gülsüm E. ZENGİN BALCI Istanbul Technical University	.....
	Prof. Dr. Nuriye Altınay PERENDECİ Akdeniz University	.....

Date of Submission : 28 March 2024
Date of Defense : 17 May 2024

To my beloved mother, who has been my biggest support in life, and the late Prof. Didem OKUTMAN TAŞ, whose guidance and support during my academic journey is remembered with eternal gratitude

FOREWORD

I would like to express my endless gratitude to my esteemed advisor, Prof. Dr. Hayrettin Güçlü İNSEL, who guided me in this study and in my entire academic life. He always set an example for me with his knowledge, intelligence, dedication, and inexhaustible energy. He is not only an advisor to me but also a supportive older brother in every aspect of life.

Foremost, I pay tribute to my honorary advisor, Prof. Dr. Emine ÇOKGÖR, who never withheld her knowledge, support, and understanding from me throughout my whole university life, who was always there for me whenever I needed and motivated me with her love for science. I will never forget your support throughout my life.

I honor the memory of Prof. Dr. Didem OKUTMAN TAŞ, who was a professor and an elder sister to me. Her intelligence and guidance enlightened me and many other students over the years. We will never forget her beautiful smile, diligence, and kindness. ITU Environmental Engineering Department will never be the same without her.

My dear and precious mother, Merih ÖZYILDIZ, you have been my biggest supporter and the foundation of my academic career. This thesis would not have been possible without your unwavering support, and I dedicate it to you with all my heart. I would also like to express my gratitude to my dear brother, Yavuz Selim ÖZYILDIZ, for helping me realize that there are alternative ways of living. Your support has been invaluable to me despite your resistance to understanding what I am doing and what I need to do to move forward on this path. Thank you both for always being there for me. You are my only family, and I am grateful for your love and support.

I would like to express my sincere love and gratitude to my esteemed professor, Prof. Dr. Melike GÜREL, who has never withheld her moral support from me for many years and never lost faith in me, and to dear Assoc. Prof. Dr. Gülsüm Emel ZENGİN, who has always been by my side with her calmness, sincerity, and understanding in the most challenging times. Without your support, this thesis would not exist today. I would like to express my gratitude to Assoc. Prof. Didem GÜVEN, whose passion for science and unwavering determination have been a constant source of inspiration. Her generous assistance and support have been invaluable throughout this process.

I would like to express my heartfelt gratitude to Prof. Dr. Tuğba ÖLMEZ-HANCI, who has shown me how laboratory work can be both enjoyable and never-ending. Even sitting in a café, she taught me how to create an experimental program on a napkin and generate new ideas. Thank you so much for your guidance and inspiration.

A special thanks to Prof. Dr. Elif PEHLİVANOĞLU MANTAŞ and Assoc. Prof. Dr. Burçak KAYNAK, thank you for always trusting me and for your understanding and supportive attitude, especially in the last years of this very complicated and stressful journey.

My dearest friends, the Ph.D. group, -Assoc. Prof. Dr. Emel TOPUZ, Dr. Nilay SAYI UÇAR, Dr. Gökçe KOR-BIÇAKCI, Dr. Gülten YÜKSEK, Dr. Burçin COŞKUN- you understood me the best during these troubled days. Without your support, friendship, and individual interventions at critical moments, I could not write these lines today. I would like to express my heartfelt gratitude to all of you.

Last but not least, I would like to express my gratitude to my dear colleagues Nergis DİLSİZOĞLU-AKYOL and Ali Tamer ÇETİNKAYA, who provided their unwavering support, especially in the last days of my Ph.D. studies. I am particularly grateful to them for their exceptional assistance and understanding during the most stressful period of this so-called journey. They have set a remarkable example of what it means to be a helpful and supportive colleague.

This thesis (Project No: MDK-2021-43447) has been partially supported by Istanbul Technical University Scientific Research Projects Department. A part of this study was supported by "Wastewater Standardization and Management Project No 1: Biological characterization and dynamic modeling in wastewater treatment plants" funded by İstanbul Water and Sewerage Administration (İSKİ).

Gökşin ÖZYILDIZ
May 2024 (Environmental and Civil Engineer, M.Sc.)

TABLE OF CONTENTS

Page

ABBREVIATIONS

AD : Anaerobic Digestion
ADM : Anaerobic Digestion Model
AOB : Ammonia Oxidizing Bacteria
ASIM : Activated Sludge Simulation Program
ASM : Activated Sludge Model
BMP : Biochemical Methane Potential
BNR : Biological Nutrient Removal
BOD : Biochemical Oxygen Demand
CBIM : Continuity-Based Interface Method
CFR : Code of Federal Regulations
COD : Chemical Oxygen Demand
DRM : Death-Regeneration Model
EAWAG : Swiss Federal Institute for Environmental Science and Technology
EBPR : Enhanced Biological Phosphorus Removal
EC : European Commission
EDM : Endogenous Decay Model
EPA : Environmental Protection Agency
FBBR : Fixed Bed Biofilm Reactor
FIM : Fisher Information Matrix
GAO : Glycogen Accumulating Organisms
GC : Gas Chromatography
GHG : Greenhouse Gas
GPS-X : General Purpose Simulator-X
GTO : Glycerol Trioleate
HPLC : High Performance Liquid Chromatography
HRT : Hydraulic Retention Time
IAWPRC : International Association on Water Pollution Research and Control
IAWQ : International Association on Water Quality
IC : Ion Chromatograph
IFAS : Integrated Fixed Film Activated Sludge

IWA : International Water Association
LCFA : Long Chain Fatty Acid
MAD : Mesophilic Anaerobic Digester
MAP : Magnesium Ammonium Phosphate
MBBR : Moving Bed Biofilm Reactor
MBR : Membrane Bioreactor
MLSS : Mixed Liquor Suspended Solids
NOB : Nitrite Oxidizing Bacteria
NPR : Nitrate Production Rate
NUR : Nitrate Utilization Rate
OUR : Oxygen Uptake Rate
PAO : Polyphosphate Accumulating Organism
PSM : Primary Sludge Mass
PSMF : Primary Sludge Mass Fraction
RNA : Ribonucleic Acid
RR : Resource Recovery
SBR : Sequencing Batch Reactors
SMA : Specific Methanogenic Activity
SRT : Sludge Retention Time
SSSP : Single Sludge Simulation Program
TKN : Total Kjeldahl Nitrogen
TN : Total Nitrogen
TP : Total Phosphorus
TS : Total Solids
TSS : Total Suspended Solids
USA : United States of America
UV : Ultraviolet
VFA : Volatile Fatty Acid
VS : Volatile Solids
VSS : Volatile Suspended Solids
WAS : Waste Activated Sludge
WWTP : Wastewater Treatment Plant

SYMBOLS

$\eta_{HYD,ana}$; η_{fe} : Reduction factor for anaerobic hydrolysis

μ_A : Autotrophic growth rate

$\mu_{A,max}$; $\hat{\mu}_A$: Maximum autotrophic growth rate

$\mu_{H,max}$; $\hat{\mu}_H$: Maximum heterotrophic growth rate

b_A : Endogenous decay rate for autotrophs

b_H : Endogenous decay rate for heterotroph in EDM

b'_H : Heterotrophic decay rate for heterotroph in DRM

C_B : Colloidal biodegradable substrate (mg COD/L)

C_I : Total inert COD concentration

C_S : Total biodegradable COD concentration

C_T : Total COD concentration

C_{TKN} : Total nitrogen concentration

C_U : Colloidal unbiodegradable organics (mg COD/L)

f_E : Coefficient for the inert component of endogenous biomass in EDM

f_{ES} : Coefficient for the soluble inert component of endogenous biomass in EDM

f_{EX} : Coefficient for the particulate inert component of endogenous biomass in EDM

f_P : Coefficient for the inert component of biomass in DRM

f_{PS} : Coefficient for the soluble inert component of biomass in DRM

f_{PX} : Coefficient for the particulate inert component of biomass in DRM

f_X : Conversion factor for COD/VSS ratio

k_d : Heterotrophic decay rate

K_{NH} : Half-saturation constant for ammonia

K_{NO} : Half-saturation constant for nitrate nitrogen

$K_{O,A}$: Half-saturation constant for dissolved oxygen for autotrophs

$K_{O,H}$: Half-saturation constant for dissolved oxygen for heterotrophs

K_S : Half-saturation constant for organic matter

NO_X : Total oxidized nitrogen concentration

q_{HYD} : Hydrolysis rate

S_B : Readily biodegradable substrate (non-VFA) (mg COD/L)

S_H : Rapidly hydrolysable COD concentration

S_I : Soluble inert COD concentration

S_{MEOL} : Methanol concentration (external carbon source) (mg COD/L)

S_N : Soluble nitrogen concentration

S_{ND} : Soluble organic nitrogen concentration

S_{NH} : Ammonia nitrogen concentration

S_{NI} : Soluble inert nitrogen concentration

S_{NO} : Oxidized nitrogen concentration

S_O : Dissolved oxygen concentration

S_P : Soluble inert microbial product concentration

S_S : Readily biodegradable COD concentration

S_U : Soluble unbiodegradable organics (mg COD/L)

S_{VFA} : Volatile fatty acid concentration (mg COD/L)

X_A : Autotrophic biomass concentration

X_B : Slowly biodegradable substrate (influent-oriented)

$X_{B,E}$: Slowly biodegradable substrate (decay-oriented)

X_E : Endogenous microbial products

X_H : Heterotrophic biomass concentration

X_I : Particulate inert COD concentration

X_N : Particulate nitrogen concentration

X_{ND} : Particulate biodegradable nitrogen concentration

X_{NI} : Particulate inert nitrogen concentration

X_P : Particulate inert microbial product concentration

X_S : Slowly biodegradable COD concentration

X_U : Particulate unbiodegradable organics (mg COD/L)

Y : Yield coefficient

Y_A : Yield coefficient for autotrophs

Y_H : Yield coefficient for heterotrophs

α_D : Coefficient of dissolved inert formation (growth origin)

η_{NO3} : Reduction factor for anoxic hydrolysis

θ_X : Sludge age

θ_h : Hydraulic retention time

LIST OF TABLES

Page

LIST OF FIGURES

Page

PLANT-WIDE PROCESS ANALYSIS TARGETING RELIABLE ESTIMATION OF BIOGAS PRODUCTION FROM ANAEROBIC SLUDGE DIGESTION

SUMMARY

Anaerobic sludge digestion is a critical and widely used technology employed in wastewater treatment plants for the stabilization of solids generated during the treatment process and for the production of biogas as a renewable energy source. This process typically involves the treatment of mixed primary and biological sludge in digesters. Primary sludge comprises inorganic solids and organic matter, whereas biological sludge is rich in active biomass and residues from biochemical reactions. The process faces challenges, such as the lower organic degradation efficiency of waste activated sludge (WAS) under both aerobic and anaerobic conditions, necessitating extended sludge retention times.

Hydrolysis, identified as the rate-limiting step in microbial degradation across various environmental conditions, significantly influences the efficiency of the anaerobic digestion process. Therefore, the nature of the degradation of the hydrolysable matter directly influences the efficiency of the anaerobic digestion process. Traditional activated sludge models, which conceptualize COD turnover through a single hydrolysable matter component (X_B), do not adequately account for the range of hydrolysis kinetics observed in practice. Despite a plethora of parameter values proposed for anaerobic hydrolysis, research into the kinetic analysis of anaerobic sludge digestion, particularly considering varying mixes of primary and waste activated sludge, remains sparse.

The appropriate selection of wastewater treatment and sludge disposal methods depends on specific aspects, including the organic matter components in the influent wastewater and the kinetic parameters specific to the biomass. Therefore, the integration of experimental studies with plant-wide modeling tools is becoming an important strategy for selecting suitable treatment systems and executing reliable process calculations.

In this study, seven large-scale wastewater treatment plants were analyzed for operational parameters and dynamic modeling was combined with plant-focused batch experiments to uncover deviations from the calculated data during the design phase. The long-term performance of three full-scale carbon and biological nutrient removal plants with anaerobic sludge digestion systems was rigorously monitored. This approach aimed to improve the understanding of process kinetics for carbon removal, nutrient removal, and anaerobic digestion. It involved COD fractionation, nitrification and denitrification kinetics, and anaerobic batch experiments. Plant-specific kinetic parameters were determined experimentally and integrated with plant-wide SUMO model simulations.

The research revealed that anaerobic hydrolysis rates are significantly lower than the available literature values. The study identified this stage as a critical point in optimizing biogas production. Anaerobic digestion batch experiments and plant-wide

model calibration showed that anaerobic hydrolysis rate is the critical parameter for biogas production. In parallel, anaerobic digestion performance and modeling studies in full-scale plants showed low biogas production efficiency.

The innovative use of plant-wide model calibration, in conjuction with anaerobic digestion tests in the study, illuminated the significant challenges posed by low anaerobic hydrolysis rates for efficient biogas production. This was demonstrated by the poor performance and low biogas yields in full-scale plants. The study also discovered that the degradation rate of primary sludge through anaerobic hydrolysis is significantly higher compared to the hydrolysis rate of biological sludge, shedding light on areas for process improvement.

In the second stage of the study, the effect of anaerobic hydrolysis rate on biogas production was investigated with mesophilic digesters in seven large-scale wastewater treatment plants. This phase was critical in understanding how the process parameters underpinning anaerobic digestion could be optimized to enhance biogas production. A linear correlation was determined between the percentage of primary sludge mass in the total sludge fed to the digester and the overall anaerobic hydrolysis rate. This correlation emphasises the heightened efficiency of primary sludge in undergoing anaerobic hydrolysis, a revelation that emerged from identifying that the rate of anaerobic hydrolysis for primary sludge was threefold greater than that observed for biological sludge. The anaerobic hydrolysis rate of primary sludge was determined to be three times higher than that of biological sludge. Furthermore, the study delineated the reduction factor for anaerobic hydrolysis ($\eta_{HYD,ana}$), falling within the range of 0.11 to 0.30. This finding is particularly noteworthy as it sits below the range recommended in the existing literature (0.30-0.50), thereby highlighting a potential area for further investigation and optimization within the field of anaerobic digestion.

In the final phase of the study, the study advocates for the adoption of an innovative model paradigm, distinguishing the anaerobic degradation kinetics of particulate biodegradable organics stemming from influent (X_B) and decay processes ($X_{B,E}$). Traditionally, plant-wide models have utilized a singular kinetic expression to represent the degradation process, necessitating the recalibration of the model for each treatment plant to accurately predict biogas flowrate, based on the varying compositions of primary and secondary sludge introduced to the digesters. This approach not only facilitates a more streamlined and accurate prediction of biogas production across different treatment facilities but also represents a significant advancement in the field by addressing the variability in sludge composition without the need for model recalibration.

By introducing a novel model approach, the study segregates the anaerobic degradation kinetics of particulate biodegradable organics derived from both influent and decay-oriented (X_B, $X_{B,E}$), significantly refining the precision of biogas production forecasts across varying treatment plants without necessitating recalibration to account for fluctuating sludge compositions. This avant-garde methodology not only elevates the predictive proficiency of plant-wide models but also addresses critical challenges in wastewater treatment, including energy conservation and environmental stewardship.

This new modeling approach sheds light on the changes that need to be made in the design criteria of BNR systems, including proper sizing of Bio-P tanks and optimization of anoxic zones for efficient denitrification. It is also expected to make major differences in process calculations for the accurate assessment of biogas

production capacity and the design and optimization of sludge disintegration processes such as thermal hydrolysis. Therefore, the proposed model facilitates a comprehensive re-evaluation of process performance and design methodologies for biological processes, including sludge fermentation and BNR processes. As a next stage of the study, it became evident that it is imperative to develop specific experimental procedures to determine new model parameters, especially related to hydrolysis under anaerobic and anoxic conditions.

The study's findings underscore the importance of adopting a model-based experimental characterization coupled with plant-wide modeling to overcome the limitations of current kinetic parameter adjustments. Through the integration of insights gleaned from kinetic batch experiments within the simulation architecture, the investigation achieves a formidable prediction of the long-term operational efficacy of wastewater treatment facilities, thereby establishing a novel benchmark for the design and enhancement of anaerobic digestion processes aimed at advancing sustainable wastewater management practices.

ANAEROBİK ÇAMUR ÇÜRÜTME PROSESİNDEN BİYOGAZ ÜRETİMİNİN GÜVENİLİR TAHMİNİNE YÖNELİK TESİS GENELİ PROSES ANALİZİ

ÖZET

Anaerobik çamur çürütme, atıksu arıtma tesislerinde arıtma işlemi sırasında oluşan katı maddelerin stabilizasyonu ve yenilenebilir enerji kaynağı olarak biyogaz üretimi için kullanılan kritik ve yaygın bir teknolojidir. Bu süreç tipik olarak çürütücülerde karışık birincil ve ikincil (biyolojik) atık çamurun birlikte stabilizasyonunu içerir. Birincil çamur inorganik katılar ve yoğun olarak organik maddelerden oluşurken, biyolojik çamur aktif biyokütle ve biyokimyasal reaksiyonlardan kaynaklanan kalıntılar bakımından zengindir. Anaerobik çürütme prosesinde, atık aktif çamurun yapısı gereği hem aerobik hem de anaerobik koşullar altında daha düşük biyolojik olarak bozunma özelliği sebebiyle çamur bekletme sürelerinin uzatılmasını gerektirmektedir.

Çeşitli çevresel koşullarda mikrobiyal bozunmada hız sınırlayıcı adım olarak tanımlanan hidroliz, anaerobik çürütme sürecinin verimliliğini önemli ölçüde etkilemektedir. Bu nedenle, hidroliz olabilen organik maddenin ayrışma kinetiği anaerobik çürütme sürecinin verimliliğini doğrudan etkilemektedir. KOİ dönüşümünü tek bir yavaş ayrışan organik madde bileşeni (X_B) üzerinden kavramsallaştıran geleneksel aktif çamur modelleri ile pratikte gözlemlenen hidroliz kinetiği birbiriyle uyuşmamakta, dolayısıyla beklenen biyogaz miktarı ile proseste elde edilen biyogaz miktarı arasında büyük farklar oluşmaktadır. Anaerobik hidroliz kinetiği için önerilen çok sayıda parametre değerine rağmen, anaerobik çamur çürütmenin kinetik analizine ilişkin araştırmalar, özellikle birincil ve biyolojik çamurun değişen karışımları dikkate alındığında, literatür verileri yeterli gelmemektedir.

Uygun atıksu arıtma ve çamur bertaraf yöntemlerinin seçimi ve konfigürasyonların belirlenmesi, giriş atıksuyundaki organik madde bileşenlerinin belirlenmesi ve söz konusu biyokütleye özgü kinetik parametreler de dahil olmak üzere belirli hususlara bağlıdır. Sonuç olarak, deneysel çalışmaların tesis bazında modelleme araçlarıyla entegrasyonu, uygun arıtma sistemlerinin seçimi ve güvenilir proses hesaplamalarının yürütülmesi için zorlu bir strateji olarak ortaya çıkmaktadır.

Bu çalışmada, yedi adet büyük ölçekli atıksu arıtma tesisinde işletme parametrelerinin kapsamlı analizi yapılmış ve tasarım esnasında hesaplanan veriler ile sapmaları aydınlatmak için tesis odaklı kesikli deneyler ile dinamik modelleme birleştirilmiştir. Bu kapsamda, üç adet anaerobik çamur çürütme sistemleri bulunan tam ölçekli karbon ve biyolojik nütrient gideren tesislerin uzun süreli performansı titizlikle izlenmiştir. Bu entegre yaklaşım sayesinde çalışma, karbon giderimi, nütrient giderimi ve anaerobik çürütme için proses kinetiği anlayışını geliştirmeyi amaçlamıştır. Bu yaklaşımla, KOİ bölümlenmesi, nitrifikasyon ve denitrifikasyon kinetiği ile anaerobik kesikli deney çalışmaları yapılmış ve tesise özgü kinetik parametreler deneysel olarak belirlenmiş ve bu parametrelerin tesis genelinde Sumo model simülasyonlarıyla entegre edilmesiyle gerçekleştirilmiştir.

Araştırma, anaerobik hidroliz hızlarının mevcut literatür değerlerinden belirgin şekilde düşük olduğunu ortaya koymuş ve bu aşamayı biyogaz üretimini optimize etmede kritik bir nokta olarak tanımlamıştır. Anaerobik çürütme kesikli deneyleri ve tesis bazında gerçekleştirilen model kalibrasyonu, anaerobik hidroliz hızının biyogaz üretiminde kritik parametre olduğunu göstermiştir. Buna paralel olarak, tam ölçekli tesislerdeki anaerobik çürütme performansı ve modelleme çalışmaları incelendiğinde tesislerde düşük biyogaz üretim verimi gözlemlenmiştir. Çalışmada anaerobik çürütme testleri ile birlikte tesis çapında model kalibrasyonunun yenilikçi kullanımı, tam ölçekli tesislerdeki düşük performans ve düşük biyogaz verimini de gösterdiği gibi, düşük anaerobik hidroliz hızlarının verimli biyogaz üretimi için yarattığı önemli zorlukları aydınlatmıştır. Ayrıca, anaerobik hidroliz yoluyla birincil çamurun bozunma oranının biyolojik çamurun hidroliz hızına kıyasla önemli ölçüde daha yüksek (~2,5-3) olduğu keşfedilmiş ve bu da proses iyileştirme alanlarına ışık tutmuştur.

Çalışmanın ikinci aşamasında, anaerobik hidroliz hızının biyogaz üretimi üzerindeki etkisi, toplamda yedi büyük ölçekli atıksu arıtma tesislerindeki mezofilik anaerobik çürütücülerde araştırılmıştır. Çürütücüye beslenen toplam çamur içindeki birincil çamur kütlesinin yüzdesi ile anaerobik hidroliz hızı arasında doğrusal bir korelasyon tespit edilmiştir. Anaerobik hidroliz için düzeltme faktörü ($\eta_{HYD,ana}$) literatürde önerilen aralığa (0,30-0,50) kıyasla daha düşük olan 0,11-0,30 aralığında belirlenmiştir.

Çalışmanın son aşamasında, giriş atıksuyu kaynaklı (X_B) ve içsel solunumdan kaynaklanan ($X_{B,E}$) yavaş ayrışan organik maddelerin anaerobik bozunma kinetiklerinin birbirinden ayrıldığı yeni bir model yaklaşımı önerilmiştir. Tek bir kinetik ifadeye sahip tesis bazlı mevcut modeller, anaerobik çürütücülere beslenen farklı birincil ve ikincil çamur oranlarına sahip her bir arıtma tesisi için biyogaz debisini hesaplamak üzere modelin yeniden kalibre edilmesini gerektirmektedir. Önerilen yeni model yapısı, iki yavaş ayrışan organik madde bileşeninin (X_B, $X_{B,E}$) bozunma kinetiğini ayırarak herhangi bir yeniden kalibrasyon ihtiyacı olmadan tüm atıksu arıtma tesislerinin biyogaz üretimini tahmin edebilmektedir.

Yeni bir model yaklaşımı öneren bu çalışma, giriş atıksuyu kaynaklı ve içsel solunumdan kaynaklanan yavaş ayrışan organik maddelerin anaerobik bozunma kinetikleri arasında ayrım yapmakta ve böylece farklı çamur bileşim oranlarına uyum sağlamak için yeniden kalibrasyona gerek kalmadan farklı arıtma tesislerinde biyogaz üretimi tahminlerinin doğruluğunu artırmaktadır. Bu yeni yaklaşım, sadece tesis genelindeki modellerin tahmin kapasitesini geliştirmekle kalmıyor, aynı zamanda enerji verimliliği ve çevresel sürdürülebilirlik gibi atıksu arıtımındaki yeni nesil zorlukları da ele almaktadır.

Çalışmanın bulguları, mevcut kinetik parametre kalibrasyonu sınırlamalarının üstesinden gelmek için tesis bazında modelleme ile birlikte model tabanlı bir deneysel karakterizasyonun benimsenmesinin önemini vurgulamaktadır. Araştırma, simülasyon bazlı kinetik kesikli testlerden elde edilen bilgilerden yararlanılarak, atıksu arıtma tesislerinin uzun vadeli işletme performansının güvenilir bir tahminini elde etmeyi sağlamakta ve sürdürülebilir atıksu yönetimi arayışında anaerobik çürütme süreçlerinin tasarımı ve optimizasyonu için yeni bir standart oluşturmaktadır.

Bu yeni modelleme yaklaşımı, Bio-P tanklarının uygun boyutlandırılması ve yüksek verimli denitrifikasyon için anoksik bölgelerin optimizasyonu dahil olmak üzere BNR sistemlerinin tasarım kriterlerinde yapılması gereken değişikliklere ışık tutmaktadır.

Biyogaz üretim kapasitesinin doğru bir şekilde değerlendirilmesi ve termal hidroliz gibi çamur parçalama süreçlerinin tasarımı ve optimizasyonu için yapılacak proses hesaplarında da büyük farklılıklar yaratması beklenmektedir. Bu nedenle, önerilen model, çamur fermantasyonu ve BNR prosesleri de dahil olmak üzere biyolojik prosesler için proses performansının ve tasarım metodolojilerinin kapsamlı bir şekilde yeniden değerlendirilmesini kolaylaştırmaktadır. Çalışmanın bir sonraki aşaması olarak, özellikle anaerobik ve anoksik koşullar altında hidroliz ile ilgili yeni model parametrelerini belirlemek için özel deneysel prosedürlerin geliştirilmesinin zorunlu olduğu ortaya çıkmıştır.

1. INTRODUCTION

The European Commission (EC) announced a set of policies called the European Green Deal to achieve climate neutrality by 2050 (Fetting, 2020). In this regard, rethinking of the municipal wastewater treatment plant design has become crucial for sustainable systems achieving the limit of technology treatment within the context of energy-efficiency issues. Currently, conventional biological nutrient removal (BNR) systems are known as the most widely used alternative to protect the environment from pollutant loads (N, P). As one further step, integrated organic carbon diversion and nutrient recovery options convert conventional treatment systems into self-sufficient resource recovery (RR) plants. In this respect, the management of organic matter utilization in wastewater and sludge processes is of great importance in the design and optimal operation of resource recovery plants.

Wastewater treatment plants are vital for maintaining a sustainable environment, but their design and planning need to be smart and tailored to meet local demands and conditions. The nature of the wastewater and characteristics of the sewer system play significant roles in choosing the process scheme, as well as in the design and layout of the treatment units. Although safety factors are integrated during the design stage, they sometimes prove inadequate in the real-world operation of full-scale facilities. Selecting design parameters with precision is crucial, factoring in the requirements for effluent quality and considerations related to energy. Regrettably, the tendency towards conservative design norms in engineering practices can result in design flaws, putting the success of costly projects at risk.

Wastewater treatment plant operators face significant challenges when it comes to managing the treatment process under dynamic conditions. These conditions may include changes in influent wastewater characteristics, which have a significant impact on the process efficiency of the treatment process. To address this challenge, engineers and decision-makers have turned to multi-component process models that offer a more detailed understanding of the complex interplay between various subsystems within the treatment process.

Plant-wide modeling methodologies have emerged as a particularly effective strategy for assessing operational performance and identifying opportunities for improvement. These methodologies take a holistic view of the treatment process, capturing the dynamic and interconnected nature of transformation processes occurring across both liquid and solid phases. This enables decision-makers and operators to make informed choices about the design and management of wastewater treatment systems, and ensure that they are optimized for maximum process and energy efficiency (Kazadi Mbamba et al., 2016). Sophisticated analytical methods and comprehensive modeling techniques are crucial for ensuring optimal process efficiency in the face of varying influent characterization and environmental conditions. These advanced tools provide engineers and decision-makers with the ability to navigate the complexities of the treatment process, and make informed decisions about how to optimize the efficiency of the system. The intricate relationship between effluent quality and process efficiency necessitates the adoption of advanced evaluation techniques and plant-wide modeling in wastewater treatment facilities (Nguyen et al., 2020). Simulation studies that consider environmental and local conditions have revealed significant limitations in treatment plants that adhere to conservative design principles, highlighting the need for flexible and robust plant-wide modeling approaches that enhance the resilience and efficiency of wastewater treatment plants (Insel et al., 2022; Jenkins and Wanner, 2014).

During the design period, plant-wide modeling studies play a crucial role in predicting the performance of wastewater treatment plants. These studies allow engineers to simulate various scenarios and evaluate the impact of design choices on process efficiency and environmental outcomes. By considering the complex interactions between different components of the treatment process, plant-wide models provide valuable insights into optimization opportunities and potential challenges that may arise during operation. Therefore, integrating plant-wide modeling into the design phase enables engineers to develop more robust and efficient treatment systems that meet regulatory requirements and environmental goals. By adopting sophisticated analytical methods and comprehensive modeling techniques, complexities of the treatment process can be navigated and robust, flexible, and optimized wastewater treatment plant designs can be ensured.

Plant-wide modeling offers a comprehensive approach to optimize the performance of wastewater treatment plants by providing insights into system-wide interactions and dynamics. By simulating various scenarios and considering the complex relationships between different components of the treatment process, engineers can identify optimization opportunities, assess the impact of design choices on process efficiency, and predict environmental outcomes more accurately.

During the operation of wastewater treatment plants, challenges such as dynamic process conditions, uncertainty in influent characteristics, and design discrepancies may arise, affecting system performance. Advanced evaluation strategies, including plant-wide modeling, facilitate real-time monitoring of process performance, rapid identification of bottlenecks, and proactive decision-making to optimize system operation. Rigorous validation of models against empirical data ensures their reliability and applicability in practical scenarios, mitigating operational risks and enhancing overall plant performance.

Process models play a crucial role in deciphering the interplay among various components of wastewater treatment processes under distinct conditions, such as aerobic, anoxic, and anaerobic environments. These models employ mass balance calculations to ascertain the efficacy of the treatment system. In the 1980s, the advent of multi-component process models marked a significant advancement in wastewater treatment, facilitating the simulation of nutrient removal processes alongside the removal of organic carbon (Dold et al., 1980; Ekama et al., 1986; Henze et al., 2000; Wentzel et al., 1992). The development of the anaerobic digestion model (ADM) represented a further enhancement by incorporating additional components beyond those considered in activated sludge models (Batstone et al., 2002; Siegrist et al., 2002). In recent times, the preference has shifted towards plant-wide simulation approaches. These approaches are favored for their ability to swiftly resolve using a singular model, thereby reducing uncertainties across interconnected processes. Plant-wide models stand out by offering substantial benefits in assessing the overall performance of the system compared to specific models. An integrated perspective offered by plant-wide simulations is indispensable for tackling emerging challenges in wastewater treatment plants, including resource recovery, energy reduction, and evaluating environmental impacts (Hvala et al., 2018).

In recent years, plant-wide modeling has been increasingly used in various fields such as estimating carbon footprint and greenhouse gas (GHG) emissions and evaluating strategies for process modification and operation of WWTPs (Kazadi Mbamba et al., 2016; Kazadi Mbamba et al., 2019; Lizarralde et al., 2019; Ikumi and Harding, 2020; Nguyen et al., 2020). However, as models become more complex and process components and their relations increase, over-parametrization can lead to severe parameter identifiability problems (Brun et al., 2001; Brun et al., 2002). To date, there have been plant-wide evaluation studies in the literature. However, most research on model-based analysis has centered around validating models with either default values from literature or data collected from laboratory studies conducted on a smaller scale (Barat et al., 2013; Grau et al., 2007; Lizarralde et al., 2015; Solon et al., 2017).

Despite their advantages, plant-wide models often involve simplifications and assumptions to manage complexity and computational demands. These simplifications may overlook certain nuances or variations in real-world processes, potentially leading to inaccuracies in predictions or optimizations. Therefore, it's essential to validate these models rigorously against empirical data and refine them iteratively to ensure their reliability and applicability in practical scenarios.

It is essential to conduct additional detailed offline experiments to gather critical information about the sensitive parameters of the model that affect the output of the model, and ultimately, the efficiency of the treatment system. For a biological nutrient removal plant with a biogas facility, it is important to analyze the characteristics of the influent wastewater, the nitrate utilization rate (NUR), the biodegradation pattern of influent organics, and the biomass activity to identify any process bottlenecks throughout the plant.

The integration of biogas production modules into plant-wide models enhances their utility in evaluating energy sustainability and resource recovery aspects of wastewater treatment plants (Kazadi Mbamba et al., 2016). By simulating the entire process from influent wastewater to biogas generation, these models provide a comprehensive understanding of biogas production potential within wastewater treatment plants. Comparing the calculated design biogas amounts with the obtained real biogas amounts during plant operation is crucial for assessing the actual biogas potential of the system. This comparison facilitates the identification of any discrepancies between

the predicted and actual biogas production, allowing for adjustments and optimizations to maximize biogas yield and energy recovery from wastewater treatment processes.

Biogas production during anaerobic digestion depends on the amount of influent organic carbon, especially the slowly biodegradable (COD) fraction, and the biodegradation characteristics (Eskicioglu et al., 2006; Yuan et al., 2019). Therefore, it is essential to perform plant-specific kinetic characterization and evaluation for reliable decision-making on treatment processes.

Furthermore, the hydrolysis process of primary sludge and secondary sludge significantly influences biogas production in anaerobic digestion. Primary sludge, consisting of settled solids from the preliminary treatment stage, undergoes hydrolysis to break down complex organic compounds into simpler compounds such as volatile fatty acids (VFA) and sugars. Similarly, secondary sludge, generated during biological treatment processes, also undergoes hydrolysis to release organic matter for subsequent digestion. The efficiency of hydrolysis directly impacts the availability of substrate for methane-producing archea during anaerobic digestion, thus influencing biogas yield. Therefore, incorporating hydrolysis kinetics into plant-wide models enables a more accurate prediction of biogas production and facilitates optimization strategies for enhancing energy recovery in wastewater treatment plants (Ekama et al., 2007).

In conclusion, the design and operation of municipal wastewater treatment plants are paramount for achieving sustainable environmental outcomes, particularly in light of initiatives such as the European Green Deal. These initiatives emphasize the need for reducing greenhouse gas emissions, promoting resource efficiency, and fostering a circular economy. The integration of plant-wide modeling techniques with newly elucidated degradation kinetics provides a powerful framework for optimizing process efficiency, identifying potential challenges, and meeting stringent regulatory requirements. By simulating various scenarios and considering the complex interactions between different components of the treatment process, engineers can develop robust and efficient treatment systems. These models allow for the anticipation of system behavior under diverse operational conditions, enabling proactive management and fine-tuning of the treatment processes to ensure consistent performance. Moreover, the advancement of biogas production modules within these models underscores the importance of resource recovery and energy minimization in

wastewater treatment. The ability to convert organic waste into biogas not only contributes to energy self-sufficiency but also reduces the carbon footprint of treatment plants. However, it is crucial to validate these models rigorously against empirical data and refine them iteratively to ensure their reliability and applicability in practical scenarios. This involves continuous monitoring and data collection from operational plants, followed by detailed analysis and model adjustments to reflect real-world conditions accurately. Through continued research and innovation, wastewater treatment plants can evolve into key contributors to a sustainable future, facilitating resource recovery and minimizing environmental impact.

2. PURPOSE OF THESIS

The primary aim of this research was to highlight the importance of using comprehensive plant-wide model-based experimental characterizations to evaluate the operational efficiencies and potential upgrade avenues within wastewater treatment facilities. This involved precisely defining COD fractionation within influents and specific kinetic parameters relevant to biomass. By applying such methodologies, it becomes possible to understand the biological processes underlying wastewater treatment, framed through real kinetic behaviors. This provides stakeholders with a better understanding of the design and operational dynamics of these plants, facilitating more informed decision-making processes.

The study focused on identifying intrinsic kinetic and operational parameters tailored to local environmental conditions. This approach allows for a robust evaluation of process performance, particularly in the context of fluctuating nitrification rates and anaerobic hydrolysis dynamics. The research reviewed seven full-scale wastewater treatment plants, each equipped with anaerobic sludge digestion facilities. A critical aspect of this study was the examination of COD turnover rates, nitrification and nitrate utilization rates, and biogas production capabilities within these systems. By conducting comprehensive plant-wide process analyses, the study enabled a direct comparison between theoretical models and the empirical conditions observed within these full-scale treatment facilities.

The study also explored the effects of varying mass fractions of primary and secondary sludge on biogas generation and the kinetic degradation processes. Data from full-scale treatment facilities was used to integrate respirometry-based influent wastewater characterization alongside specialized tests designed to assess biochemical methane potential (BMP) and specific methanogenic activity (SMA). This was complemented by the analysis of online biogas data from large-scale wastewater treatment operations in Turkey. A significant contribution of this study was the development and introduction of a novel model, Sumo1H. This model distinguishes between the anaerobic degradation kinetics of slowly biodegradable organic matter derived from

raw influent wastewater (X_B) and the decay processes of active biomass ($X_{B,E}$). Such a distinction is crucial for enhancing calibration accuracy and the comprehensive determination of process performance and biogas production within plant-wide modeling efforts. The efficacy and accuracy of the Sumo1H model were rigorously validated through calibration processes leveraging data from seven major municipal wastewater treatment facilities operational within the region, underscoring its potential applicability and utility in optimizing the operational paradigms of wastewater treatment plants.

3. LITERATURE REVIEW

3.1 The History of Process Simulation

Today, process simulators have become indispensable tools for engineers during design and operation of wastewater treatment plants. Scientific developments in wastewater treatment, advances in measurement techniques and breakthroughs in computer science and technology have contributed greatly to the success of process simulators.

The first known linear model for wastewater treatment plants was proposed by Garret and Sawyer in 1952. In the model, the amount of excess sludge produced is linked to the substrate (BOD_5) load and the organic load is given in the range of 0.25 - 0.50 kg BOD_5/kg TSS/day. In the literature, the dynamic activated sludge model was first proposed in 1974 by John F. Andrews (1974) and the development of IBM personal computers in 1983 increased the use of process models. In the 1980s, in South Africa, Dr. Peter Dold introduced the concept of multi-component model with the endogenous decay and death-regeneration model and model setup was based on COD fractions (Dold et al., 1980; Ekama et al., 1986). In the same years, SSSP (Single Sludge Simulation Program) dynamic simulation program was prepared by Bidstrup and Grady (1987). Dr. Gilles Patry laid the foundations of GPS-X (General Purpose Simulator-X) software of Hydromantis Company in 1987. In Europe, Dr. Mogenz Henze published the Activated Sludge Model No.1 (ASM1) in the International Water Association (IWA), which calculates organic carbon and biological nitrogen removal (Henze et al., 1987). Subsequently, in Canada, a defined process model for biological nitrogen and organic carbon removal was released by Dr. Peter Dold within the Biowin program (Envirosim, Biowin) in 1990. While the ASM1 model has 13 variables and 8 processes, the mathematical model developed by Envirosim consists of 82 variables and 46 processes. With Dr. Dold, the usage of GPS-X that allows the simulation of the wastewater and sludge streams of the plant together has started. Enhanced biological phosphorus removal (EBPR) was introduced into the model literature by the University of Cape Town (South Africa) with experimental and plant data (Wentzel et

al., 1992). This model includes organic carbon and biological nitrogen removal as well as enhanced biological phosphorus removal under aerobic conditions. Henze et al. (1995) published Activated Sludge Model No.2 (ASM2), which includes biological nitrogen/carbon and aerobic phosphorus storage. The effect of biological excessive phosphorus storage under anoxic conditions was characterized in University of Capetown (UCT) type activated sludge systems. In addition to aerobic phosphorus storage, the anoxic phosphorus storage process was introduced into the model matrix by Barker and Dold (1997). Under anoxic conditions, low anoxic conversion rates (Y_{HD}) have also been used by Orhon et al. (1996). The ASM2d models, which anoxic phosphorus storage processes were added, were published by International Water Association (IWA) as a technical report (1999). The ASM3 model (Gujer et al., 1999) states that organic carbon is metabolized by bacteria after being converted into storage products. However, subsequent scientific studies have shown that storage and growth processes occur simultaneously (Krishna and van Loosdrecht, 1999). The integration of intracellular metabolism in bioprocesses into the metabolic model was intensified by studies at the Delft University of Technology (Murnleitner et al., 1997; Smolders et al., 1994). These studies were followed by the scientific work carried out by Filipe and Daigger (1998). Metabolic models were not as widespread as ASM-type models and remained on an academic scale.

Anaerobic sludge digestion models have also been developed in the process model literature (Siegrist et al., 2002; Batstone et al., 2002). These models, which formulate liquid-gas interactions, in which biological and physicochemical processes are solved together, are prepared for mesophilic/thermophilic sludge digestion processes. The model known as Anaerobic Digestion Model No.1 (ADM1) is recognized as the first globally accepted extension for describing anaerobic digestion (Batstone et al., 2002). The major motivation for the development of this model was the increasing use of the plant-wide model application in plant design, operation and optimization. In a comprehensive stoichiometric model published by Ikumi et al. (2011) linked activated sludge to anaerobic and/or aerobic digestion. This model incorporates elemental balances and employs a mixed weak acid/base chemistry approach for pH calculations.

Anaerobic digestion model components were created based on protein, carbohydrate and fat components and needed to be integrated with activated sludge models for plant-based simulations. For this purpose, interfaces have been created and algorithms that

convert model components to each other have been proposed (Nopens et al., 2009). However, since the uncertainty in these algorithms creates a negative impact on the evaluation of the overall performance of the plant, they have not found practical use.

Sedimentation processes in activated sludge processes have also been integrated into general purpose models to evaluate the performance of settling ponds (Ekama et al., 1997; Takács et al., 1991; Vesilind et al., 1968). In addition, greenhouse gas emissions (N_2O) (Hiatt and Grady, 2008; Wild et al., 1995), competition between glycogenaccumulating organism (GAO) and phosphorus accumulating organisms (PAO) (Yagci et al., 2004), the effect of high temperatures on the process (Sarioglu et al, 2017), sludge reduction technologies (Cambi etc.), deammonification (Hellinga et al., 1998) and physicochemical processes (Söteman et al., 2005; Takács, 2008) have also been included in the general models and the effects of all these processes on overall performance can be calculated by the process simulators. Considering all abovementioned developments, the calculation of plant-based process calculations on a single supermodel provides great advantages in terms of overall evaluation (Ekama, 2009; Seco et al., 2020). In today's simulators (Mantis, Envirosim, Sumo©, etc.), all processes are combined in a single supermodel and model components can be calculated time-dependently by the processor according to ambient conditions.

3.2 Processes and Model Parameters

Activated sludge models are introduced to plant-wide process simulators in Gujer Matrix format, including model components, processes, kinetic and stoichiometric parameters (Gujer and Larsen, 1995) and flows between the state variables and rate expressions are shown in the model matrix. The number of state variables varies depending on the COD fractions and bacteria species introduced into the model. Reaction rates can be adjusted automatically with correction factors according to the ambient/environmental conditions (temperature, pH, etc.).

3.2.1 Heterotrophic growth

Organic matter removal in activated sludge systems is carried out by heterotrophic microorganisms. Heterotrophic bacteria perform the growth process in aerobic, anoxic and anaerobic conditions by using easily biodegradable organic matter in dissolved form. These microorganisms use the energy released by biochemical reactions as an

energy source and the organic carbon in the environment as a carbon source. Heterotrophic bacteria population has the highest fraction in activated sludge systems as it is the biomass community with the highest growth and conversion rates.

The microorganisms in the system store more than half of the organic matter removed by the microorganisms in the system to be used as an energy source in cellular activities, while the remaining part is used for new cell formation. If there is not enough organic matter in the environment, microorganisms perform endogenous respiration by self-oxidizing to provide the necessary energy source.

3.2.2 Heterotrophic decay

The reduction of heterotrophic biomass in activated sludge systems can be explained by the concept of energy used by microorganisms other than biosynthesis. Microorganisms use some of the energy produced for regeneration of cell components, movement, etc. As a result, growth is less than the amount determined by the stoichiometric conversion rate. The degradation mechanism of biomass takes place simultaneously with growth process. The decay rate is traditionally expressed by the following equation using 1st order reaction kinetics with the assumption that it decreases with a constant coefficient according to the biomass concentration (Equation 3.1).

$$\frac{dX}{dt} = -k_D \cdot X_H \tag{3.1}$$

k_d: Heterotrophic decay rate (1/day)

3.2.3 Autotrophic growth

The nitrification process is typically considered as the autotrophic transformation occurring within activated sludge systems, characterized by the sequential oxidation of saline and free ammonia nitrogen into nitrite and then nitrate, facilitated by autotrophic microorganisms under aerobic conditions. These autotrophic bacteria utilize inorganic carbon (CO_2) as their carbon source and derive energy from inorganic nitrogen compounds. The process unfolds in two primary stages: initially, ammonia-oxidizing bacteria (AOB), with *Nitrosomonas* being a common example, oxidize ammonia to nitrite. Subsequently, nitrite-oxidizing bacteria (NOB), often exemplified

by *Nitrobacter*, convert nitrite into nitrate. This transformation is governed by specific stoichiometric redox reactions that delineate the nitrification process.

$$NH_4^+ + \frac{3}{2}O_2 \xrightarrow{AOB} NO_2^- + H_2O + 2H^+ \quad (3.2)$$

$$NO_2^- + \frac{1}{2}O_2 \xrightarrow{NOB} NO_3^- \quad (3.3)$$

From the Equation 3.2 and Equation 3.3, the oxygen requirement can be calculated as 3.43 mg O_2/mg N for the oxidation of ammonia to nitrite and 1.14 mg O_2/mg N for nitrite to nitrate, totaling 4.57 mg O_2/mg N. Since the ammonia nitrogen is also used in biomass synthesis, in reality, the total oxygen requirement for the oxidation of ammonia to nitrate is lower than this value and reported down to 4.3 mg O_2/mg N (Henze et al., 2008). Nitrification is the process most affected by environmental conditions (oxygen, pH, temperature, etc.).

3.2.4 Autotrophic decay

Similar to the heterotrophic endogenous decay rate, autotrophic endogenous respiration is also expressed by using 1st order reaction kinetics. The process can be formulated as below (Equation 3.4):

$$\frac{dX_A}{dt} = -b_A \cdot X_A \quad (3.4)$$

As specific growth rates, autotrophic organisms have much lower endogenous decay rate (b_A=0.04 day^{-1}) than heterotrophic endogenous decay rate (b_H=0.24 day^{-1}).

3.2.5 Hydrolysis

Slowly biodegradable organic matter is converted into readily biodegradable organic matter by the activity of heterotrophic bacteria in the activated sludge process. The hydrolysis mechanism is expressed by a surface saturation function with a maximum hydrolysis rate and a half saturation constant. The rate of hydrolysis is not directly dependent on the concentration of slowly biodegradable organic matter, but the ratio of slowly biodegradable organic matter concentration to heterotrophic biomass concentration. The hydrolysis process can take place under aerobic, anoxic and

anaerobic conditions, but the rate of hydrolysis is lower than the aerobic conditions. Since, the slowly biodegradable organic matter is present in high concentrations in influent wastewater, it has an importance in terms of nutrient removal. In activated sludge systems, hydrolysable organic matter can be separated into more than one component as fast and slow hydrolysable organic matter fraction. In addition, colloidal substances also participate in the hydrolysis mechanism by adsorption in model simulations. Hydrolysable organic matter can be used in process modifications for pre-hydrolysis/fermentation for phosphorus removal, optimization of denitrification potential, pre-sedimentation in anaerobic digesters and increasing the amount of biogas.

3.2.6 Methanogenic activity

In activated sludge models, especially in the calculation of anaerobic sludge digester performance, the activities of acidoclastic and hydrogenotrophic methanogens are mainly effective. Acidoclastic methanogens metabolize volatile fatty acids and hydrogenotrophic methanogens metabolize hydrogen and CO_2 into methane gas. In plant simulations, methanogenic activity can also be calculated in the wastewater process stream. The process stoichiometry and kinetics of these reactions are included in the general model matrices. Detailed information on the reactions, process kinetics and microbiology of methanogenic activity is given in Anaerobic Sludge Digestion Section.

3.2.7 Phosphorus accumulating organisms

Phosphorus removal in activated sludge models is simulated by adding relevant reactions in which phosphorus accumulating organisms (PAO) storing volatile fatty acids (acetic acid, propionic acid, etc.) and releasing phosphorus under anaerobic conditions. Furthermore, the utilization of storage products under aerobic/anoxic conditions is integrated with 2 different kinetic expressions according to low and high phosphorus concentrations. In anoxic conditions, phosphorus accumulating biomass has the ability to denitrify and store phosphorus. However, this reaction has a slower kinetics compared to aerobic conditions.

Phosphorus accumulating bacteria can also contribute to the fermentation process depending on the characteristics of anaerobic conditions. In simulations, secondary

phosphorus release can be calculated when the stored substrate is depleted and the microorganism switches to endogenous respiration. For example, phosphorus release (by denitrification) can be calculated when sludge with biological excessive phosphorus removal is retained in the final sedimentation unit. K, Mg ions in the influent wastewater are also important in phosphorus storage mechanism.

3.2.8 Glycogen accumulating organisms

Glycogen accumulating organisms (GAO) have the ability to store volatile fatty acids under anaerobic conditions. However, they do not have the ability to store phosphorus. They can have higher growth rates than phosphorus accumulating organisms at high temperatures and can affect the process performance of the wastewater treatment plants. In simulations, GAO population is also included in the calculations (Yagci et al., 2004).

3.2.9 Chemical reactions

With the development of computer science and processors, pH calculations in biochemical processes has become important for the evaluation of overall process performance (Sötemann et al., 2005). Chemical reactions were first included in the ASM2/2d model to calculate phosphorus removal with metal addition. In the model, two processes were defined as precipitation and dissolution. However, recent studies have revealed that free ion effect, chemical equilibrium, adsorption and precipitate maturation should also be added in order to calculate chemical reactions properly. As it is known, $FePO_4$ crystals are formed between pH 2-4. Since, especially municipal wastewater treatment plants are operated close to neutral pH, the effect of hydroxide flocs on chemical precipitation was integrated into the models. In addition, in activated sludge systems with anaerobic digesters, struvite (MAP), calcium phosphate and vivianite must also be calculated in the reactors in order to accurately determine the phosphorus and nitrogen mass balances. Since chemical reactions depend on pH calculation and ion balance, anion and cation measurements in the inlet stream must also be introduced correctly into the model. Chemical reactions and/or pH calculations can be optionally selected.

3.2.10 Temperature effect

As a known fact, increasing temperature thermodynamically increases reaction rates. In new generation activated sludge simulators, temperature changes affect the rate constants of reactions with Arrhenius function. In activated sludge models, the Arrhenius function is an exponential expression and assumes a continuous increase with temperature. In the simulators, the process models are prepared as a single exponential model. The usable temperature range of the Arrhenius function can be taken as 10-27°C. Above this temperature, the process rates in activated sludge decrease. Especially the substrate storage rates of nitrifying bacteria and PAOs decrease with increasing temperature and the effect of temperature on the process becomes evident above 30°C (Sarioglu et al., 2017).

3.3 Wastewater Characterization in Activated Sludge Modeling

Achieving an accurate wastewater characterization, particularly with COD fractionation, is fundamental for distinguishing between organic substances based on their biodegradability properties. This differentiation is essential for the precise estimation of the electron acceptor demand and the projection of excess biological sludge production in the context of modeling. Additionally, the assessment of the inert fraction of organic matter present in wastewater plays a pivotal role as it indirectly reflects the quantity of biodegradable organic matter available. This biodegradable fraction serves as the essential substrate for microbial growth and the utilization of electron acceptors such as oxygen (O_2) and nitrate (NO_3). In contemporary modeling practices for activated sludge systems, COD is employed as a critical parameter. It effectively encapsulates the electron equivalence among the organic substrate, active biomass, and dissolved oxygen, thereby providing a comprehensive measure for the dynamic interactions within wastewater treatment processes.

In multi-component activated sludge modeling, the organic matter in the wastewater is defined in terms of COD, broken down into fractions according to the biodegradability characteristics. In this context, the total COD (C_T) of the wastewater consists of two main components: unbiodegradable or inert COD (C_I) and total biodegradable COD (C_S). Soluble inert COD (S_I), which is the soluble form of inert COD, leaves the system as it enters, unaffected by biochemical reactions whereas

particulate inert COD (X_I) accumulates in the system and leaves the system with excess biological sludge (Henze et al., 2008; Orhon and Artan, 1994).

The total biodegradable COD in wastewater has been defined by two important components, namely readily biodegradable COD (S_S) and slowly biodegradable COD (X_S), according to their degradation rates (Dold and Marais, 1986). The X_S component, which is defined as particulate organic matter in this approach, was later determined to consist of dissolved, colloidal and complex large organic matter according to particle size. The main feature of this component is that it needs extracellular hydrolysis to pass through the cell wall (Henze, 1992). The rate of hydrolysis is the rate-limiting step since it affects the rate of utilization of the slowly biodegradable organic matter by microorganisms and it varies for each organic matter, making the characterization of this component difficult. This component can be characterized according to two different hydrolysis rates as rapidly hydrolysable COD (S_H) and slowly hydrolysable COD (X_S) (Çokgör, 1997; Henze, 1992; Orhon and Artan, 1994).

The COD components present in influent wastewater are given in Figure 3.1.

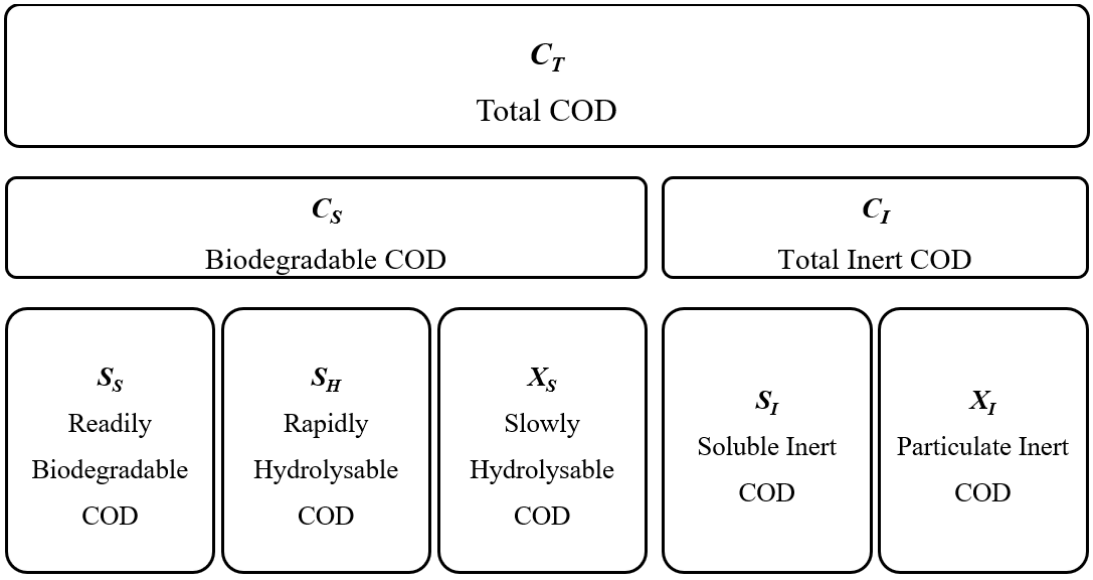

Figure 3.1 : COD fractions of influent wastewater.

Wastewater characterization in terms of organic content is very useful for the determination of the treatment process and process kinetics and also for the prediction of process performance and effluent quality.

A different COD structure is observed in the effluent streams of biological treatment systems compared to the influent wastewater. The soluble COD fractions in the

effluent includes soluble inert COD (S_I) and small amounts of biodegradable COD as well as metabolically formed and inert soluble COD, S_P. As a result, there is generally more soluble inert COD in the effluent than in the raw wastewater. The dissolved COD components in the effluent are given in Figure 3.2.

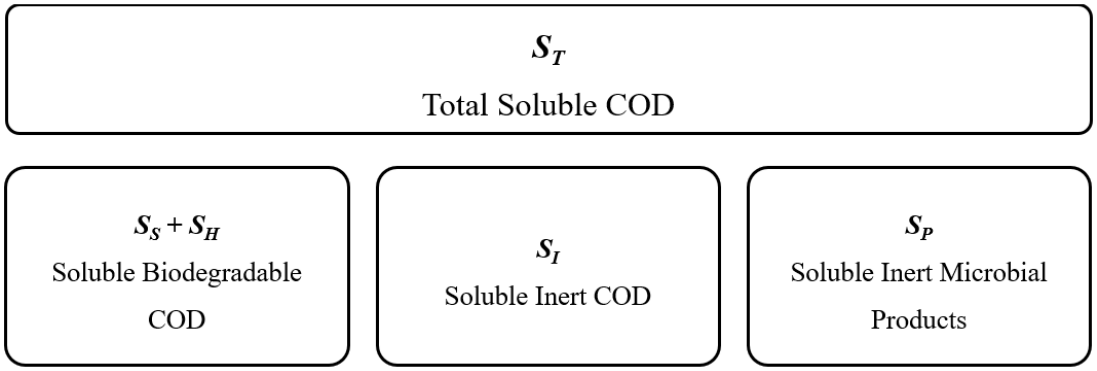

Figure 3.2 : Soluble COD fractions of the effluent wastewater.

Similarly, particulate COD has different components in the effluent stream than in the raw wastewater. Apart from the particulate inert COD (X_I) present in the raw wastewater, which is retained and accumulated by the sludge, active heterotrophic biomass (X_H) utilizing biodegradable COD as substrate is observed in the effluent. At the same time, the portion of the slowly hydrolysable organic matter, X_S, that cannot be removed according to sludge age can be observed in the effluent.

The fourth component of total particulate COD is the inert particulate COD, X_P, which is formed as a result of metabolic activities during the biochemical reactions of biomass. The components of particulate COD present in the sludge stream are given in Figure 3.3.

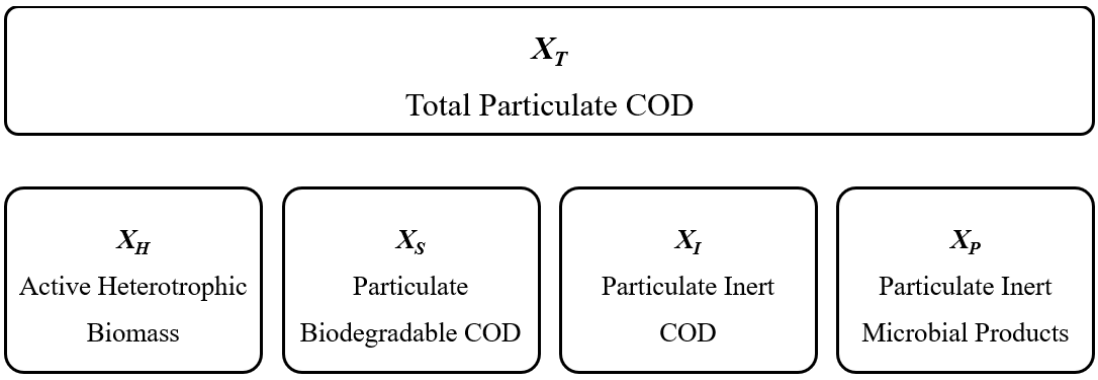

Figure 3.3 : Particulate COD fractions present in the sludge stream.

The influent wastewater characterization can vary depending on the structure of the model. Nowadays, in parallel with technological developments such as hybrid

processes, high-rate activated sludge systems, membrane bioreactors, more detailed influent fractions have to be included in the models. Therefore, the importance of flocculation and adsorption processes has increased and colloidal COD fraction has been re-integrated into the models for influent wastewater characterization (Melcer et al., 2003).

The equivalents of the influent wastewater fractions described in detail above in terms of COD fractions in the Sumo1 model (www.dynamita.com) are summarized below (Figure 3.4).

Total readily biodegradable COD concentration, S_S:

$$S_S = S_{VFA} + S_B + S_{MEOL} \quad (3.5)$$

S_{VFA}: Volatile fatty acids (mg COD/L)

S_B: Readily biodegradable substrate (non-VFA) (mg COD/L)

S_{MEOL}: Methanol (mg COD/L) (external carbon source)

Total slowly biodegradable COD concentration, X_S:

$$X_S = X_B + C_B \quad (3.6)$$

X_B: Slowly biodegradable substrate (mg COD/L)

C_B: Colloidal biodegradable substrate (mg COD/L)

C_U: Colloidal unbiodegradable organics (mg COD/L)

X_U: Particulate unbiodegradable organics (mg COD/L)

Filtered COD (1,5 μm, including colloids): $S_{C,COD} = (S_U + S_B + S_{VFA}) + C_B + C_U$

Filtered flocculated COD (1,5 μm, without colloids): $S_{COD} = S_U + S_B + S_{VFA}$

S_U: Soluble unbiodegradable organics (mg COD/L)

The filtered COD is about 40% of the influent wastewater COD. The filtered flocculated COD accounts for 60% of the filtered COD. These values may vary according to the characteristics of the sewage system and industrial contribution to the sewer system.

Calculation of biodegradable and inert COD fractions in colloidal form in plant-wide models (C_B, C_U) is given below (Melcer et al., 2003; URL-1):

- In the simulation, a fraction of COD that cannot be degraded in colloidal form (C_U) is incorporated onto particulate inert COD (X_U) by adsorption process. Accordingly, a part of the C_U is retained in the sludge stream and the non-adsorbable fraction passes to the effluent stream.

- A fraction of COD that can be degraded in colloidal form (C_B) is included in the slowly biodegradable COD (X_B) by the adsorption process. The remaining C_B is similarly calculated in the effluent stream to be discharged. Approximately 10-15% colloidal COD is present in wastewater treatment plants in Istanbul, Turkey (Sözen et al., 2008).

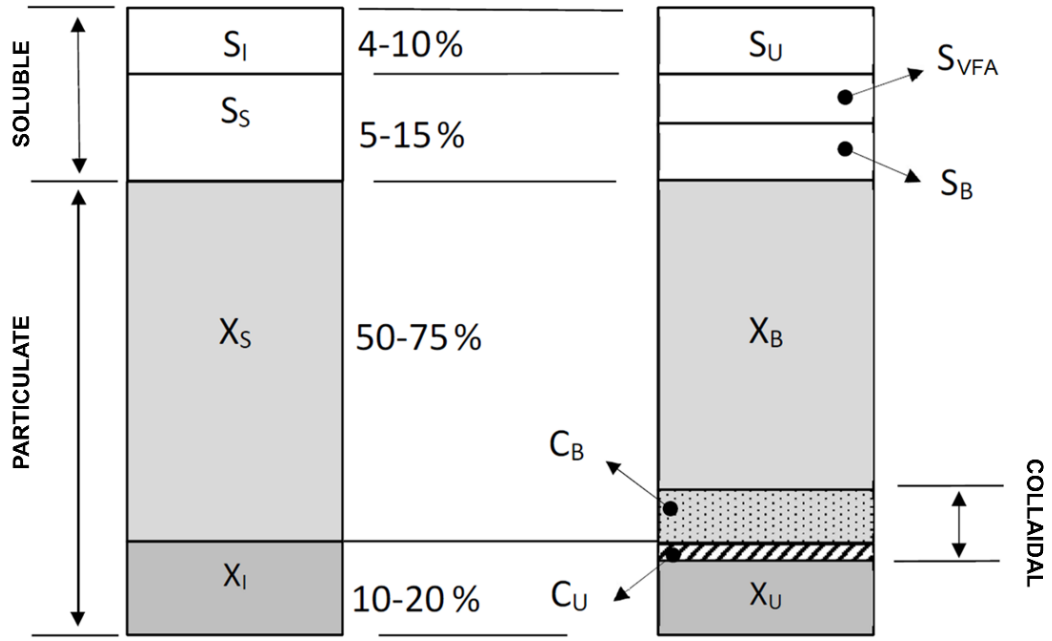

Figure 3.4 : Comparison of COD fractions.

Determination of influent COD fractions has a great importance in selection of advanced biological wastewater treatment plant configuration. It should be noted that COD fractions may differ for each plant and therefore different plant configurations may be required. In order to apply activated sludge models directly to industrial wastewater treatment plants, suitable COD fractions for the specific industry must be defined in the model (Orhon et al., 2009). For example, in wastewater applications, slowly biodegradable COD fraction in dissolved form (S_H) is integrated into the model (Ubay Cokgor et al., 1998). Soluble organic matter is particularly important for industrial wastewater as it contributes to the COD concentration in the effluent and affects the bioreactor volume.

For the simulation of nitrification and denitrification processes, the influent nitrogen fractions in wastewaters should also be defined. In Figure 3.5, influent nitrogen concentrations are fractionated considering soluble and particulate nitrogen forms. In domestic/urban wastewater, influent nitrogen is generally in the form of TKN and oxidized nitrogen forms are nearly absent. Approximately 80-90% of the influent TKN is in soluble form. Influent NH_4-N is measured between 65-80% of the influent TKN concentration (Henze et al., 2008). In Istanbul wastewater, this ratio was measured between 55-75% (İnsel et al., 2020). Particulate and soluble unbiodegradable nitrogen concentrations are 8-10% of the influent TKN value. In urban wastewater, oxidized forms of nitrogen are generally absent in the influent wastewater except under special conditions. Especially in long sewerage systems, NH_4-N can be converted into oxidized nitrogen by oxygen gained at pumping stations or at stack drops. In these cases, the NO_X-N parameter should be added to the influent as a model component.

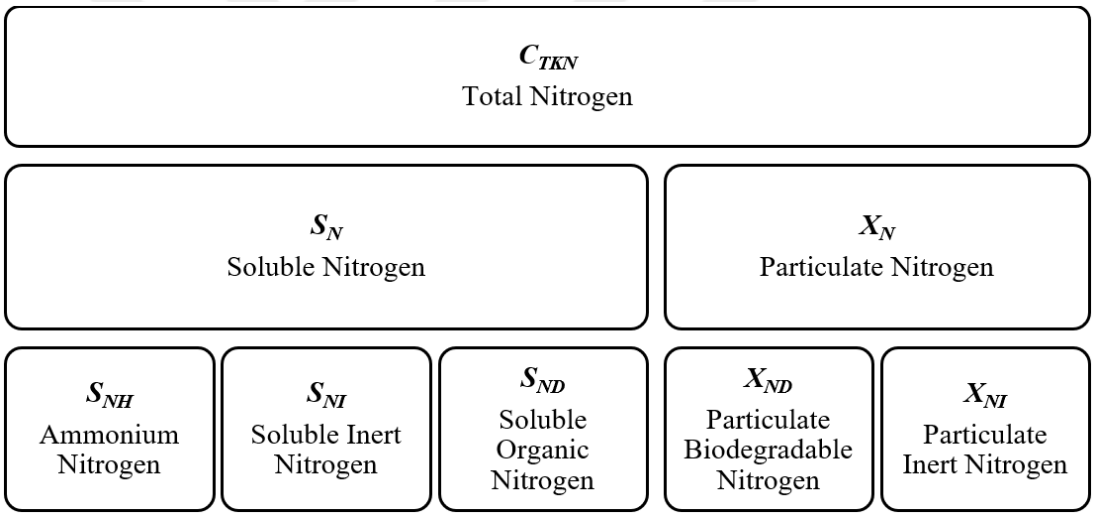

Figure 3.5 : Influent nitrogen fractions.

3.4 Multi-Component Activated Sludge Models

3.4.1 Endogenous decay approach

In the context of the endogenous decay model (EDM), organic matter in wastewater is classified as biodegradable (S_S and X_S) and unbiodegradable (S_I and X_I) organic matter in dissolved and particulate form. S_P and X_P are defined as soluble and particulate microbial products resulting from metabolic activities in the reactor and X_H is defined as active heterotrophic biomass.

In the EDM, it is assumed that the active biomass is converted into particulate inert microbial products with a ratio of f_{EX} and into soluble inert microbial products with a ratio of f_{ES}. The particulate inert microbial products accumulate in the activated sludge system like the influent particulate inert materials and leave the system with excess biological sludge.

The rate of decrease in total biomass (X) was described by McKinney as in Equation 3.7.

$$\frac{dX}{dt} = \frac{dX_H}{dt} + \frac{dX_P}{dt} \tag{3.7}$$

The formation of particulate inert microbial products is expressed by Equation 3.8.

$$\frac{dX_P}{dt} = -f_{EX} \cdot \frac{dX_H}{dt} \tag{3.8}$$

In the endogenous decay approach, the decay mechanism reflects the respiration process and the electron acceptor (oxygen) is consumed during endogenous respiration. When the decay process of this mechanism is expressed with Equation 3.1, it takes the form of Equation 3.9.

$$\frac{dX_H}{dt} = -b_H \cdot X_H \tag{3.9}$$

b_H: Endogenous decay rate for EDM (1/day)

Substituting Equation 3.9, the expression for the decrease in active heterotrophic biomass, into Equation 3.8 gives the expression for the formation of particulate inert microbial products (Equation 3.10).

$$\frac{dX_P}{dt} = f_{EX} \cdot b_H \cdot X_H \tag{3.10}$$

The relationship between the two decay rates, k_D and b_H, can be expressed by Equation 3.11:

$$k_d = (1 - f_{EX}) \cdot \frac{X_H}{X} \cdot b_H \tag{3.11}$$

Soluble inert microbial products are the result of growth and decay mechanisms (Artan, 1987; Orhon et al., 1989). When the dominant of these two mechanisms is considered and the other mechanism is neglected, the result will not be affected.

If the growth mechanism is considered to be dominant, the expression for the formation of dissolved inert microbial products becomes as in Equation 3.12.

$$\frac{dS_P}{dt} = -\alpha_D \cdot \hat{\mu}_H \cdot \frac{S_S}{K_S + S_S} \cdot X_H \tag{3.12}$$

α_D: Coefficient of dissolved inert formation (growth origin) [-]

When the decay mechanism is dominant in the formation of the soluble inert microbial product, the formation expression is considered as in Equation 3.13.

$$\frac{dS_P}{dt} = -f_{ES} \cdot b_H \cdot X_H \tag{3.13}$$

As can be seen from the above equations, it is assumed that during the degradation mechanism, biomass is converted into particulate inert microbial products at f_{EX} and soluble inert microbial products at f_{ES} instead of being oxidized. Figure 3.6 shows a schematic representation of the EDM.

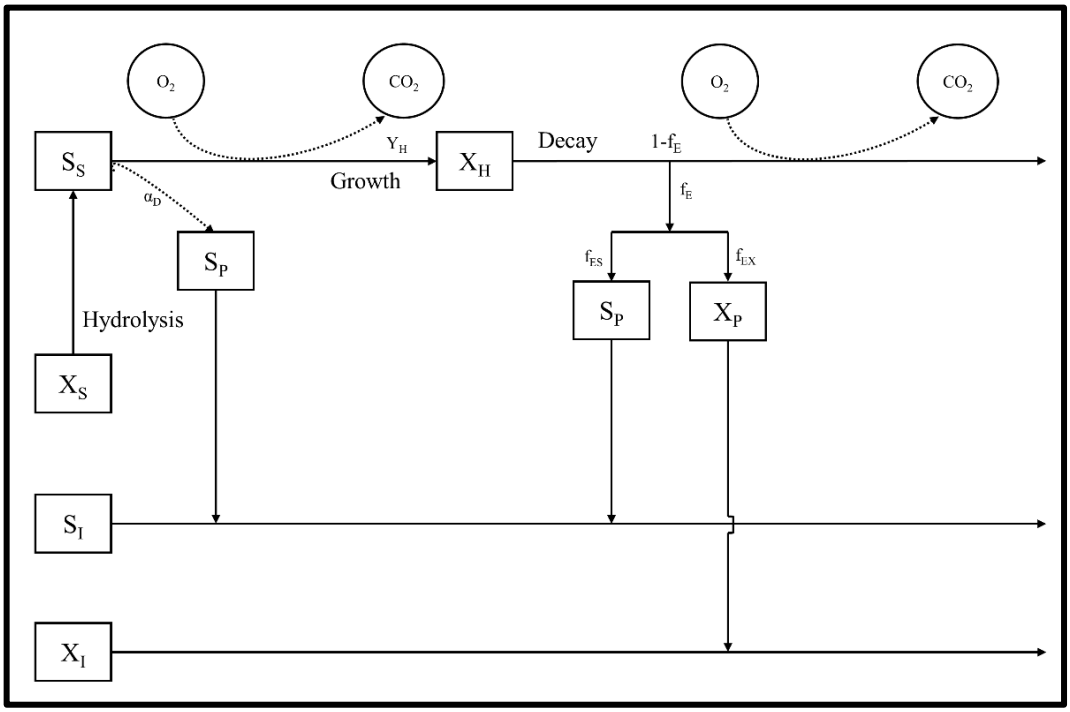

Figure 3.6 : Schematics of EDM (Orhon and Artan, 1994).

The matrix given in Table 3.1 shows the kinetics and stoichiometric relations in the EDM for carbon removal.

3.4.2 Death-regeneration approach and ASM1 model

The death-regeneration concept was first suggested by Dold et al. in 1980, and then modified by Henze et al. in 1987 in the ASM1 model, which provides the basis for many other activated sludge models.

In the death-regeneration model (DRM), active heterotrophic biomass (X_H) is converted into inert particulate matter (X_P) at a rate of f_{XP} and into slowly hydrolysable particulate matter (X_S) at a rate of (1-f_{XP}). This fraction is then converted by hydrolysis process back into the readily biodegradable fraction, which is used for growth and finally is considered to be converted into soluble microbial product (S_P). According to this approach, no electron acceptor is consumed in any process other than the growth mechanism. When the decay process of this mechanism is expressed similarly to Equaiton 3.7, it takes the form of Equation 3.14.

$$\frac{dX_H}{dt} = -b'_H \cdot X_H \tag{3.14}$$

b'_H: Heterotrophic decay rate for DRM (1/day)

The difference between the decay rates of the EDM and the DRM is expressed as Equation 3.15.

$$b'_H = \frac{b_H}{1 - f_X \cdot Y_H \cdot (1 - f_P)} \tag{3.15}$$

In Equation 3.13, f_P is the coefficient for the inert component of biomass in the DRM. Figure 3.7 shows a schematic representation of the death-regeneration approach.

The matrix given in Table 3.2 shows the process stoichiometry and kinetics of the DRM for carbon removal.

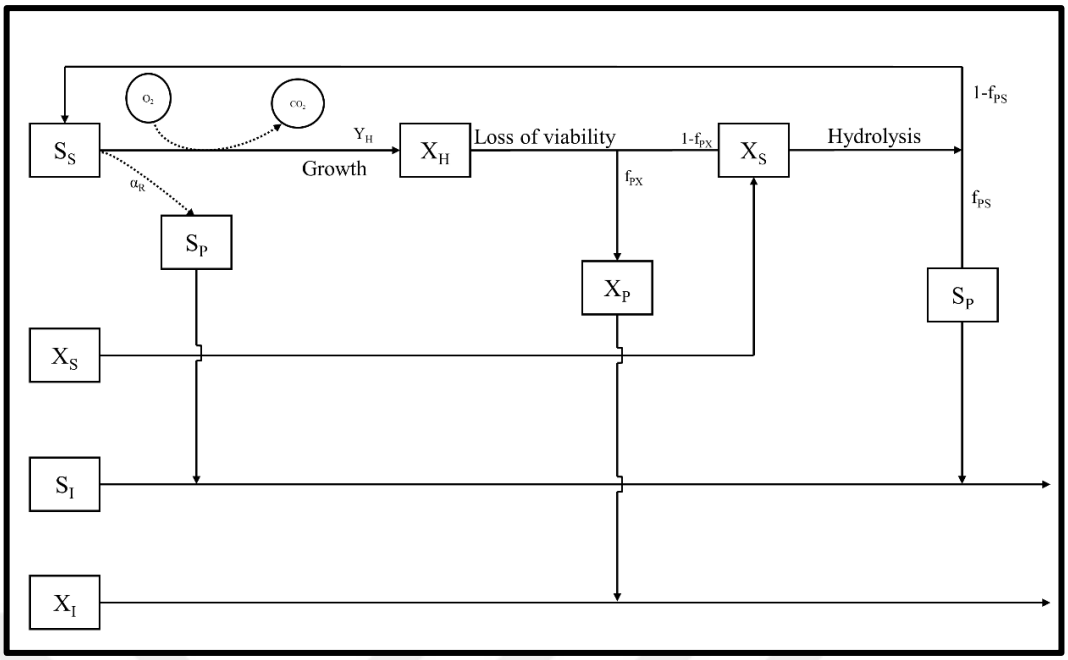

Figure 3.7 : Schematics of DRM (Orhon and Artan, 1994).

In 1987, based on the death-regeneration concept, the International Association on Water Pollution Research and Control (IAWPRC) Task Group developed the IAWQ Activated Sludge Model No.1, which will be the basis for subsequent models (Henze et al., 1987; Henze, 2004). ASM1 approach is considered to be the key milestone, especially when it comes to organic carbon removal, and still maintains its scientific importance (Orhon et al., 2009).

The ASM1 model covers nitrification and denitrification kinetics in addition to organic carbon removal and was developed primarily for municipal/urban wastewater. However, it can also be used for industrial wastewaters with precise calibrations for model parameters (Henze, 2004; Orhon et al., 2009; Pala-Özkök, 2012). The matrix representation of the ASM1 model is given in Table 3.3.

Table 3.1 : Matrix representation of carbon removal stoichiometry and kinetics in EDM (Orhon and Artan, 1994).

Component, i →	1	2	3	4	5	6	7	8	Process Rate
Process, j ↓	S_I	S_S	X_I	X_S	X_H	X_P	S_P	S_O	$ML^{-3}T^{-1}$
Growth		$-\frac{1}{Y_H}$			1		α_D	$-\frac{(1-\alpha_D \cdot Y_H - Y_H)}{Y_H}$	$\hat{\mu}_H \cdot \frac{S_S}{K_S + S_S} \cdot X_H$
Hydrolysis		1		-1					$k_h \frac{X_s/X_H}{K_X + X_s/X_H} \cdot X_H$
Decay					-1	f_{EX}	f_{ES}	-(1- f_{EX}- f_{ES})	$b_H \cdot X_H$
Parameter, ML^{-3}	COD	COD	COD	COD	Cell COD	COD	COD	O_2	

Table 3.2 : Matrix representation of carbon removal stoichiometry and kinetics in DRM (Orhon and Artan, 1994).

Component, i →	1	2	3	4	5	6	7	8	Process Rate
Process, j ↓	S_I	S_S	X_I	X_S	X_H	X_P	S_P	S_O	$ML^{-3}T^{-1}$
Growth		$-\frac{1}{Y_H}$			1		α_R	$-\frac{(1-\alpha_R \cdot Y_H - Y_H)}{Y_H}$	$\hat{\mu}_H \cdot \frac{S_S}{K_S + S_S} \cdot X_H$
Hydrolysis		1- f_{PS}		-1			f_{PS}		$K_h \cdot X_H$
Decay				1- f_{PX}	-1	f_{PX}			$b'_H \cdot X_H$
Parameter, ML^{-3}	COD	COD	COD	COD	Cell COD	COD	COD	O_2	

Table 3.3 : Matrix representation of ASM1 model (Henze et al., 2000).

Component, i →	1	2	3	4	5	6	7	8	9	10	11	Process Rate
Process, j ↓	S_I	S_S	X_I	X_S	X_H	X_A	X_P	S_O	S_{NO}	S_{NH}	S_{ALK}	$ML^{-3}T^{-1}$
Heterotrophic growth		$-\frac{1}{Y_H}$			1			$-\frac{(1-Y_H)}{Y_H}$		$-i_{XB}$	$-\frac{i_{XB}}{14}$	$\hat{\mu}_H \cdot \frac{S_S}{K_S+S_S} \cdot \frac{S_O}{K_{O,H}+S_O} \cdot X_H$
Autotrophic growth						1		$-\frac{(4{,}57-Y_A)}{Y_A}$	$\frac{1}{Y_A}$	$-i_{XB}$ $-\frac{1}{Y_A}$	$-\frac{i_{XB}}{14}$ $-\frac{1}{7 \cdot Y_A}$	$\hat{\mu}_A \cdot \frac{S_{NH}}{K_{NH}+S_{NH}} \cdot \frac{S_O}{K_{O,A}+S_O} \cdot X_A$
Hydrolysis, X_S		1		-1								$k_{hX} \frac{X_s/X_H}{K_{XX}+X_s/X_H} \cdot \frac{S_O}{K_{O,H}+S_O} \cdot X_H$
Heterotrophic decay				1- f_P	-1		f_P					$b_H \cdot X_H$
Autotrophic decay				1- f_P		-1	f_P					$b_H \cdot X_A$
Parameter, ML^{-3}	COD	COD	COD	COD	Cell COD	Cell COD	COD	O_2	N	N	$CaCO_3$	

3.5 Plant-wide Process Simulators

The insightful findings from simulation/modeling studies, particularly those that incorporate the variability of environmental conditions, have cast a spotlight on the profound inadequacies inherent in the conventional approaches to designing wastewater treatment plants (Insel et al., 2022; Jenkins and Wanner, 2014). These studies, by integrating a spectrum of variable factors such as diurnal influent loads, diverse temperature ranges, varying precipitation patterns, and the potential for inhibitory substances, reveal that traditional design calculations may not adequately prepare these plants to handle the complexities of real-world environmental conditions. This revelation brings to the fore the critical necessity for a comprehensive reevaluation and optimization of the design methodologies employed in the planning and construction of wastewater treatment plants.

To address these challenges, the employment of process simulators emerges as a pivotal strategy. These advanced tools offer the capability to simulate a wide array of environmental and operational scenarios, providing detailed insights into how different factors interact and impact the overall performance of the treatment processes. By leveraging the predictive power of process simulators, engineers and plant designers can explore a multitude of design variations and operational strategies, enabling them to identify and implement solutions that enhance the robustness, efficiency, and adaptability of wastewater treatment plants. This approach not only ensures that plants are better equipped to deal with the uncertainties of environmental conditions but also contributes to the advancement of sustainable and resilient wastewater management practices. In this context, the optimization of wastewater treatment plant design under variable conditions is not merely a recommendation but a fundamental requirement for ensuring the long-term effectiveness and sustainability of wastewater treatment infrastructures in the face of evolving environmental challenges.

Plant-wide process simulators serve many purposes such as determination of plant-based design principles and process control, creation of automation scenarios, selection of appropriate equipment in automation, evaluation of the performance of wastewater and sludge treatment processes, bottleneck analysis, improvement of treatment efficiency, calculation of capacity increase, reduction of operating costs, calculation of greenhouse gas emissions, personnel training etc. (İnsel, 2004; Olsson

et al., 2005). When plant-specific wastewater characterization, model parameters and operating conditions are introduced to the software, system performance analysis can be investigated, process problems can be identified and results very close to reality can be obtained (Insel et al., 2012).

The working principle of these programs is based on the general mass balance and the model that carries out the process calculations and works in the background. The mass balances depend on the selected reactor technology and plant configuration. Models are available in the library of simulator programs or can be created by the user.

Multicomponent process models consisting of processes and variables have become indispensable parts of process simulators for wastewater treatment processes, anaerobic/aerobic sludge digestion, innovative treatment processes and process simulators with the development of computer technology. On the other hand, libraries related to physicochemical processes integrated with biological processes (chemical phosphorus precipitation, Magnesium Ammonium Phosphate (MAP) Crystallization, etc.) and membrane bioreactors have also taken their place in commercial programs. Commonly used academic and commercial simulator software are summarized in Table 3.4.

The correct use of simulators requires that the plant should be reflected into in the software closest way to reality. The accuracy of the assumptions made in the plant simulation and the data introduced to the simulator will ensure realistic results. According to this;

1. Influent wastewater characterization, organic matter (COD), nitrogen and phosphorus fractions
2. Inert/organic matter concentrations in the inlet
3. Appropriate model (kinetic and stoichiometric) coefficients for wastewater/process
4. Wastewater treatment plant configuration and process flow
5. Operational conditions (MLSS, volumes, air flow rate, all flow rates, sludge age, etc.)
6. Process control system (aeration, sludge age, internal recirculation, sludge recirculation, etc.)

should be introduced to the software to represent the real conditions (İnsel, 2004; Rieger et al. 2012). Otherwise, both the obtained results and the reliability of these results are at the risk of the user. The processes and reactor technologies used in process simulators are summarized in Table 3.5. Schematic representation of model components in wastewater treatment plant simulation is given in Figure 3.8.

Table 3.4 : Simulation software used in process modeling and simulation (İnsel et al., 2022).

Software	Country	Company/Institution
AQUASIM	Switzerland	EAWAG
ASIM	Switzerland	EAWAG
BioWin	Canada	Envirosim
GPS-X	Canada	Hydromantis
SIMBA#	Germany	ifak
STOAT	England	Water Research Centre
SUMO	France	Dynamita
WEST	Denmark	DHI Technologies

Since, the simultaneous use of different plant configurations and complex reactor hydraulics make it impossible to solve the abovementioned stoichiometric calculations manually in a reasonable time, the use of simulators for performance analysis has become essential. On the other hand, wastewater treatment plant simulators are also widely used to determine appropriate process control strategies. Especially during the operation phase, simulators are also used for scenario analysis and operator training without risking the plant operation (Makinia and Zaborowska, 2020; Vanrolleghem et al., 2003).

Brief information about commercially used plant-wide process simulators can be found in the following sections.

Table 3.5 : Processes and technologies in plant-wide simulators.

Biological / Chemical Processes	Separation Processes	Reactor Technologies
Nitrification/Denitrification	Primary Sedimentation	Completely Stirred Reactors
Biological Phosphorus Removal	Thickening Processes	Plug Flow Reactors
Sludge Production and Oxygen Uptake	Final Sedimentation	Sequencing Batch Reactors
Fermentation – Anaerobic Digestion	Reactive Sedimentation	Membrane Bioreactors
Nutrient Recovery	Flocculation	MBBR Systems
Greenhouse Gas Emissions	Chemical Precipitation	Trickling Filters
Aeration/Gas Transfer	Filtration	Membrane Oxygen Systems
pH - Alkalinity	Cyclone Separators	Hybrid Processes
Anammox Process	Membrane Filtration	Granular Activated Sludge
Realtime Process Control		Thermal Hydrolysis

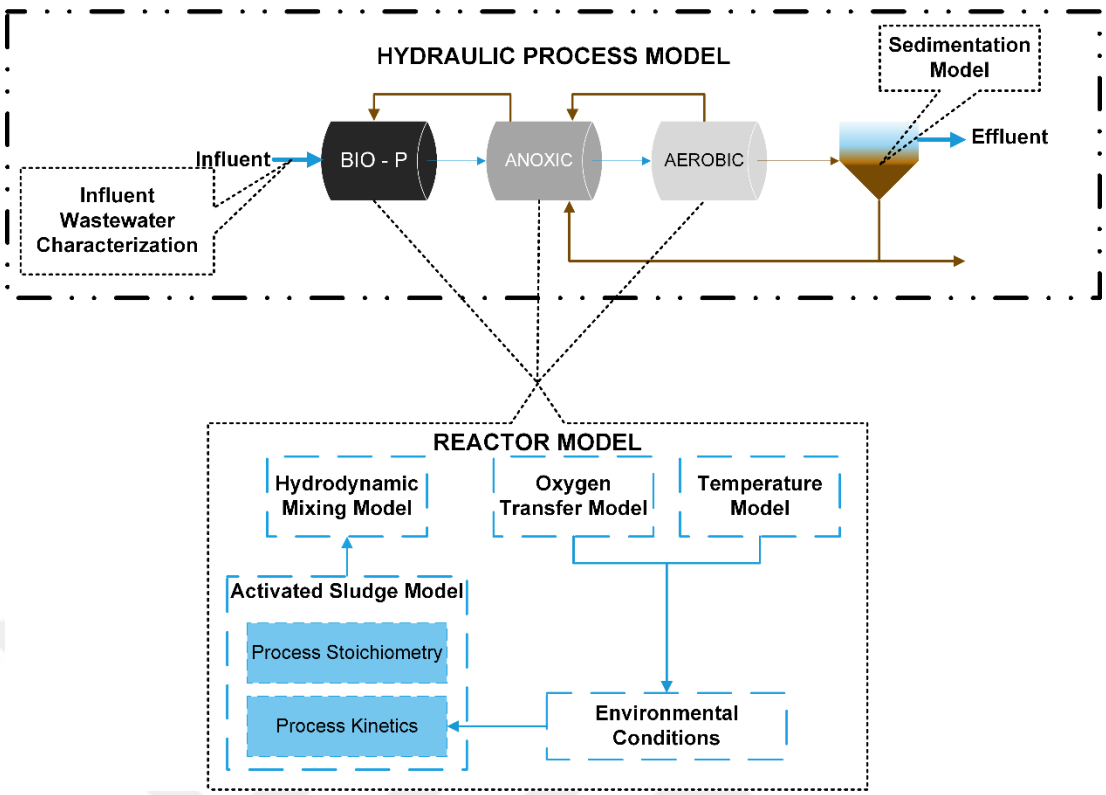

Figure 3.8 : Model components of wastewater treatment plant simulation.

3.5.1 AQUASIM

AQUASIM was firstly designed by Swiss Federal Institute for Environmental Science and Technology (EAWAG) in 1994. Then, AQUASIM Version 2.0 was released in 1998. AQUASIM is a universal simulation software designed specifically for the simulation and identification of aquatic systems. The software has the ability to introduce seven different variables and two types of processes. Additionally, six different types of reactor compartments can be defined to the systems to be simulated (Table 3.6). AQUASIM allows its users to represent the configuration of the system under investigation as a set of compartments that can be connected to each other. The software also enables sensitivity analysis, parameter estimation, and uncertainty analysis. It allows estimation and calibration of multi-state variables at once using a real-time data set as shown (Reichert, 1998). Main window of AQUASIM is given in Figure 3.9.

Table 3.6 : Processes, variables and compartments in AQUASIM (Reichert, 1998).

Variables	Processes	Compartments
State variables	Dynamic Processes	Mixed reactor compartment
Program variables	Equilibrium Processes	Biofilm reactor compartment
Constant variables		Advective-diffusive reactor compartment
Real list variables		Saturated soil column compartment
Variable list variables		River section compartment
Formula variables		Lake compartment
Probe variables		

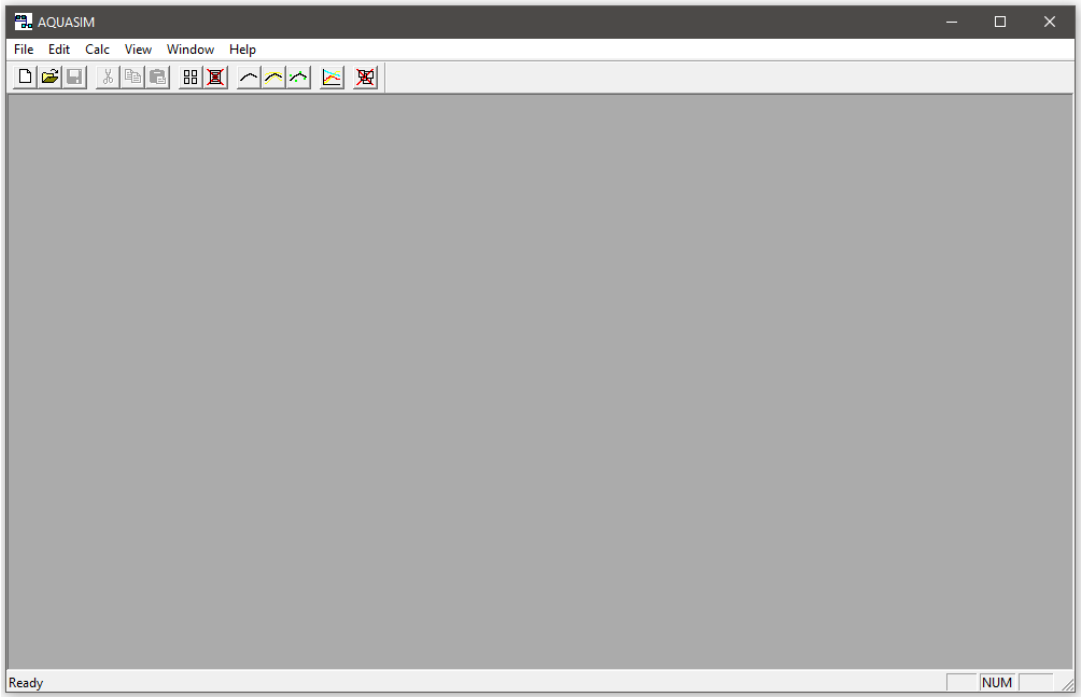

Figure 3.9 : Main window of AQUASIM.

3.5.2 Activated Sludge Simulation Program (ASIM)

ASIM, an acronym for Activated Sludge Simulation Program, stands as a sophisticated dynamic simulation software, meticulously designed for the modeling of biological wastewater treatment plants. This robust tool enables the detailed simulation of activated sludge systems, offering flexibility through the capability to model up to 10 distinct reactors in series. This feature is further enhanced by the inclusion of options for sludge return and internal recirculation lines, allowing for a comprehensive representation of the treatment process.

The software is adeptly equipped with a suite of built-in models, including the Activated Sludge Model No. 1 (ASM1), Activated Sludge Model No. 2 (ASM2), and an extended version of ASM2 that incorporates ferrous oxidation models. These models serve as the foundational frameworks within ASIM, enabling users to accurately simulate a wide range of biological and chemical processes occurring

within wastewater treatment systems. One of the hallmark features of ASIM is its incorporation of process control loops. These loops are instrumental in facilitating the simulation of varying load conditions, be it diurnal or seasonal, as well as accommodating fluctuations in temperature and operational parameters. This level of detail provides users with the ability to model and predict the performance of wastewater treatment plants under a diverse array of environmental conditions and operational strategies. Through its comprehensive modeling capabilities, ASIM empowers engineers and wastewater treatment professionals to explore, analyze, and optimize the design and operation of activated sludge systems. This contributes significantly to the advancement of wastewater treatment technologies, ensuring facilities are equipped to efficiently manage and treat wastewater in alignment with environmental regulations and sustainability goals. A diagram of the simulation environment of ASIM is provided in Figure 3.10.

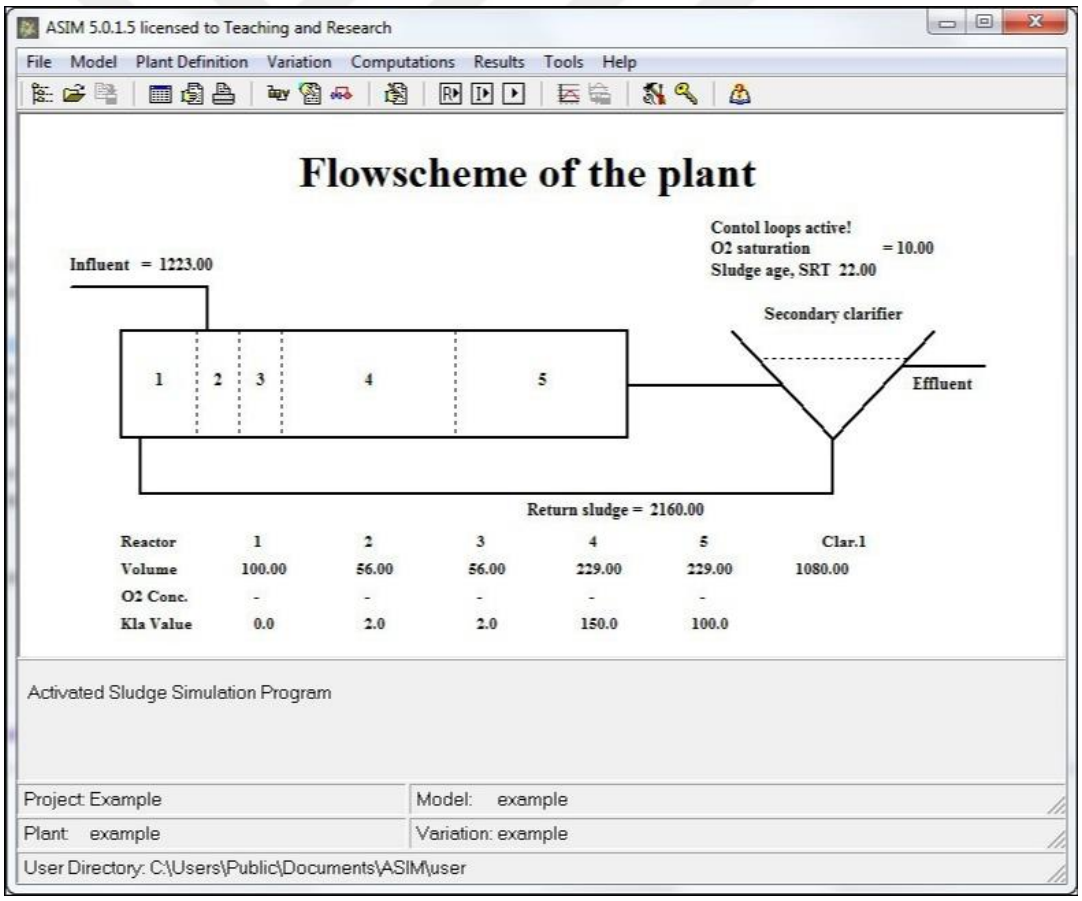

Figure 3.10 : Simulation environment of ASIM.

3.5.3 BioWin

BioWin stands as a leading-edge process simulator, meticulously engineered to facilitate the simulation of biological wastewater treatment systems. It offers users the unparalleled flexibility to connect various process units, creating an integrated model that mirrors the complexity of real-world wastewater treatment operations. Central to its functionality is the adoption of the Activated Sludge Model No. 1 (ASM1) extension, which incorporates the Enhanced Biological Phosphorus Removal (EBPR) process as proposed by the International Association on Water Quality (IAWQ). This inclusion ensures that BioWin aligns with globally recognized standards for modeling biological processes in wastewater treatment. The simulation of the settling process within BioWin is notably advanced, utilizing the double-exponential settling function introduced by Takacs et al. (1991). This mathematical model is pivotal for accurately predicting the sedimentation behavior of sludge, a critical aspect of the wastewater treatment process that influences overall system performance and efficiency.

BioWin provides users with the option to select between two comprehensive models: the "CNP" and "CN" models. The "CNP" model encompasses the simulation of carbon, nitrogen, and phosphorus removal processes, offering a holistic approach to modeling the nutrient removal capabilities of a treatment system. In contrast, the "CN" model focuses on the removal of carbon and nitrogen, catering to scenarios where phosphorus removal is not a primary concern. This flexibility allows users to tailor the simulation to reflect the specific operational goals and regulatory requirements of the wastewater treatment facility being modeled. By integrating these advanced modeling capabilities, BioWin empowers engineers and wastewater treatment professionals to conduct detailed analyses and optimization of biological treatment processes. The software’s intuitive design and comprehensive functionality make it an invaluable tool for enhancing the understanding and improvement of wastewater treatment systems, ultimately contributing to the development of more efficient, sustainable, and effective treatment solutions. User interface of BioWin is given in Figure 3.11.

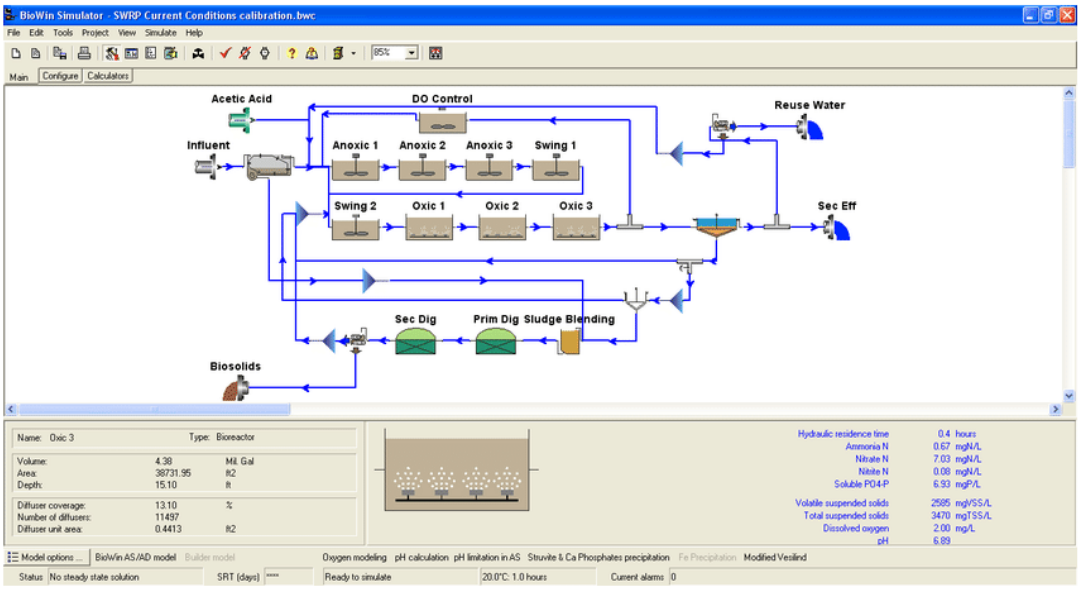

Figure 3.11 : Simulation environment of BioWin.

3.5.4 General Purpose Simulator-X (GPS-X)

GPS–X is the first commercially used dynamic process modeling software used for wastewater treatment plants developed by Hydromantis Inc., Hamilton. GPS-X emerges as a sophisticated software platform renowned for its advanced capabilities in modeling and optimizing wastewater treatment processes. Offering comprehensive simulation functionalities, GPS-X facilitates detailed analysis of treatment units including biological treatment, physical treatment, advanced treatment technologies, and sludge handling processes commonly found in wastewater treatment plants. The software has built-in biological model based on IAWPRC model (based on ASM1) and "noreac1d" model for settling processes. The software enables parameter optimization, sensitivity analysis, and Monte Carlo analysis. This provides a convenient way of adjusting model parameters based on nonlinear dynamic optimization. GPS-X also offers advanced tools for scenario modeling enabling users to assess the robustness of treatment processes under varying operating conditions and design configurations. Notable features include its advanced optimization capabilities, support for integration with third-party software, and specialized modules for modeling advanced treatment technologies such as membrane bioreactors (MBRs), sequencing batch reactors (SBRs), and fixed-film reactors, making it a versatile tool for wastewater treatment simulation. Using GPS–X "Advanced Tools" module, users are able to create Python scripts and integrate it into GPS–X to manipulate variables in the simulation. User interface of GPS–X is given in Figure 3.12.

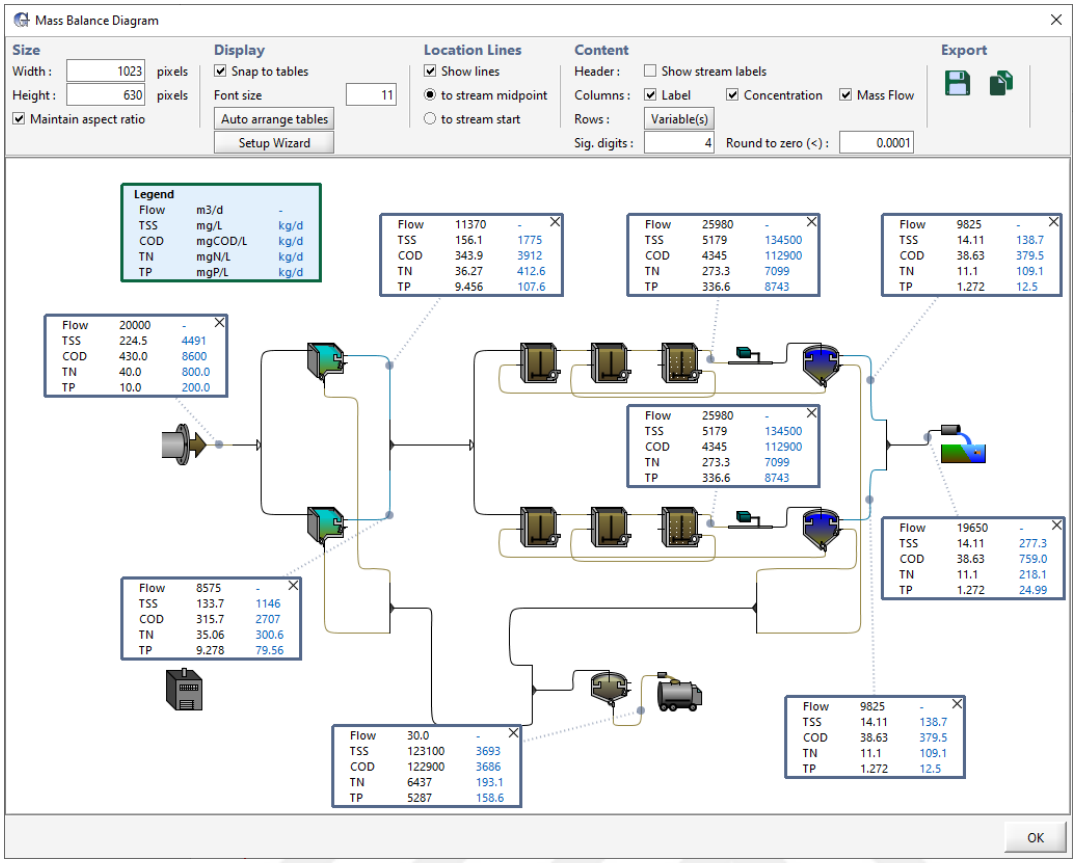

Figure 3.12 : Simulation environment of GPS–X.

3.5.5 SIMBA#

SIMBA is a simulation environment based on Matlab™ & Simulink™ firsly released in 1994. A wide range of processes in wastewater treatment (MBBR, FBBR, MABR, TF, Granular) as well as sludge treatment and anaerobic digestion processes can be modeled using SIMBA. The software is mostly compatible with DWA A131 2016 standard. Models and matrix can be freely edited or modified in SIMBA using the editor in Gujer Petersen matrix notation. The software already has 5 different built-in models as default options: ASM1, ASM3, ASM3 with biological P removal, extended ASM model (ASM_inCTRL) and extended ASM_XL_laf model with anammox option (as a result of the NoNitriNox Project). For settling processes, it has also four different options. User interface of SIMBA# is given in Figure 3.13. Noteworthy features include its advanced calibration and validation tools, support for scenario analysis and risk assessment functionalities, and specialized modules for modeling specific treatment processes mainly like enhanced biological phosphorus removal (EBPR), biological nitrogen removal (BNR), and integrated fixed-film activated sludge (IFAS) systems, making it a comprehensive tool for optimizing biological

processes in wastewater treatment plants. SIMBA's advanced capabilities extend to dynamic simulation, enabling users to model transient conditions, diurnal variations, and seasonal fluctuations in influent characteristics, and assess the resilience of treatment processes to changing operating conditions and external disturbances. Additionally, SIMBA offers advanced reporting and visualization tools, allowing users to communicate simulation results effectively, analyze trends in treatment plant performance, and identify opportunities for process optimization and resource recovery.

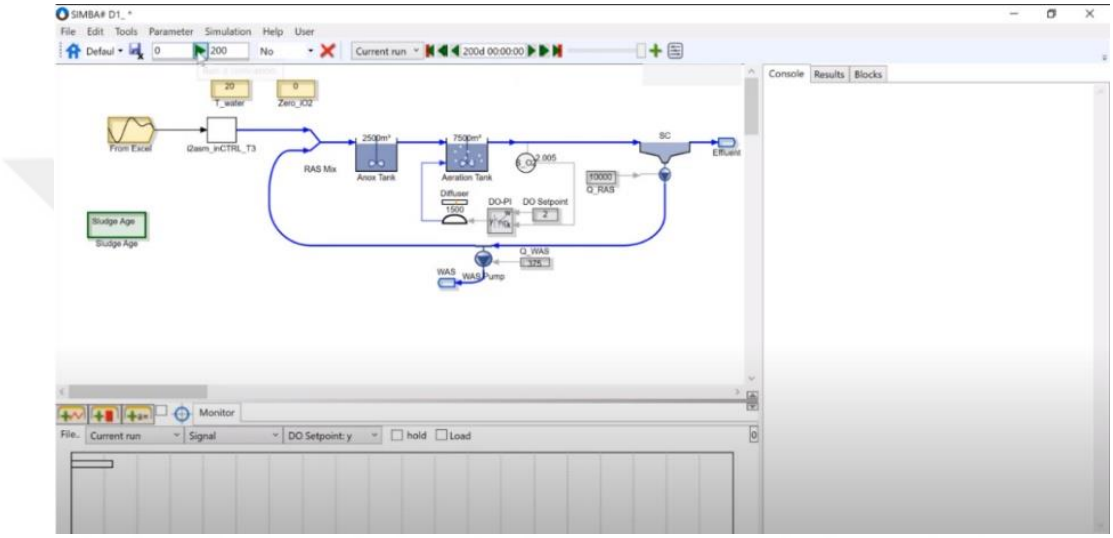

Figure 3.13 : Simulation environment of SIMBA#.

3.5.6 STOAT™

STOAT is a modular dynamic modeling software for the simulation of wastewater treatment systems. STOAT includes various compartments for different processes including mesophilic and thermophilic anaerobic sludge digestion and sludge incineration and heat exchangers. The software includes built-in IAWQ extension of ASM1 model called *IAWQ#1* and the double-exponential settling function proposed by Takacs et al. (1991), called *Generic*. STOAT is also compatible with other tools such as for the sewer system modeling (MOSQITO) and for river impact modeling (MIKE 11) to provide integrated modeling package. User interface of STOAT is given in Figure 3.14.

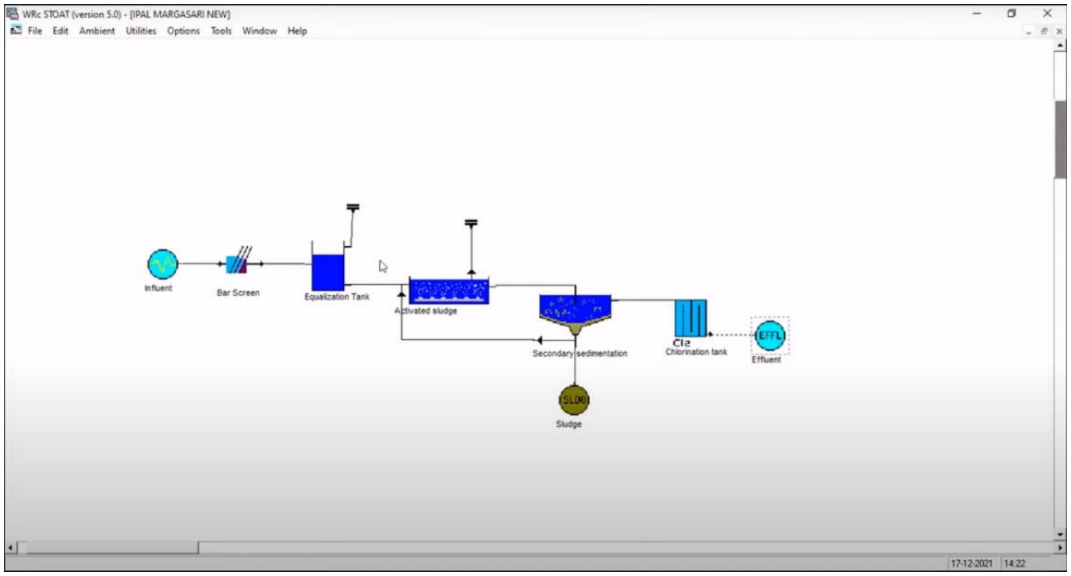

Figure 3.14 : Simulation environment of STOAT.

3.5.7 WEST

WEST is a simulation platform for dynamic modeling and simulation of aquatic systems including wastewater treatment plants, rivers, sewer systems and urban catchments. Control strategies can be implemented to the system by adding sensors and controller units to the layout without additional codes. New models can be implemented and/or existing models can be modified using model editor consisting of a code editor and graphical Gujer Petersen Matrix editor. WEST also allows the integration with SCADA system and data management systems on the real-scale WWTPs. The software includes tools for parameter estimation, scenario analysis, and uncertainty analysis, making it easy to adjust model parameters. The user interface for WEST is displayed in Figure 3.15.

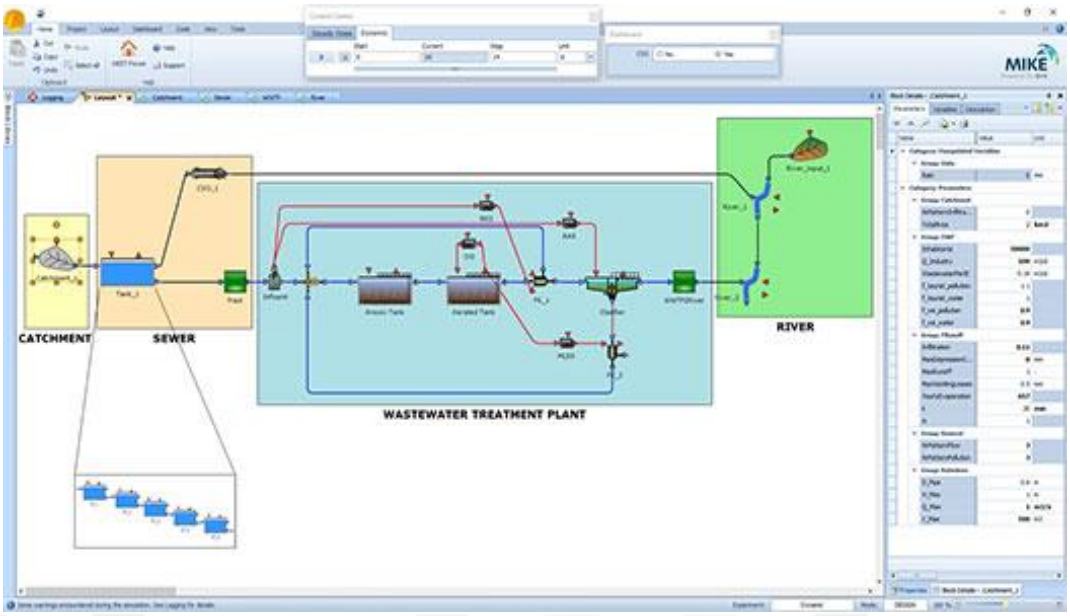

Figure 3.15 : User interface of WEST.

3.5.8 Super Model (SUMO®)

SUMO is a third-generation wastewater process simulation software released firstly in 2017 by Dynamita, France. SUMO allows users to simulate plant-wide dynamic model using built-in three different full plant models (Mini_Sumo, Sumo1, Sumo2), three focus models (Sumo2C, Sumo2S, Sumo4N) and museum models (ASM1, ASM2d, ASM2d_TUD, ASM3, ASM3_BioP, Barker-Dold). Biological processes including BOD removal, nitrogen and phosphorus removal, anaerobic digestion processes, photosynthesis and other biological conversions including flocculation, hydrolysis, ammonification, endogenous products conversion, anaerobic methanol conversion and assimilative reduction of nitrate/nitrite are implemented in all these models together with physico-chemical reactions with pH and alkalinity calculations and chemical removal of phosphorus and chemical precipitation. In Sumo22, carbon footprint calculations with database and reverse osmosis process units are also included to the plant-wide model (URL-1). User interface of SUMO is given in Figure 3.16.

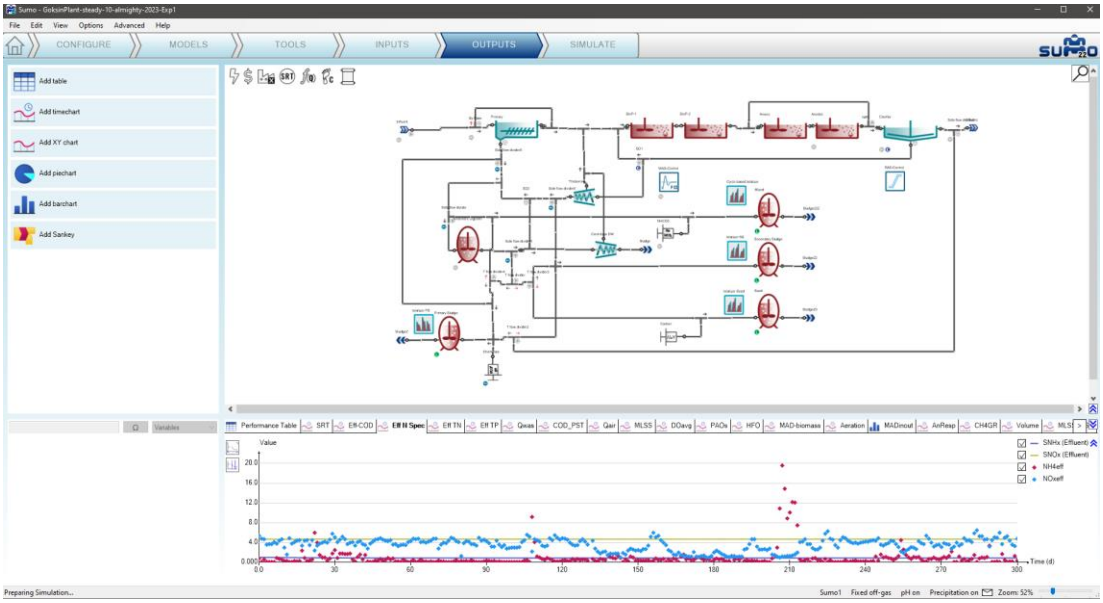

Figure 3.16 : User interface of SUMO.

Since it has open source plantwide code (MS Excel), users easily modify existing models and/or built their own model in plant-wide mode using the MS Excel template provided by the software itself (Figure 3.17). It is easy to add processes and kinetic conversions to the current model by modifying the Gujer kinetic matrix. In addition, new process units can be incorporated into these models. Currently, there are 107 state variables included in default models, and there are five symbols distinguish the types of state variables: soluble (S), particulate (X), colloidal (C), gaseous (G) and enthalpy (H). The list of state variables in the default models are given in Table A.1 (see Appendix A).

Additionally, SUMO integrates state-of-the-art algorithms for off-gas emission calculations, enabling users to assess greenhouse gas emissions and air quality impacts associated with wastewater treatment operations. Furthermore, SUMO's versatile platform allows for seamless integration with external tools and databases, facilitating data exchange and interoperability for comprehensive modeling and analysis. Its user-friendly interface, coupled with advanced visualization and reporting capabilities, empowers users to gain insights into treatment plant performance and make informed decisions for process optimization and environmental sustainability. SUMO also offers advanced features for dynamic control and optimization, including real-time data integration, model predictive control, and adaptive optimization algorithms, enabling users to implement optimal control strategies and respond to changing operating conditions effectively. Moreover, SUMO's extensive library of process units

and customizable modules enables users to model complex treatment processes with high fidelity, ensuring accurate representation and analysis of real-world treatment plant operations. Continuous research and development efforts, coupled with user feedback and industry collaboration, ensure that SUMO remains at the forefront of wastewater treatment simulation software, providing cutting-edge solutions to address the evolving challenges of the water industry. SUMO's advanced capabilities extend to scenario analysis, allowing users to evaluate the performance of different treatment strategies, assess the impact of regulatory changes, and explore innovative process configurations for enhanced sustainability and resilience in wastewater treatment operations. Additionally, SUMO's intuitive modeling environment and extensive documentation support users at all skill levels, facilitating knowledge transfer and skill development in wastewater treatment modeling and optimization.

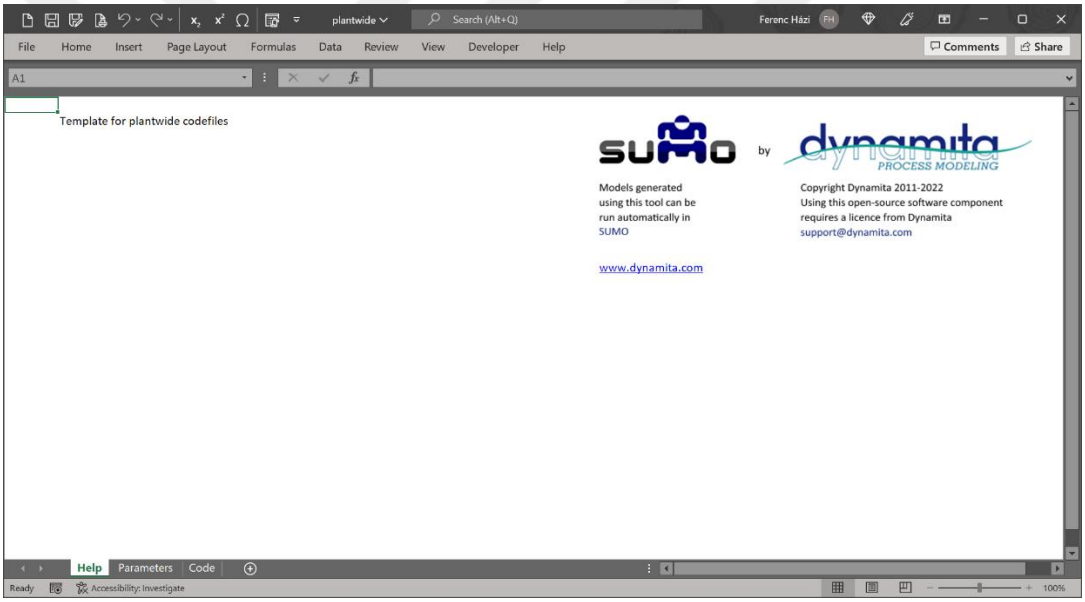

Figure 3.17 : MS Excel template of plant-wide code.

3.6 Anaerobic Sludge Digestion

Wastewater contains water which comprises of with both biodegradable and inert solids, alongside pathogenic organisms. The fundamental aim of a wastewater treatment plant is to efficiently extract these constituents from wastewater prior to its release into aquatic ecosystems. Through the treatment process, liquid effluents are purified and then reintroduced to the natural water cycle, while solid residues are segregated for subsequent treatment stages and eventual disposal.

During the comprehensive treatment phases—primary, secondary, and tertiary—a significant volume of sewage sludge emerges as a residual by-product. The specific quantity and properties of this sludge are influenced by a myriad of factors, including the initial characteristics of the incoming wastewater, the structural design and operational scheme of the treatment facility, and the particular sludge management strategies employed. It's noteworthy that, even within a singular plant, the profile of sludge generation may exhibit notable variability on a seasonal or daily basis. This variation is attributed to the substantial fluctuations in both the quality and volume of the influent wastewater.

Given that sewage sludge represents the predominant component extracted through the wastewater treatment process, the methodologies adopted for its management, treatment, and ultimate disposal are subjects of critical importance. The strategic handling of sewage sludge not only addresses environmental and public health concerns but also plays a vital role in the overall efficacy and sustainability of wastewater treatment operations. This necessitates ongoing assessment and optimization of sludge treatment and disposal practices, ensuring they are responsive to the changing dynamics of wastewater treatment and are aligned with environmental conservation goals.

The U.S. Environmental Protection Agency (EPA) defines sewage sludge as "*The solid, semisolid, or liquid residue generated during the treatment of domestic sewage in a treatment works. Sewage sludge includes, but is not limited to, domestic septage, scum, and solids removed during primary, secondary, or advanced wastewater treatment processes. The definition of sewage sludge also includes a material derived from sewage sludge (i.e., sewage sludge whose quality is changed either through further treatment or through mixing with other materials).*" in the regulation called "40 Code of Federal Regulations (CFR)", "Part 503 - A Guide for Land Appliers on the Requirements of the Federal Standards for the Use or Disposal of Sewage Sludge" (EPA, 1994). Primary sludge is formed by the settling of raw wastewater and mainly consist of particulate organic matter in the influent wastewater. Secondary sludge is produced during biological reactions in the system (e.g. conventional activated sludge systems or BNR).

To be able to protect human and environmental health, sludge stabilization is an essential step. Due to inherent characteristics of the raw sludge (high organic matter

content, pathogens, unpleasant odor, etc.), sludge stabilization aims primarily stabilizing the biodegradable fraction of organic matter, reducing the number of pathogens, minimizing unpleasant odors, and eliminating the potential for putrefaction. In sludge stabilization, achieved biological reduction of the volatile content and addition of different chemicals to the sludge determine the elimination and reduction of these nuisance conditions, and turn the sludge into an inappropriate environment for microorganisms to survive (Metcalf and Eddy, 2014).

Sludge stabilization methods can be classified into three categories: biological methods which include composting, and aerobic or anaerobic digestion, chemical methods (alkaline), and thermal methods such as autothermal thermophilic digestion. The use of these processes not only helps in reducing the volume of sludge but also generates renewable energy (methane) and enhances sludge dewaterability, besides improving health and aesthetic factors.

Bioreactor sludge is usually combined with primary sludge and can be subjected to various methods of treatment, with anaerobic digestion being the most widely used process.

Anaerobic digestion is a natural process that can convert almost all types of organic materials, as well as many synthetic compounds, into biogas. The biogas primarily consists of methane and carbon dioxide, and has gained significant attention worldwide due to its potential as a source of energy and its ability to mitigate greenhouse gas (GHG) effects. The production of methane through anaerobic digestion has become increasingly popular in recent years (Li et al., 2011; Lyberatos and Skiadas, 1999; Zhang et al., 2014). Non-renewable energy still has the highest percentage of energy supply and this contributes to environmental challenges due to high quantities of greenhouse gas emissions. This challenge could only be overcome by the usage of renewable energy sources which include solar energy, wind energy, hydropower, geothermal and biogas (Obileke et al., 2020).

Anaerobic digestion is a well-established technology used to stabilize sludge and convert organic waste into bioenergy. In the conventional AD process, a mixed sludge is broken down by microbes in the absence of molecular oxygen. Generally, the process of anaerobic digestion of complex organic materials to methane can be achieved through a sequence of four stages, as shown in Figure 3.18**.** These stages include hydrolysis, acidogenesis, acetogenesis, and methanogenesis (Appels et al.,

2008; Gavala et al., 2003). Biogas is composed of 50% to 75% CH_4, 25% to 45% CO_2, and trace amounts of N_2 (<2%), O_2 (<2%), H_2 (<1%), hydrogen sulfide, other gases, and water vapor (Tyagi and Lo, 2013).

The anaerobic digestion process of sludge provides numerous benefits. It produces methane gas which is a renewable energy source and can be used for electricity and/or heat generation. Additionally, it stabilizes organic matter that can be used as soil amendment, reduces sludge volume, decreases GHG emissions, reduces pathogens, decreases fossil fuel usage, and provides flexibility in waste composition.

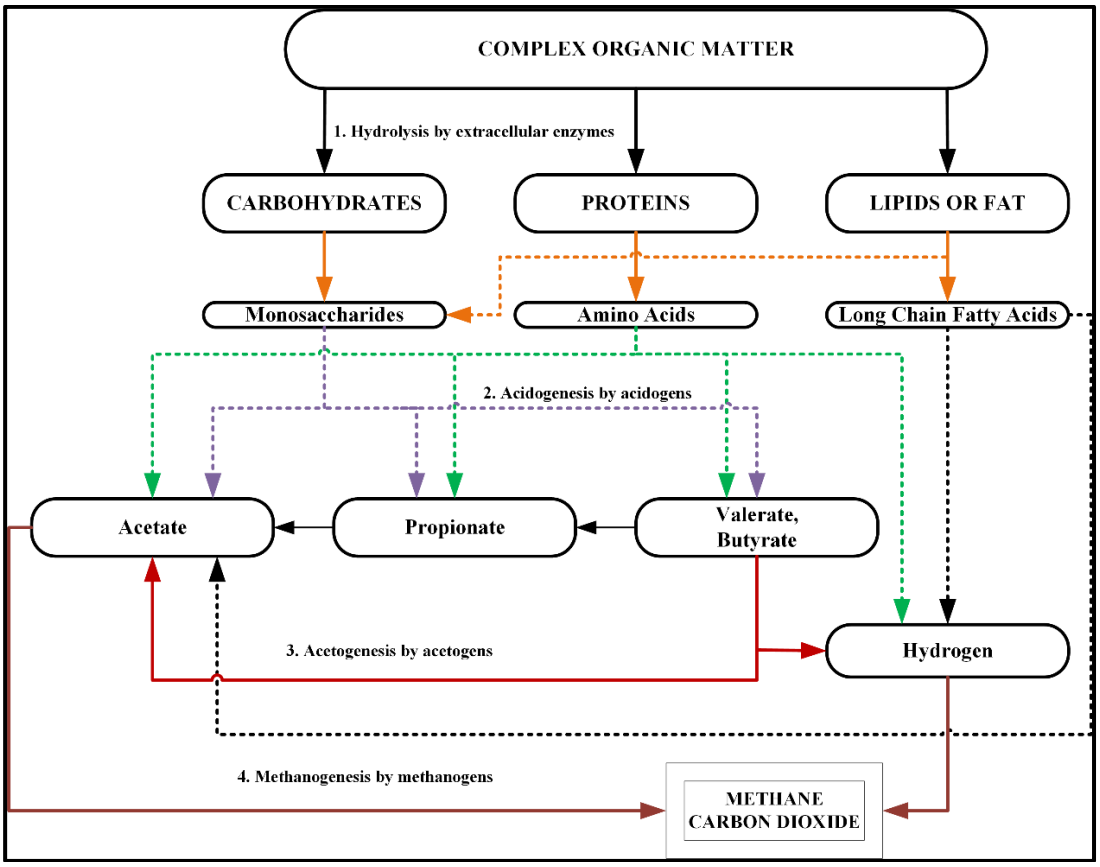

Figure 3.18 : Reaction steps in anaerobic digestion.

Anaerobic sludge digestion is a cost-effective and eco-friendly method used for sludge stabilization. It is considered a modern WWTP approach due to its above-mentioned advantages. The anaerobic digestion (AD) process, although beneficial, also has a few drawbacks. The challenges in anaerobic digestion systems include the necessity for long hydraulic retention times (HRT) because the methane-producing microorganisms have slower growth rates. Additionally, there are low biodegradation efficiencies, and the complex activated sludge floc structure has slower and limited degradability. There are also complex organic compounds that are either non-biodegradable or

biodegradable. The high capital costs arise due to the large reactor volume and longer start-up time needed for biomass development. Poor dewaterability, low supernatant quality, and potential odor production are other significant challenges.

3.6.1 Anaerobic metabolism

3.6.1.1 Hydrolysis

During the first step of the anaerobic metabolism, high molecular weight particulate and insoluble organic materials are transformed into soluble compounds. These compounds can then be further broken down into simple monomers, which are utilized by bacteria to perform fermentation. The complex organic material can be simplified into three categories: carbohydrates, lipids, and proteins. Carbohydrates are degraded into simple sugars, proteins are hydrolyzed into amino acids, and lipids are broken down into long chain fatty acids (LCFAs). These monomers can then penetrate the cell membranes of bacteria and be metabolized.

The three parallel hydrolysis processes are facilitated by extracellular enzymes produced by a variety of facultative and obligate anaerobes, also known as hydrolytic bacteria. These bacteria produce enzymes that are released into the liquid and then attached to the surface of soluble substances. In some cases, the process can also be carried out by enzymes from organisms that are directly attached to the insoluble substrate surface nearby.

3.6.1.2 Acidogenesis

Acidogenesis, commonly referred to as fermentation within the context of anaerobic digestion, is a critical biochemical process through which microorganisms break down hydrolyzed substrates in an oxygen-free environment. This step is characterized by the unique ability of the substrates to serve simultaneously as electron donors and acceptors, eliminating the requirement for external electron donors or acceptors. Through acidogenesis, the complex organic compounds that have been previously hydrolyzed are transformed into a suite of simpler molecules. The primary products of this transformation are short-chain VFAs, which include substances such as acetate, propionate, and butyrate.

In addition to VFAs, the acidogenic phase also results in the production of hydrogen (H_2), carbon dioxide (CO_2), ammonia (NH_3), and a spectrum of other minor by-

products. These compounds collectively represent the intermediate metabolites that are essential for the subsequent phases of anaerobic digestion, notably acetogenesis and methanogenesis. The production of these intermediates during acidogenesis plays a pivotal role in the overall efficiency and effectiveness of the anaerobic digestion process, facilitating the conversion of complex organic matter into valuable bioenergy carriers like methane in the later stages. This step is thus integral to the biological process of breaking down organic waste materials in the absence of oxygen, contributing to the sustainable generation of biogas and the recycling of organic waste.

3.6.1.3 Acetogenesis

Within the multifaceted stages of anaerobic digestion, acetogenesis stands as a pivotal phase where VFAs, which are the intermediary products derived from the preceding acidogenesis process, undergo further fermentation. This step is crucial for the synthesis of acetate, carbon dioxide (CO_2), and hydrogen (H_2), which serve as vital substrates for the subsequent production of methane by acetogenic bacteria. Additionally, LCFAs initially broken down during the hydrolysis phase, are further degraded into acetate, CO_2, and H_2 during acetogenesis. This results in the predominant generation of high levels of acetate and H_2, which are essential for the methanogenesis stage.

However, the successful conversion of propionate and butyrate into acetate and hydrogen hinges on maintaining a low hydrogen concentration within the system. Elevated levels of H_2 can inhibit this conversion process (McCarty and Smith, 1986). The presence of high hydrogen concentrations interferes with the thermodynamic feasibility of the reaction, thereby halting the conversion of propionate and butyrate into the necessary precursors for methane production. This underscores the importance of regulating hydrogen levels within the anaerobic digestion environment to ensure the efficient progression of acetogenesis and, by extension, the overall success of the biogas production process.

3.6.1.4 Metanogenesis

Methanogenesis represents the culminating phase in the anaerobic digestion process, driven by a specialized group of microorganisms known as methanogens. These *Archaea* are characterized by their strict obligate anaerobic nature, thriving only in environments devoid of oxygen. The primary role of methanogens within the

anaerobic digestion framework is the conversion of VFAs into methane (CH_4), a reaction that underscores the bioenergy potential of this biological process. However, the efficiency of methanogenesis is inherently moderated by the slow metabolic rates of methanogens, which, in turn, are attributed to their heightened sensitivity to fluctuations in environmental parameters.

The biodegradation of complex, slowly degradable substrates, such as the excess sludge typified by intricate microbial flocs, presents additional challenges within the anaerobic digestion sequence. In such contexts, the hydrolysis stage is identified as the rate-limiting step, by various researchers (Appels et al., 2008; Ariunbaatar et al., 2014; Droste, 1997; Elliott and Mahmood, 2007; Gavala et al., 2003; Metcalf and Eddy, 2014; Tyagi and Lo, 2011). This bottleneck occurs because the breakdown of complex organic matter into simpler compounds, which are then available for subsequent fermentation and acetogenesis phases, progresses at a significantly slower pace. The inherent complexity and recalcitrance of these substrates necessitate extended hydrolysis durations, thereby extending the overall timeline for methanogenesis and, consequently, methane production. These dynamic underscores the importance of optimizing the initial stages of anaerobic digestion, particularly hydrolysis, to enhance the efficiency and throughput of methane generation from complex organic wastes.

3.6.2 Process microbiology of anaerobic digestion

3.6.2.1 Fermentative bacteria

During the first stage of anaerobic digestion, fermentative bacteria is responsible for hydrolysis and acidogenesis processes. This process involves the anaerobic species belonging to the families Streptococcaceae and Enterobacteriaceae, and the genera of *Bacteroides, Bifidobacterium, Butyrivibrio, Clostridium, Eubacterium,* and *Lactobacillus*. *Bacillaceae, Enterobacteriaceae,* and *Lactobacillaceae* are all present in digesting sludge, with Bacillaceae being the most predominant (Novaes, 1986).

Acetovibrio, Bacteroides, Cellulomonas, Clostridium, Erwinia, Fibrobacter, Firmicutes, Prevotella, Ruminococcus, Succinivibrio, and *Microbispora* are some of the key bacteria involved in hydrolysis step, where the fermentative bacteria such as the *Clostridia*, ferment the hydrolyzed products of proteins, such as peptides and amino acids, to VFAs, CO_2, H_2, NH_4^+, and S^{2-} (Zhen et al., 2017).

Obligatory and facultative anaerobic bacteria such as *Bacteroides, Clostridium, Desulfovibrio, Desulfobacter, Eubacterium, Geobacter, Lactobacillus, Phodopseudomonas, Peptoccus,* and *Sarcina* are responsible for acidogenesis process (Zhen et al., 2017).

The diversity of substrates and the prevailing environmental conditions are critical in dictating the metabolic end products within microbial ecosystems. Among these factors, the concentration of hydrogen (H_2) plays a crucial role. Specifically, acetate, carbon dioxide (CO_2), and H_2 serve as the primary substrates for methanogens, with their metabolic conversion being thermodynamically viable only under conditions of low hydrogen partial pressure. Conversely, an elevated partial pressure of H_2 is associated with a shift in metabolic pathways, culminating in the production of propionate and additional organic acids (Novaes, 1986). This dynamic interplay between hydrogen partial pressure and substrate utilization underscores the intricate balance within microbial communities, significantly influencing their metabolic outputs and ecological roles.

In recent years, the paradigm of waste management has shifted towards a more sustainable and resource-efficient approach, underscored by an escalating interest in the valorization of waste streams. This burgeoning focus aims to extract value-added products from various waste materials, thereby transforming what was traditionally viewed as refuse into a trove of economically and environmentally beneficial resources. This interest is driven by the dual objectives of mitigating environmental impacts associated with waste disposal and creating new revenue streams through the recovery of valuable compounds. When organic matter is not completely broken down by fermentative bacteria, it leads to the formation of useful byproducts such as organic acids, solvents, nisin, hydrogen, and others. Lactic acid bacteria can produce lactic acid and nisin, while acidogenesis by fermentative bacteria, particularly the *Clostridia* genus, produces hydrogen (Khanal, 2008).

3.6.2.2 Hydrogen-producing acetogenic bacteria

This microbial consortium is responsible for the conversion of C3+ organic acids (such as propionate and butyrate), ethanol, and selected aromatic compounds (including benzoate) into acetate, hydrogen (H_2), and carbon dioxide (CO_2). This conversion process, however, faces thermodynamic challenges under anaerobic conditions,

particularly in the context of hydrogen-producing bacteria, where the anaerobic oxidation of these substrates is thermodynamically disadvantaged. The pivotal role of a symbiotic association between hydrogen-producing acetogenic bacteria and hydrogen-consuming methanogenic archea is thus emphasized (Hungate, 1967). Methanogenic archea expedite the consumption of hydrogen, thereby maintaining a low hydrogen partial pressure. This low pressure, in turn, cultivates an optimal environment for the acetogenic bacteria to degrade organic compounds into acetate, H_2, and CO_2 through a mechanism known as "interspecies hydrogen transfer."

For the thermodynamic favorability of propionic acid oxidation to acetate, it is essential that the hydrogen partial pressures are maintained below 10^{-4} atm. Similarly, for the oxidation processes of butyrate and ethanol to be favorable, hydrogen partial pressures should not exceed 10^{-3} atm and 1 atm, respectively (Pohland, 1992). Notably, in the anaerobic digestion of sewage sludge and other complex compounds or wastes, propionate oxidation is of significant importance, with up to 30% of electrons being associated with this process, highlighting its critical role in the microbial energy metabolism. The bulk of the hydrogen production is attributed to the oxidation of long-chain fatty acids and other intermediate volatile fatty acids to acetic acid, illustrating the complex interplay of microbial processes in energy conversion and substrate utilization.

Desulfovibrio, Moorella, Pelotomaculum, Syntrophobacter, Syntrophus, Syntrophomonas, and *Syntrophothermus* are mostly responsible for acetogenesis process (Zhen et al., 2017).

Propionic acid accumulation is worse under thermophilic conditions than under mesophilic conditions. It is equally important to optimize reactor configuration, nutrient supplement, characteristics of substrate, and microbial community for propionic acid metabolism.

3.6.2.3 Homoacetogens

Homoacetogenesis is a process that has gained a lot of attention lately because of its ability to produce acetate. Acetate is an essential precursor to methane generation. The bacteria responsible for homoacetogenesis can be either autotrophs or heterotrophs. Autotrophic homoacetogens use a mixture of hydrogen (H_2) and carbon dioxide (CO_2) as their carbon source for cell synthesis. Some homoacetogens can also utilize carbon

monoxide (CO) as a carbon source. On the other hand, heterotrophic homoacetogens use organic substrates, such as formate and methanol, as a carbon source to produce acetate as the end product. Two mesophilic homoacetogenic bacteria, *Acetobacterium woodii*, and *Clostridium aceticum* were isolated from sewage sludge (Khanal, 2008; Novaes, 1986). Homoacetogenic bacteria have high thermodynamic efficiency, which prevents the accumulation of H_2 and CO_2 during growth on multicarbon compounds (Khanal, 2008; Zeikus, 1981).

3.6.2.4 Methanogens

Microorganisms were previously classified primarily based on their physical properties. However, currently, classification is based on genetic characteristics known as phylogeny. This method considers an organism's evolutionary history. Methanogens were once classified as bacteria, but now they are classified as *Archaea* due to the presence of membrane lipids, the absence of basic cellular characteristics such as peptidoglycan, and distinctive ribosomal RNA. Methanogens are obligate anaerobes and are considered a rate-limiting species in anaerobic digestion. They are most commonly found in oxygen-free environments that are rich in organic matter such as swamps, marshes, ponds, lakes, and marine sediments.

There are two distinct groups of methanogenic microorganisms that are responsible for producing methane. The first group is aceticlastic or acetotrophic methanogens, which are responsible for splitting acetate into CH_4 and CO_2. The second group is H_2-utilizing or hydrogenotrophic methanogens (mainly *Methanobacterium* and *Methanoculleus*), which use H_2 as the electron donor and CO_2 as the electron acceptor for methane production. Hydrogenotrophic methanogens are responsible for methane production from H_2 and CO_2, while acetotrophic methanogens are responsible for the CH_4 and CO_2 generation from acetate. The most common aceticlastic methanogenic organisms are from the genera *Methanosarcina* and *Methanosaeta*. *Methanosarcina spp.* have a spherical shape and a doubling time of approximately 1.5 days, while *Methanosaeta spp.* have a rod-like or filamentous shape with a doubling time of around 4 days (Droste, 1997). As a result, *Methanosaeta spp.* require longer sludge retention times during anaerobic digestion process to thrive and become more prevalent.

3.6.3 Process fundamentals of anaerobic digestion

Although the efficiency and stability of anaerobic digestion process mostly depends on the feed sludge characteristics, AD process also related to environmental and operational conditions due to sensitivity of microbial population to these factors. The most important factors that could affect the performance of AD process are: 1) SRT, 2) temperature, 3) alkalinity, pH, VFAs and 4) ammonia

3.6.3.1 Sludge retention time (SRT)

One of the most operational condition for design of AD process is sludge retention time. Effective pathogen destruction and methane production due to removal of organic materials is directly related to design of AD with a proper sludge retention time. Peak loads of toxic substances and system failures can be avoided and process stability can be achieved with longer SRTs. Also, more homogeneous digester content can be provided with larger digester volumes (Parkin and Owen, 1986). Studies have reported the following remarks (Appels et al., 2008; Metcalf and Eddy, 2014):

1. SRTs shorter than 5 days is inadequate for proses stability due to increasing VFA concentrations resulted with washing out of methanogens from the system.
2. Between 5 to 8 days, relatively high VFA concentrations are obtained to be able to ensure complete breakdown of compounds such as lipids.
3. A SRT between 8 to 10 days is sufficient for process stability and low VFA concentration and degradation of lipids can be achieved.
4. SRTs greater than 10 days is also adequate for stabilizing the majority of organic matter degradation.
5. A SRT greater than 30 days is required for conversion of nearly all degradable solids.

3.6.3.2 Temperature

The kinetics of hydrolysis and methane generation in AD processes are significantly influenced by temperature, which directly impacts the population dynamics, metabolic rates, and growth kinetics of microorganisms within an anaerobic reactor. Methanogens, the Archaea responsible for methane production, exhibit a particularly high sensitivity to abrupt temperature fluctuations compared to other microbial

inhabitants of anaerobic digesters. Both the physical and chemical characteristics of the substances present in the reactor, as well as the rates of biochemical reactions, are subject to alterations by temperature variations.

Anaerobic digestion facilities are commonly operated within the mesophilic temperature range of 30 – 40°C, which is conducive to a stable microbial environment and efficient digestion processes. Alternatively, some digesters are designed for operation under thermophilic conditions, maintaining temperatures between 50–60°C. The adoption of thermophilic digestion has gained popularity due to its associated benefits, including accelerated digestion rates, enhanced methane yield, and more effective pathogen reduction (Lu et al., 2008; Metcalf and Eddy, 2014).

Despite these advantages, thermophilic digestion presents several challenges that must be carefully managed. These include the necessity for additional energy to maintain elevated temperatures, difficulties in the dewatering process, and a heightened vulnerability to toxic compounds owing to the lower microbial diversity characteristic of thermophilic environments. Furthermore, issues such as potential ammonia toxicity, diminished quality of the supernatant, and reduced operational stability underscore the complexities of managing thermophilic systems (Chen et al., 2008; Gianico et al., 2013; Lu et al., 2008; Parkin and Owen, 1986).

3.6.3.3 Alkalinity, pH, and volatile fatty acids (VFAs)

Monitoring digester stability and maintaining system equilibrium are critical for the effective operation of anaerobic digestion (AD) processes. To achieve this, the measurement of pH, alkalinity, and volatile fatty acid (VFA) concentration emerges as the paramount performance indicators. Despite the varied pH preferences among the microbial consortia engaged in AD, a significant majority demonstrate optimal growth at neutral pH levels. Specifically, methanogenic archaea thrive within a pH range of 6.6 to 8.0, whereas fermentative bacteria exhibit a broader pH tolerance, functioning effectively across a spectrum from pH 4.0 to 8.5 (Metcalf and Eddy, 2014; Rittmann and McCarty, 2001). It is also documented that pH values exceeding 8.3 or dropping below 6.1 significantly impair biogas production, underlining the critical role of pH regulation in optimizing AD performance (Arshad et al., 2011; Lay et al., 1997).

The presence of carbon dioxide (CO_2) in high concentrations (25–35%) within digesters, which leads to the consumption of alkalinity through the formation of

carbonic acid, further emphasizes the necessity for substantial alkalinity levels to stabilize pH near neutrality. As a guideline, total alkalinity, measured as equivalent calcium carbonate ($CaCO_3$), should ideally fall within the range of 2,000 to 5,000 mg/L in a well-functioning digester (Metcalf and Eddy, 2014). This requirement for high alkalinity underscores the intricate balance between microbial needs and chemical dynamics within the AD process, ensuring optimal operational conditions and maximizing biogas yield.

Increase in the volatile fatty acid concentration is directly affect the alkalinity. VFAs are intermediate products of acidogenesis stage in digestion process and consume alkalinity. Due to effects on biogas production, VFA concentration should be monitored as an operational parameter of the anaerobic digester. An unbalanced anaerobic digestion process in terms of VFA concentration affects the separation of the acid producer and consumer in kinetic processes, due to the build-up of VFAs. Typically, methane production kinetics for methanogens are slower than production kinetics for for volatile fatty acids. To establish adequate methanogenic population for stable digestion process, VFA concentration should be between 50 mg/L to 300 mg/L and pH should be higher than 7. However, due to unstable digester operation, VFA production rate may exceed the methanogenic VFA utilization rate. This leads an increase in VFA concentration and decrease in pH, based on the amount of alkalinity present (Metcalf and Eddy, 2014).

3.6.3.4 Ammonia

The pH stabilization in anaerobic digestion systems is critically dependent on the balance between the ammonia and bicarbonate systems (Angelidaki and Ahring, 1993). In AD process, it has been reported that ammonia nitrogen between 50–200 mg/L is beneficial for cell synthesis. However, excessive accumulation of free ammonia in the digester can be toxic and inhibit methanogenesis. Ammonia nitrogen is produced from degradation of nitrogenous matter, mainly proteins and urea, in anaerobic digestion process and can be present in two different forms as ammonium ion (NH_4^+) or dissolved ammonia gas (NH_3). These two forms have an equilibrium between each other, controlled by pH value (hydrogen ion concentration). Ammonia toxicity/inhibition is related with dissolved ammonia gas if the pH value is higher than 7.2 while ammonium ion concentration may become inhibitory at lower pH values

(equal or lower than 7.2). Dissolved ammonia gas concentration has an inhibitory effect at a much lower concentration than the ammonium ion (McCarty, 1964).

3.6.4 Modeling of anaerobic digestion of sludge

Anaerobic technology, historically utilized predominantly for sludge digestion and stabilization, has recently expanded its application to encompass the treatment of low-cost, varying-strength wastewaters, while concurrently facilitating energy recovery through the production of methane and hydrogen. This technological evolution marks a significant departure from the traditional reliance on empirical guidelines for the design, operation, and control of anaerobic processes. The advent of comprehensive anaerobic process models has been instrumental in this transformation, serving as a cornerstone for the rapid advancements in this field. These mathematical models have emerged as invaluable tools for the design, operation, control, and optimization of a wide array of anaerobic processes. By offering a quantifiable framework for understanding the complexities of anaerobic digestion, these models enable precise long-term performance forecasting and optimization, thereby enhancing the efficiency, reliability, and sustainability of anaerobic treatment systems.

There are various models available for anaerobic processes, ranging from simple kinetic models to more complicated structured models.

The anaerobic digestion of sludge represents a multifaceted process facilitated by various microbial consortia, capable of proceeding at two distinct thermal regimes: within the mesophilic (25–40°C) or thermophilic range (>45°C). Notably, the majority of treatment systems are engineered to function at or below mesophilic temperatures (de la Rubia et al., 2002; de Mes et al., 2003; McCarty, 1964; Metcalf and Eddy, 2014; Parkin and Owen, 1986).

Sewage sludge constitutes a heterogeneous mixture of components, predominantly particulate in nature, exhibiting varied biodegradability profiles and metabolic trajectories. Particulate complex organic substances, such as carbohydrates, lipids, and proteins, are impervious to direct microbial access due to their inability to cross the cellular membrane. The hydrolysis stage initiates the process, wherein these particulate organics are enzymatically degraded into smaller, soluble molecules; carbohydrates are broken down into sugars, lipids into LCFAs, and proteins into amino acids. These solubilized entities are then converted through acidogenesis into CO_2 and H_2.

Following this, the acetogenesis commences, during which LCFAs and alcohols are oxidized by proton-reducing acetogens to produce acetic acid and hydrogen. The culminating phase involves CH_4 production, where methanogenic acetoclastic bacteria and CO_2 reducing methanogens catalyze the conversion of acetic acid and the reduction of carbon dioxide with hydrogen, respectively.

The whole process is executed through the synergistic actions of four distinct microbial consortia: acidogens, acetogens, acetoclastic methanogens, and carbon dioxide reducing bacteria. A pivotal factor influencing the efficiency of this process is the disequilibrium in the kinetic behaviors of the various bacterial groups involved.

Hydrolysis process is slow and its rate depends on the nature of the particulate matter involved. This can cause a decrease in the overall process kinetics, resulting in considerable delays during the initial start-up phase. (de Mes et al., 2003; Eastman and Ferguson, 1981; Gujer and Zehnder, 1983; Li and Noike, 1987; Metcalf and Eddy, 2014). The speed of acidogenesis is much faster than methanogenesis, meaning that any disturbance that reduces methanogenic activity can negatively impact the process efficiency. This issue is worsened by methanogenic archea's high sensitivity to environmental conditions.

3.6.4.1 Simple component models

Hydrolysis limiting step models

These models detailing the anaerobic digestion of sludge adopt a simplified method for characterizing the substrate. These models treat the sludge matrix, without distinguishing among the different components. Additionally, these models define the process kinetics based on the limiting or controlling step, which is the slowest process in the sequence. This slowest stage can lead to failure of process under critical conditions.

Earlier studies conducted by Gossett and Belser (1982) as well as Pavlostathis (1985) revealed that methanogenesis does not consistently serve as the predominant rate-limiting stage in anaerobic sludge digestion, contrary to its typical portrayal in models of the anaerobic degradation process. The degradation of this complex matrix involves transforming the viable fraction of the sludge into substrates that anaerobic microorganisms can use, accomplished by processes such as cell lysis and/or hydrolysis. This initial phase is typified by slow rates and is deemed limiting step in

simplistic models. Additionally, the hydrolytic conversion of complex organic compounds into soluble substrates, essential for acidogenic bacteria, significantly influences the availability of substrates for methanogenic microorganisms, given that the kinetic rates of acidogenesis surpass methanogenesis by an order of magnitude.

Eastman & Ferguson model

The Eastman & Ferguson model involves a continuous stirred tank reactor (CSTR) that treats primary sewage sludge. The acidogenic phase comprises two stages - hydrolysis and fermentation. During the hydrolysis stage, biodegradable solids break down into smaller soluble molecules. In the second fermentation stage, acid-forming bacteria convert these soluble intermediates into fermentation products. The model posits that cell decay adds to the accumulation of fermentation products and assumes that the levels of oxygen, nitrate, and sulfate are minimal. Additionally, the only electron acceptors in the system are organics and CO_2. The metabolic pathway in this model is depicted in Figure 3.19 (Eastman and Ferguson, 1981).

The kinetics of hydrolysis concerning particulate biodegradable chemical oxygen demand (COD), denoted as F, is posited to adhere to a first-order kinetic model under conditions of unvarying pH and temperature. This model stands as the most rudimentary empirical formulation capable of encapsulating the aggregate effects emanating from the intricate biological activities transpiring within an anaerobic digestion environment. Consequently, it is frequently employed in the characterization of anaerobic systems processing heterogeneous substrates, such as sewage sludge. Herein, F symbolizes the non-viable or non-living fraction of the suspended solid phase, whereas the microbial entities growing on the soluble substrate generated through hydrolysis are designated as biomass (X). The growth kinetics of the biomass are delineated by Monod kinetics, and the endogenous decay is represented through a 1^{st} order kinetic model in relation to the concentration of active biomass. Along with biomass, the digestion process yields fermentation products (P), encompassing both soluble and gaseous constituents. Eastman & Ferguson model matrix and list of symbols and default values can be found in Table 3.7 and Table 3.8, respectively.

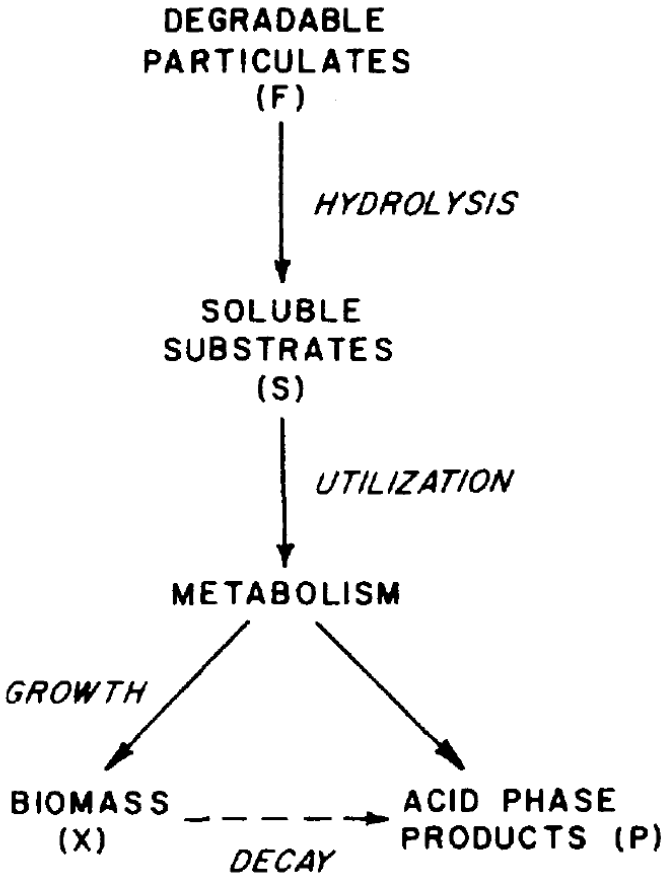

Figure 3.19 : Schematic diagram of model proposed by Eastman & Ferguson (Eastman and Ferguson, 1981).

Table 3.7 : Eastman & Ferguson model matrix (Eastman and Ferguson, 1981).

Component, i → / Process, j ↓	1 *F*	2 *S*	3 *P*	4 *X*	Rate g COD L^{-1} h^{-1}
Hydrolysis of particulate COD	*-1*	*1*			$k_h \cdot F$
Substrate utilization		*-1*	*1-Y*	*Y*	$\frac{1}{Y} \cdot \frac{\hat{\mu} S X}{K_S + S}$
Cell decay			*1*	*-1*	$k_d \cdot X$

Table 3.8 : List of symbols and default values of Eastman & Ferguson model (Eastman and Ferguson, 1981).

Symbol	Definition	Value pH=5.15 T=35°C	Units
k_h	Hydrolysis constant	3	h^{-1}
$\hat{\mu}$	Maximum specific growth rate		h^{-1}
K_S	Saturation constant		g COD/L
Y	Growth yield coefficient	0.48	g COD/g COD
k_d	Decay coefficient	0.018	h^{-1}
F	Particulate degradable substrate in the influent		g COD/L
S	Soluble degradable substrate in the influent		g COD/L
X	Active biomass concentration in the influent		g COD/L

Pavlostathis & Gosset model

According to the model proposed by Pavlostathis and Gossett (1986), biologically generated sludge is considered as the standard substrate for anaerobic sludge digestion. The study found that there are two potential limiting processes for the biomass retention times used in this process: death or lysis of cell and hydrolysis process. The authors' research showed that non-hydrolyzed proteins constituted about 80% of the biodegradable COD in the digester's effluent, indicating that hydrolysis or other preliminary conversion mechanisms are critical for the process sequence. Figure 3.20 depicts a diagram illustrating the proposed conversion process by Pavlostathis & Gossett model.

The sludge composition model elucidated herein provides a more comprehensive delineation than the framework previously expounded by Eastman & Ferguson. As mentioned by Gossett and Belser (1982), the biodegradable fraction of the activated sludge is predominantly constituted by the biodegradable fraction of viable microorganisms. This fraction is divided into two BOD subcategory; soluble and particulate. After the decay of these organisms, cellular lysis occurs, liberating intracellular soluble BOD, characterized by its low molecular weight components. After that, the residual intracellular soluble BOD from decayed cells undergoes modification via intracellular hydrolysis processes—facilitated by still partially active intracellular enzymes—thereby converting intracellular particulate BOD into soluble BOD, accompanied by the extracellular diffusion of these soluble entities. Concurrently, the particulate BOD of dead cells is diminished through extracellular hydrolysis, instigated by the active biomass within the digester. The culmination of these mechanisms results in the release of soluble BOD into the bulk phase, where it is assimilated by acidogenic bacteria. This model now integrates the conventional two phase pathway of anaerobic digestion, comprising acidogenesis and methanogenesis.

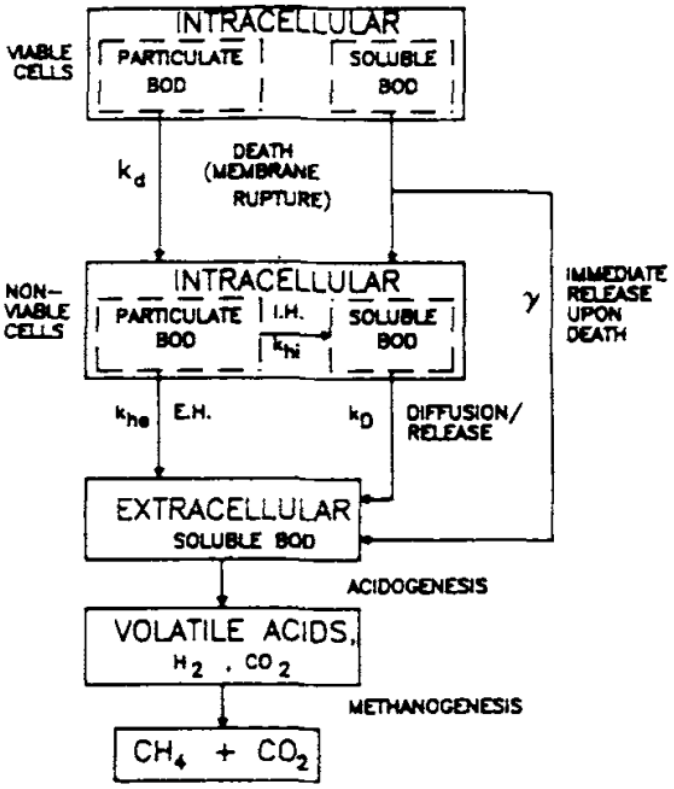

Figure 3.20 : Conceptual model of Pavlostathis & Gosset model (Pavlostathis and Gosset, 1986).

However, this model is quite complex due to the large number of parameters that need to be evaluated. Additionally, there is a lack of reliable methods for evaluating these parameters, so some simplification is necessary for their practical implementation. Although death and lysis are technically different in final products, evaluating and distinguishing their characteristic parameters is challenging. The authors attempted to measure cell lysis rate but were unsuccessful. Therefore, it is best to combine the two processes into a single process as death/lysis for modeling purposes. This model simplifies the process of death and lysis, assuming that there is no delay between them and that the soluble substrate is released into the bulk phase immediately after cell membrane rupture.The simplified model assumes that the entire pool of intracellular substrate (γ) is released by the death/lysis process and then solubilized by hydrolysis. The model also assumes that the biodegradable fraction (f_d) is the same in both the activated sludge to be digested and the anaerobic biomass.. Figure 3.21 shows the schematics of the simplified model. γ is the fraction of cell BOD released as soluble BOD upon cell death/lysis, k_h is the hydrolysis rate coefficient whereas k_d is the death/lysis rate coefficient. Matrix representation of Pavlostathis & Gosset model can be found in Table 3.9.

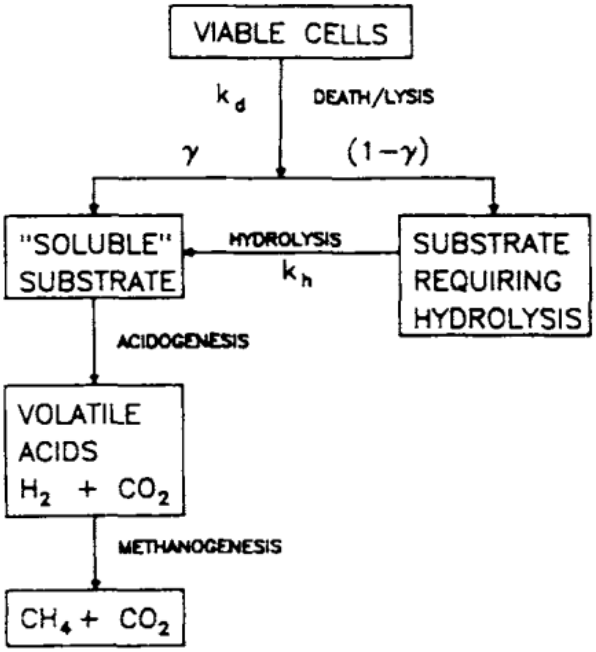

Figure 3.21 : Schematics of simplified Pavlostathis & Gosset model (Pavlostathis and Gosset, 1986).

Table 3.9 : Matrix representation of Pavlostathis & Gosset model (Pavlostathis and Gosset, 1986).

Component, i → / Process, j ↓	1 F	2 S^A	3 S^B	4 X_a^{AS}	5 X_a^A	6 X_a^B	7 CH_4	Rate g COD L^{-1} h^{-1}
Cell death/lysis	$(1-\gamma) f_d$	γf_d		-1				$k_d \cdot X_a^{AS}$
Particulate hydrolysis	-1	1						$k_h \cdot F$
Soluble substrate utilization in the acidogenic phase		-1	$1-Y^A$		Y^A			$\frac{k^A S^A X_a^A}{K_S^A + S^A}$
Soluble substrate utilization in the methanogenic phase			-1			Y^B	$1- Y^B$	$\frac{k^B S^B X_a^B}{K_C^B + S^B}$
Decay of acidogenic active biomass								$B^A \cdot X_a^A$
Decay of methanogenic active biomass								$b^B \cdot X_a^B$

Default values of kinetic and stoichiometric parameters listed in Table 3.10 and the symbols list of the variables can be found in Table 3.11 proposed by Pavlostathis and Gosset (1986).

Table 3.10 : List of symbols and default values of kinetic and stoichiometric parameters of Pavlostathis & Gossett model (Pavlostathis and Gosset, 1986).

Symbol	Definition	Value	Units
f_d	Net biodegradable fraction of active biomass	0.73	g COD/g COD
γ	Fraction of cell COD released as soluble fraction upon cell death/lysis	0.3	g COD/g COD
k_d	Cell decay constant	2	day^{-1}
k_h	Hydrolysis constant	0.15	day^{-1}
b^A	Decay coefficient for acidogens	0.1	day^{-1}
Y^A	Yield coefficient for acidogens	0.2	g $COD_{biomass}$/g $COD_{utilized}$
k^A	Maximum specific substrate utilization rate for acidogens	8	g $COD_{utilized}$/g $COD_{biomass}$/day
K_S^A	Semi-saturation constant for acidogenesis	0.045	g COD/L
b^B	Decay coefficient for methanogens	0.015	day^{-1}
Y^B	Yield coefficient for methanogens	0.057	g $COD_{biomass}$/g $COD_{utilized}$
k^B	Maximum specific substrate utilization rate for methanogens	6.2	g $COD_{utilized}$/g $COD_{biomass}$/day
K_C^B	Semi-saturation constant for methanogenesis	0.045	g COD/L

Table 3.11 : List of symbols and definitions of composition variables in Pavlostathis & Gossett model (in the unit of g COD/L) (Pavlostathis and Gosset, 1986).

Symbol	Definition
F	Degradable particulate (non-viable) COD concentration
S^A	Soluble substrate concentration degradable in the acidogenic phase
S^B	Volatile acid concentration
X_a^{AS}	Viable AS biomass
X_a^A	Active acidogenic microorganism concentration
X_a^B	Active methanogenic microorganism concentration

3.6.4.2 Advanced component models

Angelidaki et al. model

The dynamic model developed by Angelidaki et al. stands as a seminal contribution, underpinned by extensive experimental validation, and is pivotal for the simulation of co-digestion processes involving a variety of waste types in conjunction with sewage sludge. This model delineates substrates on the basis of their analytical composition, primarily categorizing organic wastes into lipids, carbohydrates, and proteins. The composition of substrates is carefully assessed, focusing on both primary organic components and inorganic constituents, including ammonia, phosphate, cations, and anions, alongside their biodegradation intermediates such as volatile fatty acids (VFAs).

Figure 3.22 serves as a graphical illustration of the metabolic pathways integral to the model, showcasing a series of biodegradation steps. Initially, the model depicts the hydrolysis of carbohydrates (designated as step A) followed by the hydrolysis of insoluble proteins (designated as step B). Subsequently, it outlines a suite of eight

biological conversions, each facilitated by distinct microbial groups. These groups are integral to the model's comprehensive representation of biodegradation dynamics, including glucose-fermenting acidogens, lipolytic bacteria, and long-chain fatty acid (LCFA)-degrading acetogens. Additionally, the model accounts for amino acid-degrading acidogens, propionate-degrading acetogens, butyrate-degrading acetogens, valerate-degrading acetogens, and acetoclastic methanogens. Collectively, these elements underscore the model's robustness in simulating the intricate processes underlying the co-digestion of diverse waste streams (Angelidaki et al., 1999).

In the model proposed by Angelidaki et al., carbohydrates are classified into three distinct categories: soluble, insoluble, and inert fractions. The model articulates that the insoluble fraction of carbohydrates is subjected to enzymatic hydrolysis, a process through which soluble carbohydrates are generated. These soluble carbohydrates are then metabolized by acidogenic bacteria, resulting in the formation of VFAs (Angelidaki et al., 1999).

Lipids within the model are exemplified by glycerol trioleate (GTO), which undergoes metabolism by a specialized subset of acidogenic bacteria. This metabolic process converts GTO into glycerol and LCFAs. Subsequently, glycerol is transformed into propionate through a biochemical reaction that, although not kinetically limiting, is not explicitly represented in the model's systematic delineation and is subsumed under the hydrolysis of GTO. Notably, LCFAs are characterized by their inhibitory effects across all stages of the process, culminating in their degradation by acidogenic microorganisms into acetate and hydrogen (Angelidaki et al., 1999).

Proteins within the model are analogized to gelatin, which is considered to contain both soluble and inert fractions. The model hypothesizes that the insoluble proteinaceous materials undergo hydrolysis, yielding amino acids. These amino acids are then converted through subsequent stages of degradation into acetate, propionate, butyrate, and valerate, reflecting the model's comprehensive approach to simulating the biodegradation of complex organic substrates (Angelidaki et al., 1999).

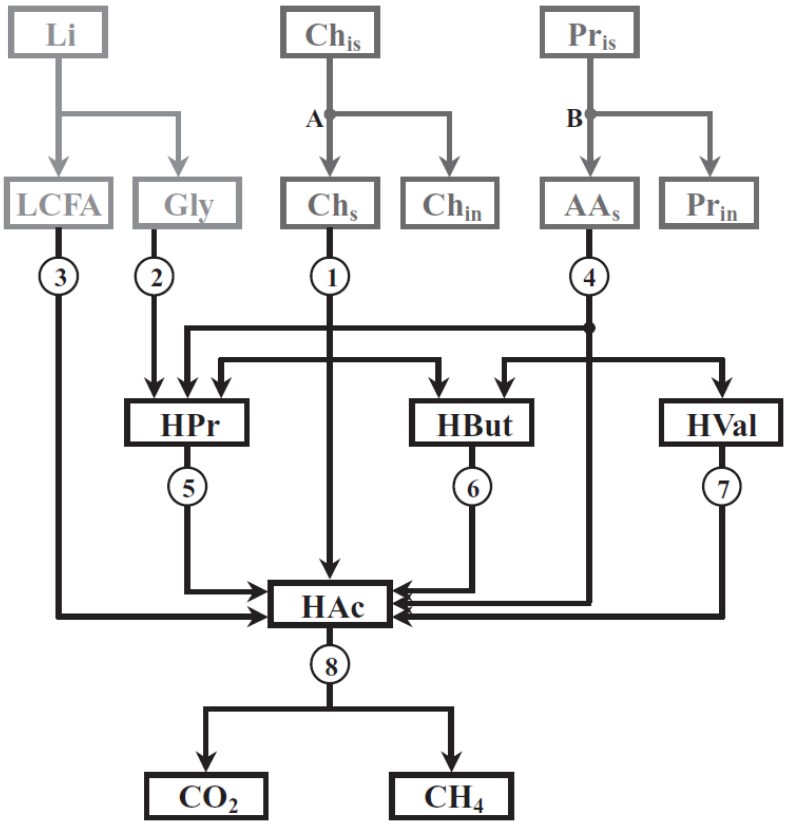

Figure 3.22 : Schematics of Angelidaki et al. model (1999).

In Angelidaki et al. model, the hydrolysis phase is depicted through the employment of a first-order kinetic equation. This assumption is substantiated by prior empirical inquiries, which assert the superiority of this kinetic model in encapsulating the intricate chemical and biological interactions inherent in the system (Noike et al., 1985; Pavlostathis and Gossett, 1986; Pavlostathis et al., 1988). Furthermore, the decay of biomass is similarly delineated using a simplistic first-order formula, whereby the resultant decay constituents; namely carbohydrates and proteins, are reintegrated as substrates for acidogenic organisms. The entirety of the biological phenomena within this framework is kinetically characterized via Monod kinetics, incorporating a limiting adjunct for ammonia nitrogen, serving as a nutrient (or cosubstrate) for the biomass growth. Moreover, terms accounting for non-competitive inhibition by LCFAs are integrated for all bacterial stages barring the acetogenic phase, which is described by Haldane inhibition model. Inhibition of LCFA fermentation by acetate is acknowledged, alongside the inhibition of the hydrolytic phase by VFAs. The model also includes Haldane inhibition by free ammonia for the acetoclastic phase. Conclusively, the model accommodates the influence of pH and temperature on the kinetics of the process.

Table 3.12 enumerates the proposed kinetic parameters, while the list of symbols representing the kinetic parameters and composition variables is outlined in Table 3.13. Table 3.14 displays the rate equations of Angelidaki et al (1999) model in matrix form.

Table 3.12 : Processes and kinetics proposed by Angelidaki et al. (1999).

Parameter, i → / Process, j ↓	k_0 d^{-1}	μ_{max} d^{-1}	K_S g/L	$K_{S,NH3}$ g/L	$K_{I,VFA}$ g/L	$K_{I,HAc}$ g/L	$K_{I,NH3}$ g/L	$K_{I,LCFA}$ g/L	pH_1 -	pK_h -	k_{dec} d^{-1}
A		1	-		0.33				-	-	-
B		1	-		0.33				-	-	-
1		5.1	0.5	0.05				5.0	-	-	-
2		0.53	0.01	0.05				5.0			
3		0.55	0.02	0.05				5.0			
4		6.38		-				-			
5		0.49	0.259	0.05		0.96		5.0	6.0	8.5	
6		0.67	0.176	0.05		0.72		5.0	6.0	8.5	
7		0.69	0.175	0.05		0.4		5.0			
8		0.60	0.120	0.05			0.26	5.0	6.0	8.5	
9											0.24

Table 3.13: List of symbols and definitions of kinetic parameters and variables for Angelidaki et al. (1999) model.

Symbol	Definition	Units
k_0	Non inhibited hydrolysis rate	day^{-1}
K	Inhibited hydrolysis rate	day^{-1}
k_{dec}	Cell decay rate	day^{-1}
$\mu_{max(T)}$	Maximum growth rate	day^{-1}
K_S	Half saturation constant	g/L
$K_{S,NH3}$	Half saturation constant for the total ammonia	g/L
$K_{I,i}$	Inhibition constant for the substrate	g/L
I_i	Substrate inhibition function	g/L
$Ch_{is/in/s}$	Carbohydrates insoluble/soluble/inert	g/L
$Pr_{is/in}$	Proteins insoluble/inert	g/L
Li	Lipids	g/L
AA_s	Soluble amino acids	g/L
Gly	Glycerol	g/L
X	Biomass	g/L
[VFA]	Total volatile fatty acids	g/L
[GTO]	Glycerol trioleate (lipids)	g/L
$[C_6H_{10}O_5]$	Glucose (carbohydrates)	g/L
[AA]	Amino acids	g/L
[LCFA]	Long chain fatty acids	g/L
[HAc]	Acetic acid	g/L
[HPr]	Propionic acid	g/L
[HBu]	Butyric acid	g/L
[HVa]	Valeric acid	g/L
$[T\text{-}NH_3]$	Total ammonia	g/L
$[NH_3]$	Free ammonia	g/L
pH	$-\log[H^+]$	
pK_1	Lower pH limit for 50% microorganism inhibition	
pK_h	Higher pH limit for 50% microorganism inhibition	

Table 3.14 : Angelidaki et al. (1999) model matrix.

Component, i → / Process, j ↓	1 Ch_{is}	2 Ch_{in}	3 Ch_s	4 Li	5 $LCFA$	6 Pr_{is}	7 Pr_{in}	8 AA	9 NH_3-N	10 Ac	11 Pr	12 Bu	13 Va	14 CH_4	15 CO_2	16 H_2S	17 X	Process Rate kg COD·m^{-3}d^{-1}
A. Carbohydrate enzymatic hydrolysis	*-1*	*0.5*	*0.5*															$k_0 \cdot I_{VFA-T} \cdot Ch_{is}$
B. Protein enzymatic hydrolysis						*-1*	*0.2*	*0.8*										$k_0 \cdot I_{VFA-T} \cdot Pr_{is}$
1. Carbohydrate acidogenesis			*-12.86*						*-0.124*	*3.543*	*2.937*	*3.079*			*2.413*		*1*	$\mu_{max(T)} \cdot \left(\frac{(C_5H_{10}O_5)_S}{(C_5H_{10}O_5)_S + K_S}\right) \cdot I_{NH3-T} \cdot I_{LCFA} \cdot I_{pH}$
2. Lipolysis				*-192.16*	*183.90*				*-0.124*		*15.151*				*-0.278*		*1*	$\mu_{max(T)} \cdot \left(\frac{GTO}{GTO + K_S}\right) \cdot I_{NH3-T} \cdot I_{LCFA} \cdot I_{pH}$
3. LCFA acetogenesis					*-9.387*				*-0.124*	*18.208*				*1.905*	*-6.267*		*1*	$\mu_{max(T)} \cdot I^*_{LCFA} \cdot I_{NH3-T} \cdot I_{pH}$
4. Amino acid acidogenesis								*-14.493*	*2.061*	*9.282*	*1.178*	*1.045*	*0.705*		*1.723*	*0.018*	*1*	$\mu_{max(T)} \cdot \left(\frac{AA}{AA + K_S}\right) \cdot I_{NH3-T} \cdot I_{LCFA} \cdot I_{pH}$
5. Propionate acetogenesis									*-0.124*	*8.006*	*-10.57*			*1.509*	*1.01*		*1*	$\mu_{max(T)} \cdot \left(\frac{HPr}{HPr + K_S}\right) \cdot I_{NH3-T} \cdot I_{LCFA} \cdot I_{HAc} \cdot I_{pH}$
6. Butyrate acetogenesis									*-0.124*	*15.366*		*-11.92*		*0.965*	*-3.303*		*1*	$\mu_{max(T)} \cdot \left(\frac{HBu}{HBu + K_S}\right) \cdot I_{NH3-T} \cdot I_{LCFA} \cdot I_{HAc} \cdot I_{pH}$
7. Valerate acetogenesis									*-0.124*	*7.247*	*10.029*		*-13.82*	*0.966*	*-3.305*		*1*	$\mu_{max(T)} \cdot \left(\frac{HVa}{HVa + K_S}\right) \cdot I_{NH3-T} \cdot I_{LCFA} \cdot I_{HAc} \cdot I_{pH}$
8. Acetoclastic methanogenesis									*-0.124*	*-24.135*				*6.082*	*16.726*		*1*	$\mu_{max(T)} \cdot \left(\frac{HAc}{HAc + K_S}\right) \cdot I_{NH3-T} \cdot I_{LCFA} \cdot I_{pH}$
9. Cell decay	*0.18*						*0.82*										*-1*	$k_{dec} \cdot X$

ADM1 model

Anaerobic Digestion Model No.1 (ADM1) is one such model that can be considered as the first internationally-used model to describe anaerobic digestion (Batstone et al., 2002; Jenkins and Wanner, 2014). ADM1 model is a standardized and comprehensive model published by the International Water Association (IWA) and it can be used in combination with other wastewater treatment models such as activated sludge models (ASMs) published by IWA in 1987. A common approach has been adopted in terms of units and nomenclature to ensure consistency across the different models. Moreover, a comprehensive stoichiometric model that link ASM models to anaerobic and/or aerobic digestion by Ikumi et al. (2011). The model includes elemental balances and mixed acid/base reactions for pH calculations. As mentioned before, continuity-based interface method (CBIM) approach is suggested by Vanrolleghem et al. (2005), by interfacing ASM1 to ADM1 for the excess sludge line and return lines (Jenkins and Wanner, 2014).

In the anaerobic digestion process, four primary stages of reaction occur, each of which is accompanied by a multitude of concurrent reactions and the formation of intermediate products (Batstone et al., 2002; Gavala et al., 2003). To model these reactions in a cohesive and systematic framework, the International Water Association Task Group introduced the Anaerobic Digestion Model No. 1 (ADM1) (Appels et al., 2008; Batstone et al., 2002; Donoso-Bravo et al., 2011). The ADM1 framework encapsulates a variety of biochemical mechanisms responsible for transforming complex organic substrates into biogas, as depicted in (Figure 3.18). These mechanisms encompass the disintegration/hydrolysis of intricate organic substances, followed by acidogenesis, acetogenesis, and methanogenesis. Within the ADM1 paradigm, deceased microorganisms are assimilated as part of the intricate organic matter, serving as substrates after decay, degraded into carbohydrates and proteins. The catalysis of anaerobic digestion processes, either intra- or extracellularly by enzymes, leverages available organic material, inclusive of both soluble and particulate forms. Such processes have been extensively verified and are supported by a consensus within the scientific community (Batstone, 2006; Batstone et al., 2002; Gujer and Zehnder, 1983). The phases of acidogenesis or fermentation are characterized by the assimilation of sugars, amino acids, and long-chain fatty acids (LCFAs). Concurrently, acetogenesis involves the assimilation of valerate, butyrate,

and propionate, whereas methanogenesis is marked by the assimilation of acetate and hydrogen.

Within ADM1, the comprehensive mechanism of anaerobic digestion is dissected into four primary stages, which are further delineated into nineteen distinct processes. These processes facilitate a detailed understanding and simulation of the complex biochemical reactions involved in the conversion of organic matter to biogas. Initially, the disintegration of complex organic matter is accounted for by a singular process, emphasizing the breakdown of solid organic substances into a form more amenable to microbial action.

Subsequently, the hydrolysis stage encompasses three processes, each tailored to the breakdown of specific components of organic matter: carbohydrates, proteins, and lipids. This differentiation acknowledges the varied pathways through which these macromolecules are degraded into simpler molecules that can be readily assimilated by microorganisms.

The progression of the digestion process is marked by eight distinctive processes associated with the uptake of various substrates, including sugars, amino acids, long-chain fatty acids (LCFAs), butyrate, valerate, propionate, acetate, and hydrogen. Each of these processes is critical for the successive stages of acidogenesis, acetogenesis, and methanogenesis, facilitating the conversion of intermediate products into methane and carbon dioxide.

Finally, the ADM1 model integrates seven processes for the decay of organic substrates: sugars, amino acids, LCFAs, butyrate, valerate, propionate, acetate, and hydrogen. These decay processes are pivotal in the model, accounting for the turnover and recycling of microbial biomass and the release of substrates back into the digestion cycle, thereby ensuring the continuity and efficiency of the biogas production process. This intricate structuring of the ADM1 into specific processes underscores the model's comprehensive approach to simulating the complex dynamics of anaerobic digestion.

Within ADM1, the disintegration and hydrolysis phase are postulated to adhere to first-order kinetics. This dynamic is succinctly encapsulated by Equation 3.16, where r_h signifies the rate of hydrolysis, and k_h denotes the hydrolysis rate coefficient, measured in the unit of day^{-1}.

$$-r_h = k_h \cdot S \tag{3.16}$$

Subsequent processes in ADM1 are predicated on the application of Monod-type kinetics, eschewing Michaelis-Menten growth kinetics. The rationale for this preference, lies in the employment of substrate uptake kinetics for the articulation of changes in variable and inhibition phenomena among microorganisms (Batstone et al., 2002). This approach facilitates the segregation of growth from uptake activities, thereby enabling variable yields.

The model considers eight distinct groups of microorganisms for the uptake of substrates, and the decay of these biomasses is incorporated into the ADM1 framework. Notably, the original ADM1 does not encompass sulfate reducers. The specified groups are as follows:

1. Sugar degraders: These organisms catalyze the conversion of monosaccharides into butyrate, propionate, acetate, and hydrogen.
2. Amino acid degraders: This group is responsible for transforming amino acids into valerate, butyrate, propionate, acetate, and hydrogen.
3. Long-chain fatty acid degraders: These microorganisms convert long-chain fatty acids (LCFA) into acetate and hydrogen.
4. Valerate and butyrate degraders: This category involves the conversion of valerate and butyrate into propionate, acetate, and hydrogen.
5. Propionate degraders: Propionate and hydrogen are converted into acetate and hydrogen by these degraders.
6. Acetate degraders: The conversion of acetate into methane is facilitated by these organisms.
7. Hydrogen degraders: This group converts hydrogen into methane.
8. Sulfate reducers: These organisms are responsible for converting sulfate into sulfide, though they are excluded from the original ADM1 model.

ADM1 employs approximately 32 differential equations to capture the dynamic behaviors of various components within the AD process (Gerber and Span, 2008). This mathematical framework is pivotal for understanding and predicting the changes in concentrations of substances involved in AD over time. The model uses a matrix format to articulate the kinetic and stoichiometric yield coefficients, meticulously incorporating the kinetics and inhibition functions pertinent to each of the nineteen

processes identified within the ADM1 framework. This matrix representation outlines the relationship between substrates, microorganisms, and products, facilitated by kinetics that describe the rates of reactions and yields that quantify the conversion efficiency of substrates to products. The inclusion of inhibition functions within this matrix is crucial, as these functions account for the conditions under which the efficiency of biochemical reactions is reduced due to the presence of inhibitory substances or unfavorable environmental conditions.

The model distinguishes between different types of inhibition that affect the AD processes:

Noncompetitive inhibition, particularly involving ammonia and hydrogen, affects nearly all AD processes with the exception of hydrolysis. This form of inhibition occurs when an inhibitor binds to an enzyme at a site other than the active site, altering the enzyme's activity without blocking substrate binding (Batstone et al., 2002).

Empirical inhibition by pH and secondary substrate inhibition are applicable across all AD processes, acknowledging the critical role of pH in microbial activity and the potential inhibitory effects of excess substrate concentrations (Batstone et al., 2002).

Competitive inhibition is specifically associated with the uptake processes for butyrate and valerate. In this context, competitive inhibition arises when substances compete with the substrate for binding to the active site of an enzyme, effectively decreasing the reaction rate for substrate conversion (Batstone et al., 2002).

The model's matrix representation, as detailed in Table 3.15 for soluble components and Table 3.16 for particulate components, provides a comprehensive overview of the stoichiometric and kinetic parameters governing the transformation of these components throughout the AD process. This structured approach facilitates a deep understanding of the complex interactions within the AD system, enabling researchers and practitioners to predict system behavior under various conditions and to optimize the AD process for enhanced biogas production.

ADM1 is heralded as a potent instrument for the design and optimization of anaerobic digesters. Its comprehensive framework enables the detailed simulation of biochemical processes involved in anaerobic digestion, facilitating full-scale design endeavors and process optimization efforts. This capability not only aids in the effective scaling of anaerobic digestion technologies from laboratory to industrial scales but also enhances

the efficiency and stability of biogas production processes. Moreover, ADM1 serves as a robust foundation for further model development and validation studies, offering a standardized approach for researchers to refine and expand upon (Batstone et al., 2002; Mendes et al., 2015; Otuzalti et al., 2018).

The utility of ADM1 extends to its applicability across a wide array of substrates, as evidenced by its successful application to various types of organic material (Mendes et al., 2015; Otuzalti et al., 2018). This adaptability underscores the model's versatility in predicting the digestion behavior of diverse feedstocks, ranging from municipal waste to industrial effluents and agricultural residues. Such breadth of application is crucial for the evolving landscape of waste management and renewable energy production, where the efficient and environmentally responsible conversion of organic waste into energy is of paramount importance.

Despite its extensive capabilities, ADM1 does have limitations, particularly in its consideration of liquid-solid transformations. The model currently does not account for processes such as the precipitation and solubilization of ions, which can play significant roles in the overall dynamics of anaerobic digestion systems. These transformations can influence the bioavailability of nutrients, the formation of inhibitory compounds, and the overall process stability. Their exclusion from the model may limit the accuracy of predictions in systems where such phenomena are critical to the digestion process. As such, ongoing research and development efforts aimed at integrating these aspects into ADM1 or subsequent models would significantly advance the field of anaerobic digestion modeling, paving the way for more comprehensive and accurate system designs and optimizations.

Table 3.15 : Matrix representation of ADM1 model for soluble components (i= 1-12, j= 1-19) (Batstone et al., 2002).

Component, i → / Process, j ↓	1 S_{su}	2 S_{aa}	3 S_{fa}	4 S_{va}	5 S_{bu}	6 S_{pro}	7 S_{ac}	8 S_{h2}	9 Sc_{H4}	10 S_{IC}	11 S_{IN}	12 S_I	Process Rate kg COD·m^{-3}d^{-1}
Disintegration												$f_{sI,Xc}$	$k_{dis} \cdot X_C$
Hydrolysis of carbohydrates	*1*												$k_{hyd,ch} \cdot X_{Ch}$
Hydrolysis of proteins		*1*											$k_{hyd,pr} \cdot X_{pr}$
Hydrolysis of lipids	*1-$f_{fa,li}$*		*$f_{fa,li}$*										$k_{hyd,li} \cdot X_{li}$
Uptake of sugars	*-1*				*(1-Y_{su})·$f_{bu,su}$*	*(1-Y_{su})·$f_{pro,su}$*	*(1-Y_{su})·$f_{ac,su}$*	*(1-Y_{su})·$f_{h2,su}$*		$-\sum_{i=1-9,11-24} C_i v_{i,5}$	*-(Y_{su})·N_{bac}*		$k_{m,su} \cdot \frac{S_{su}}{K_S + S_{su}} \cdot X_{su} \cdot I_1$
Uptake of amino acids		*-1*		*(1-Y_{aa})·$f_{va,aa}$*	*(1-Y_{aa})·$f_{bu,aa}$*	*(1-Y_{aa})·$f_{pro,aa}$*	*(1-Y_{aa})·$f_{ac,aa}$*	*(1-Y_{aa})·$f_{h2,aa}$*		$-\sum_{i=1-9,11-24} C_i v_{i,6}$	N_{aa} *-(Y_{aa})·N_{bac}*		$k_{m,aa} \cdot \frac{S_{aa}}{K_S + S_{aa}} \cdot X_{aa} \cdot I_1$
Uptake of LCFA			*-1*				*(1-Y_{fa})·0.7*	*(1-Y_{fa})·0.3*			*-(Y_{fa})·N_{bac}*		$k_{m,fa} \cdot \frac{S_{fa}}{K_S + S_{fa}} \cdot X_{fa} \cdot I_2$
Uptake of valerate				*-1*		*(1-Y_{c4})·0.54*	*(1-Y_{c4})·0.31*	*(1-Y_{c4})·0.15*			*-(Y_{c4})·N_{bac}*		$k_{m,c4} \cdot \frac{S_{va}}{K_S + S_{va}} \cdot X_{c4} \cdot \frac{1}{1 + S_{bu}/S_{va}} \cdot I_2$
Uptake of butyrate					*-1*		*(1-Y_{c4})·0.8*	*(1-Y_{c4})·0.2*			*-(Y_{c4})·N_{bac}*		$k_{m,c4} \cdot \frac{S_{bu}}{K_S + S_{bu}} \cdot X_{c4} \cdot \frac{1}{1 + S_{va}/S_{bu}} \cdot I_2$
Uptake of propionate						*-1*	*(1-Y_{pro})·0.57*	*(1-Y_{pro})·0.43*		$-\sum_{i=1-9,11-24} C_i v_{i,1}$	*-(Y_{pro})·N_{bac}*		$k_{m,pro} \cdot \frac{S_{pro}}{K_S + S_{pro}} \cdot X_{pro} \cdot I_2$
Uptake of acetate							*-1*		*(1-Y_{ac})*	$-\sum_{i=1-9,11-24} C_i v_{i,1}$	*-(Y_{ac})·N_{bac}*		$k_{m,ac} \cdot \frac{S_{ac}}{K_S + S_{ac}} \cdot X_{ac} \cdot I_3$
Uptake of hydrogen								*-1*	*(1-Y_{h2})*	$-\sum_{i=1-9,11-24} C_i v_{i,1}$	*-(Y_{h2})·N_{bac}*		$k_{m,h2} \cdot \frac{S_{h2}}{K_S + S_{h2}} \cdot X_{h2} \cdot I_1$
Decay of X_{su}													$k_{dec,Xsu} \cdot X_{Su}$
Decay of X_{aa}													$k_{dec,Xaa} \cdot X_{aa}$
Decay of X_{fa}													$k_{dec,Xfa} \cdot X_{fa}$
Decay of X_{c4}													$k_{dec,Xc4} \cdot X_{c4}$
Decay of X_{pro}													$k_{dec,Xpro} \cdot X_{pro}$
Decay of X_{ac}													$k_{dec,Xac} \cdot X_{ac}$
Decay of X_{h2}													$k_{dec,Xh2} \cdot X_{h2}$
Parameter, ML^{-3}	Monosacc. kg COD·m^{-3}	Amino acids kg COD·m^{-3}	LCFAs kg COD·m^{-3}	Total valerate kg COD·m^{-3}	Total butyrate kg COD·m^{-3}	Total propionate kg COD·m^{-3}	Total acetate kg COD·m^{-3}	Hydrogen gas kg COD·m^{-3}	Methane gas kg COD·m^{-3}	Inorganic carbon kmole C·m^{-3}	Inorganic nitrogen kmole N·m^{-3}	Soluble inerts kg COD·m^{-3}	Inhibition factors $I_1 = I_{pH}\, I_{IN,lim}$ $I_2 = I_{pH}\, I_{IN,lim} \cdot I_{h2}$ $I_3 = I_{pH}\, I_{IN,lim} \cdot I_{NH3,Xax}$

Table 3.16 : Matrix representation of ADM1 model for particulate components (i= 13-24, j= 1-19) (Batstone et al., 2002).

Component, i →	13	14	15	16	17	18	19	20	21	22	23	24	Process Rate
Process, j ↓	X_c	X_{ch}	X_{pr}	X_{li}	X_{su}	X_{aa}	X_{fa}	X_{c4}	X_{pro}	X_{ac}	X_{h2}	X_I	kg COD·m^{-3}d^{-1}
Disintegration	-1	$f_{ch,xc}$	$f_{pr,xc}$	$f_{li,xc}$								$f_{XI,Xc}$	$k_{dis} \cdot X_C$
Hydrolysis of carbohydrates		*-1*											$k_{hyd,ch} \cdot X_{Ch}$
Hydrolysis of proteins			*-1*										$k_{hyd,pr} \cdot X_{pr}$
Hydrolysis of lipids				*-1*									$k_{hyd,li} \cdot X_{li}$
Uptake of sugars					Y_{su}								$k_{m,su} \cdot \frac{S_{su}}{K_S + S_{su}} \cdot X_{su} \cdot I_1$
Uptake of amino acids						Y_{aa}							$k_{m,aa} \cdot \frac{S_{aa}}{K_S + S_{aa}} \cdot X_{aa} \cdot I_1$
Uptake of LCFA							Y_{fa}						$k_{m,fa} \cdot \frac{S_{fa}}{K_S + S_{fa}} \cdot X_{fa} \cdot I_2$
Uptake of valerate								Y_{c4}					$k_{m,c4} \cdot \frac{S_{va}}{K_S + S_{va}} \cdot X_{c4} \cdot \frac{1}{1 + S_{bu}/S_{va}} \cdot I_2$
Uptake of butyrate								Y_{c4}					$k_{m,c4} \cdot \frac{S_{bu}}{K_S + S_{bu}} \cdot X_{c4} \cdot \frac{1}{1 + S_{va}/S_{bu}} \cdot I_2$
Uptake of propionate									Y_{pro}				$k_{m,pro} \cdot \frac{S_{pro}}{K_S + S_{pro}} \cdot X_{pro} \cdot I_2$
Uptake of acetate										Y_{ac}			$k_{m,ac} \cdot \frac{S_{ac}}{K_S + S_{ac}} \cdot X_{ac} \cdot I_3$
Uptake of hydrogen											Y_{h2}		$k_{m,h2} \cdot \frac{S_{h2}}{K_S + S_{h2}} \cdot X_{h2} \cdot I_1$
Decay of X_{su}	1				-1								$k_{dec,Xsu} \cdot X_{Su}$
Decay of X_{aa}	1					-1							$k_{dec,Xaa} \cdot X_{aa}$
Decay of X_{fa}	1						*-1*						$k_{dec,Xfa} \cdot X_{fa}$
Decay of X_{c4}	1							-1					$k_{dec,Xc4} \cdot X_{c4}$
Decay of X_{pro}	1								*-1*				$k_{dec,Xpro} \cdot X_{pro}$
Decay of X_{ac}	1									-1			$k_{dec,Xac} \cdot X_{ac}$
Decay of X_{h2}	1										-1		$k_{dec,Xh2} \cdot X_{h2}$
Parameter, ML^{-3}	Composites kg COD·m^{-3}	Carbohydrates kg COD·m^{-3}	Proteins kg COD·m^{-3}	Lipids kg COD·m^{-3}	Sugar degraders kg COD·m^{-3}	AA degraders kg COD·m^{-3}	LCFA degraders kg COD·m^{-3}	Valerate and butyrate degraders kg COD·m^{-3}	Propi.degraders kg COD·m^{-3}	Acetate degraders kg COD·m^{-3}	Hydrogen degraders kg COD·m^{-3}	Particulate inerts kg COD·m^{-3}	Inhibition factors $I_1 = I_{pH}\, I_{IN,lim}$ $I_2 = I_{pH}\, I_{IN,lim} \cdot I_{h2}$ $I_3 = I_{pH}\, I_{IN,lim} \cdot I_{NH3,Xax}$

3.6.4.3 Anaerobic hydrolysis

The hydrolysis process, which is the breakdown of complex organic matter into simpler substances, can take place under aerobic, anoxic, and anaerobic conditions. However, it is important to note that the rate of hydrolysis is generally lower under anoxic and anaerobic conditions compared to aerobic conditions (Henze et al., 2008; Henze et al., 1995).

Hydrolyzable organic matter, which refers to organic substances that can be broken down through hydrolysis, plays a significant role in several process modifications within wastewater treatment and biogas production systems. For instance, pre-hydrolysis or fermentation processes can be employed to enhance phosphorus removal from wastewater. Additionally, optimizing the denitrification potential, can be achieved by utilizing hydrolyzable organic matter.

Moreover, anaerobic digesters can be improved by incorporating hydrolyzable organic matter. This not only aids in the removal of organic pollutants but also enhances the overall efficiency of biogas production. Process modifications aimed at increasing the amount of biogas generated are particularly important for improving the sustainability and energy efficiency of anaerobic digesters.

Therefore, it is of great importance to determine the effects and understand the kinetics of hydrolysis for the fraction of organic matter that degrades slowly. This fraction typically exists in the form of particulate and/or colloidal organic matter. Comprehensive knowledge of these hydrolysis kinetics is essential for optimizing carbon removal and nutrient removal processes in wastewater treatment. Additionally, it is crucial for maximizing biogas production in anaerobic digesters, thereby contributing to more efficient and sustainable waste management practices.

The hydrolysis of organic polymers is typically performed by extracellular enzymes known as hydrolases. These enzymes are secreted by microorganisms and work outside the cell to break down complex organic materials into simpler, more easily degradable molecules. Under anaerobic conditions, where oxygen is absent, hydrolysis may or may not be the rate-limiting step in the bioconversion of organic matter.

Solubilization is not exclusively an enzymatic process facilitated by biologically produced enzymes. It can also occur due to various physicochemical reactions. These reactions do not require the direct involvement of biological catalysts but can result

from the interaction of organic polymers with their environment, including changes in pH, temperature, and the presence of other chemicals.

Describing the entire hydrolysis process with reliable kinetics is extremely challenging due to its complexity. The hydrolysis of complex, insoluble substrates depends on numerous parameters such as the size of the particles being hydrolyzed, the pH of the environment, the production rate of enzymes by microorganisms, and the diffusion and adsorption of these enzymes onto the particles. Each of these factors can significantly influence the rate and efficiency of hydrolysis.

Typically, the hydrolysis of organic polymers is described using a first-order kinetic model, which assumes that the rate of hydrolysis is directly proportional to the concentration of the substrate. This model is often applied because the enzymatic activity responsible for hydrolysis is not directly coupled to the growth rate of the bacteria producing the enzymes (Gujer and Zehnder, 1983). However, while a first-order kinetic model may be suitable for complex and heterogeneous substrates, other hydrolysis functions might be more appropriate for single, homogeneous substrates (Pavlostathis and Giraldo-Gomez, 1991). For instance, substrates that are uniform in composition and structure may follow different kinetic patterns (Gavala et al., 2003).

McCarty and Mosey suggested that hydrolysis could be considered a microbial process and proposed an alternative to the first-order kinetic model (McCarty and Mosey, 1991) (Equation 3.17). They introduced the "pseudo-Monod" equation, which includes a high saturation constant ranging from 5000 to 10000 mg/L. This equation accounts for the microbial nature of hydrolysis and provides a more nuanced understanding of the kinetics involved, especially under conditions where enzyme concentrations are significantly high.

$$r_S = K_h \cdot S \tag{3.17}$$

K_h: Hydrolytic constant

S: Substrate concentration

Another approach was suggested by Vavilin et al. (1996) that hydrolysis of complex organic substances is considered as a two-phase mechanism. The first phase of this process is bacterial colonization. During this phase, hydrolytic bacteria, which produce enzymes capable of breaking down complex organic materials, colonize or cover the

surface of the solid substrates. The rate at which this colonization occurs is influenced by the available contact area between the bacteria and the solid surfaces. Essentially, the more extensive the surface area that the bacteria can access, the faster the colonization process will proceed. This phase is critical because it sets the stage for the subsequent enzymatic activity. The second phase involves the actual degradation of the solid substrate by the hydrolytic enzymes produced by the bacteria. These enzymes work by breaking down the solid surface at a constant depth per unit of time. This means that the enzymes progressively degrade the surface layer of the solid material, facilitating its conversion into simpler compounds. This degradation process continues uniformly over time, provided that the environmental conditions remain favorable for enzyme activity. The rate of hydrolysis during this two-phase process can be mathematically expressed and is governed by a specific Equation 3.18.

$$r_S = K_h \cdot S_F^{1/3} \cdot S^{2/3} \tag{3.18}$$

where S_F is the concentration of influent biodegradable organic matter. The hydrolytic constant K_h of the two-phase model is a function of the ratio between the characteristic sizes of bacteria and particles hydrolyzed according to Equation 3.19.

$$K_h = 6r_{mS} \cdot \frac{\rho_B}{\rho_S} \cdot \frac{\delta}{d_S} \tag{3.19}$$

where r_{mS} is the maximum specific hydrolysis rate, ρ_B and ρ_S are the bacterial and particles densities, whereas, δ denotes the depth of the bacterial layer and d_S is the current diameter of particles.

Verstraete et al. (1981) suggested the following equation (Equation 3.20) by interpolating the experimental data from literature related to the anaerobic digestion of sewage sludge:

$$\frac{dX_S}{dt} = -k \cdot X_B^{0.5} \cdot X_S \tag{3.20}$$

The equation can be viewed as an adaptation of the first-order reaction equation, where the reaction rate's dependence on biomass concentration is modified by a superscript of 0.5. This adjustment accounts for the effective availability of the substrate to the biomass. Specifically, this mathematical formulation considers the reduction in the

effect of biomass concentration at higher concentrations, where insufficient substrate limits the accessibility of the biomass. In such cases, a portion of the biomass cannot interact with the substrate, leading to a decrease in the reaction rate.

Valentini et al. (1997) introduced a more generalized version of the earlier equation (Equation 3.20). In this updated form, the superscript value applied to the biomass concentration (X_B) is not fixed at 0.5 but is instead a parameter (A) that must be determined through data correlation (Equation 3.21). This allows for greater flexibility and accuracy in modeling the reaction dynamics based on empirical data.

$$\frac{dX_S}{dt} = -k \cdot X_B^A \cdot X_S \tag{3.21}$$

where A is a constant in the range 0 to 1.

More complex models that aim to account for the mechanisms involved in the hydrolysis process often incorporate the idea that the substrate removal rate is influenced by the biomass concentration. These models typically employ a function that represents a surface-limited reaction, meaning that the reaction primarily occurs at the interface where the solid substrate and the microorganisms meet. In this context, the process is conceptualized as a surface reaction. The efficiency and rate of hydrolysis process are significantly affected by how well the particulate substrates and microorganisms can interact at their surfaces (Insel et al., 2003).

To accurately model this surface reaction mechanism, the Contois equation is often used. The Contois equation posits that the degradation rate of the substrate is governed by the ratio of the substrate concentration (X_S) to the biomass concentration (X_B). This ratio reflects the availability of the substrate relative to the amount of biomass present, and it provides a more precise representation of the dynamics involved in the hydrolysis process (Equation 3.22).

$$\frac{dX_S}{dt} = -k_C \cdot X_B \cdot \frac{{}^{X_S}/_{X_B}}{K_X + {}^{X_S}/_{X_B}} \tag{3.22}$$

While studies on the removal and degradation kinetics of readily biodegradable organic matter (S_S) in activated sludge systems are widely available in the literature, detailed information on the effect of slowly biodegradable organic matter (X_S) and

hydrolysis kinetics on oxygen consumption rate, as well as carbon and nutrient removal and biogas production, is lacking. In Activated Sludge Model No.2, the hydrolysis kinetics of slowly biodegradable organic matter was identified as a weak point (Henze et al., 1995). In this model, hydrolysis reduction factors under anaerobic and anoxic conditions were defined as η_{fe} and η_{NO3}, respectively (Henze et al., 1995). The correction factors for hydrolysis in anaerobic and anoxic conditions were specified as 0.1 and 0.6, respectively, but there is no corresponding literature providing these correction factors derived from experimental methods (Ekama and Wentzel, 1999).

Henze and Mladenovski (1991) experimentally determined the hydrolysis rate of nitrogenous compounds under aerobic, anaerobic, and anoxic conditions as 0.12 d^{-1}, 0.06 d^{-1}, and 0.03 d^{-1}, respectively, and determined the η_{fe} value as 0.5 and the η_{NO3} value as 0.25. Mino et al. (1995) conducted batch studies with pure enzyme, pure culture, and activated sludge samples to determine the hydrolysis rate of slowly hydrolyzable COD under anaerobic, anoxic, and aerobic conditions using starch as a model substrate. In the starch sample, anaerobic and anoxic correction factors were found to be close to 1.0, and it was emphasized that this value could not be 1.0 if similar studies were carried out with high molecular weight compounds (proteins, fats, polynucleotides, etc.) (Mino et al., 1995).

Goel et al. (1999) proposed a method for measuring the oxygen consumption rate in EBPR systems by separating the hydrolysis process from the storage process. In this method, oxygen consumption rate measurements were performed in two parallel batch reactors fed with raw wastewater and filtered wastewater. Drewnowski and Makinia (2011) conducted a series of experiments, highlighting the lack of information in the literature on the effect of slowly biodegradable COD on nitrogen and phosphorus removal. In their study, they determined the nitrate consumption rate and specific phosphorus release/uptake rates of biomass in anoxic and anaerobic phases in two parallel reactors, where raw wastewater and pretreated wastewater (where readily biodegradable wastewater were separated from raw wastewater). However, only the comparative results of raw wastewater and pretreated wastewater were given, and no data on hydrolysis kinetics were generated (Drewnowski and Makinia, 2011; Drewnowski, 2014).

Slowly biodegradable particulate organic matter in the influent wastewater accumulates in the primary or secondary sludge, depending on the presence of a

primary settling process and the operating conditions of the activated sludge process, such as sludge age and retention time. In the death regeneration model proposed in the 1980s, active biomass is transformed into slowly decomposable organic matter through the decay process. Current plant-wide models are based on the death regeneration model, and model matrices are constructed according to this approach. However, these models do not distinguish between the slowly biodegradable organic matter (X_S) already present in the influent wastewater and X_S that is transformed from biomass due to the decay process. One possible explanation for this common practice is the real difficulty in anaerobic digestion of sludge to differentiate the active biomass (X_B) from the sludge volatile solids representing the substrate (X_S).

The recent development of more efficient microbial characterization techniques to determine the active fraction of the biomass will make it easier to evaluate these two components. This advancement will enable the implementation of more reliable models, enhancing the accuracy of simulations and predictions in wastewater treatment processes. Improved characterization will help optimize treatment efficiency, better understand microbial dynamics, and potentially lead to more effective strategies for managing and treating wastewater (Tomei et al., 2009).

4. MATERIALS AND METHOD

4.1 Conceptual Framework

In this study, the prediction capability of a general process model has been investigated by using biogas production of anaerobic sludge digesters operated in 7 full-scale wastewater treatment plants in Turkey. The robustness of the multi-component model has been checked with different percentages of primary and secondary sludge mass fed to the anaerobic digesters. In this regard, the conceptual framework combining the experimental and modeling work have been identified in Figure 4.1.

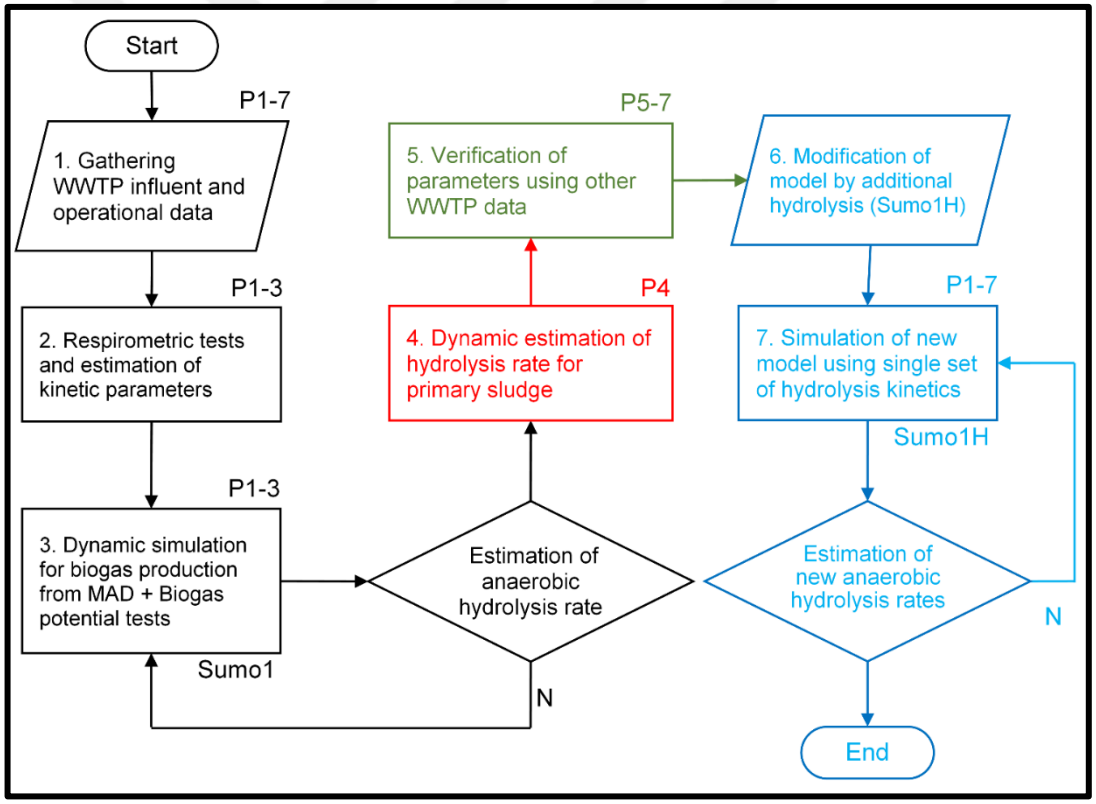

Figure 4.1 : Iterative steps for experimental design and modeling.

The biogas yields produced from different primary sludge fraction masses fed into anaerobic sludge digesters in wastewater treatment plants were simulated using the Sumo1 model (www.dynamita.com). The plants were categorized by their capacities, and the average biogas yields were calculated by manipulating the reduction factor for anaerobic hydrolysis ($\eta_{HYD,ana}$) in the model to simulate daily biogas flowrates. These

results were then compared to the average biogas measurement results of seven full-scale wastewater treatment plants. It should be noted that studied wastewater treatment plants have different levels of information obtained from different projects. In this respect, the modeling results of WWTPs P1-P4 are used for constructing the theoretical framework and calibration of the new model approach. The remaining WWTP results are used for model validation. The organization of the study is summarized as follows:

Step 1. Gathering WWTP Data: The design information and operational data of all wastewater treatment plants (P1–P7) were collected and analyzed in this step. The mass balances were checked in accordance with the actual capacity of each plant (Vanrolleghem et al., 2003).

Step 2. Respirometric Analysis and Nitrification-Denitrification Tests for Influent Wastewater: Batch respirometric experiments conducted with composite wastewater samples to identify influent COD fractions together with growth and hydrolysis kinetics (Ekama et al.,1986; Insel et al., 2003). Duplicate respirometric tests reflect the batch tests conducted to reflect the winter and summer characterization of 3 plants, denoted as P1, P2, and P3. The procedures for influent COD fractionation and model kinetics were adopted from Insel et al (2022) for those plants. The denitrification batch tests were performed to determine the reduction factors for the growth process and hydrolysis under anoxic conditions through assessing nitrate utilization profiles following the protocol suggested by Melcer et al. (2003) and Sözen et al. (1998).

Step 3. Dynamic Process Simulations: Dynamic simulations were conducted to mimic the long-term performance of plant and daily biogas production of the anaerobic digesters. The Sumo1 (Dynamita, Sumo22) plant-wide model was used in plant-wide simulation studies. The anaerobic hydrolysis reduction factor ($\eta_{HYD,ana}$) of the model was calibrated using real-time biogas production data of plants encoded with P1, P2, and P3. In addition, the sludges sampled from anaerobic digesters were subjected to SMA tests and BMP tests with raw sludge. The Modified-Gompertz model was used to compare the rates with kinetics obtained from the Sumo1 model. The original Sumo1 model matrix can be downloaded along with the program from the official website of the Sumo simulation platform (URL-1).

Step 4. Dynamic Simulation for Primary Sludge Digestion: The plant coded as P4 data is used to simulate daily biogas production of an anaerobic digester fed only with

thickened primary sludge. The average influent wastewater COD fractionation and the model kinetics of plants P1–P3 were used in dynamic simulations. The reduction factor for the anaerobic hydrolysis parameter was calibrated according to the biogas production and Volatile Solids (VS) destruction in digesters.

Step 5. Anaerobic Hydrolysis Rate vs. Sludge Mass Fractions: The same approach was applied to the treatment plants P5, P6, and P7, where each plant had different primary and secondary sludge mass fractions fed to the anaerobic digesters. Annual average biogas flowrates were used in model calibration. The objective here is to obtain a correlation between primary sludge mass contribution on model recalibration using biogas flowrate.

Step 6. Modification of Activated Sludge Model: In the current model the degradation of particulate organic matter (X_B) is controlled with hydrolysis kinetics adjusted by a reduction factor ($\eta_{HYD,ana}$) under anaerobic conditions. However, in this step, the model needed recalibration in each case where the primary sludge (fed to the digester) had different fractions. As a result, the model was modified (as Sumo1H) accordingly by extending X_B to (a) influent particulate biodegradable COD, X_B, and (b) particulate biodegradable COD produced by endogenous processes, $X_{B,E}$.

Step 7. Validation of the Modified Model: In the last step, a modified plant-wide model (Sumo1H) was used to estimate the average biogas flowrates of all digesters (P1–P7), without any recalibration effort. Thus, a unique parameter set for degradation kinetics of X_B and $X_{B,E}$ was proposed for the use in design, operation, and optimization of anaerobic digesters.

The simulation layouts for all wastewater treatment plants were prepared in Sumo22 simulation platform developed by Dynamita. Simulation layouts and aerial views of plants are given in Table 4.1. The design capacity of the studied plants is also summarized in the Materials and Method section.

Table 4.1 : Aerial views and simulation layouts of the plants.

No	Aerial View	Simulation Layout
P1		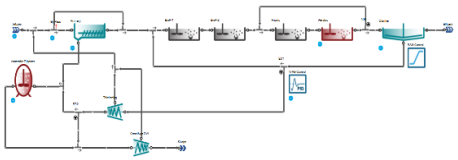
P2		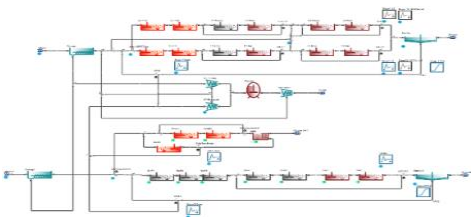
P3		
P4		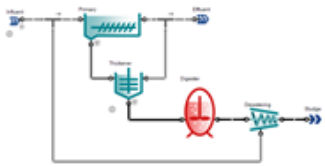
P5		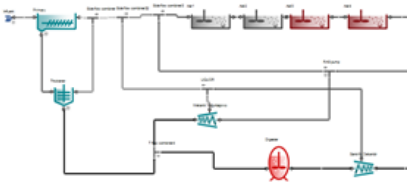
P6		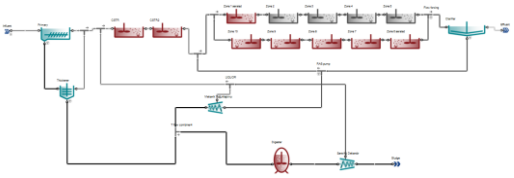
P7		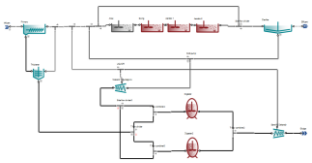

4.2 Description of Studied Wastewater Treatments

Studied WWTPs were full-scale biological carbon and nutrient removal wastewater treatment plants located in different regions of Turkey. The average capacities of the plants were in the range between 65,000 m^3/day to 640,000 m^3/day and the influent COD concentrations were in the range between 330 mg/L and 1200 mg/L.

WWTP No. 1 (P1): The plant is located in the Marmara Region of Turkey. It has an average capacity of 400,000 m^3/day. Influent average COD, total Kjeldahl nitrogen (TKN), and total phosphorus (TP) concentrations of 480 mg/L, 50 mg N/L, and 5 mg P/L, respectively. The plant has primary sedimentation, Bio-P, and anoxic/aerobic activated sludge basins followed by final clarifiers. Primary and secondary sludge is mechanically thickened and sent to mesophilic anaerobic digesters operated at 18 days of SRT. The primary sludge fraction in the total sludge fed to the anaerobic sludge digester is about 34%. The TSS removal efficiency in the primary sedimentation unit is 30%. The activated sludge plant is operated at an SRT of 20 days. The average biogas production from anaerobic digester is around 16,000 m^3/day.

WWTP No.2 (P2): The plant is located in the Marmara Region of Turkey. The wastewater flowrate is 390,000 m^3/day with an average influent COD, TKN, and TP concentrations of 615 mg/L, 60 mg N/L, and 8 mg P/L, respectively. The plant is equipped with primaries followed by Bio-P reactors and oxidation ditch type anoxic/aerobic activated sludge tanks with a total SRT of 10 days. The TSS removal efficiency in primary sedimentation is 30%. Only thickened WAS is sent to mesophilic anaerobic digesters (MAD) operated with an SRT of 20 days. The average biogas production from anaerobic digester is recorded as 10,000 m^3/day.

WWTP No.3 (P3): The plant has average capacity of 300,000 m^3/day located in the Marmara Region of Turkey. The average influent COD, TKN, and TP concentrations are 515 mg/L, 65 mg N/L, and 7 mg P/L, respectively. The plant comprises primary sedimentation, Bio-P and anoxic/aerobic activated sludge basins followed by final clarifiers. The TSS removal efficiency in primary sedimentation unit is 30%. The plant consists of BNR and high rate activated sludge systems. Anoxic and total sludge ages of activated sludge system are 3 days and 9 days, respectively. The primary sludge is subjected to gravity; the secondary sludge is mechanically thickened before the MAD operated with an SRT of 20 days. The primary sludge fraction in the total sludge mass

fed to the digester is around 60%. The average biogas production from MAD is approximately 12,300 m^3/day.

WWTP No.4 (P4): The plant is located in the central region of Turkey. It receives an average flowrate of 150,000 m^3/day. The influent COD, TKN, and TP concentrations are 1200 mg/L, 85 mg N/L, and 9.5 mg P/L, respectively. The plant comprises of primary sedimentation tanks, selector tank, Bio-P tanks and anoxic/aerobic activated sludge basins and final clarifiers. Only primary sludge is thickened and sent to MAD. The average biogas production from the digester is reported as 9,500 m^3/day.

WWTP No.5 (P5): The plant is located in the central region of Turkey. The influent flowrate is recorded as 640,000 m^3/day. The COD, TKN, and TP concentrations of 330 mg/L, 36 mg N/L, and 7 mg P/L, respectively. The plant was equipped with primary sedimentation, surface aeration type activated sludge system and final clarifiers. The sludge is thickened and conveyed to anaerobic sludge digesters. The TSS removal efficiency in primary sedimentation unit is 60% and SRT of high rate activated sludge system is 2.5 days. The primary sludge fraction in the total sludge mass fed to the MAD is about 49%. The average biogas production from MAD is 40,000 m^3/day.

WWTP No.6 (P6): The plant is located in southern part of Turkey and has an average capacity of 65,000 m^3/day. It is in the neighborhood of a large touristic area. The COD, TKN, and TP concentrations are 550 mg/L, 45 mg N/L, and 10 mg P/L, respectively. The system is equipped with primary sedimentation tanks, closed-loop bioreactors followed by final clarifiers. The sludge is thickened and diverted to anaerobic sludge digester. The TSS removal efficiency of primaries is 40% and the total SRT of activated sludge system is 9 days. The primary sludge fraction in the total sludge mass is around 60%. The mixed thickened sludge is fed to MAD with a total retention time of 20 days. The average biogas production from digester is measured as 2,300 m^3/day.

WWTP No.7 (P7): The plant is located in the eastern side of Turkey. It has an average influent capacity of 88,000 m^3/day and designed as a carbon and nitrogen removal activated sludge process with an influent average COD, TKN, and TP concentrations of 400 mg/L, 35 mg N/L, and 7.5 mg P/L, respectively. The plant comprises of primary sedimentation, oxidation ditch type anoxic/aerobic activated sludge basins followed by final clarifiers. The TSS removal efficiency in primary sedimentation unit is 30% and the SRT of activated sludge is 10 days. Primary sludge is subjected to gravity

thickening process while secondary sludge is mechanically thickened and mixed sludge diverted to MAD, operated at 20 days of SRT. The primary sludge fraction fed to MAD is around 80%. The average biogas production from digester is around 5,000 m^3/day.

4.3 Biodegradability Characteristics of Influent Wastewater

4.3.1 Determination of inert COD fractions

Particular and soluble inert fractions of wastewaters have also a major role to identify operating conditions of treatment plants and discharge standards. In this context, detailed experimental study had been conducted on the influent wastewater to identify the soluble inert (S_{I1}) and particulate inert (X_{I1}) COD fraction of wastewater. Soluble inert COD (S_{I1}) is the most significant fraction of organic matter in the effluent of wastewater treatment plants, since this fraction is discharged without any biochemical reaction in activated sludge systems. In activated sludge operation, the particulate inert COD (X_{I1}) is accumulated in the system depending on sludge age and influent concentration. Respectively, it contributes to the quantity of waste sludge. Therefore, sludge quantity in the activated sludge system and the efficiency of the activated sludge system can be determined by experimental identification of particulate inert COD fraction (X_{I1}), as well.

The procedure suggests the operation of three aerated batch reactors to the point of cessation of biological activity. After monitoring the final threshold values of COD in each reactor, the COD fractions and stoichiometric parameters of microbial products can be determined independently (Orhon et al., 1999).

In the experiment, a triad of aerated batch reactors were employed, each receiving a distinct feed: the first reactor was supplied with the raw wastewater sample, the second reactor received the soluble (filtered) wastewater sample, and the third was administered a glucose solution, the COD value of which was approximately equivalent to that of the filtered wastewater reactor. (Figure 4.2). All reactors were initially seeded with around 20 mg VSS/L of biomass. Each run was continued for 40–50 days by taking aliquots for periodic COD measurements until all biological activity was completed. At the end, no appreciable change was any longer detected in the COD levels. The experiments were conducted at room temperature (22±1°C) and at a pH

range of 7.0–8.0. The soluble (filtered) COD was defined as the filtrate through Millipore polyamide membrane filters (0.45 µm).

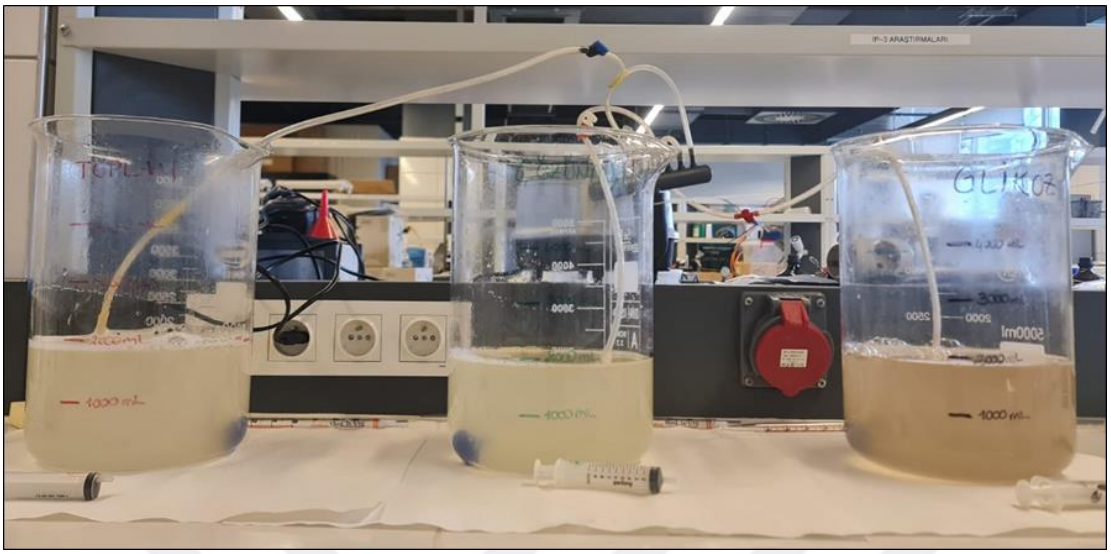

Figure 4.2 : Reactor set-up for identification of inert COD fractions.

The concentration of soluble COD within the glucose reactor is projected to diminish from an initial value, S_{G1}, to a final value, denoted as $(S_G)_1$, whereas this is the value of soluble residual COD, symbolized as $(S_P)_G$. Subsequently, the fraction of biodegradable COD is converted into soluble inert microbial products, with the yield value of Y_{SP} and stoichiometric coefficient f_{ES} may be defined as:

$$Y_{SP} = f_{ES} \cdot Y_H = \frac{(S_P)_G}{S_{G1}} \tag{4.1}$$

$$f_{ES} = \frac{1}{Y_H} \frac{(S_P)_G}{S_{G1}} \tag{4.2}$$

Similarly, the residual COD in filtered wastewater reactor, $(S_T)_2$, includes soluble inert COD of wastewater, $(S_T)_2$, and soluble microbial products, $(S_P)_2$,

$$(S_T)_2 = S_{I1} + (S_P)_2 \tag{4.3}$$

Soluble inert microbial products,

$$(S_P)_2 = f_{ES} \cdot Y_H \cdot (S_{T1} - S_{I1}) \tag{4.4}$$

and soluble inert COD may be computed as follows:

$$S_{I1} = \frac{(S_T)_2 - f_{ES} \cdot Y_H \cdot S_{T1}}{(1 - f_{ES} \cdot Y_H)} \tag{4.5}$$

f_{EX} can be calculated based on the idea that in the aerated reactor, all biological activity is completed and the biomass completed the decay process and is also fully mineralized after a long operation time ($\theta_X = \theta_h \cong \infty$). A filtered wastewater sample is fed into the reactor, which makes it very convenient for this purpose. During the experiment, the only particulate COD fraction remaining is $(X_P)_2$, and it can be expressed as in Equation 4.6.

$$X_P = f_{EX} \cdot Y_H \cdot C_S \tag{4.6}$$

And, f_{EX} may be calculated as follows:

$$(X_P)_2 = (C_T)_2 - (S_T)_2 = Y_{XP} \cdot (S_{T1} - S_{I1}) \tag{4.7}$$

$$Y_{XP} = f_{EX} \cdot Y_H = \frac{(X_P)_2}{S_{S1}} \tag{4.8}$$

$$f_{EX} = \frac{1}{Y_H} \cdot \frac{[(C_T)_2 - (S_T)_2]}{(S_{T1} - S_{I1})} \tag{4.9}$$

Results obtained from the the raw wastewater reactor are required for the determination of particulate inert COD, X_{I1}. The stoichiometric expressions that can be inferred from the experimental data obtained are enumerated as follows:

$$(X_T)_1 = (C_T)_1 - (S_T)_1 = X_{I1} + (X_P)_1 \tag{4.10}$$

Particulate inert microbial products, $(X_P)_1$,

$$C_{S1} = C_{T1} - X_{I1} - S_{I1} \tag{4.11}$$

$$(X_P)_1 = f_{EX} \cdot Y_H \cdot (C_{T1} - X_{I1} - S_{I1}) \tag{4.12}$$

And particulate inert COD may be computed as following expressions:

$$X_{I1} = \frac{(X_T)_1 - f_{EX} \cdot Y_H \cdot (C_{T1} - S_{I1})}{(1 - f_{EX} \cdot Y_H)} \quad (4.13)$$

4.3.2 Respirometric analysis and modeling studies

Biodegradable COD components in composite wastewater samples from 3 wastewater treatment plants were determined through respirometric experiments. These experiments measured the respiration of heterotrophic bacteria in laboratory conditions, alongside modeling studies that helped determine the COD fractions, growth rate, and hydrolysis rates (Ekama et al., 1986; Spanjers and Vanrolleghem, 1995; Ubay Çokgör et al., 1998). To conduct the experiments, 1 liter of biomass was taken from the activated sludge unit of each wastewater treatment plant and aerated until the endogenous respiration level was reached. This level represents the biomass activity at the absolute starvation level when there is no substrate left in the mineral medium (wastewater) in which the biomass is contained, and the substrate accumulated in the biological sludge and the cell has been consumed. The respiration level was monitored during the aeration period, and the endogenous respiration level was determined by identifying the point at which the OUR curve remained constant at the lowest level for a long time. Depending on the character of the wastewater and the biomass, the time to reach this level varies. Once the endogenous respiration level was reached, 1 liter of raw wastewater was added, and the oxygen utilization rate (OUR) was measured using a respirometer. The aim was to determine the fraction of COD that is biodegradable from the area under the respirometric profile. Due to the applied loading rate and low hydrolysis rates, the relevant components were determined with the help of modeling studies (Ekama et al., 1986; Spanjers and Vanrolleghem, 1995, Orhon and Okutman, 2003). OUR measurements were performed using an Applitek Ra-COMBO 1000 respirometer (Figure 4.3). All respirometric tests were conducted at 20°C and a nitrification inhibitor was used to avoid any potential interference of nitrification on the OUR profile (Formula 2533, Hach Company, USA). The entire respirometric profile was evaluated using a dynamic modeling and system identification method as described in Insel et al. (2003). The AQUASIM program developed by the Technical University of Zurich (ETH) was used for parameter estimation (Reichert, 1998). The influent wastewater was analyzed for VFA

measurements using Shimadzu HPLC at UV210 nm using an SCR-101H organic acid-specific column.

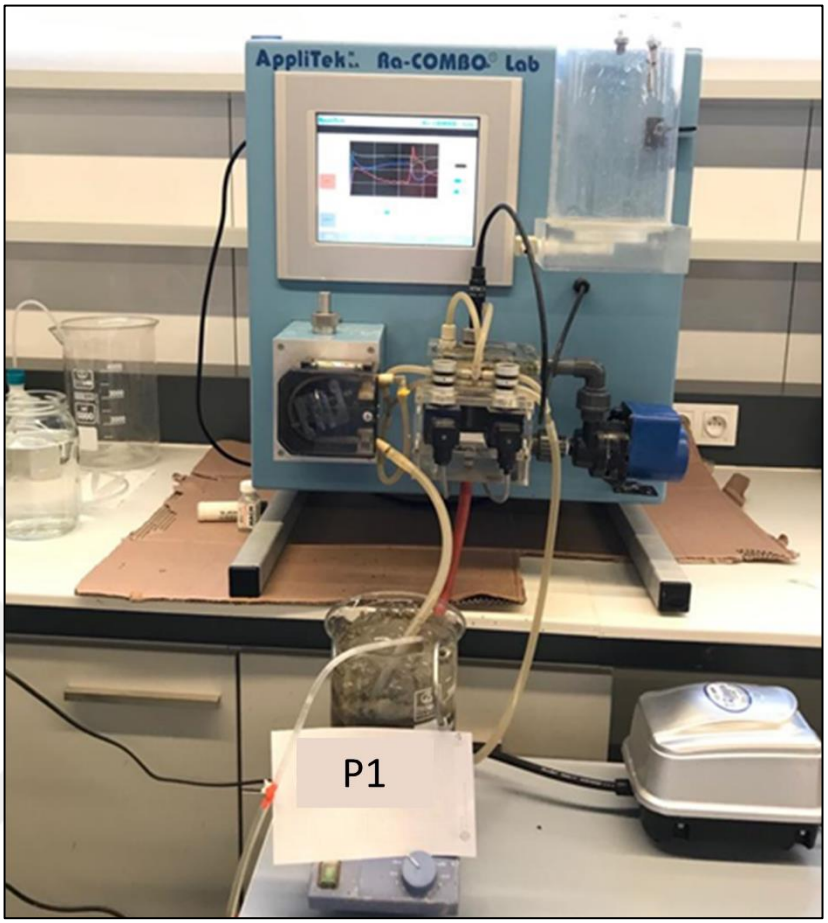

Figure 4.3 : Continuous respirometer (AppliTek Ra-Combo 1000).

4.4 Nitrification and Denitrification Batch Tests

The biological nitrogen removal process is limited by the nitrification process and it is crucial to determine the net growth rate of nitrifying bacteria to ensure effective nitrogen removal in municipal wastewater treatment plants. The net growth rate can be measured under laboratory conditions using acclimated activated sludge, and experimental results can be obtained within 5-10 days. To measure the nitrification rate, the nitrate production rate (NPR) test should be planned to represent the winter (lowest design temperature) conditions of the plants. The average temperature for the lowest two-week period reported in the WWTP can be considered. For the batch test, the effluent of the wastewater treatment plant is aerated in a water jacketed aerobic reactor until it reaches a constant temperature. Then, a low concentration of biomass and a suitable ammonium source (NH_4Cl) are added. Oxidized nitrogen is then

monitored against time by taking at least 2 samples per day. The initial nitrogen concentration of batch reactors should be adjusted to approximately 70-100 mg N/L. To prevent pH oscillations, CO_2 gas connected to pH control should be passed through the system. If there is an alkalinity deficiency, bicarbonate can be added at the beginning of the experiment. Finally, total oxidized nitrogen (NO_X) profile obtained at the end of the experiment is analyzed by parameter estimation. The net growth rate of nitrifying bacteria can be calculated by fitting the Equation 4.14 solution to the nitrate production profile using the least squares method. Simplex algorithm is preferred as iteration method using the Solver tool of MS Excel.

$$S_{NO,t} = S_{NO,0} + \frac{\mu_{A,max} \cdot X_{A,0}}{Y_A \cdot (\mu_A - b_A)} \cdot \left[e^{(\mu_{A,max} - b_A)\, t} - 1\right] \qquad (4.14)$$

The autotrophic and heterotrophic activated sludge kinetics were determined through aerobic and anoxic batch tests. A high F/M nitrification test was conducted on sludge samples obtained from full-scale WWTPs during winter and summer periods (Melcer et al., 2003). The aerobic experiment was conducted by adjusting the high F/M batch conditions and controlling the pH over several days. Aeration was used to saturate the effluent of the wastewater treatment plant with oxygen until it reached a constant temperature of 15°C in a water-jacketed 5-liter aerobic reactor (Figure 4.4).

Figure 4.4 : Temperature and pH–controlled nitrification rate measurement system.

After adding 70–100 mL of biomass to the sample, NH_4Cl was added, and the initial nitrogen concentration of batch reactors was adjusted to approximately 70-100

mg N/L. To maintain a pH range of 7.2-7.8 and avoid pH oscillations that may occur during the experiment due to the high amount of alkalinity added, CO_2 gas was passed through the system in a controlled manner. During the experiment under aerobic conditions, filtered nitrite/nitrate analysis was performed every day. The experiment was stopped when nitrate was obtained equal to the initial ammonium nitrogen concentration. 700 mg/L $CaCO_3$ alkalinity was added for 100 mg N/L. Experimental conditions for both winter and summer periods are given in Table 4.2. Initial biomass concentrations and F/M ratios adjusted in the batch tests were compatible with the WWTPs' operational conditions and autotrophic biomass activity.

Table 4.2 : Experimental conditions for nitrification tests.

Winter Conditions				
Parameter	**Unit**	**P1**	**P2**	**P3**
Duration of experiment	day	8	20	10
Volume	mL	4000	4000	4000
Seed biomass	mL	70	60	100
Biomass concentration (t=0)	mg TSS/L	155	143	130
Added NH_4-N	mg N/L	70	70	70
NO_X concentration (t=0)	mg N/L	4.1	1.5	8.3
Oxygen concentration	mg/L	8.3	8.2	8.3
Alkalinity ($NaHCO_3$)	g	3363	3363	3363
pH	-	7.2	7.2	7.2
Temperature	°C	15±1	15±1	15±1
Summer Conditions				
Parameter	**Unit**	**P1**	**P2**	**P3**
Duration of experiment	day	3	5	5
Volume	mL	4000	4000	4000
Seed biomass	mL	55	55	90
Biomass concentration (t=0)	mg/L	140	193	135
Added NH_4-N	mg N/L	70	70	70
NO_X concentration (t=0)	mg N/L	0.1	8.4	10.9
Oxygen concentration	mg/L	8.6	8.8	8.8
Alkalinity ($NaHCO_3$)	g	3363	3363	3363
pH	-	7.25	7.25	7.25
Temperature	°C	25±0.3	25±0.3	25±1

The denitrification rate represents the specific rate of nitrate consumption throughout different phases of microbial growth under anoxic conditions. Respirometric experiments, designed to operate in the absence of oxygen, enable the observation of nitrate utilization rate (NUR) profiles, which delineate successive phases of declining magnitude. Within the context of microbial growth mechanisms, there are three phases can be characterized. The initial phase is marked by a period of maximal growth,

characterized by the consumption of readily biodegradable substrate (S_S). This phase exhibits the highest rate of nitrate consumption, reflecting the utilization of easily accessible electron donors for growth and denitrification. The subsequent phase is noted for the depletion of readily bidegradable substrate, pivoting towards the consumption of slowly biodegradable substrate (X_S). During this stage, hydrolysis of the slowly biodegradable substrate becomes the rate-limiting step, significantly influencing the overall nitrate utilization rate. The final phase involves the utilization of endogenous decay products as electron donors for denitrification. This stage signifies a shift towards internal metabolic reserves, following the exhaustion of external substrates.

The differential in nitrate utilization rates across these phases elucidates the dominant biochemical mechanisms at play within each period. Specifically, the contrast in nitrate consumption between the first and second phases provides a quantitative measure of the rate attributable solely to the degradation of easily biodegradable substrate during the initial growth period. According to Henze et al. (1987), assuming constancy in the rates of hydrolysis and endogenous decay across all periods, this differential facilitates the determination of the denitrification rate based on the consumption of readily degradable substrate in the first phase.

The elucidation of the denitrification rate is instrumental in calculating the anoxic retention time, which is crucial for optimizing the process conditions for efficient denitrification. Furthermore, it informs the determination of the nitrate load (flowrate) required for recirculation, ensuring that denitrification processes are adequately supported by the supply of nitrate as an electron acceptor. This nuanced understanding of nitrate consumption dynamics across different substrate utilization phases underscores the complexity of microbial denitrification processes and their pivotal role in environmental biotechnology applications.

The methodology espoused by Melcer et al. (2003) and Sözen et al. (1998) for conducting denitrification batch tests emphasizes the importance of dissecting the NUR profiles into clearly defined phases. This approach allows for a nuanced understanding of how different substrates and microbial activities contribute to the overall denitrification process under anoxic conditions. Through these evaluations, researchers can derive specific anoxic reduction factors for both growth and

hydrolysis, thereby enhancing the predictive accuracy and operational efficiency of wastewater treatment processes aimed at nitrate removal.

The denitrification batch tests, as delineated by Melcer et al. (2003) and Sözen et al. (1998), were designed to quantify the anoxic reduction factors pertinent to microbial growth and hydrolysis (Figure 4.5). Activated sludge and influent wastewater from the activated sludge systems of the treatment plants were mixed at a ratio of 1/1 and experiments were carried out in 2 L reactors. The experiments were conducted using reactors equipped with magnetic stirrers. To ensure complete mixing and remove oxygen from the environment, nitrogen gas was continuously passed through the reactors. Each set was started by adding 139 g of $NaNO_3$/L solution, which was prepared to obtain the desired COD/NO_3 ratio. All experiments were stopped after 430 minutes. The supernatant was filtered through 0.22 μm filters for NO_3-N and NO_2-N analysis, initially at intervals of 10 minutes and then every 30 minutes. Samples for NO_X analysis were stored at +4°C until quantification with Ion Chromatograph (IC).

Figure 4.5 : Reactor set-up for NUR tests.

Experimental conditions for both winter conditions and summer conditions are given in Table 4.3.

Table 4.3 : Experimental conditions for nitrate utilization tests.

Winter Conditions				
Parameter	**Unit**	**P1**	**P2**	**P3**
Nitrate (t=0)	mg N/L	23.5	16.3	75.7
Total COD (t=0)	mg COD/L	202	215	235
TSS (t=0)	mg TSS/L	3730	2820	3800
VSS (t=0)	mg VSS/L	1945	1775	2430
Temperature	°C	15±1	15±1	15±1
Summer Conditions				
Parameter	**Unit**	**P1**	**P2**	**P3**
Nitrate (t=0)	mg N/L	68	73	71.8
Total COD (t=0)	mg COD/L	275	315	313
TSS (t=0)	mg TSS/L	4295	2805	2625
VSS (t=0)	mg VSS/L	2220	1640	1595
Temperature	°C	25±3	25±0.3	25±1

4.5 Methanogenic Activity and Biochemical Methane Potential Tests

Acetoclastic microorganisms are responsible for the conversion of acetic acid into carbon dioxide and methane, which marks the final stage of the methanization process. These microorganisms are quite delicate in nature, and they are used to monitor the performance of the system. To determine the activity of acetoclastic microorganisms in the anaerobic digesters, specific methanogenic activity (SMA) tests are conducted using inoculum sludge taken from the outlet weir of anaerobic sludge digesters. Additionally, experiments are carried out to determine the biochemical methane potential that the sludge can produce biogas for each wastewater treatment plant.

To evaluate the specific methanogenic activity and biochemical methane potential of the sludge, anaerobic batch tests were conducted (Owen et al., 1979; Speece, 1988). The tests were carried out in 3,450 mL flask reactors capped with a rubber stopper and flushed with N_2 gas. The experiments were performed in a constant temperature room at 35±1°C. (Figure 4.6). The seed sludge used in the tests was obtained from the mesophilic anaerobic digestion unit of each WWTPs.

Figure 4.6 : Reactor set-up for biochemical methane potential tests.

The mixed sludges (WAS and primary) obtained from the WWTPs were used as substrate for BMP tests, whereas acetate was the sole substrate for SMA tests. F/M ratios adjusted in the BMP tests were compatible with the WWTPs' anaerobic digester operations (See the Materials and Method section). Each test was run in triplicate and control reactors were run in parallel. The gas production was monitored through a manometer (Lutron PM-9107, Lutron Electronic Enterprise, Taiwan) (Figure 4.7). Detailed experimental conditions are given in Table 4.4 and Table 4.5.

Figure 4.7 : Reactor set-up for SMA batch tests and manometer.

Table 4.4 : Biochemical methane potential tests experimental conditions.

Parameter	Unit	P1	P2	P3
TS_{feed}	%	7.74	6.40	6.52
VSS/TSS (feed)	%	50	51	53
TS_{seed}	%	5.73	4.79	3.60
VSS/TSS (seed)	%	40	45	44
V_{Total}	mL	3680	3490	3450
$V_{Efective}$	mL	2159	2020	2020
V_{Seed}	mL	2000	1845	1900
$V_{Bicarbonate}$	mL	20	20	20
V_{Feed}	mL	139	155	100
pH (initial)	-	7.19	7.49	7.29
pH (final)	-	7.56	7.54	7.37

Table 4.5 : Specific methanogenic activity tests experimental conditions.

Parameter	Unit	SMA Test	Control
V_{Total}	mL	120	120
$V_{Efective}$	mL	60	60
$V_{Acetate}$	mL	0.52	-
V_{Seed}	mL	6	6
$V_{Bicarbonate}$	mL	0.6	0.6
$V_{Mineral}$	mL	53	53

4.6 Data Collection and Dynamic Plant-wide Modeling Studies

All wastewater treatment plants' design information and operational data (P1–P7) were collected and analyzed in this step (See Section 4.2). The mass balances were checked in accordance with the actual capacity of each plant (Vanrolleghem et al., 2003). Dynamic simulations were conducted to mimic the long-term performance of plant and daily biogas production of the anaerobic digesters. The Sumo1 model was used in plant-wide simulation studies. The wastewater treatment plant configurations introduced to the Sumo22 simulation platform (from Dynamita) are illustrated in Table 4.1. The average influent wastewater COD fractionation and the model kinetics of plants P1–P3, obtained from the batch studies, were used in dynamic simulations. The plant coded as P4 data is used to simulate daily biogas production of anaerobic digester fed only with thickened primary sludge. For the plants coded P5-P7, annual average biogas flowrates were used in model calibration.

4.7 Analytical Works

Total solids (TS), total suspended solids (TSS), volatile suspended solids (VSS), and total volatile solids (TVS) were measured according to Standard Methods procedures numbered “2540 (Solids)” (APHA, 2012). Chemical oxygen demand (COD), ammonium nitrogen (NH_4-N), total kjeldahl nitrogen (TKN), and total phosphorus (TP) were analyzed in accordance with Standard Methods procedures numbered 5220, 4500-NH_3, 4500-N_{org}, and 4500-P, respectively.

Nitrite and nitrate nitrogen were measured using ion chromatography (Dionex Corporation, Sunnyvale, CA, USA) with an analytical column of AS9A and a conductivity detector. Duplicate samples were analyzed for each parameter.

Volatile fatty acids (VFAs) were determined using high performance liquid chromatography (HPLC, Shimadzu Prominence LC-20A) equipped with an organic acid specific column SCR-101H (Shimadzu, Japan) and a UV detector (at a 210 nm wavelength). The column was operated at 60°C and 0.025% (v/v) H_2SO_4 was used as mobile phase at a flow rate of 0.7 mL/min. The standard chemicals and solutions for the calibration curve for acetic acid, lactic acid, propionic acid, butyric acid, valeric acid, formic acid and succinic acid were purchased from Merck Group.

The methane and carbon dioxide content of the biogas were analyzed using a gas chromatography (GC) (Agilent Technologies, Model 7890A) equipped with two columns and two thermal conductivity detectors. Methane was separated using a 25 m Agilent Molsieve fused silica 0.53 mm i.d. column, while carbon dioxide was separated using a 25 m HP-PLOT Q fused silica 0.53 mm i.d. column. Helium was used as the carrier gas with a constant flow of 5 mL/min, and the 10:1 split injector was maintained at 150°C, while the detector temperature was set at 150°C.

5. RESULTS AND DISCUSSION

5.1 Influent Wastewater Characterization

The results of the experiments aimed to determine the influent COD fractions, the heterotrophic biomass activity and degradation kinetics of P1, P2, and P3 by using respirometric measurements and modeling studies for both winter and summer conditions are presented in this section. Batch respirograms and model results of P1, P2 and P3 are presented in Figure 5.1, Figure 5.2 and Figure 5.3, respectively.

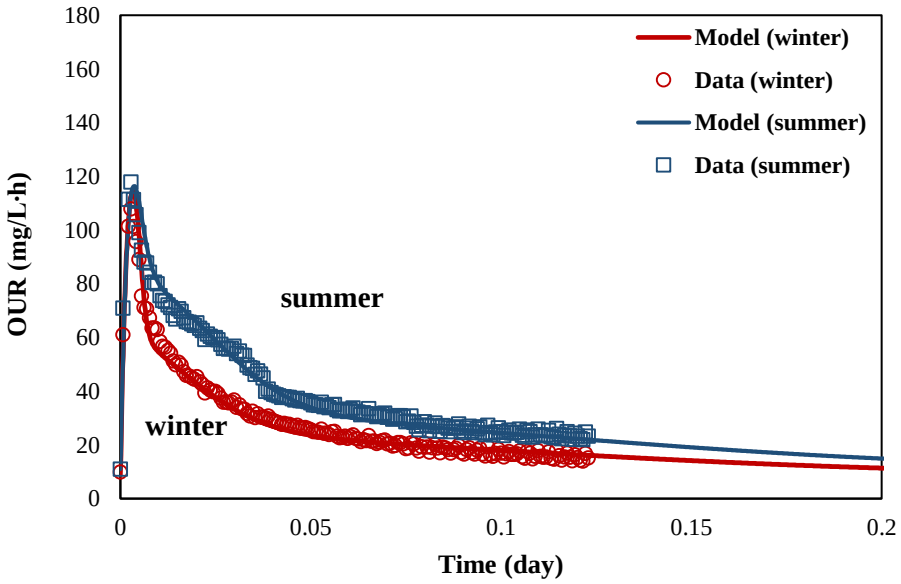

Figure 5.1 : Batch respirometric tests for P1.

The influent COD fractions of wastewater are summarized in Table 5.1 and Table 5.2 for winter and summer conditions, respectively. Soluble COD represents the fraction of influent wastewater that is filtered through a 0.45 µm filter, while colloidal COD represents the organic materials between 0.1 micron and 1.2 micron. This fraction can be approximated analytically by flocculation or filtration using the method suggested by Mamais et al. (1993). Firstly, influent COD fractions were measured and calculated using the methods available for multi-component activated sludge modeling and suggested by ASMs. Then, these fractions were converted into COD fractions accepted by the Sumo model for future dynamic simulation studies.

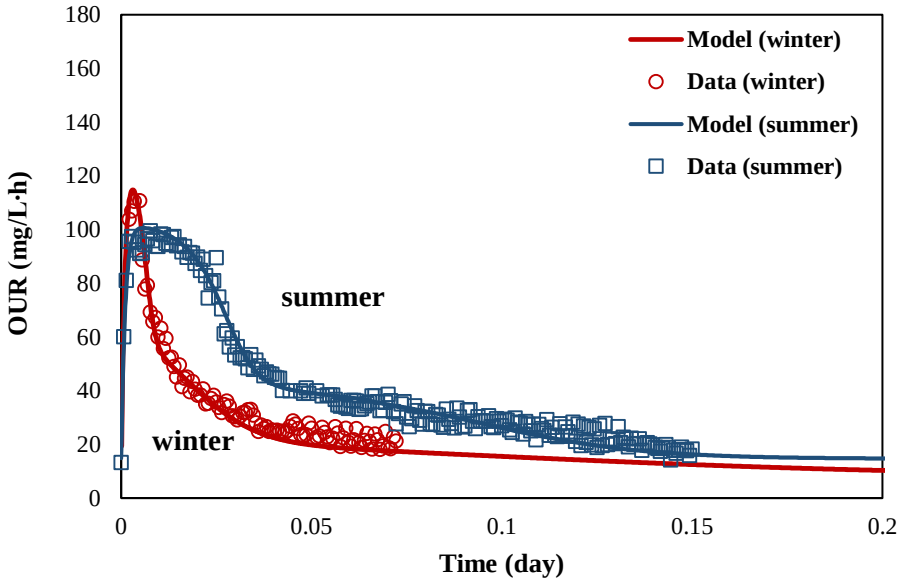

Figure 5.2 : Batch respirometric tests for P2.

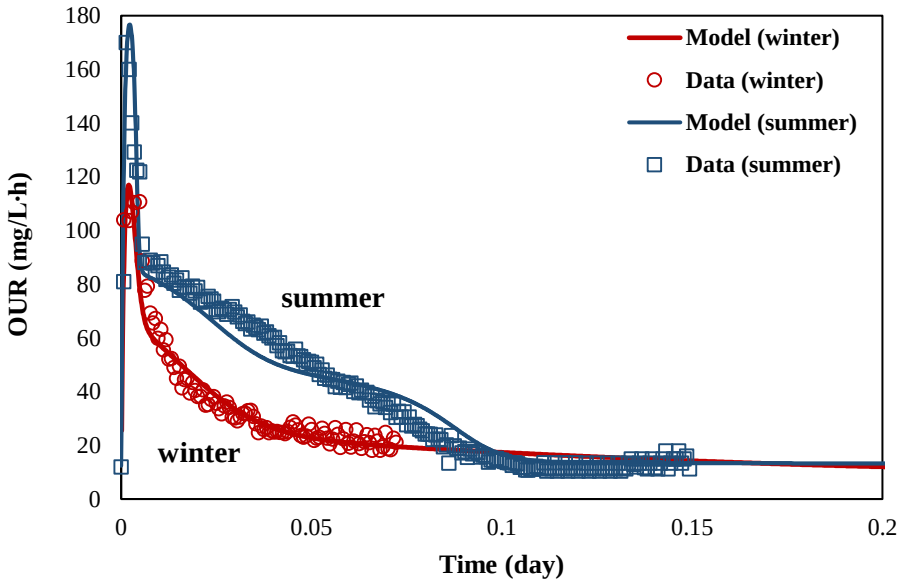

Figure 5.3 : Batch respirometric tests for P3.

Table 5.1 : Influent COD fractions (winter conditions).

Parameter	P1		P2		P3	
	mg/L	%	mg/L	%	mg/L	%
Total COD, C_T	405		430		470	
Soluble COD, S_T	120	30	115	27	135	29
Influent VFA, S_{VFA}	5	1	7	2	5	1
Fermentable COD, S_B	21	5	37	8	23	5
Hydrolysable COD, X_B	230	57	210	49	236	50
Colloidal COD, C_B	94	23	110	26	132	28
Total biodegradable COD, C_S	350	86	364	85	396	84
Soluble inert COD, S_{I1}	30	7	55	13	45	10
Particulate inert COD, X_{I1}	25	6	11	3	29	6

Table 5.2 : Influent COD fractions (summer conditions).

Parameter	P1		P2		P3	
	mg/L	%	mg/L	%	mg/L	%
Total COD, C_T	550		630		625	
Soluble COD, S_T	185	33.6	330	52.4	160	25.6
Influent VFA, S_{VFA}	6	1.1	11.2	1.8	8.4	1.3
Fermentable COD, S_B	14	2.5	44.8	7.1	31.6	5.1
Hydrolysable COD, X_B	310	56.4	320	50.8	354	56.5
Colloidal COD, C_B	160	29	150	23.8	140	22.4
Total biodegradable COD, C_S	490	89	526	83.5	534	85.3
Soluble inert COD, S_{I1}	28	5.1	62	9.8	42	6.7
Particulate inert COD, X_{I1}	32	5.8	42	6.7	49	7.8

The ratio of soluble inert COD to total wastewater COD was obtained as 6-13% in the wastewater treatment plants for the winter period. In comparison, this value ranges between 5% and 10% for the summer period, which is consistent with the literature. Henze et al. (2008) stated that the influent VFA/S_S ratio in typical domestic wastewater is 0.15. According to this ratio, the VFA levels for P1, P2, and P3 are in line with the literature.

The data obtained from respirometric analyses were used in the modeling and system identification method, as described in Insel et al. (2003), and the model results are presented in Table 5.3.

Table 5.3 : Estimated model parameters for P1, P2 and P3.

Parameter	Symbol	Unit	P1	P2	P3
Max. specific growth rate for OHOs	μ_{OHO}	day^{-1}	4.0	4.0	3.5
Decay rate for OHOs	b_{OHO}	day^{-1}	0.4	0.4	0.4
Half satur. of readily bio. for OHOs	$K_{SB,AS}$	g COD/m^3	5	5	10
Half satur. of O2 for OHOs	$K_{O2,OHO,AS}$	g O_2/m^3	0.35	0.20	0.20
Maximum hydrolysis rate	q_{HYD}	day^{-1}	1.1	1.4	1.8
Half saturation for hydrolysis	$K_{HYD,AS}$	g COD/g COD	0.06	0.06	0.06
Yield of OHOs on VFA (aerobic)	$Y_{OHO,VFA,ox}$	g COD/g COD	0.58	0.64	0.66

Based on the literature, the maximum specific growth rate and half saturation constant for domestic wastewater are reported as 2.0 – 6.6 day^{-1} and 3 – 20 mg COD/L, respectively (Henze et al. 2000; Henze et al., 2008; Ubay Çokgör et al., 1998). This study found that the modeling values were consistent with these literature values. The literature also suggests that the maximum hydrolysis rate in domestic wastewater is expected to be in the range of 1.5 – 4.7 day^{-1} (Henze et al. 2000; Henze et al., 2008; Ubay Çokgör et al., 1998). However, when comparing the maximum hydrolysis rates obtained in the study with the literature values, it was observed that they were low, particularly for P1 and P2 plants. The low hydrolysis rates obtained were also supported by the results of the NUR tests.

5.2 Determination of Nitrification and Denitrification Rates

5.2.1 Nitrate production rate

Determining nitrification rate and selecting the correct value is crucial for estimating the required aerobic sludge age and calculating the volume of the aerobic tank. In this context, a total of 6 nitrification tests were conducted in P1, P2 and P3 plants, with 2 tests in each plant representing both summer and winter periods. Representative sample days were selected for each WWTP using the data obtained from previous studies (İnsel et al., 2022; Sözen, 1995). The nitrification rate was determined by modeling the average values obtained from the tests estimated using the Solver tool of MS Excel (Equation 4.14).

The minimum temperature of 15°C was considered for the winter months and design temperature as specified in tender documents of wastewater treatment plants. The experimental and model results of the nitrate production rate tests performed under winter conditions for the P1, P2, and P3 plants are given in Figure 5.4, Figure 5.5 and Figure 5.6, respectively. For winter conditions, maximum autotrophic growth rates were calculated as 0.36, 0.30, and 0.30 day^{-1} for P1, P2 and P3, respectively. At 15°C, it was found that the maximum growth rates of the plants were very similar to each other. For the calculations, the decay rate of nitrifying bacteria was accepted as 0.1 day^{-1} (Güneş et al., 2018).

When compared with other examples in the world, it was observed that the nitrification rates of P1, P2, and P3 plants were quite low (Figure 5.7). The maximum autotrophic growth rate ($\mu_{A,max}$) at a process temperature of 15°C was reportedly 0.64 day^{-1} in the USA (Melcer et al., 2003) and 0.65 day^{-1} in Europe (Henze et al., 2000; Wichern et al., 2003). In particular, the average maximum growth rate of six different full-scale wastewater treatment plants in Germany was reported as $\mu_{A,max}$ 0.73 day^{-1} for 15°C (Wichern et al., 2003). Overall, the data suggests that the nitrification rates in the three plants are relatively low when compared to other examples worldwide.

When the maximum growth rate measured in the plants in Germany is compared with the values measured in the wastewater treatment plants in the region, it is noteworthy that the rate in Germany is 2.0-2.5 times higher. It is thought that this is mainly due to the difference in the character of urban wastewater coming to the treatment plant due

to the difference in wastewater sources discharged to the sewerage system in Europe and Turkey.

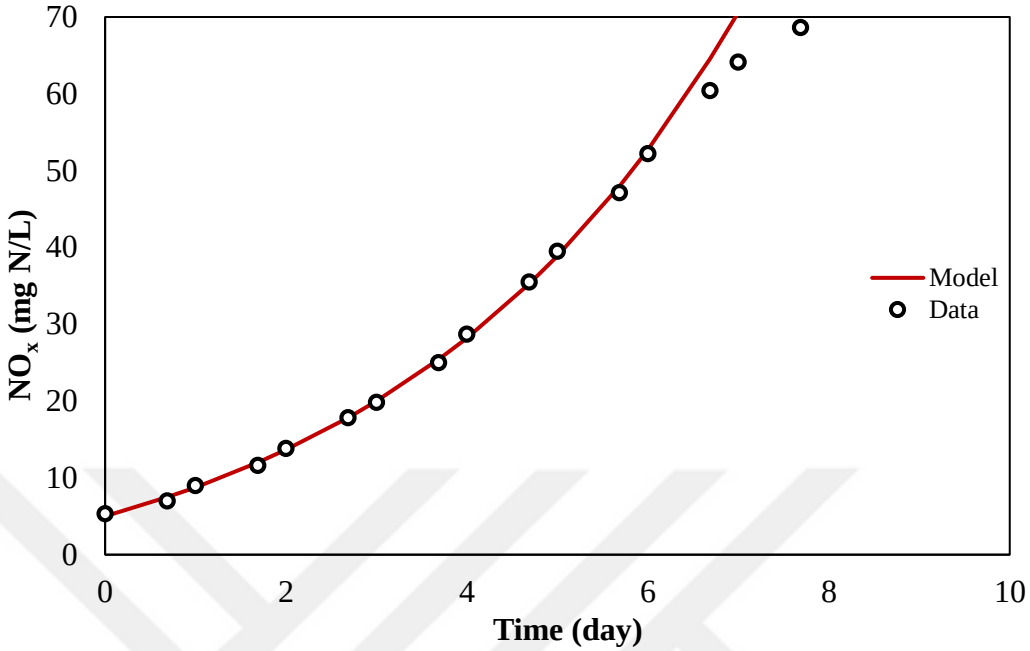

Figure 5.4 : Nitrate production profile for P1 (winter conditions).

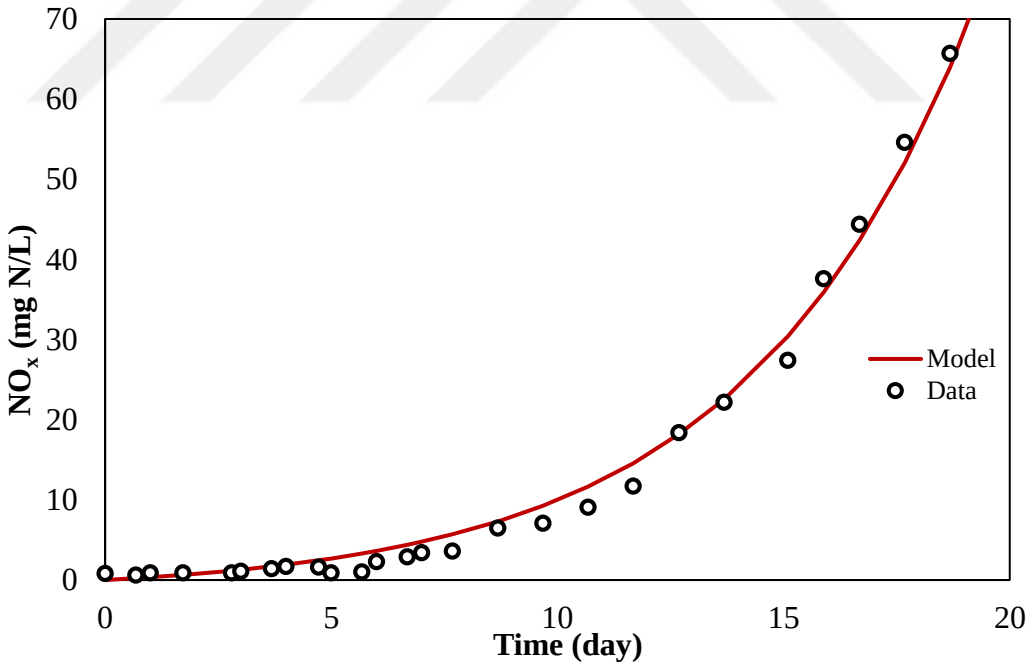

Figure 5.5 : Nitrate production profile for P2 (winter conditions).

As expected, the nitritification rate decreases with decreasing temperature in winter. It was observed that nitrate production tests carried out for winter conditions completed in 10 days (20 days for the P2 plant), while for summer conditions this duration is far lower (3–4 days).

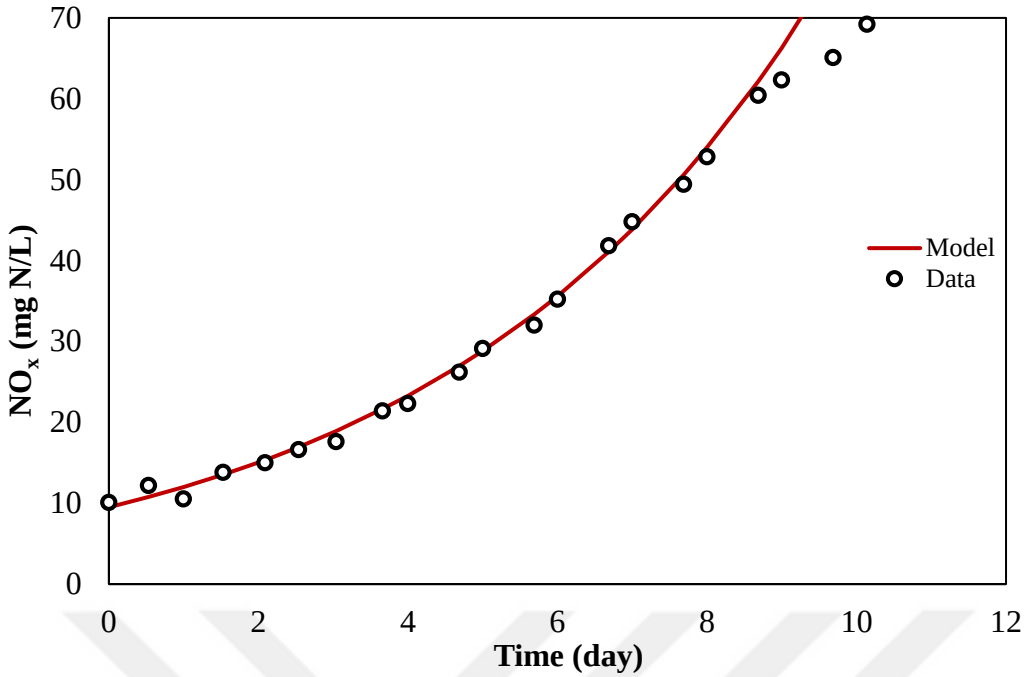

Figure 5.6 : Nitrate production profile for P3 (winter conditions).

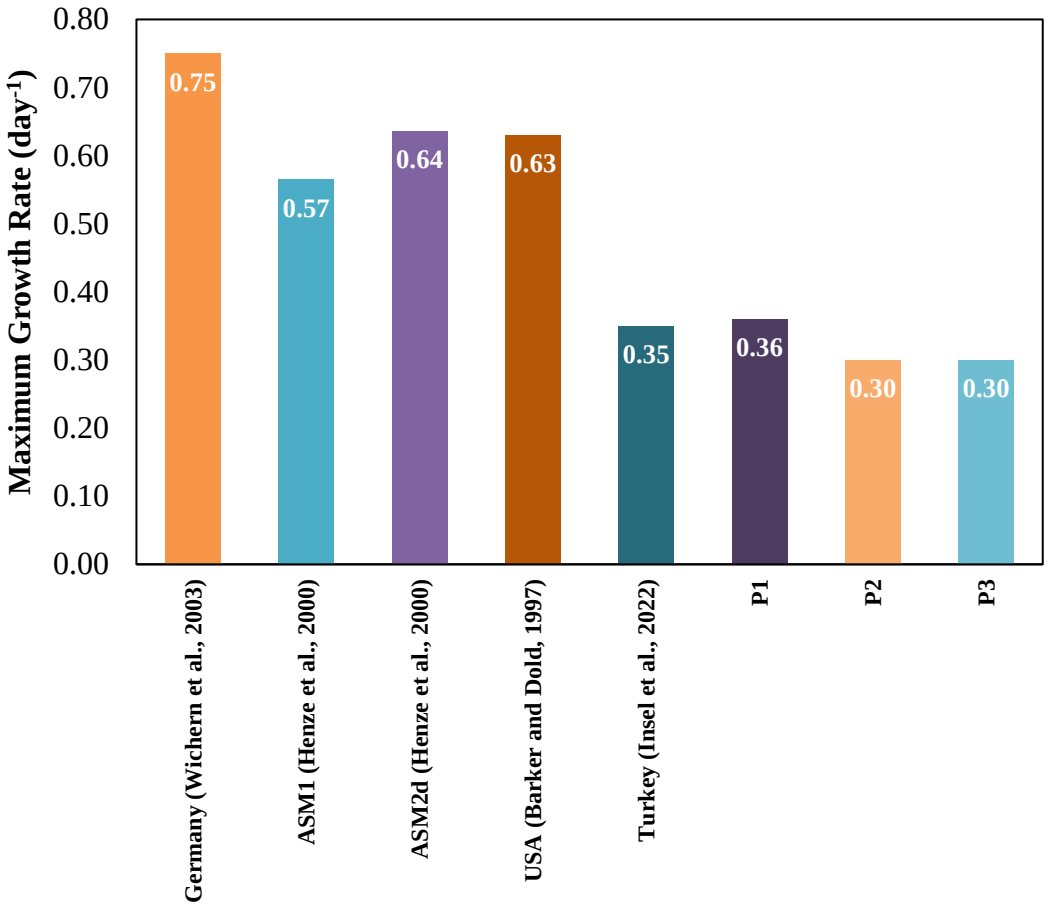

Figure 5.7 : Maximum autotrophic growth rates (15°C).

The tests for determining the nitrification rate for the summer period were conducted at 25°C, representing the average water temperature during the summer months. The experimental and model results of the nitrate production rate tests performed under summer conditions for the P1, P2, and P3 plants are given in Figure 5.8, Figure 5.9 and Figure 5.10, respectively. For summer conditions, maximum autotrophic growth rates were calculated as 0.95, 0.90 and 0.75 day^{-1} for P1, P2 and P3, respectively. Similar to the 15°C results, it was found that the maximum growth rates of the plants were very similar to each other at 25°C, too. For the calculations, the decay rate of nitrifying bacteria was accepted as 0.2 day^{-1}.

Compared to other examples in the world, nitrification rates of P1, P2 and P3 plants are quite low. It is understood that the maximum autotrophic growth rate ($\mu_{A,max}$) at a process temperature of 25 °C is 1.5 day^{-1} in USA (Melcer et al., 2003) and 1.2 day^{-1} in Europe (Henze et al., 2000; Wichern et al., 2003). In particular, the average maximum growth rate of 6 different full-scale wastewater treatment plants in Germany was reported to be 1.6 day^{-1} for 25°C (Wichern et al., 2003).

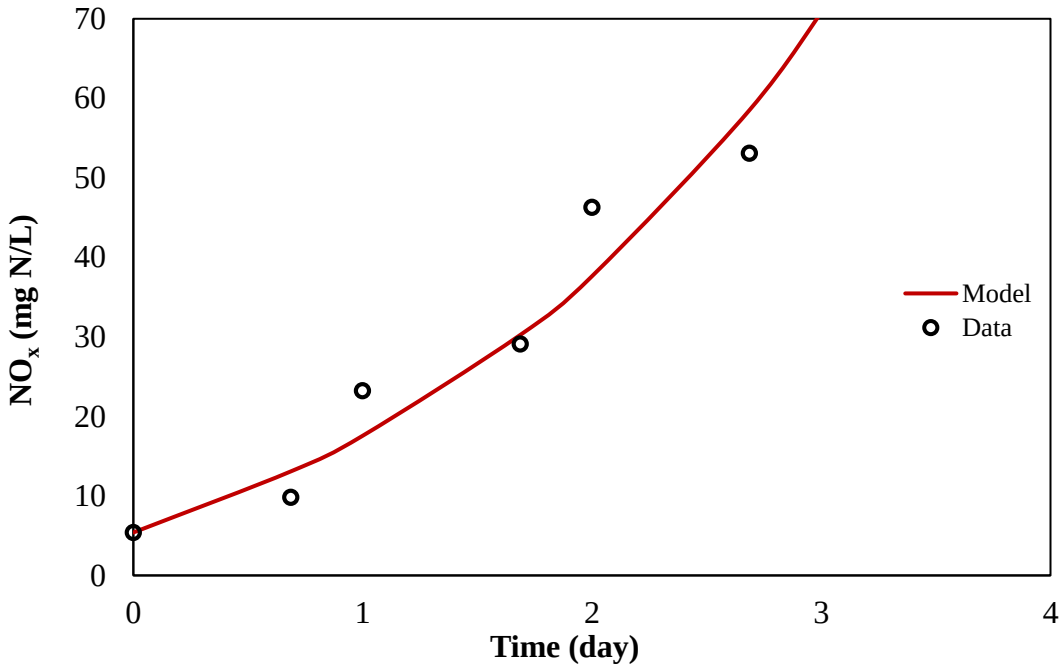

Figure 5.8 : Nitrate production profile for P1 (summer conditions).

When the maximum growth rate measured in the plants in Germany is compared with the values measured in the wastewater treatment plants in the region, it is noteworthy that the rate in Germany is 1.60 – 2.15 times higher. It is thought that this is mainly due to the difference in the character of urban wastewater coming to the treatment plant

due to the difference in wastewater sources discharged to the sewerage system in Europe and Turkey.

Studies conducted at related WWTPs in Turkey since 1995 have shown that autotrophic growth rates have been consistently low. These studies reported that the heavy inflow of industrial wastewater to the WWTPs has significantly affected the autotrophic growth rates. The presence of industrial wastewater introduces various complex and potentially inhibitory substances into the treatment systems, which can hinder the growth and activity of autotrophic microorganisms (İnsel et al., 2022; Sözen et al., 2008; Sözen et al., 1998; Sözen et al., 1996; Sözen, 1995).

To achieve complete nitrification in the current single sludge activated sludge configurations at the plants, a higher sludge age than the design sludge age accepted in the ATV-131 (2000) standards is needed. This means that an aerobic volume approximately 2.0 – 2.5 times higher is required.

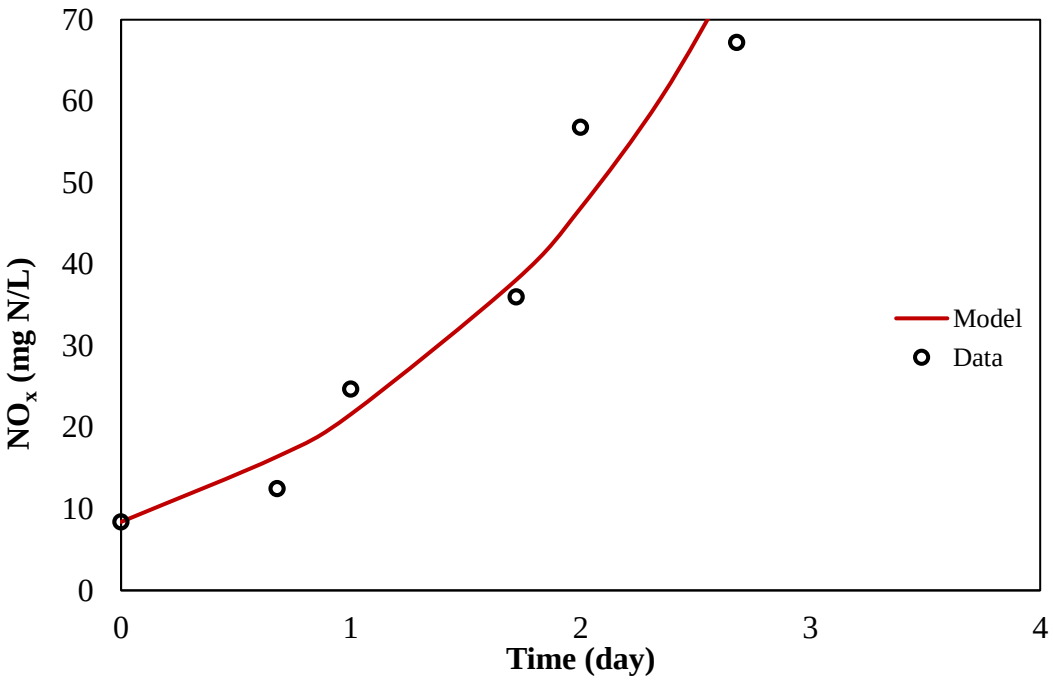

Figure 5.9 : Nitrate production profile for P2 (summer conditions).

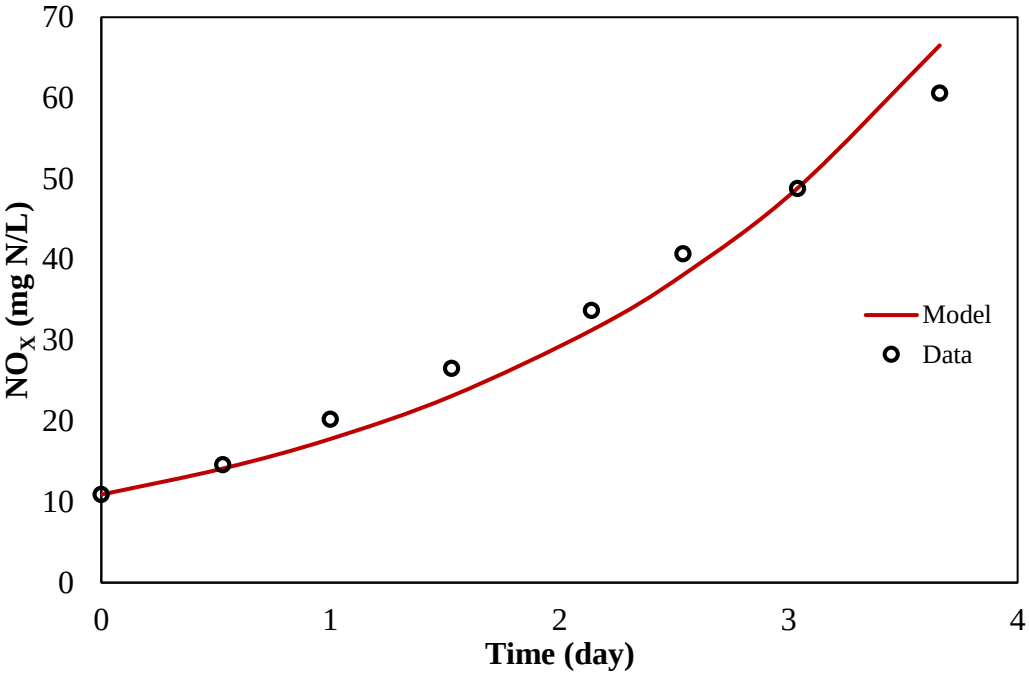

Figure 5.10 : Nitrate production profile for P3 (summer conditions).

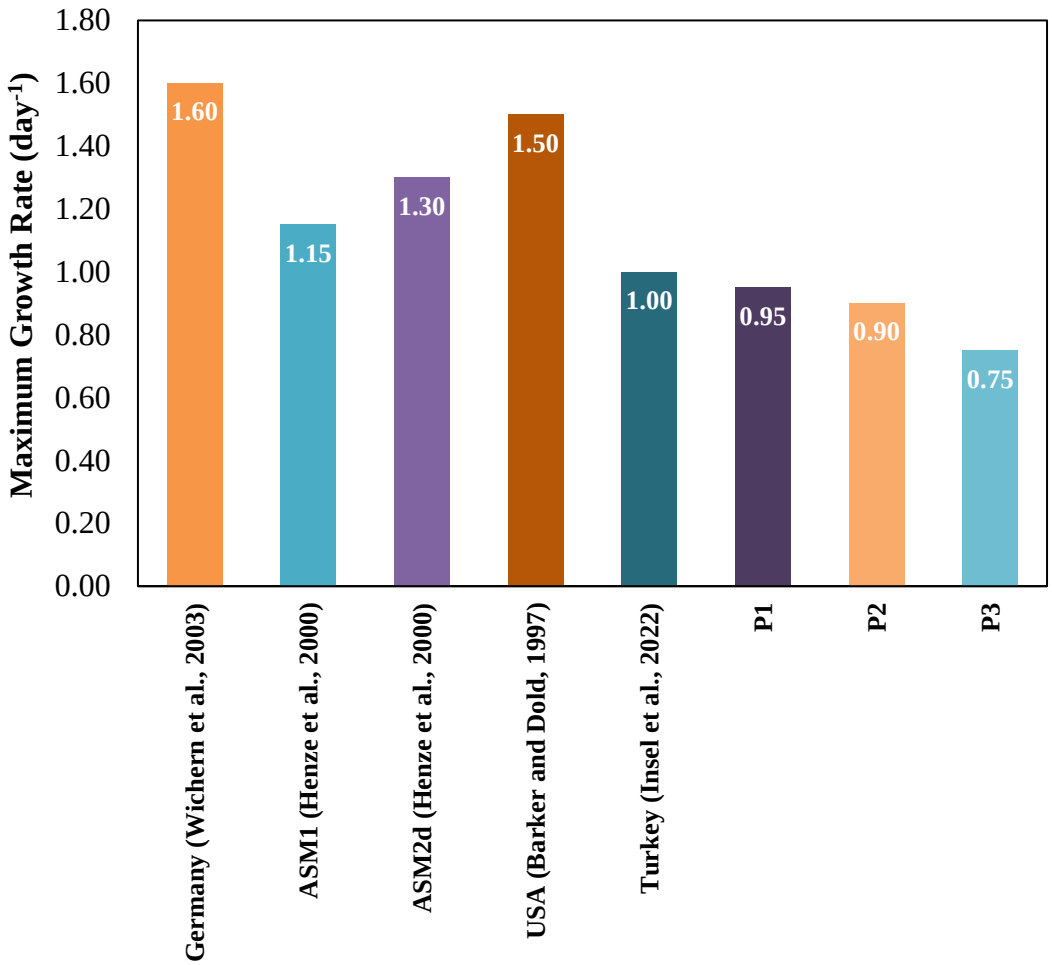

Figure 5.11 : Maximum autotrophic growth rates (25°C).

5.2.2 Nitrate utilization rate

As in carbon removal, heterotrophic microorganisms are involved in the denitrification process. Most biological wastewater treatment plants remove both nitrogen and carbon, so it's crucial to determine the kinetic coefficients of these microorganisms in both aerobic and anoxic environments. To design an effective system, it's also important to consider the adaptation of microorganisms and the change in their maximum growth rate during the transition from an oxygenated environment (where carbon removal occurs) to an anoxic environment (where nitrogen removal takes place). Respirometric measurements are a common method used to determine growth rates.

The NO_3-N and NO_2-N profiles obtained in the denitrification rate determination experiments for P1 in winter conditions are presented in Figure 5.12. As can be seen from the figure, while almost all of the nitrate is consumed within 200 minutes, it is seen that some of the nitrate is reduced during this time to cause the accumulation of approximately 10 mg NO_2-N/L nitrite. It is seen that the nitrite formed does not remain in the environment and is consumed until the end of the experiment. In this way, it can be said that all of the approximately 24 mg NO_3-N/L nitrate in the system was reduced.

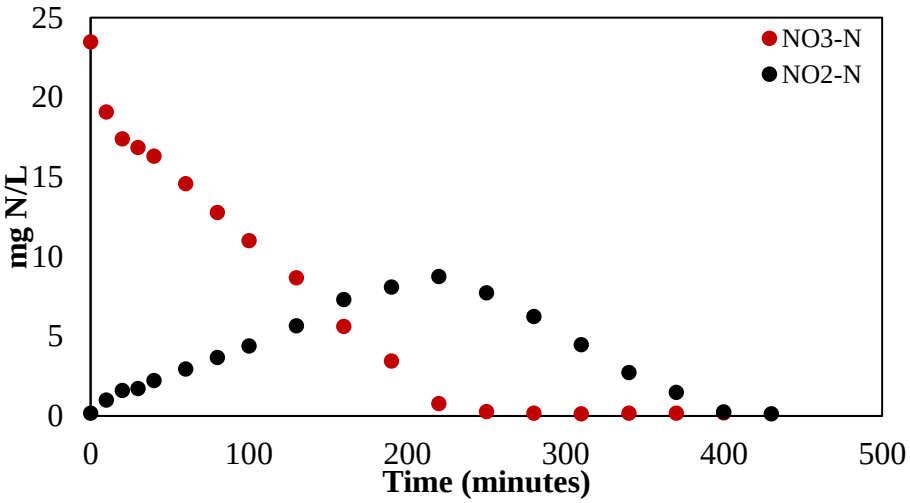

Figure 5.12 : Nitrate and nitrite profiles during NUR test for P1 (winter period).

The results of the NUR test conducted for P2 under winter conditions are presented in Figure 5.13. The test showed that all of the 16 mg/L nitrate nitrogen was used up in about 300 minutes. An intermediate product of nitrate reduction, approximately 10 mg N/L nitrite accumulation, was detected. During the experiment, around 5 mg N/L of the accumulated nitrite was reduced, while 5 mg N/L remained in the medium without

being used. It is possible to say that this is mostly due to the type of organic matter and microbial culture in the wastewater because the amount of carbon supplied to the medium during this experiment was not limited.

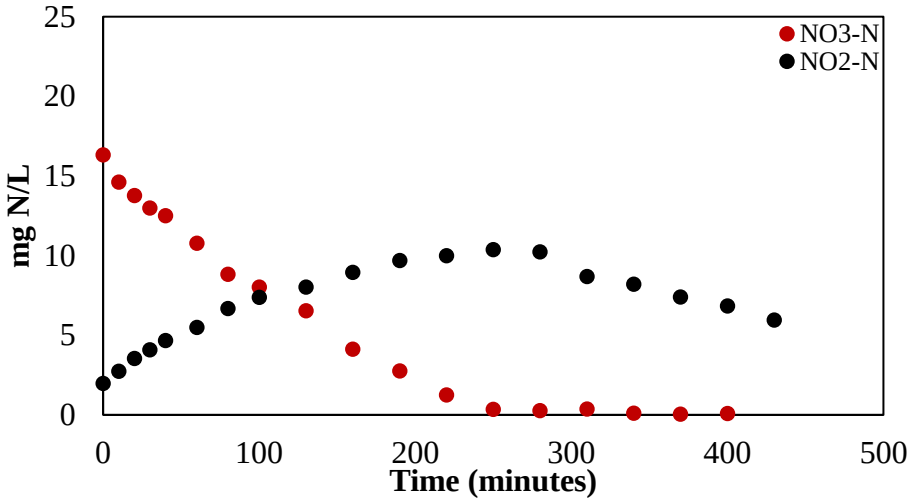

Figure 5.13 : Nitrate and nitrite profiles during NUR test for P2 (winter period).

The results of the denitrification rate determination test for P3 during the winter period are presented in Figure 5.14. During the experiment, approximately 76 mg N/L nitrate in the medium could not be completely reduced and 35 mg N/L nitrate remained in the medium at the end of the experiment. During the experiment, no significant amount of nitrite formation was observed and no nitrite accumulated in the medium.

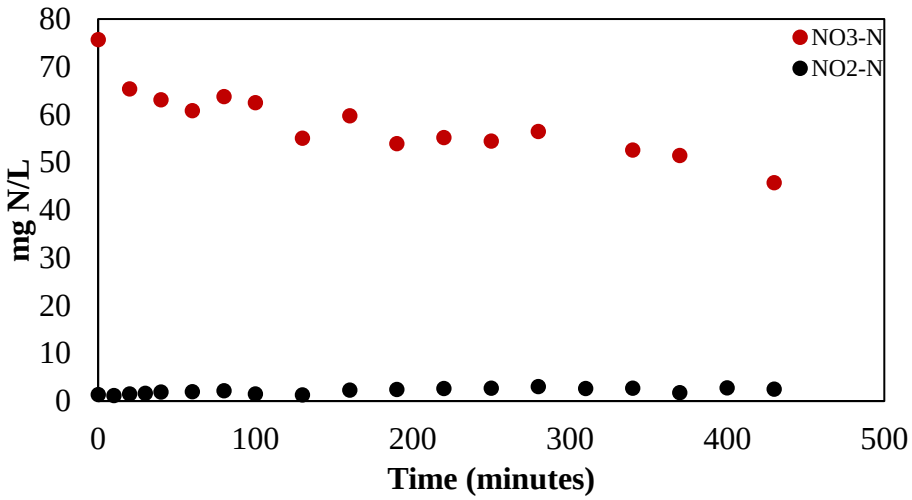

Figure 5.14 : Nitrate and nitrite profiles during NUR test for P3 (winter period).

The same set of NUR experiments was repeated for P1, P2, and P3 during the summer period.

The results of nitrate utilization rate experiments conducted for P1 during the summer period are shown in Figure 5.15. The figure indicates that out of 68 mg N/L nitrate, approximately 20 mg/L was reduced, leaving behind 45 mg N/L nitrate nitrogen. During the experiment, a small portion of nitrate was converted into nitrite, leading to the accumulation of nitrite nitrogen (approximately 5 mg N/L).

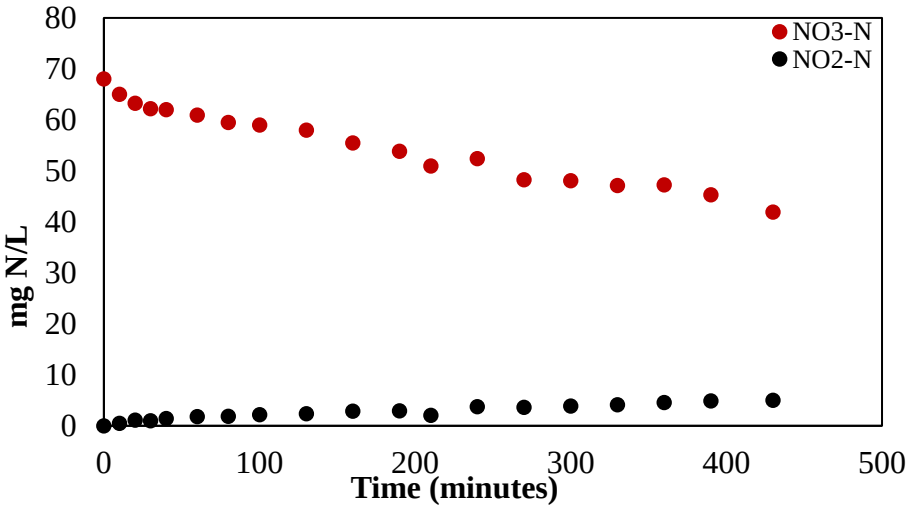

Figure 5.15 : Nitrate and nitrite profiles during NUR test for P1 (summer period).

The results of the NUR test carried out on P2 during the summer are shown in Figure 5.16. The test reduced 32 mg N/L nitrate, leaving 41 mg N/L nitrate nitrogen in the medium. As an intermediate product of the denitrification process, around 12 mg N/L nitrite nitrogen accumulation was detected and not reduced. This outcome is mainly due to the type of organic matter and microbial culture present in the wastewater.

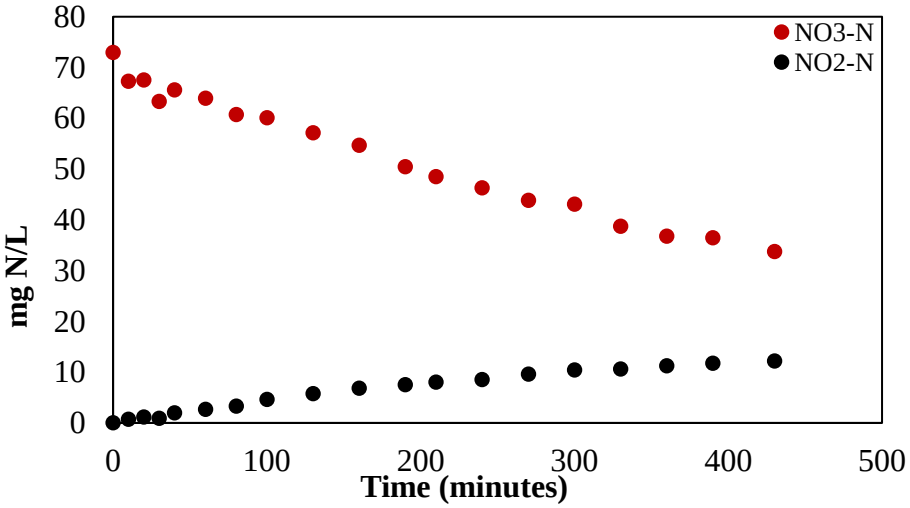

Figure 5.16 : Nitrate and nitrite profiles during NUR test for P2 (summer period).

The results of the NUR test conducted for P3, which represents the summer period, are illustrated in Figure 5.17. The experiment carried out for 430 minutes revealed that

around 72 mg of NO_3-N/L nitrate in the medium could not be reduced. Furthermore, 48 mg N/L nitrate nitrogen remained at the end of the experiment. During the experiment, a small amount of nitrite formation (3.86 mg N/L) was observed in the medium, which remained in the medium without undergoing any reduction.

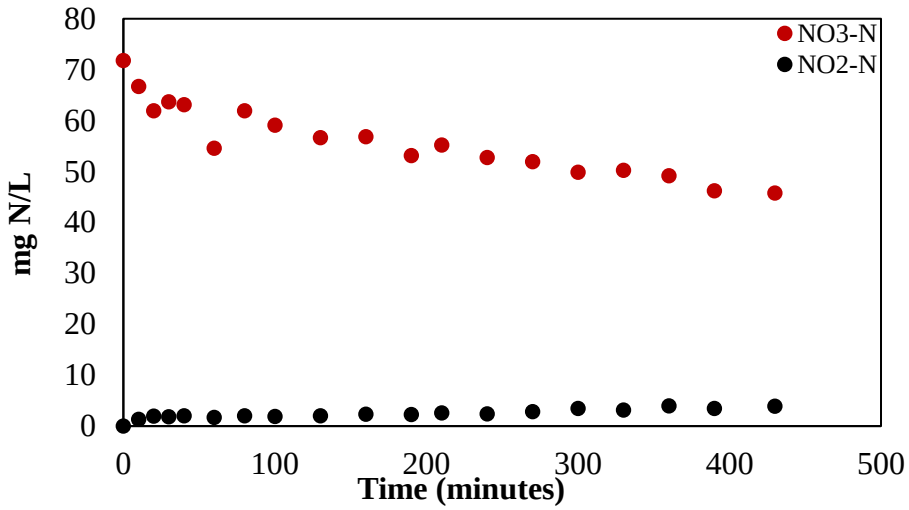

Figure 5.17 : Nitrate and nitrite profiles during NUR test for P3 (summer period).

With the data obtained in the tests, NUR profiles were created considering the nitrite-nitrate electron balance as described in Sözen et al. (1998). The denitrification rate constants depending on the COD fraction of the wastewater on the NUR profiles obtained on plant basis are shown in Figure 5.18, Figure 5.19, and Figure 5.20 for K_1, K_2 and K_3 winter period experiments. Here, K_1 represents the rate obtained in the phase where easily biodegradable organic matter is consumed, K_2 represents the rate obtained in the phase where rapidly hydrolysable organic matter is consumed, K_3 represents the rate obtained in the phase where slowly hydrolysable organic matter is consumed. Table 5.4 presents the calculated denitrification rate constants for each plant.

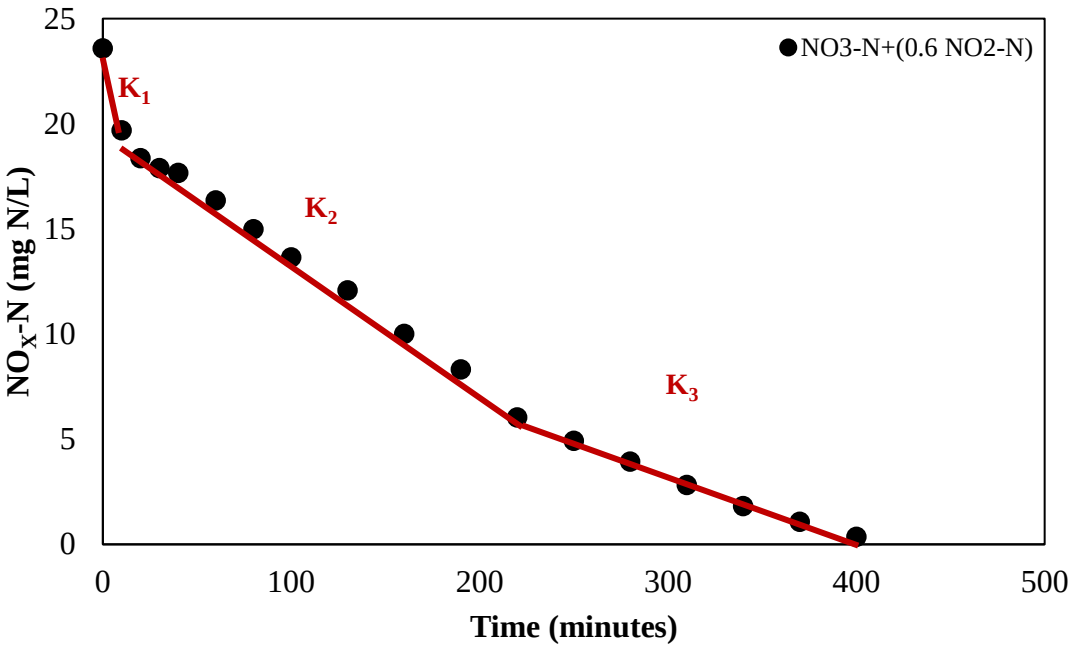

Figure 5.18 : NUR profile and denitrification rate constants for P1 (winter period).

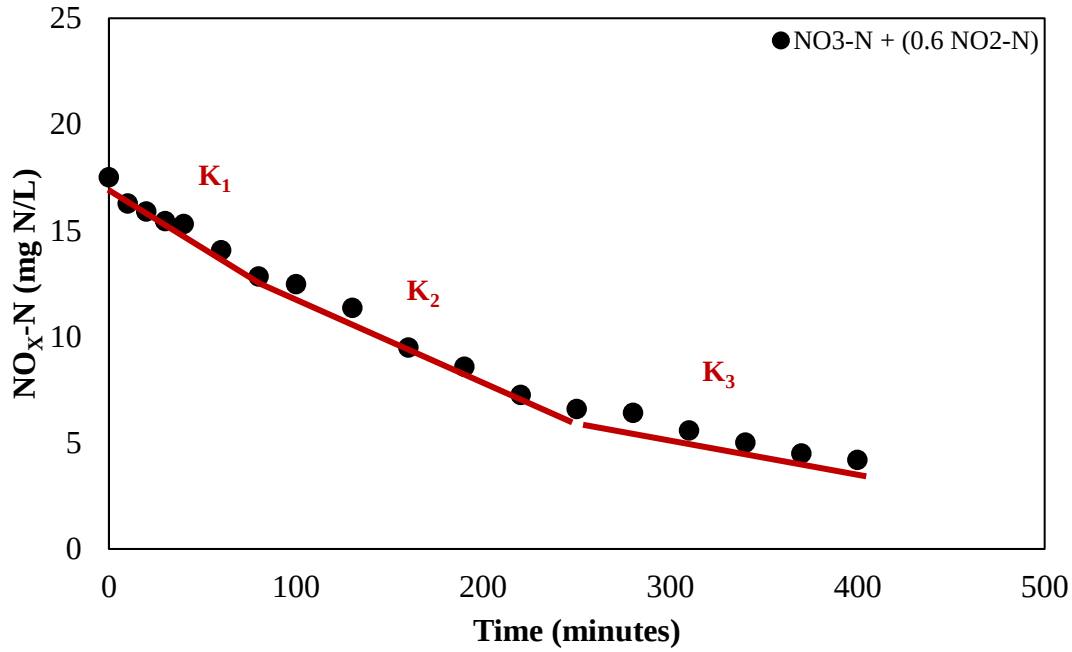

Figure 5.19 : NUR profile and denitrification rate constants for P2 (winter period).

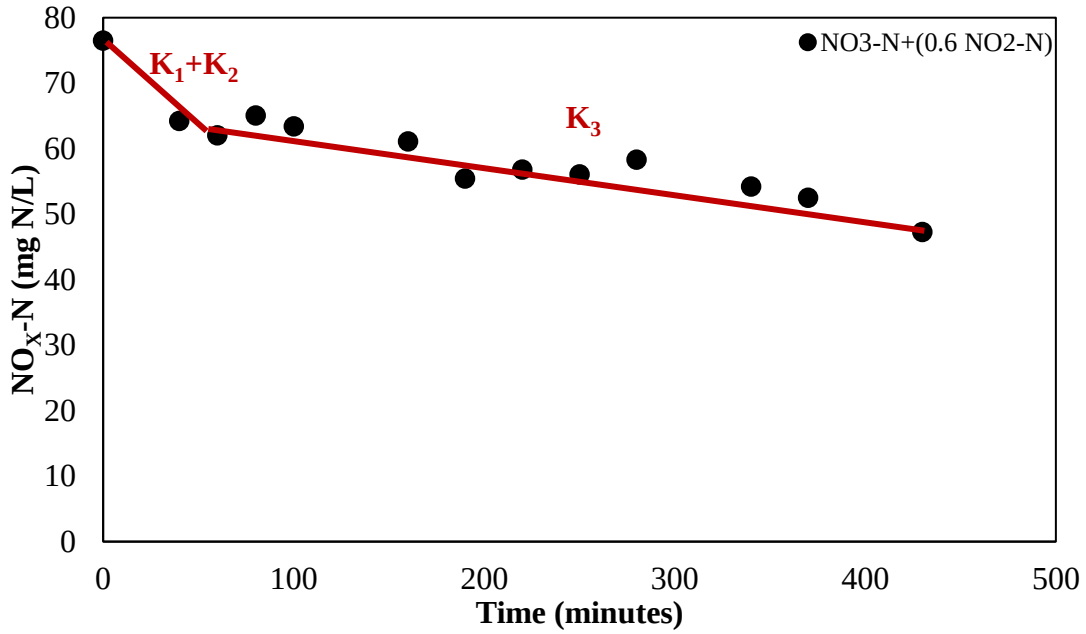

Figure 5.20 : NUR profile and denitrification rate constants for P3 (winter period).

The NUR profiles obtained for plants P1, P2, and P3 during the summer period experiments are shown in Figure 5.21, Figure 5.22 and Figure 5.23. K_1 represents the rate obtained during the phase where easily biodegradable organic matter is consumed, K_2 represents the rate obtained during the phase where rapidly hydrolysable organic matter is consumed, and K_3 represents the rate obtained during the phase where slowly hydrolysable organic matter is consumed. Table 5.4 presents the calculated denitrification rate constants for each plant.

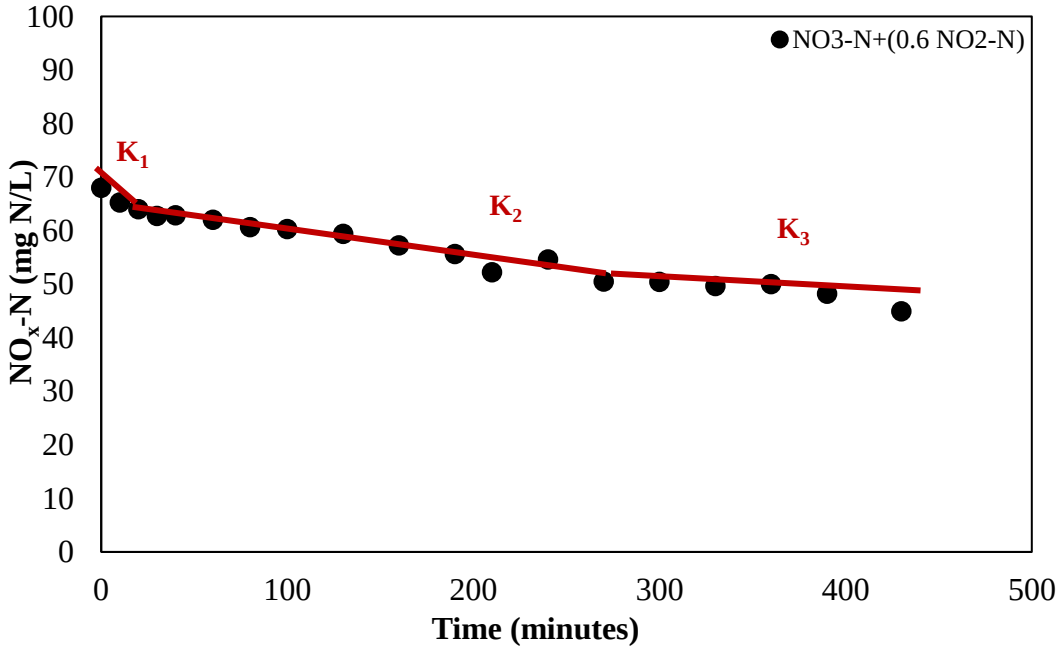

Figure 5.21 : NUR profile and denitrification rate constants for P1 (summer period).

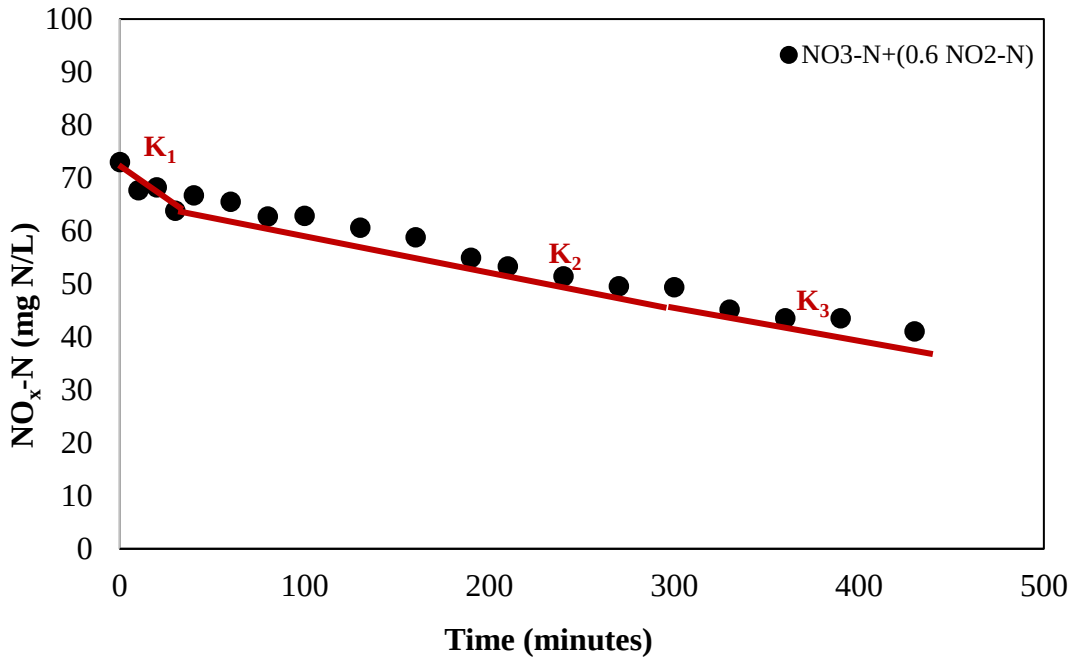

Figure 5.22 : NUR profile and denitrification rate constants for P2 (summer period).

In the experiments conducted during the winter period, as shown in Table 5.4, it can be observed that the denitrification process in P3 plant occurred with two rate constants (K_1+K_2 and K_3), while in P1 and P2 plants, the same process was observed with three rate constants (K_1, K_2, and K_3).

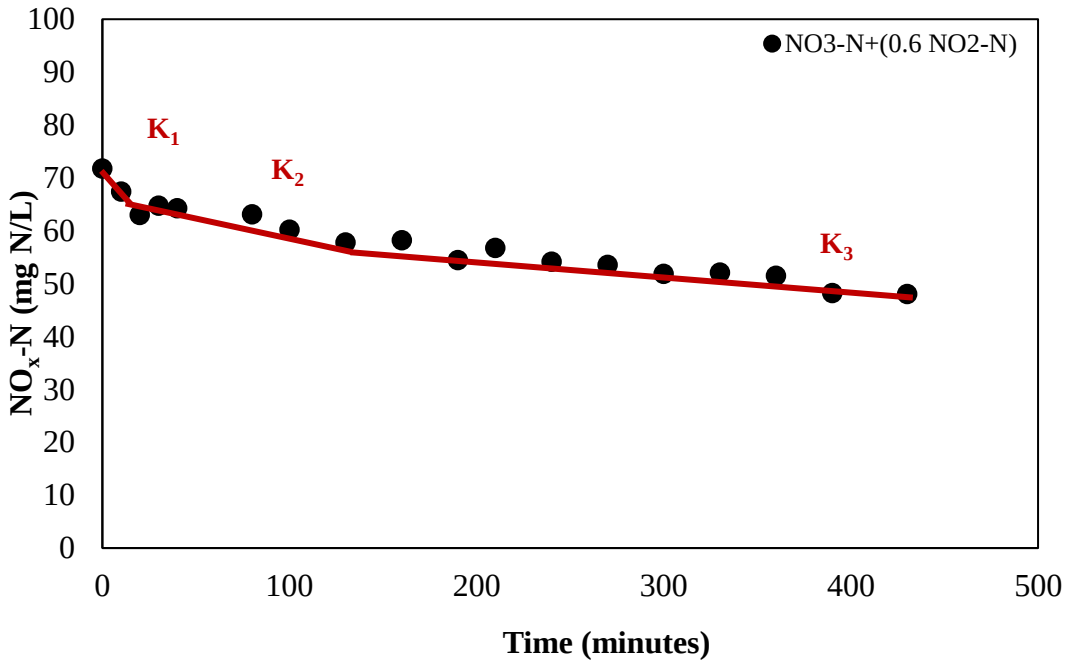

Figure 5.23 : NUR profile and denitrification rate constants for P3 (summer period).

Table 5.4 : Denitrification rate constants.

Rate Constant	Winter Period			Literature	
mg N/g VSS·hour	**P1**	**P2**	**P3**	**Sözen et al., 1998**	**Van Haandel et al., 1982**
K_1	12.00	2.33	10.70*	5.50 – 30.25	34.20
K_2	2.00	1.10	-	2.75 – 20.90	4.30
K_3	1.08	0.47	1.70	2.75 – 10.45	3.20
Summer Period					
K_1	7.04	14.20	16.26		
K_2	1.54	4.48	3.02		
K_3	0.50	2.19	1.22		

Depending on the different wastewater characteristics of the plants, anoxic biodegradation occurs at different rates. For this reason, the denitrification rates obtained in the plants can also differ. When the denitrification rates for each plant are compared, it is seen that the denitrification rates are close to each other except for P2 for the winter period. When the K_1 rates for each plant for the summer period are compared, it is seen that the highest rate is realized as 16.26 and 14.20 for P2 and P3 plants, respectively, while it is calculated as 7.4 for P1. As seen from the respirometric tests, it was determined that the characteristic of the influent wastewater of P1 plant is relatively low in easily biodegradable substrate content.

On the other hand, when the findings are compared with the values in the literature, it is observed that the K_1 value for P1 and P3 plants is within the range given by Sözen et al. (1998) and Van Haandel et al. (1982), while the K_1 value obtained for P2 in the experiments conducted in the winter period was below the lower limit of this range. In the P2 plant, the nitrification process does not occur for about ten months during the year. Therefore, the denitrification process does not take place during this period. In this respect, the low measured denitrification rate can be expected. The purpose of the NUR tests is to determine the denitrification rates, and therefore, the test procedure requires a limited test period. This time does not reflect the actual hydraulic retention time of the treatment plant; nitrite remaining in the environment can be consumed entirely and not accumulate unless there is a carbon constraint. Therefore, the actual situation regarding nitrite accumulation in the plants can only be revealed by measuring the nitrogen components in the instantaneous samples taken from the reactors in the plants.

The plants are suffering from low nitrification rates compared to that of design values. So, the plants will require considerable process upgrades and/or modifications.

5.3 Anaerobic Batch Tests

Specific methanogenic activity and biochemical methane potential of biological sludges, representing the anaerobic digester of P1, P2, and P3, were measured in laboratory-scale batch anaerobic reactors. The SMA test is used to monitor the anaerobic digester's performance by measuring the activity of acetoclastic microorganisms. The difference between the amount of methane production from the control reactor versus the methane production in sets with acetate added is considered as net methane production. When this value is converted to the amount of methane produced per unit of time, the SMA value is obtained. SMA profiles belonging to P1, P2, and P3 are presented in Figure 5.24**,** Figure 5.25**,** and Figure 5.26, respectively.

The maximum SMA level for all 3 plants was reached within 5 days. Accordingly, SMA values for the sludges of P1, P2, and P3, were calculated as 70, 50, and 75 L CH_4/kg VSS/day, respectively. The Sumo1 model was used to determine the kinetics of acetoclastic methanogens by using the methane data as shown in Figure 5.24**,** Figure 5.25**,** and Figure 5.26.

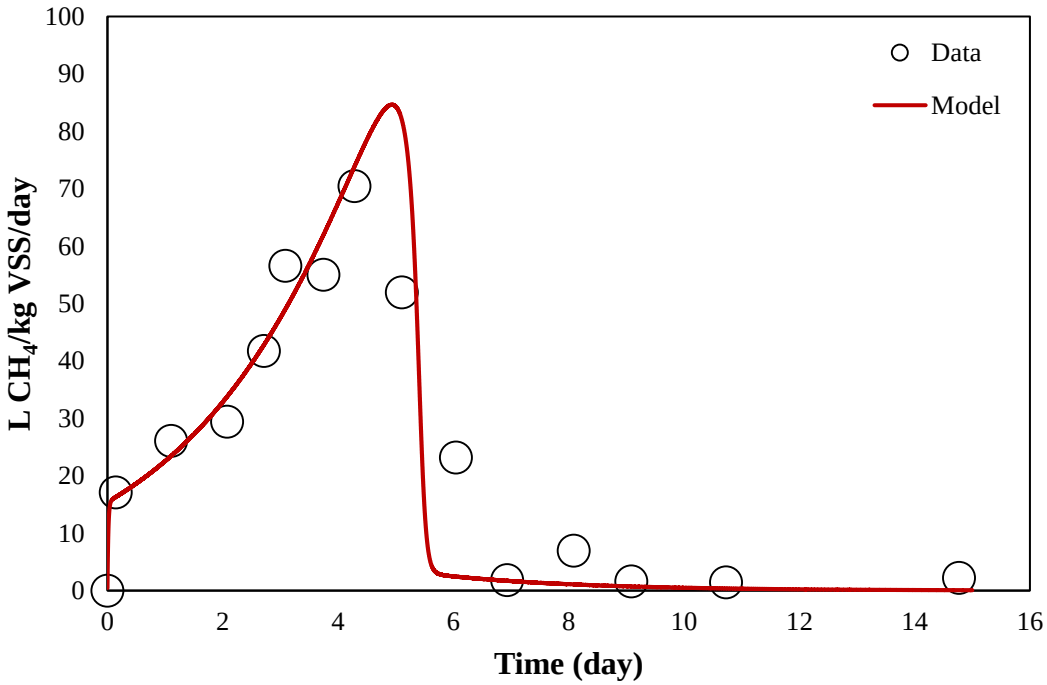

Figure 5.24 : Methanogenic activities for P1.

The objective was to identify whether the biogas production rate is limited by methanogenesis or not. As the obtained process kinetics are quite close to the default values, one can conclude that biogas production is not limited by methanogenesis, but

by hydrolysis. The lowest SMA level was determined for P2, which has approximately 30% lower activity compared to the other plants.

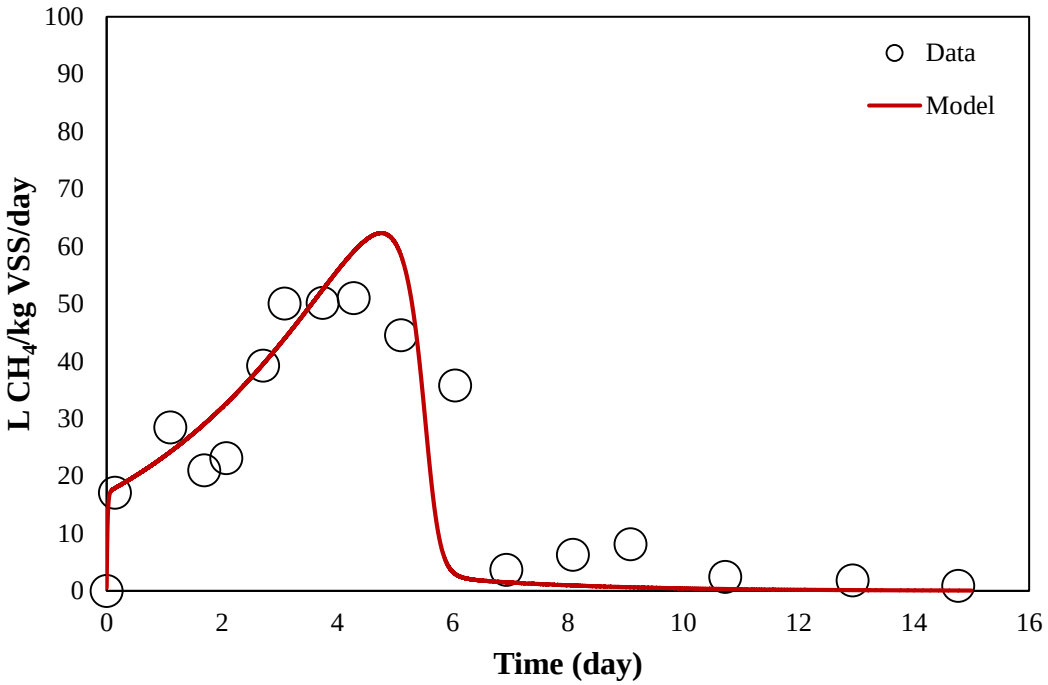

Figure 5.25 : Methanogenic activities for P2.

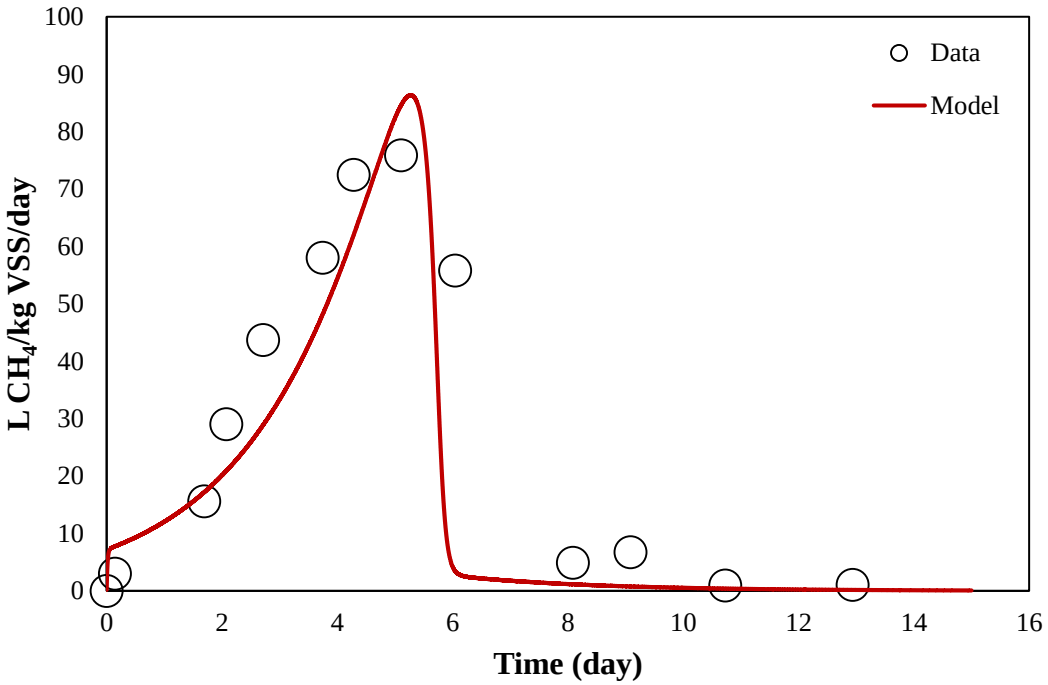

Figure 5.26 : Methanogenic activities for P3.

The cumulative methane productions belonging to P1, P2, and P3 are shown in Figure 5.27 and Figure 5.28 with both the Modified-Gompertz model and first-order kinetics

model, respectively. The Modified-Gompertz model has been widely used to predict methane production of anaerobic digestion systems (Etuwe et al. 2016). The maximum methane production rate (R_m) and maximum biogas yield potential (y_m) parameters of the Modified-Gompertz model were estimated using the Solver tool of MS Excel. For plants labeled as P1, P2, and P3, the R_m parameter was calculated as 30, 22, and 50 L CH_4/kg VS/day and the y_m parameter was calculated as 320, 195, and 230 L CH_4/kg VS, respectively (Figure 5.27). The highest R_m and y_m values were obtained for the plants encoded with P3 and P1. Similar values were reported by Donoso-Bravo et al. (2010) for R_m and y_m as 35.5 L/kg VS/day and 243.5 L/kg VS, for secondary sludge and by Ortega-Martinez et al. (2016) as 27.5 L/kg VS/day and 250 L/kg VS for mixed sludge, respectively. Biochemial methane potential data was also modeled with the first-order kinetics as compared to the Modified-Gompertz model (Figure 5.28**)**. The rate constants for BMP tests of P1, P2, and P3 were estimated to be 0.15, 0.13, and 0.29 day^{-1}, respectively. Similar results ranging from 0.166 day^{-1} to 0.22 day^{-1} were reported for secondary sludge in the literature (Donoso-Bravo et al., 2010; Mahmoud et al., 2023).

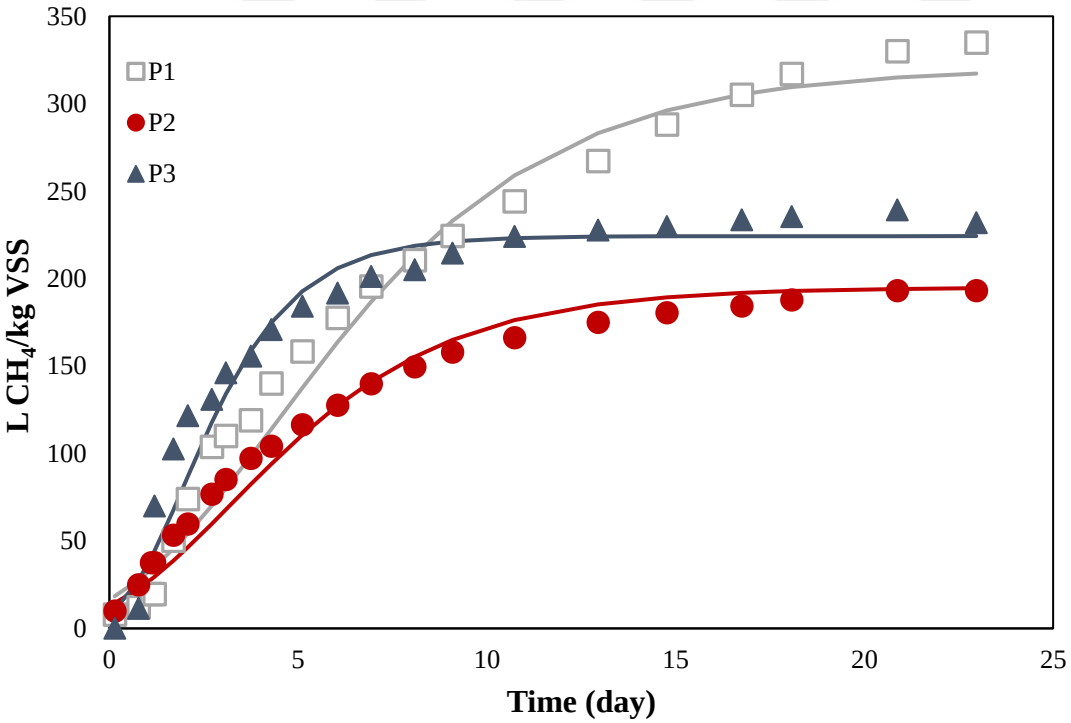

Figure 5.27 : Cumulative methane profiles with Modified-Gompertz model.

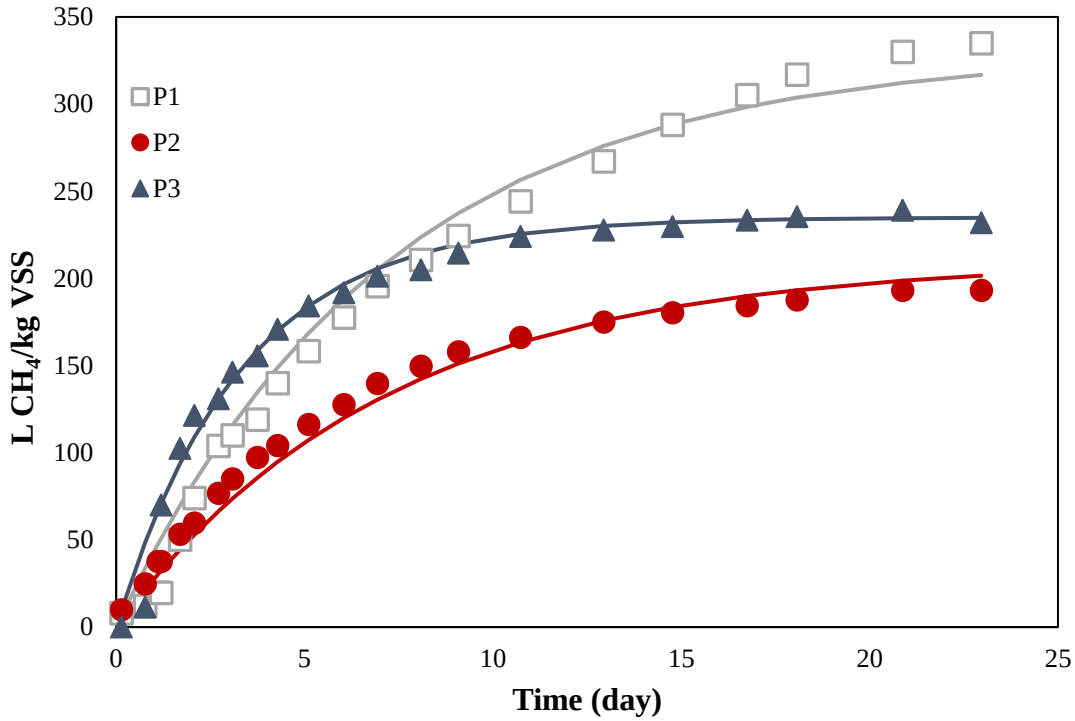

Figure 5.28 : Cumulative methane profiles with first order kinetics.

In the literature, the cumulative methane production is given as 200 L CH_4/kg VS_{fed} for low biodegradable sludge. However, for highly biodegradable sludge, this value can reach up to 420 L CH_4/kg VS_{fed}. Previous studies have shown an average range of methane potential measurements of 365-470 L CH_4/kg VS_{fed} (Bourgier et al., 2007; Cano et al., 2015; Kor, 2019; Koupaie and Eskicioglu et al., 2016). The maximum methane potential value that can be achieved is 550 L CH_4/kg VS_{fed} (Metcalf and Eddy, 2014; Rosenthal, 2020). To compare the cumulative methane potential measurements of the plants with those in literature, their capacity and biodegradability rate were considered (Figure 5.29). As a result, it was found that the feed sludge taken from the anaerobic digesters of the P1 plant has a high methane generation capacity but is slowly biodegradable sludge. On the other hand, the feed sludge of the P2 plant has a low methane production capacity but has fast biodegradable characteristics. Similarly, the feed sludge in the anaerobic digesters of the P3 plant has a low level of methane production capacity, but it is a sludge with a very fast biodegradable structure.

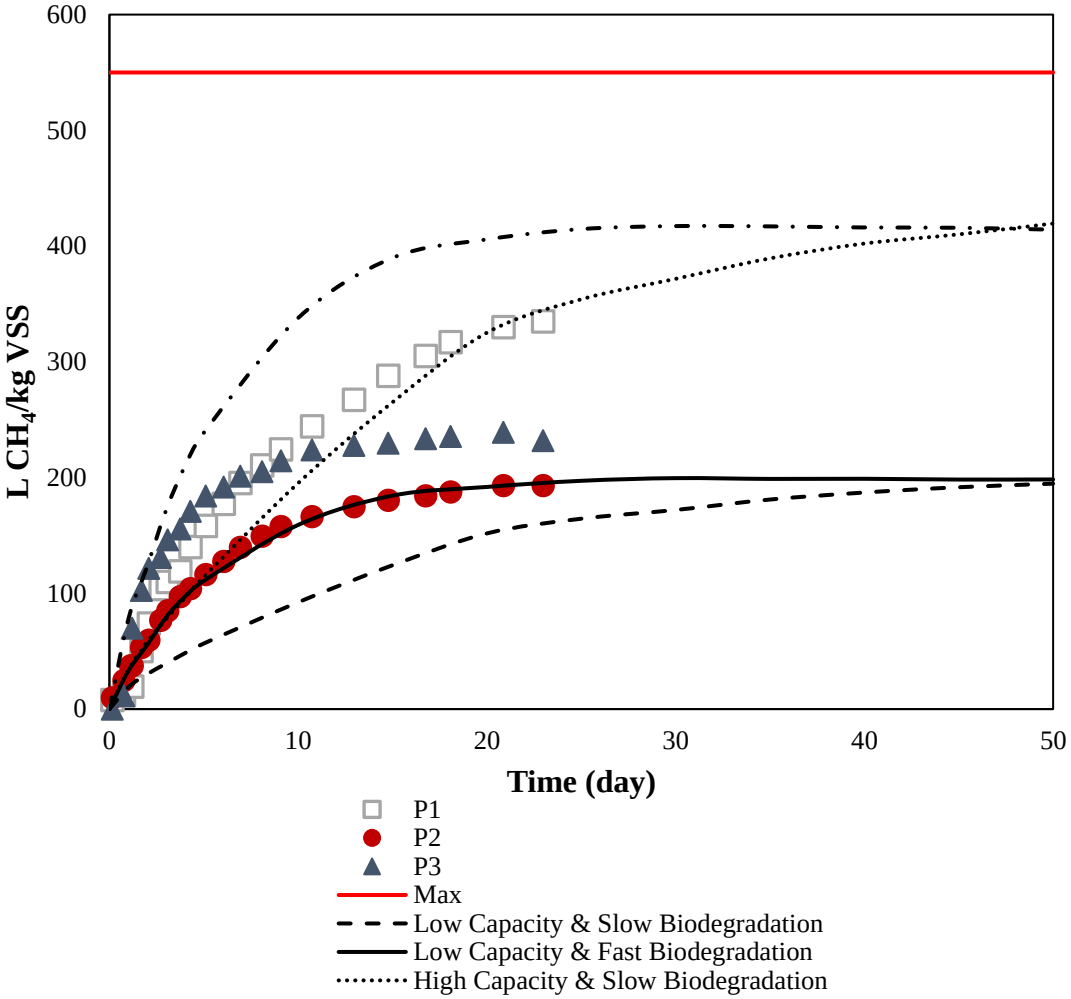

Figure 5.29 : Comparison of cumulative methane profiles.

5.4 Determination of Process Kinetics and Dynamic Modeling Studies

5.4.1 Process performance and dynamic simulations of P1

The P1 plant has been designed to remove organic carbon, nitrogen, and phosphorus from wastewater, with an average daily flow rate of 400,000 m^3/day. The treatment process involves primary settling tanks, Bio-P, aeration tanks, and secondary sedimentation tanks. The primary sludge and biological excess sludge (secondary sludge) produced from the process are thickened and directed to anaerobic digestion tanks for the production of biogas.

To simulate the plant's performance, a dynamic simulation was conducted using data collected over a one-year period. To optimize and shorten the simulation time, parallel units within the treatment plant were aggregated and introduced to the simulation program as a single unit. Specifically, the aeration basins, which consist of four parallel

lines, had their volumes combined for the purposes of the simulation. This aggregation allows for a more efficient computation while still accurately representing the plant's operations. Data for the simulation were entered into the Sumo simulation platform on a daily basis. Before initiating the dynamic simulation, the plant was operated with a constant load for a full year. This preliminary phase was crucial as it allowed the activated sludge within the system to reach the desired concentration and achieve a stable operational state. Maintaining a constant load during this period ensured that the biomass within the system had sufficient time to acclimate and grow to optimal levels, which is essential for accurate simulation results.

The process flow diagram of the plant is shown in Figure 5.30. Influent flowrate, wastewater temperatures and influent COD, TN, and TP concentrations are given in Figure 5.31-Figure 5.36.

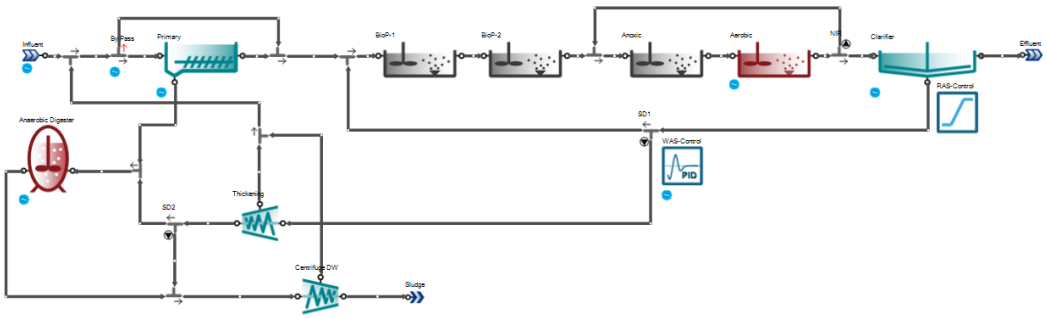

Figure 5.30 : Simulation layout for P1 (Sumo).

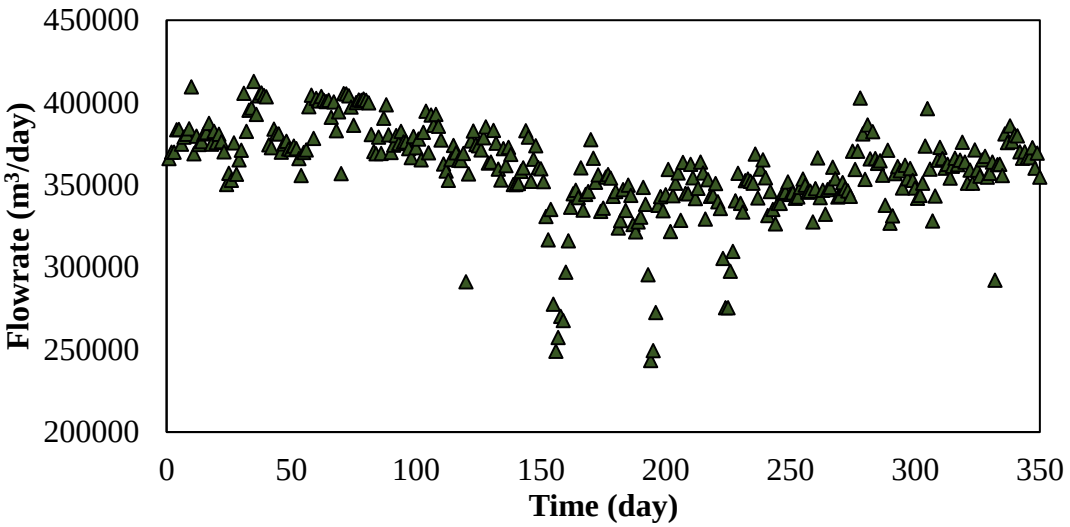

Figure 5.31 : Influent flowrate for P1.

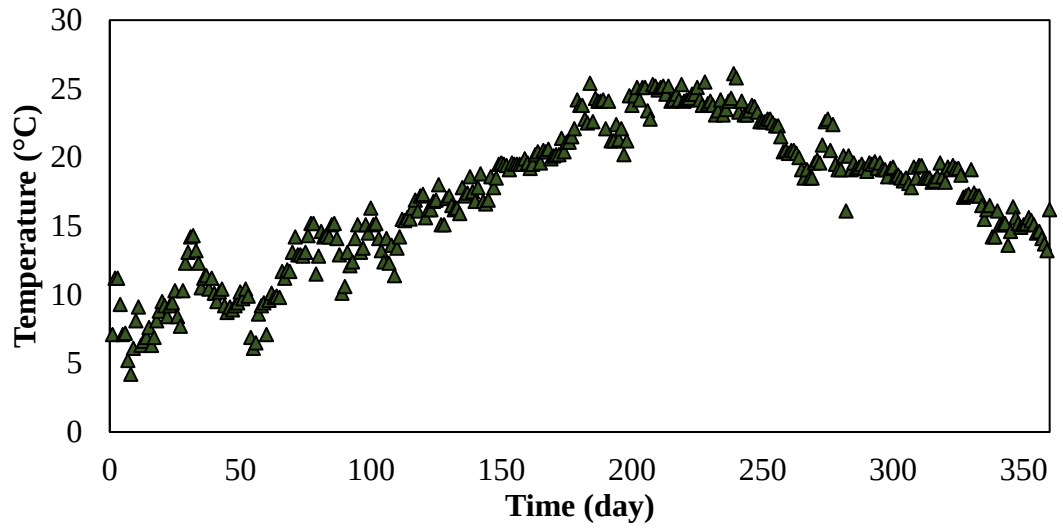

Figure 5.32 : Influent wastewater temperature profile for P1.

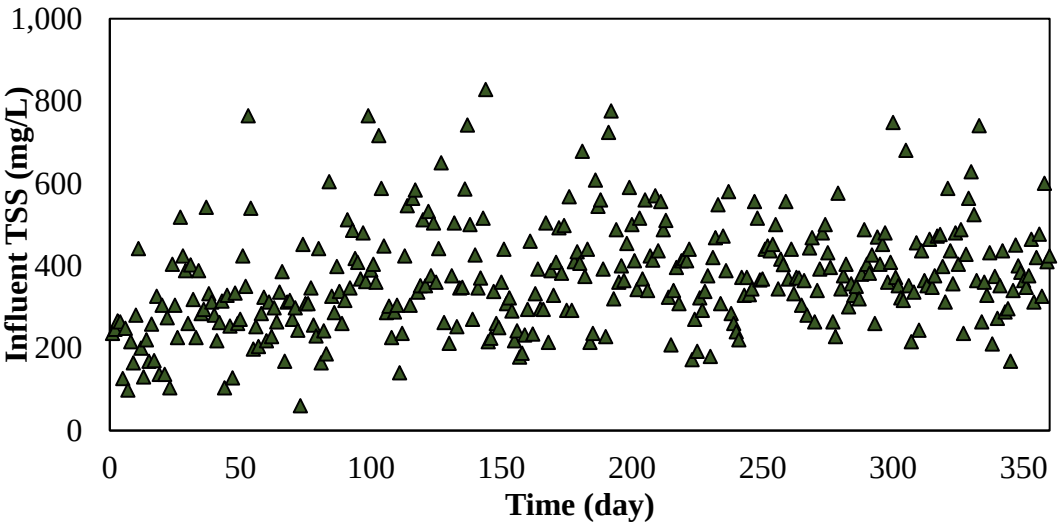

Figure 5.33 : Influent TSS concentrations for P1.

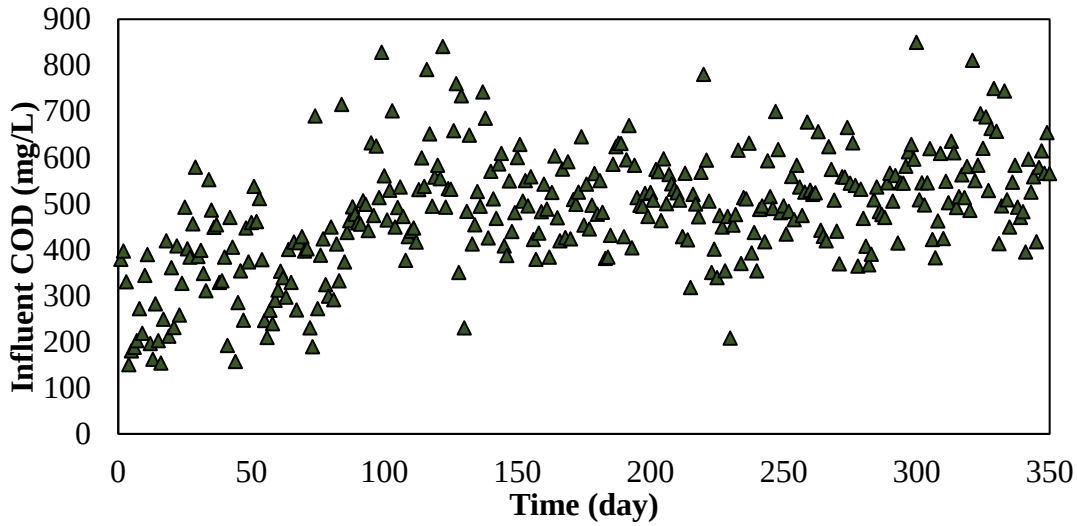

Figure 5.34 : Influent COD concentrations for P1.

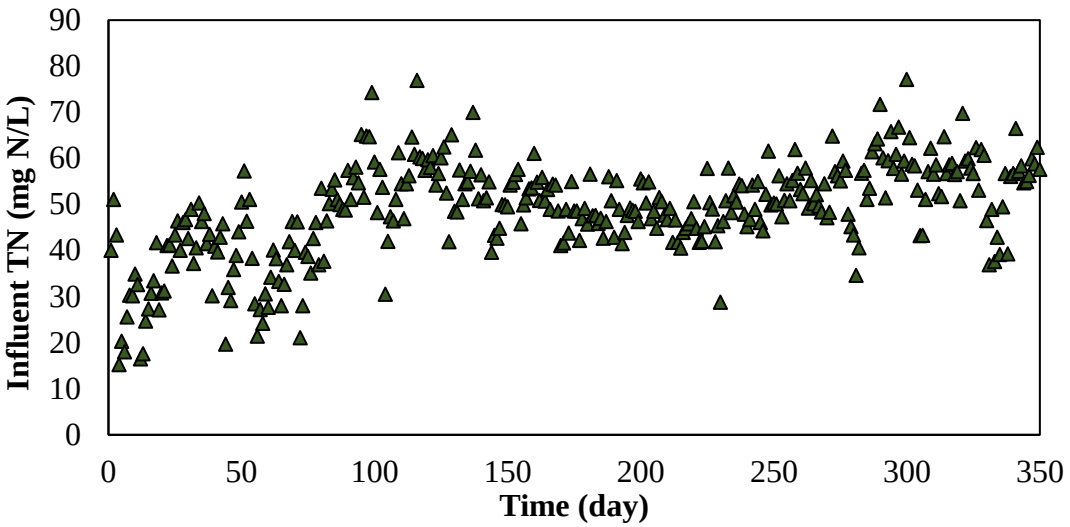

Figure 5.35 : Influent TKN concentrations for P1.

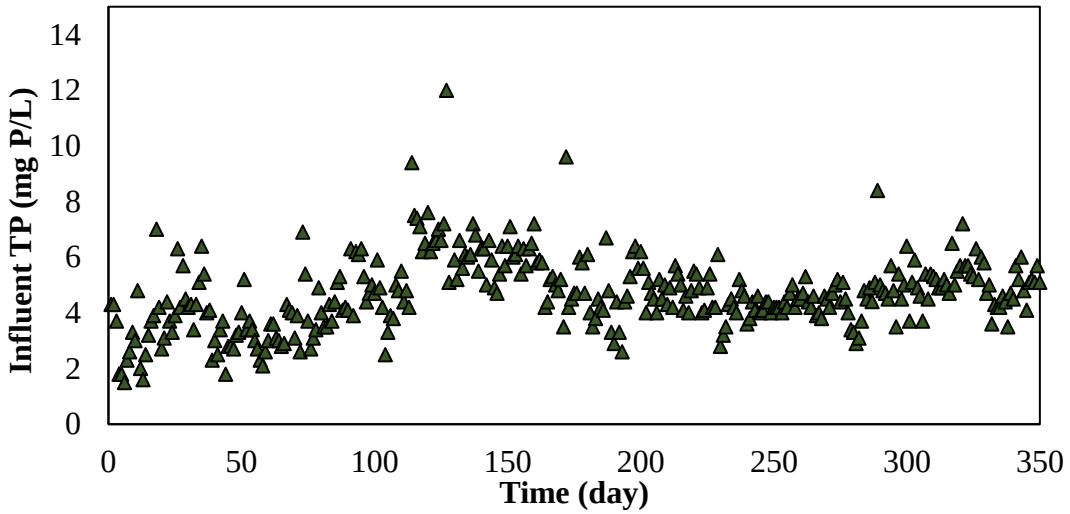

Figure 5.36 : Influent TP concentrations for P1.

The average values of the dynamic data introduced to the Sumo software can be found in Table 5.5. The average flowrate was found to be 407,467 m^3/day, with an average influent wastewater temperature of 17°C. Based on a year's worth of data, the influent wastewater COD concentration ranged between 150-850 mg/L. The average COD concentration was calculated to be 482±128 mg/L, while the influent average TSS concentration was 372±141 mg/L. The influent average TN concentration was determined to be 49±10 mg N/L. The influent TP concentration ranged between 1.5-26 mg P/L, with an average value of 4.8±1.9 mg P/L.

Based on the experimental characterization studies presented in the previous sections, wastewater fractions and the values for kinetic parameters used in dynamic simulations for the P1 plant were determined and introduced to the Sumo simulation program.

Effluent concentrations of COD, TN (and nitrogen forms), and TP together with simulation results can be found in Figure 5.37 - Figure 5.39.

Table 5.5 : Influent data for P1 simulations.

Parameter	Unit	Value
Flowrate	m^3/day	407,467
Influent temperature	°C	17
Chemical oxygen demand	mg COD/L	482±128
Total suspended solids	mg TSS/L	372±141
Total nitrogen	mg N/L	49±10
Total phosphorus	mg P/L	4.8±1.9

As can be seen from Figure 5.37–Figure 5.39, model simulation and effluent concentrations are in good fit. According to the data obtained from the plant, the effluent COD concentration was calculated as 44±25.1 mg/L, while this value was calculated as 43.6±15.9 mg/L in the simulation data (Figure 5.37). Figure 5.38 shows the forms of nitrogen in the effluent stream for plant P1. The plant generally performs efficient nitrification during the one-year period. While the average NH_4-N concentration in the effluent was calculated as 1.6±3.1 mg N/L in the plant data, this average was calculated as 1.1±1.0 mg N/L in the model results (Figure 5.38a). Based on the data provided by the plant's operation, it has been identified that two aeration basins were deactivated (25% of total volume) on the 190th day of the simulation, and were reactivated after a period of 2 weeks. It can be concluded that the peak value of ammonia nitrogen observed in Figure 5.38a is attributed to this event. The average TN concentration in the effluent was calculated as 6.8±3.6 mg N/L in the plant data, this average was calculated as 7.3±1.8 mg N/L in the model results (Figure 5.38c).

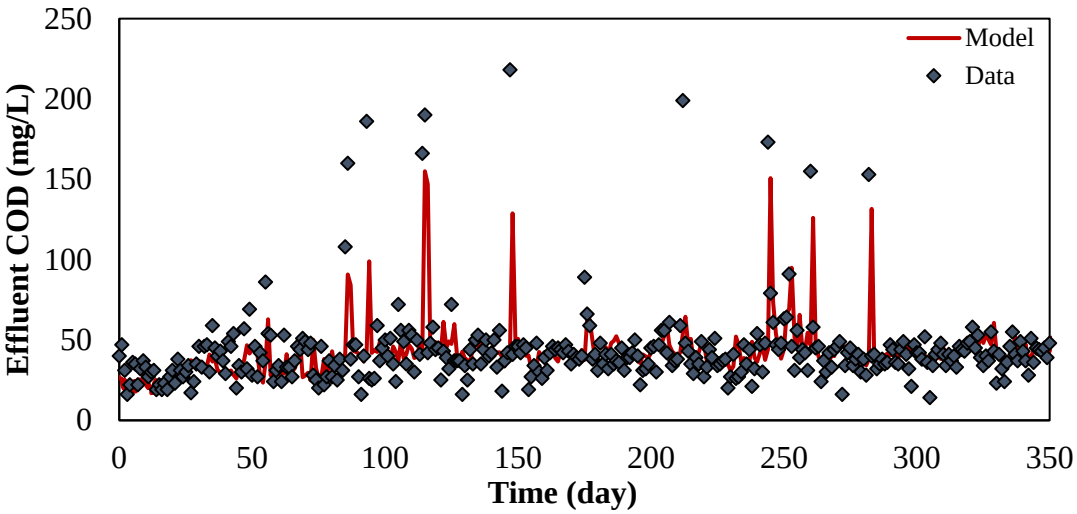

Figure 5.37 : Effluent COD concentrations and simulation results for P1.

Figure 5.39 shows the effluent concentration of TP for P1 plant. The average TP concentration in the effluent was calculated as 0.8±0.7 mg P/L in the plant data, this average was calculated as 0.7±0.5 mg P/L in the model results. The peak values of TP observed in Figure 5.39 can be attributed to biomass escaping in final sedimentation tanks.

The parameters used in the model calibration of the P1 plant model are listed in Table 5.6, along with the default values employed in the model. These parameters are crucial for ensuring the model accurately represents the plant's operations. The simulation results reveal that the maximum specific nitrifier growth rate and anaerobic hydrolysis rate for the P1 plant are lower compared to those reported in the literature (Henze et al., 2000, Melcer et al., 2003, Wichern et al., 2003).

The maximum specific autotrophic growth rate, which affects the efficiency of the nitrification process, was found to be lower, indicating a slower conversion of ammonia to nitrate in the P1 plant. Similarly, the anaerobic hydrolysis rate, which describes the breakdown of complex organic matter under anaerobic conditions, was also lower. This suggests a slower degradation process, potentially impacting the plant's overall performance in terms of organic matter removal and biogas production.

Figure 5.40 presents the biogas flowrates and simulation results for the P1 plant. The average biogas flowrate of the P1 plant was calculated around 16,000 m^3/day and this value is almost 30% of the design value accepted in tender documents (60,000 m^3/day).

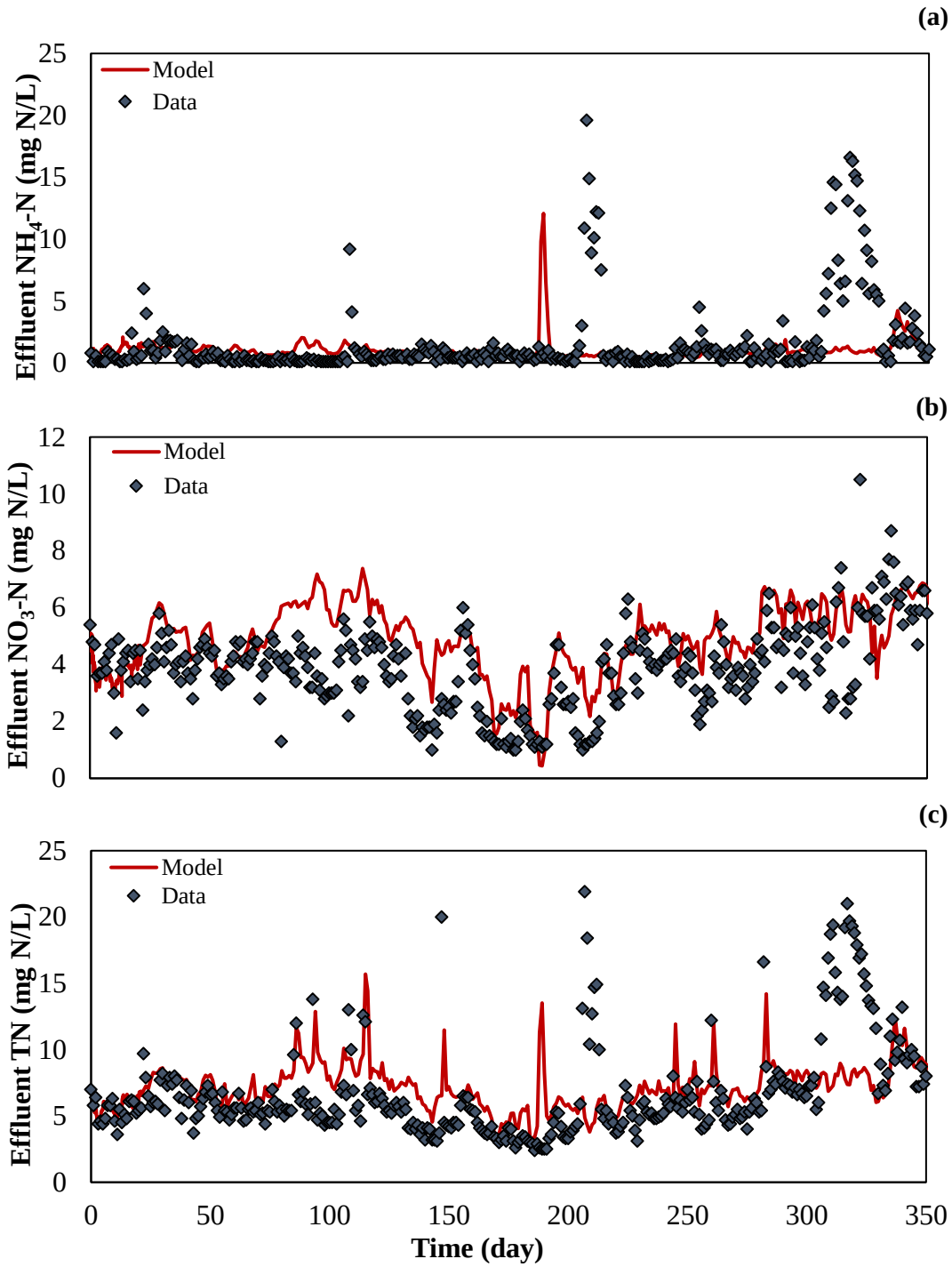

Figure 5.38 : Effluent NH_4-N (a), NO_X-N (b), and TN (c) concentrations and simulation results for P1.

The reduction of the correction factor for anaerobic hydrolysis was necessary to achieve the calibration of biogas flowrates. This indicates that the biogas yield is low due to the slow anaerobic hydrolysis rate in the anaerobic digestion process. The reason for the low nitrification and hydrolysis rates is attributed to the intensive

industrial discharge (İnsel et al, 2022, İnsel et al., 2020; Sözen, 1995; Sözen et al., 2008; Sözen et al., 1998; Sözen et al., 1996).

This value is lower than the model default value ($\eta_{HYD,ana}$) of 0.50, indicating that the anaerobic hydrolysis process operates at 76% of its full capacity. In summary, the parameter $\eta_{HYD,ana}$ is the correction factor of the maximum hydrolysis rate (q_{HYD}) in activated sludge under anaerobic conditions. This means that under anaerobic conditions, the hydrolysis rate of slowly biodegradable organic matter is calculated as $\eta_{HYD,ana} \cdot q_{HYD}$. This parameter is the rate-limiting factor in the anaerobic sludge digestion model and directly impacts the biogas flow rate.

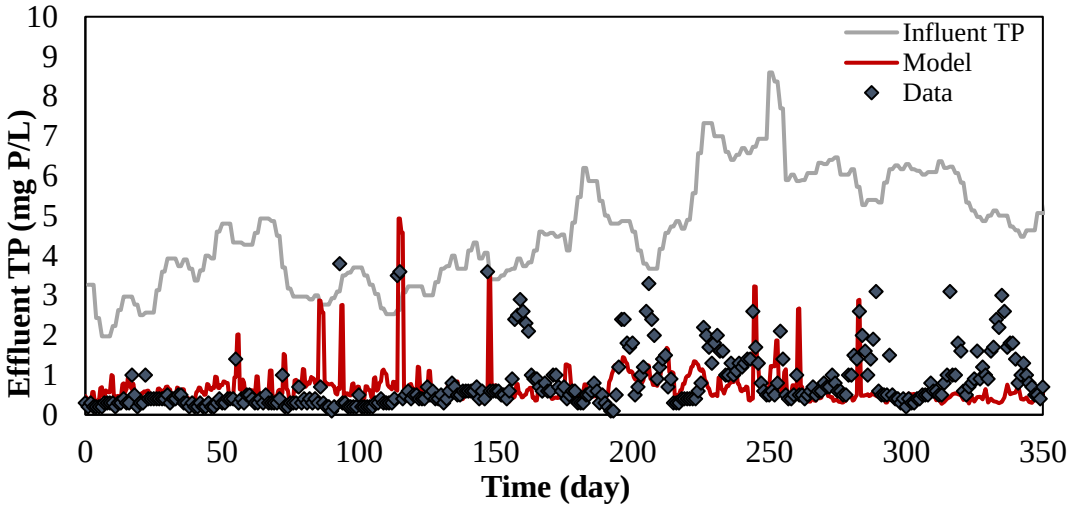

Figure 5.39 : Effluent TP concentrations and simulation results for P1.

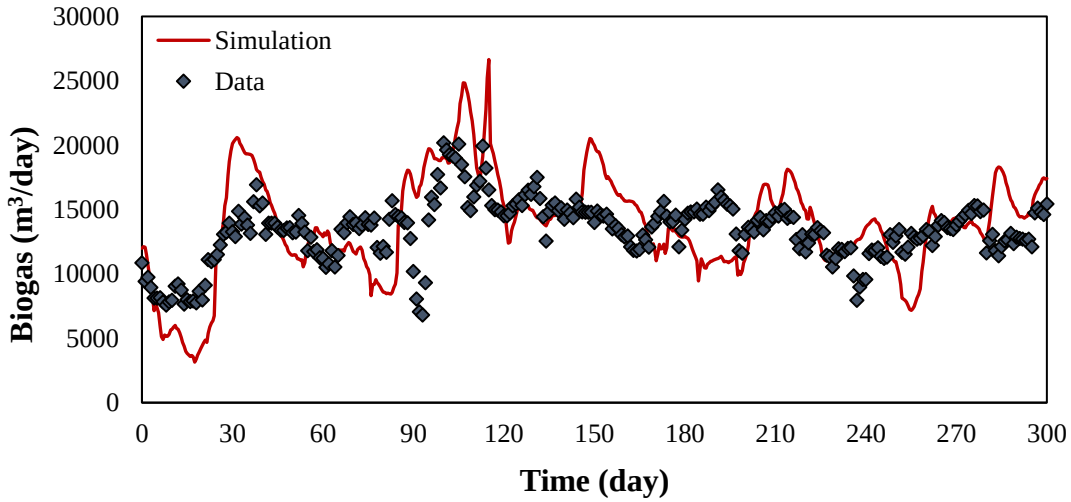

Figure 5.40 : Biogas flowrates for P1.

Table 5.6 : Model kinetic parameters for P1 (20°C).

Parameter	Symbol	Info	Unit	P1	Default
Max. specific growth rate for NITO	μ_{NITO}	Exp.	day^{-1}	0.65	0.90
Half saturation for NITO (NH_x)	$K_{O2,NITO,AS}$	Calibr.	g N/m^3	0.4	0.7
Max. specific growth rate for OHO	μ_{OHO}	Exp.	day^{-1}	4.0	4.0
Decay rate for OHO	b_{OHO}	Exp.	day^{-1}	0.4	0.62
Maximum hydrolysis rate	q_{HYD}	Exp.	day^{-1}	1.1	2.00
Half saturation for hydrolysis	$K_{HYD,AS}$	Exp.	g COD/g COD	0.06	0.05
Correction for anaerobic hydrolysis	$\eta_{HYD,ana}$	Calibr.	-	0.23	0.50
COD of volatile organics	$i_{CV,X}$	Meas.	g COD/g VSS	1.45	1.80
Maximum growth rate of AMETO	μ_{AMETO}	Exp.	day^{-1}	0.5	0.3
Half saturation of VFA for AMETO	K_{VFA}	Exp.	mg COD/L	350	400

5.4.2 Process performance and dynamic simulations of P2

The P2 plant is divided into two stages, with an average flow rate of 390,000 m³/day and 240,000 m³/day for the first and second stages, respectively. This plant is designed for organic carbon and nutrient removal. It has primary clarifiers followed by Bio-P reactors and oxidation ditch type anoxic/aerobic activated sludge tanks with a total SRT of 10 days. The sludge produced in the plant is directed to the further sludge processes and is digested in the plant's anaerobic digesters.

The first and second stages of the plant were integrated and reflected together in the simulation, ensuring a comprehensive representation of the entire plant's operations. The simulation was conducted throughout the plant to capture all relevant processes and interactions. For the simulations, the built-in Sumo1 model, which includes modules for organic carbon removal, nitrogen/phosphorus removal, and sludge digestion processes, was selected to provide a detailed and accurate portrayal of the plant's performance. Data were entered into the Sumo simulation program on a daily basis, capturing the day-to-day variations and ensuring a dynamic simulation that reflects real operational conditions. The process flow diagram of the plant, illustrating the various stages and units involved, is shown in Figure 5.41. Influent flowrate, wastewater temperatures and influent COD, TN and TP concentrations are given in Figure 5.42-Figure 5.47.

Due to the maintenance and repair works carried out in various units of the plant, the simulations were conducted with 160 days of dynamic data. This period was chosen to ensure that the simulation could provide a realistic and uninterrupted analysis of the plant's performance, accounting for any temporary disruptions caused by the maintenance activities. Moreover, it is important to note that during the simulation

period, the anaerobic digester in plant P2 received only secondary sludge. This specific operational condition was considered in the simulation to accurately reflect the treatment process and the resulting biogas production. This detail is crucial for understanding the digestion process and its impact on the overall performance of the plant.

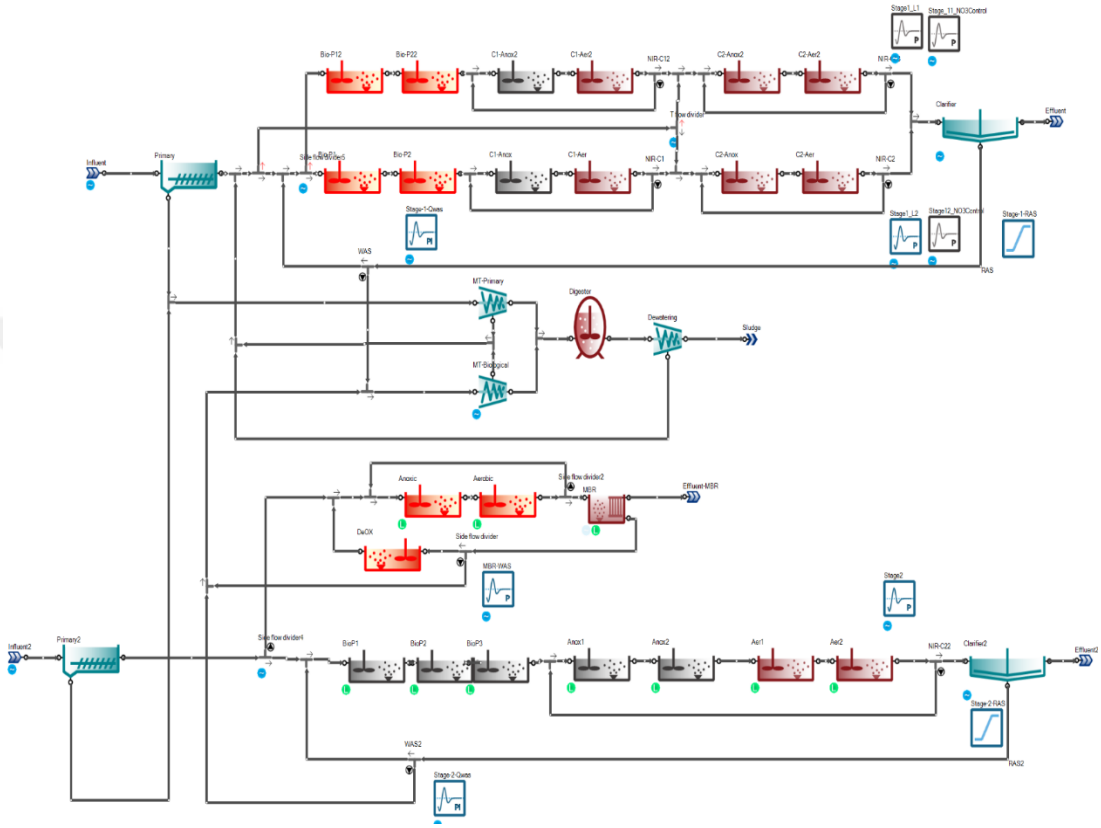

Figure 5.41 : Simulation layout for P2 (Sumo).

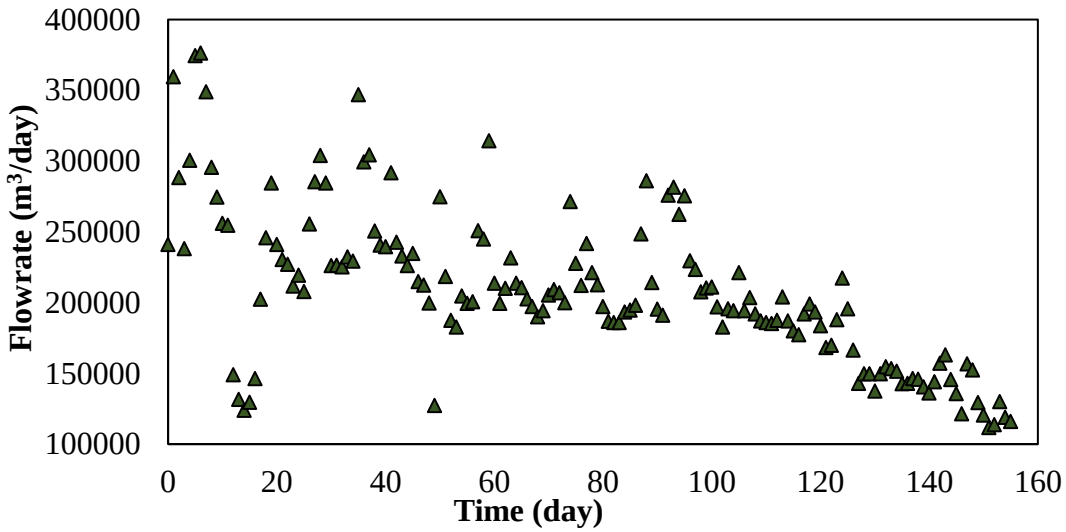

Figure 5.42 : Influent flowrate for P2.

The average values of the dynamic data introduced to the Sumo software can be found in Table 5.7. The average flowrate was found to be 208,500 m^3/day, with an average influent wastewater temperature of 20°C. Based on 160-day worth of data, the influent wastewater COD concentration ranged between 130-1100 mg/L. The average COD concentration was calculated to be 540±128 mg/L, while the influent average TSS concentration was 315±113 mg/L. The influent average TN concentration was determined to be 63±14 mg N/L. The influent TP concentration ranged between 1.5-20 mg P/L, with an average value of 6.7±2.5 mg P/L.

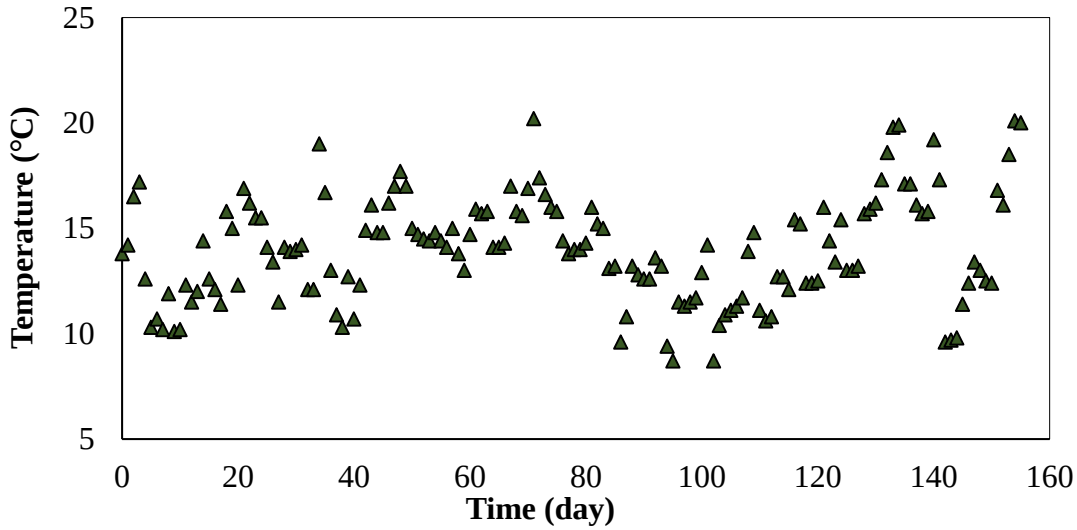

Figure 5.43 : Influent wastewater temperature profile for P2.

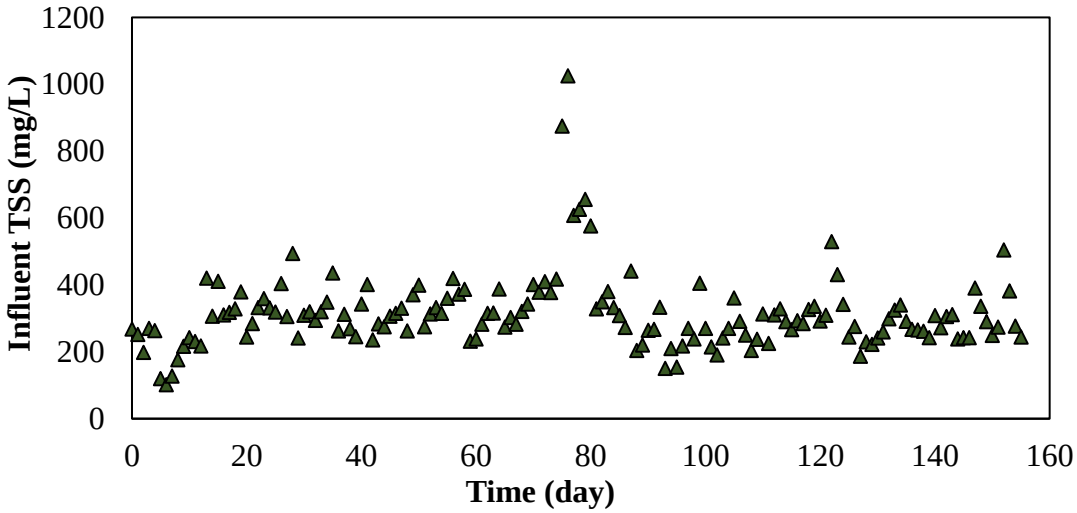

Figure 5.44 : Influent TSS concentrations for P2.

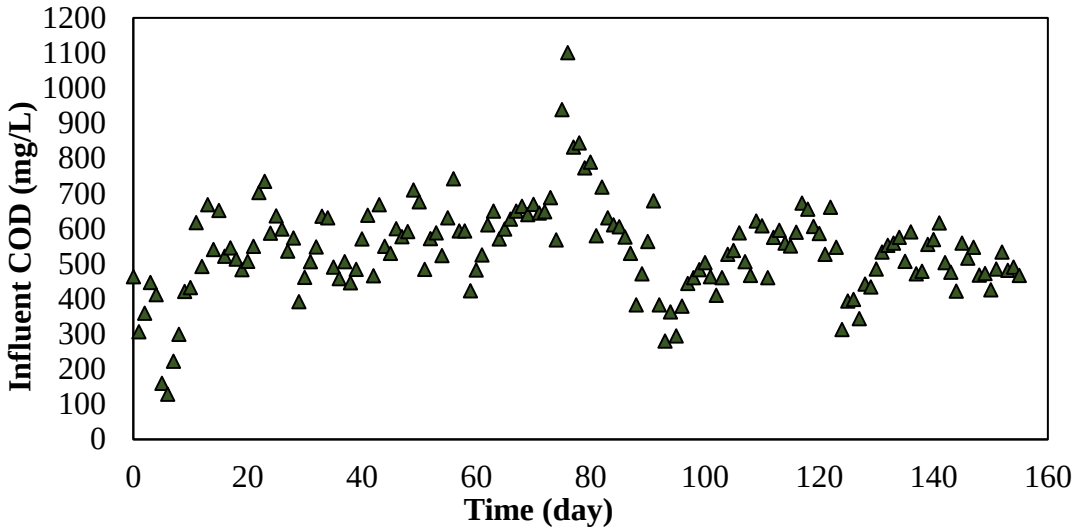

Figure 5.45 : Influent COD concentrations for P2.

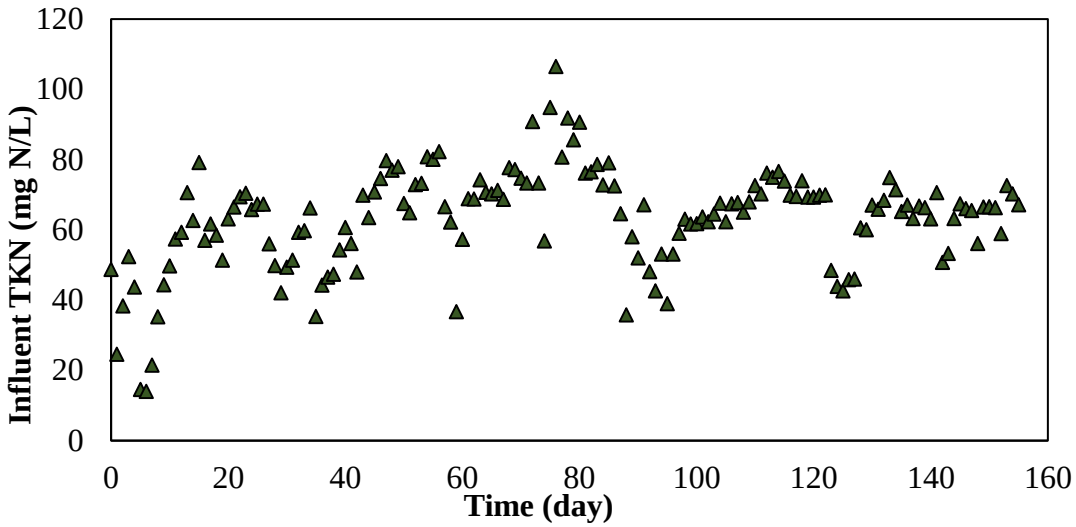

Figure 5.46 : Influent TKN concentrations for P2.

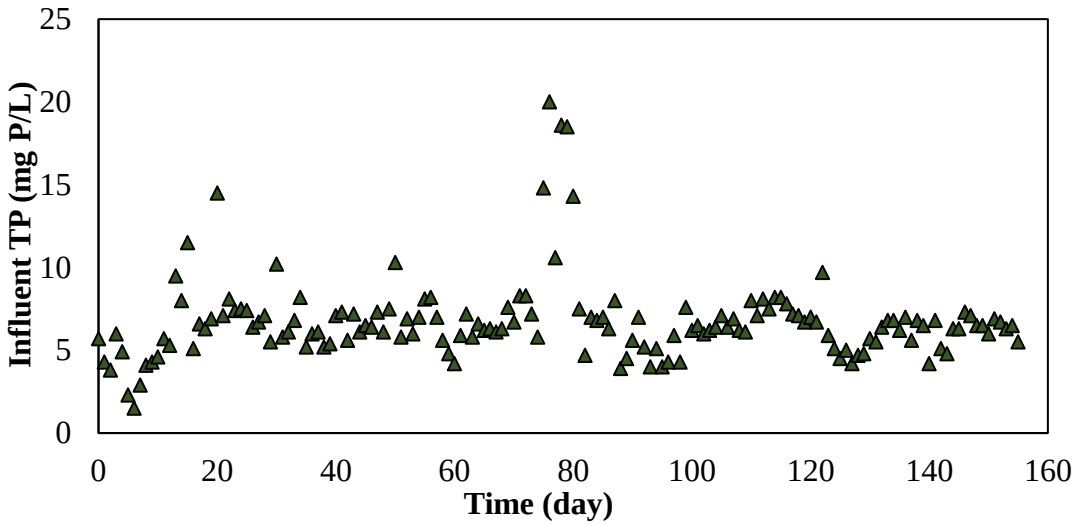

Figure 5.47 : Influent TP concentrations for P2.

Table 5.7 : Influent data for P2 simulations.

Parameter	Unit	Value
Flowrate	m^3/day	208,500
Influent temperature	°C	20
Chemical oxygen demand	mg COD/L	540±128
Total suspended solids	mg TSS/L	315±113
Total nitrogen	mg N/L	63±14
Total phosphorus	mg P/L	6.7±2.5

Based on the experimental characterization studies presented in the previous sections, wastewater fractions and the values for kinetic parameters used in dynamic simulations for the P2 plant were determined and introduced to Sumo simulation program. Effluent concentrations of COD, TN (and nitrogen forms) and TP together with simulation results can be found Figure 5.48-Figure 5.50.

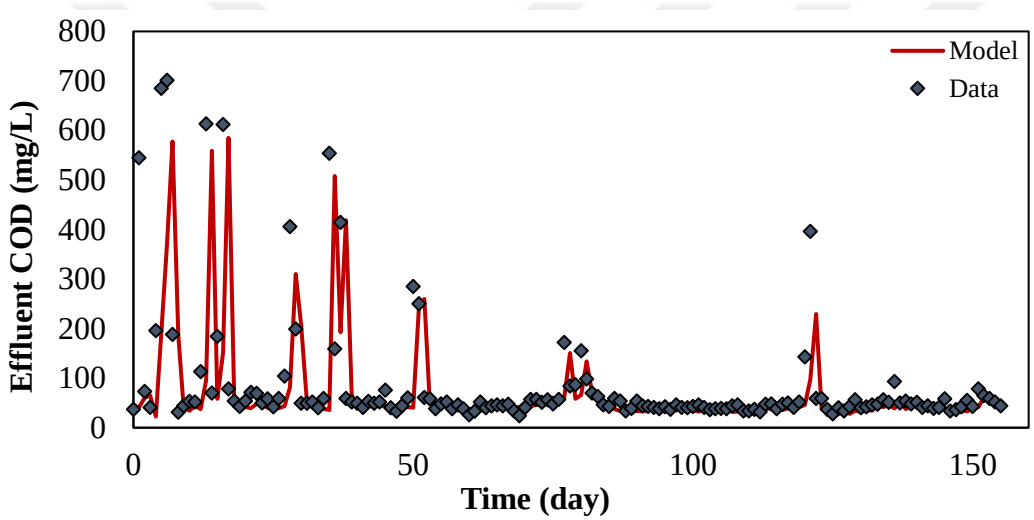

Figure 5.48 : Effluent COD concentrations and simulation results for P2.

As can be seen from Figure 5.48-Figure 5.50, model simulation and effluent concentrations are in good fit. During the 150-day period, the plant's effluent COD concentration was calculated as 88±124 mg/L, while the simulation data yielded a value of 72±99 mg/L (Figure 5.48). The COD peak values shown in Figure 5.48 can be attributed to biomass escaping the final sedimentation tanks. Figure 5.49 shows the forms of nitrogen in the effluent stream for plant P2. During the 150-day period when the modeling was conducted, it was observed that the nitrification efficiency in the plant was quite low. This low efficiency had a significant impact on the effluent ammonia concentration and, consequently, the effluent total nitrogen concentration. While the average NH_4-N concentration in the effluent was calculated as 6.4±6.4 mg N/L in the plant data, this average was calculated as 6.1±5.8 mg N/L in the model results (Figure 5.49a). The average concentration of TN in the effluent was 18.2±12.2

mg N/L in the plant data and 16.0±7.7 mg N/L in the model results. The reason for the high average values can be attributed to both the high ammonia concentrations due to low nitrification efficiency and the high amount of organic nitrogen due to the high amount of TSS in the effluent from the final sedimentation tanks. Also, the peaks observed around 80th day are due to the influent concentrations exceeding the plant's design capacity.

Figure 5.50 displays the effluent concentration of TP for P2 plant. The plant data indicates that the average TP concentration in the effluent was 3.1±3.3 mg P/L, while the model results suggest an average of 2.3±3.8 mg P/L. The occurrence of peak values of TP observed in Figure 5.50 can be attributed to the escape of biomass in final sedimentation tanks. The peaks observed around 80th day are due to the influent TP concentrations exceeding the plant's design capacity.

Figure 5.51 presents the biogas flowrates and simulation results for the P2 plant. According to the tender documents of the plant, the design biogas flowrate was projected to be 40,000 m³/day (İnsel et al., 2020). However, actual operational data from the P2 plant's SCADA system indicated that the average biogas production from the digesters was 9,117 m³/day. In comparison, the model simulations predicted a biogas flowrate of 9,836 m³/day. This simulated value corresponds to approximately 25% of the design biogas flow rate, highlighting a significant discrepancy between the expected and actual biogas yields. To achieve accurate calibration of the biogas flowrates, it was necessary to reduce the correction factor for anaerobic hydrolysis. This adjustment underscores that the biogas yield is low due to the slow anaerobic hydrolysis rate within the digestion process. This finding is consistent with observations from the P1 plant, where similar issues were noted. This indicates that the biogas yield is low due to the slow anaerobic hydrolysis rate in the anaerobic digestion process. As previously discussed for P1 plant, this value is lower than the model default value ($\eta_{HYD,ana}$) of 0.50. The primary reason for these low nitrification and hydrolysis rates is attributed to heavy industrial discharges into the wastewater system (İnsel et al., 2022; İnsel et al., 2020; Sözen, 1995; Sözen et al., 2008; Sözen et al., 1998). These discharges introduce complex and potentially inhibitory substances that can hinder the microbial activity necessary for effective anaerobic digestion.

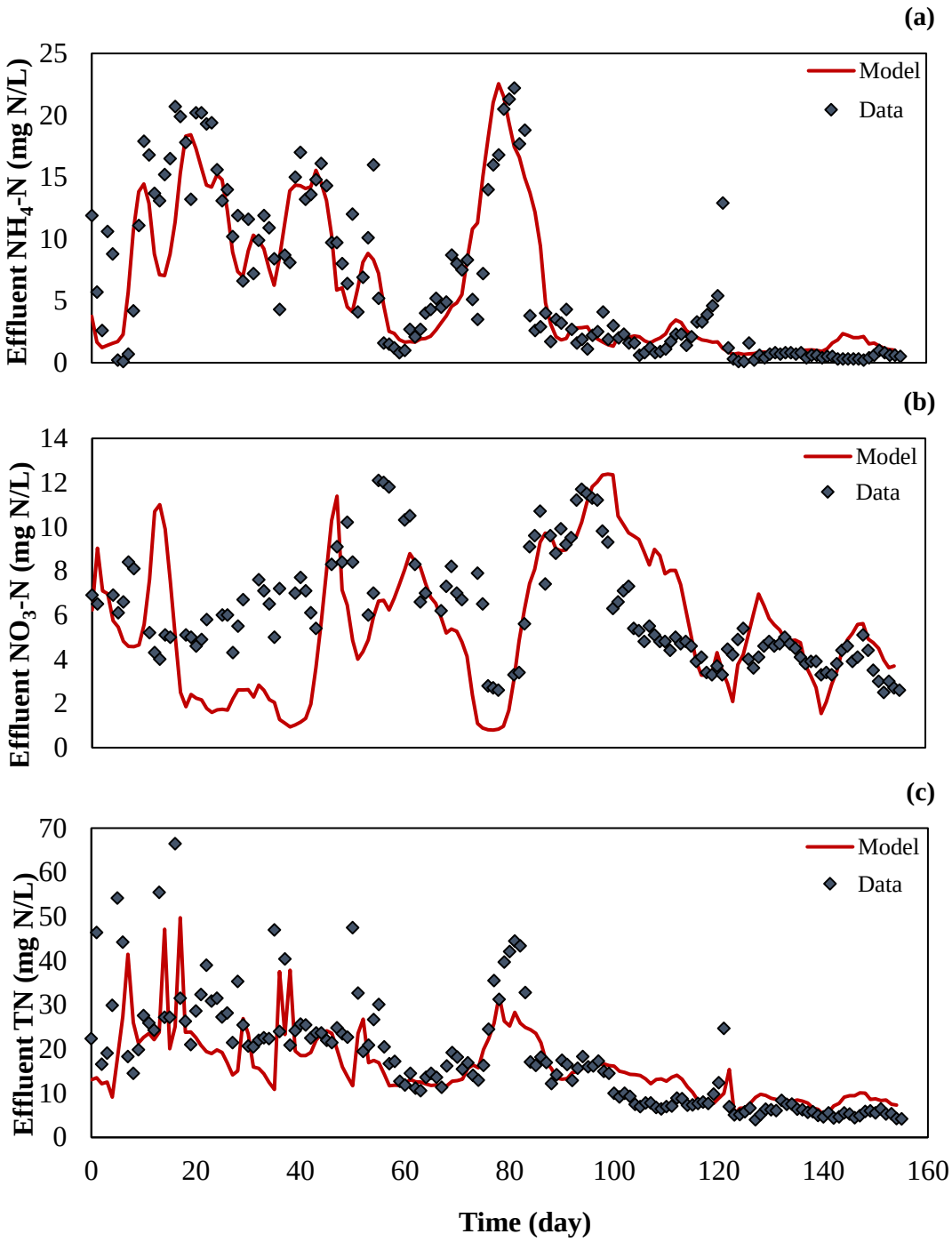

Figure 5.49 : Effluent NH_4-N (a), NO_X-N (b), and TN (c) concentrations and simulation results for P2.

The parameters used in the model calibration of the P2 plant model are listed in Table 5.8, along with the default values employed in the model. The simulation results reveal that the maximum specific nitrifier growth rate and anaerobic hydrolysis rate for the P2 plant are lower in comparison to the literature (Henze et al., 2000, Melcer et al., 2003, Wichern et al., 2003).

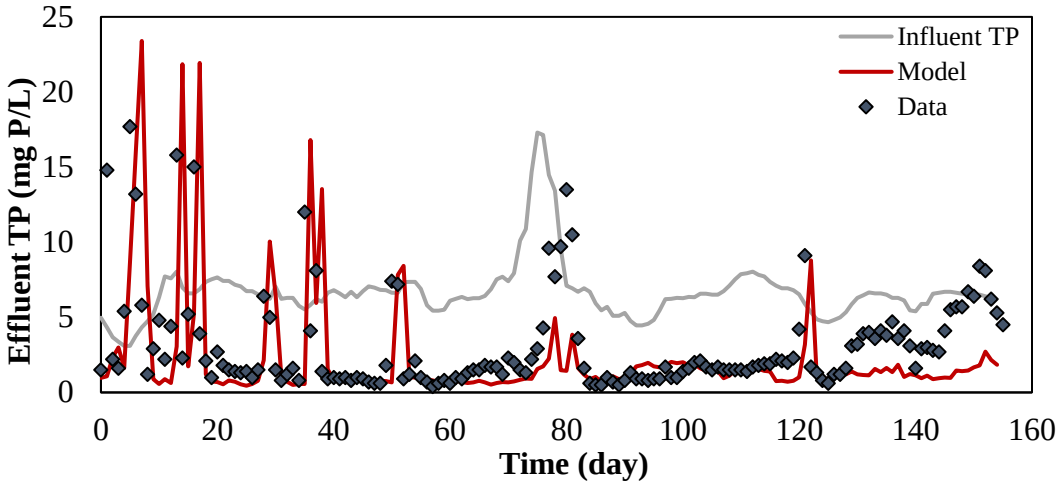

Figure 5.50 : Effluent TP concentrations and simulation results for P2.

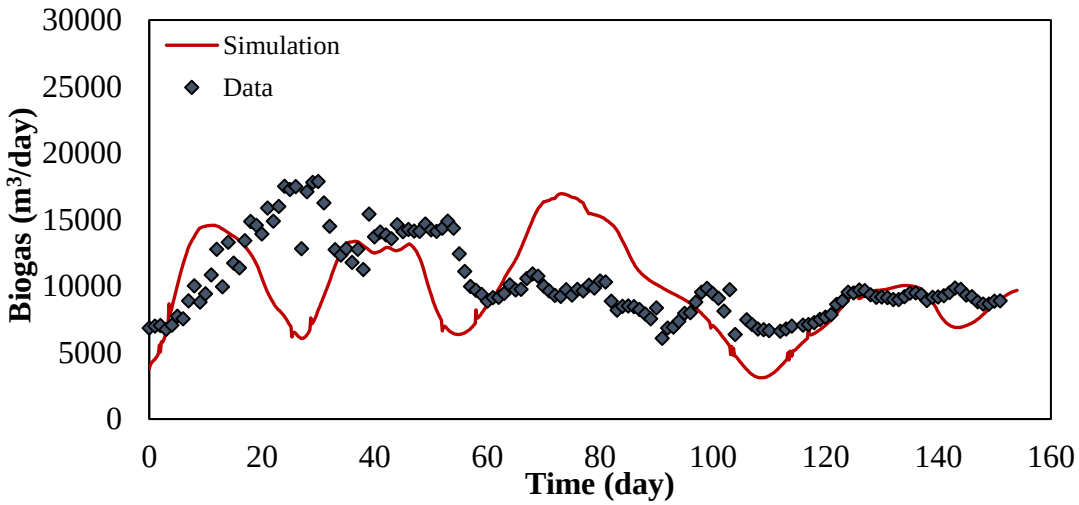

Figure 5.51 : Biogas flowrates for P2.

Table 5.8 : Model kinetic parameters for P2 (20°C).

Parameter	Symbol	Info	Unit	P2	Default
Max. specific growth rate for NITO	μ_{NITO}	Exp.	day^{-1}	0.55	0.90
Half saturation of NH_x for NITO	$K_{O2,NITO,AS}$	Calibr.	g N/m^3	0.7	0.7
Max. specific growth rate for OHO	μ_{OHO}	Exp.	day^{-1}	4.0	4.0
Decay rate for OHO	b_{OHO}	Exp.	day^{-1}	0.4	0.62
Maximum hydrolysis rate	q_{HYD}	Exp.	day^{-1}	1.4	2.00
Half saturation for hydrolysis	$K_{HYD,AS}$	Exp.	g COD/g COD	0.06	0.05
Correction for anaerobic hydrolysis	$\eta_{HYD,ana}$	Calibr.	-	0.11	0.50
COD of volatile organics	$i_{CV,X}$	Meas.	g COD/g VSS	1.50	1.80
Maximum growth rate of AMETO	μ_{AMETO}	Exp.	day^{-1}	0.5	0.3
Half saturation of VFA for AMETO	K_{VFA}	Exp.	mg COD/L	650	400

5.4.3 Process performance and dynamic simulations of P3

The P3 plant has been designed to remove organic carbon, nitrogen, and phosphorus from wastewater, with an average daily flow rate of 300,000 m^3/day. The plant

comprises primary sedimentation tanks, Bio-P tanks and anoxic and aerobic activated sludge basins followed by final clarifiers. The plant consists of BNR and high rate activated sludge systems. Anoxic and total sludge ages of activated sludge system are 3 days and 9 days, respectively. The primary sludge is subjected to gravity; the secondary sludge is mechanically thickened before the MAD operated with an SRT of 20 days.

The P3 plant's high rate and BNR stages, as well as its sludge flows, were planned in conjunction with each other to achieve a comprehensive solution for the entire plant. The data obtained from the plant's operations was analyzed and then entered into the simulation program in MS Excel format. To reduce simulation time, parallel lines are represented as a single line. For instance, four aeration basins serving for the high rate plant are depicted as a single basin. Similarly, units such as primary settling tanks, activated sludge reactors, final sedimentation tanks, and anaerobic sludge digesters, which operate in parallel, are combined and treated as a single line. To determine the overall process performance and shorten the simulation time, the tank volumes are combined to obtain a single volume for units with the same characteristics (Vanrolleghem et al., 2003). The primary sludge fraction in the total sludge mass fed to the digester is around 60%. Daily data for a year was entered into Sumo simulation program, followed by a dynamic simulation run. Figure 5.52 depicts the plant's process flow diagram. Influent flowrate, wastewater temperatures and influent COD, TN, and TP concentrations are given in Figure 5.53-Figure 5.58.

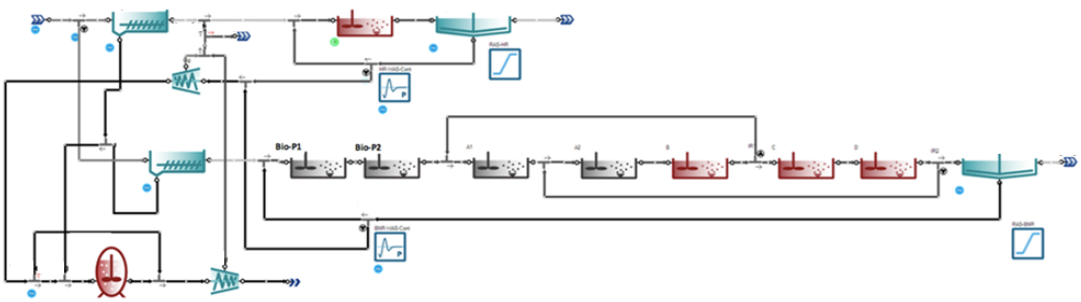

Figure 5.52 : Simulation layout for P3 (Sumo).

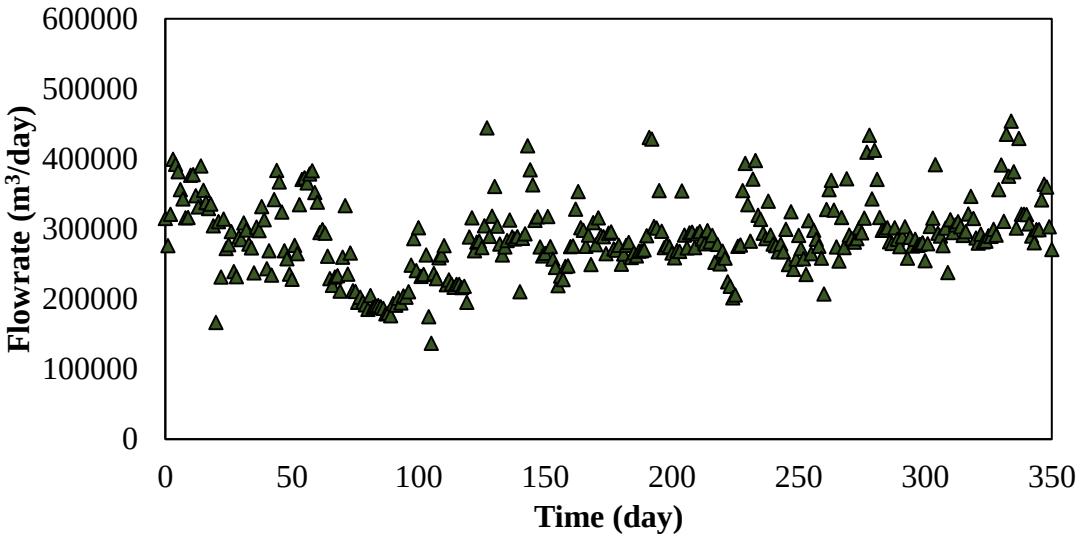

Figure 5.53 : Influent flowrate for P3.

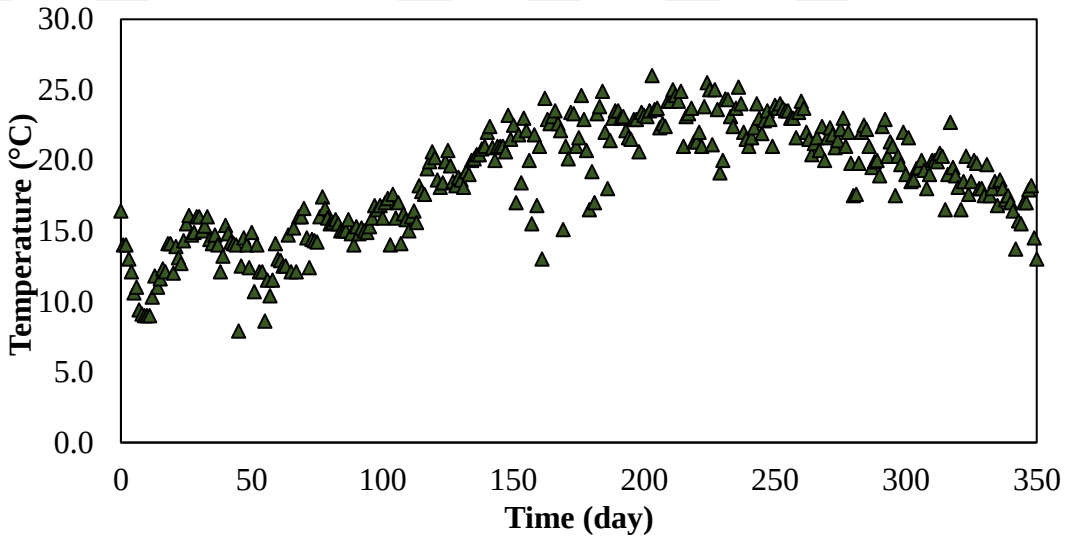

Figure 5.54 : Influent wastewater temperature profile for P3.

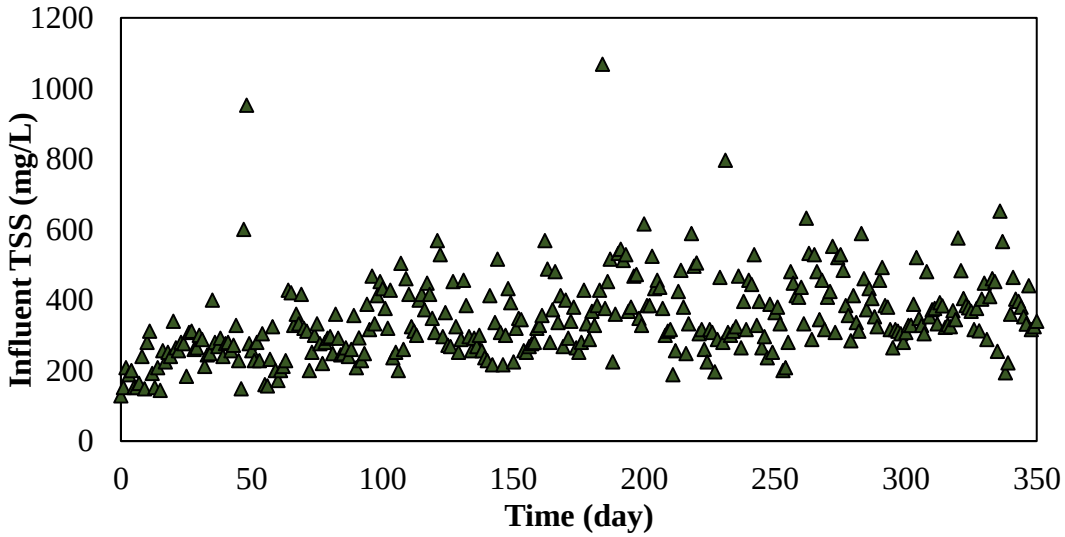

Figure 5.55 : Influent TSS concentrations for P3.

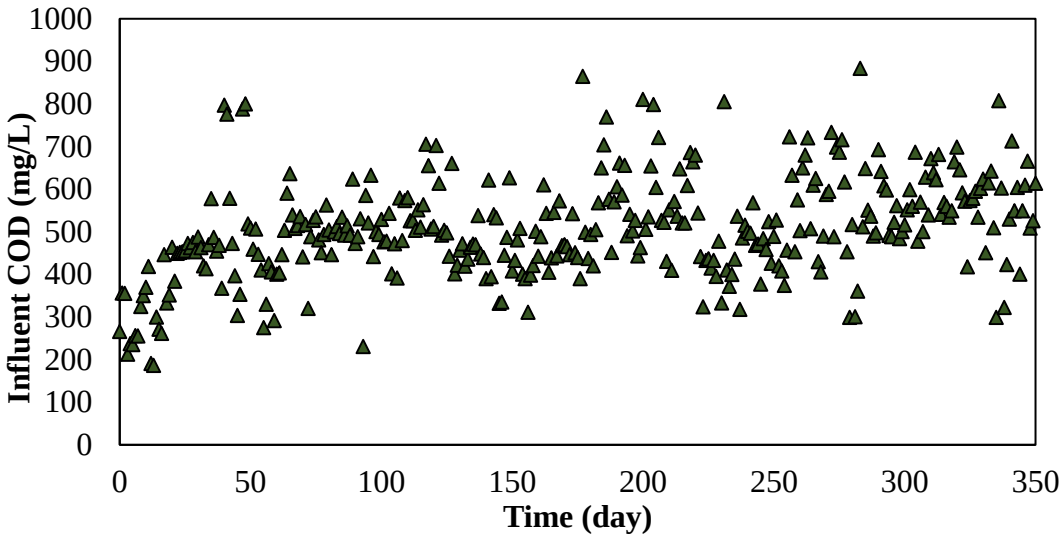

Figure 5.56 : Influent COD concentrations for P3.

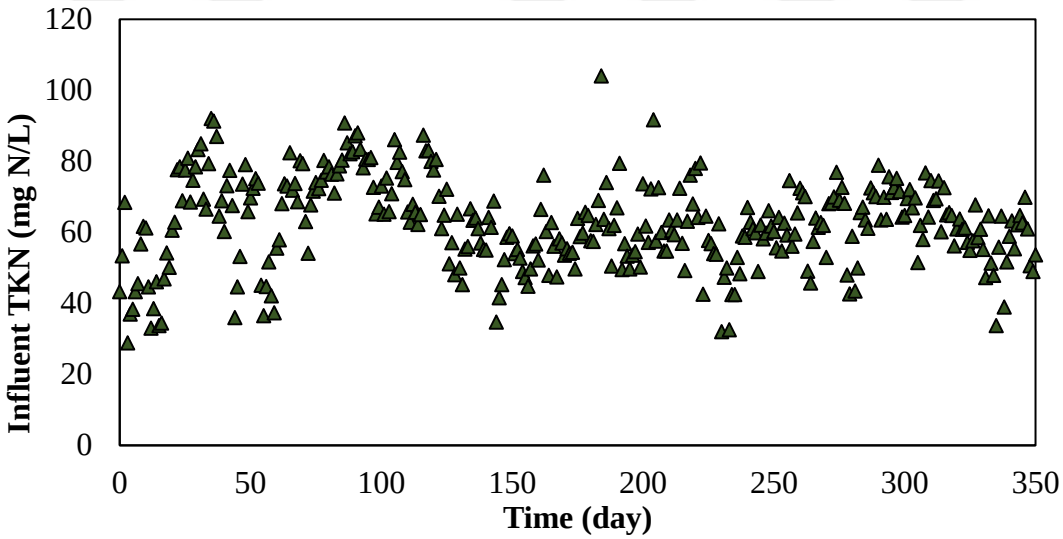

Figure 5.57 : Influent TKN concentrations for P3.

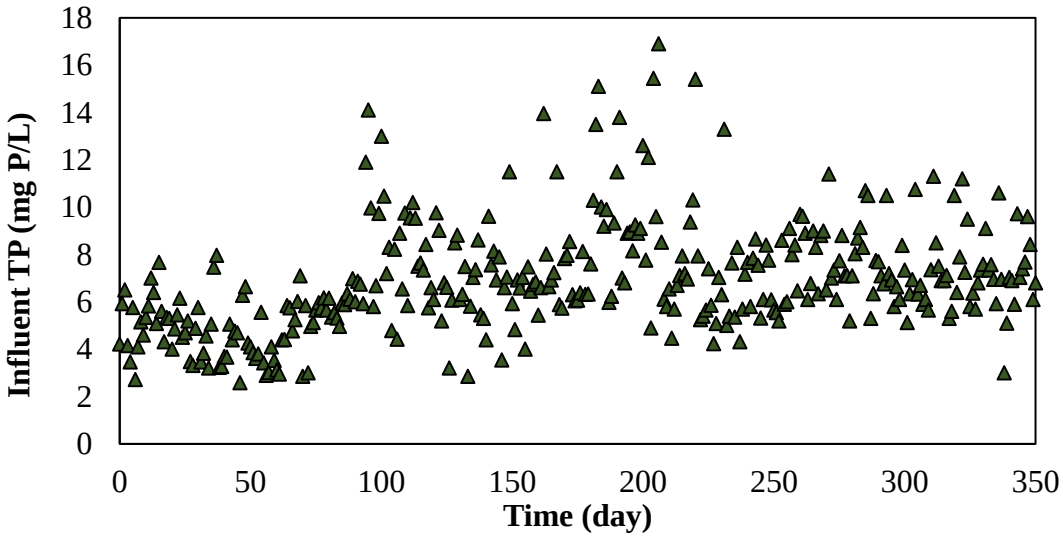

Figure 5.58 : Influent TP concentrations for P3.

The average values of the dynamic data introduced to the Sumo software can be found in Table 5.9. The average flowrate was found to be 291,600 m^3/day, 65% of influent flowrate directed to the BNR system while 35% of wastewater treated with high rate activated sludge system. The average influent wastewater temperature was calculated as 18.5°C. Based on a year's worth of data, the influent wastewater COD concentration ranged between 190-885 mg/L. The average COD concentration was calculated to be 507±120 mg/L, while the influent average TSS concentration was 346±115 mg/L. The influent average TN concentration was determined to be 63±13 mg N/L. The influent TP concentration ranged between 2.6-17 mg P/L, with an average value of 6.9±2.3 mg P/L.

Table 5.9 : Influent data for P3 simulations.

Parameter	Unit	Value
Flowrate	m^3/day	291,600
Influent temperature	°C	18.5
Chemical oxygen demand	mg COD/L	507±120
Total suspended solids	mg TSS/L	346±115
Total nitrogen	mg N/L	63±13
Total phosphorus	mg P/L	6.9±2.3

Based on the experimental characterization studies presented in the previous sections, wastewater fractions and the values for kinetic parameters used in dynamic simulations for the P3 plant were determined and introduced to Sumo simulation program. Effluent concentrations of COD, TN (and nitrogen forms) and TP together with simulation results can be found Figure 5.59-Figure 5.61. Upon analyzing the modeling results of the P3 plant, it is evident that the model calibration aligns well with the plant data.

After analyzing the plant's data for one year, it was found that the effluent COD concentration was 77±58 mg/L, while in the simulation data, it was calculated as 65±43 mg/L (Figure 5.59).

Figure 5.60 displays the different forms of nitrogen present in the effluent stream of plant P3 over a one-year period. The plant has demonstrated efficient nitrification during this period. According to the data, the average concentration of NH_4-N in the effluent was calculated as 0.9±1.8 mg N/L, while in the model results, this average was calculated as 0.7±1.2 mg N/L (Figure 5.60a). Similarly, the average TN concentration in the effluent was calculated as 14.0±4.9 mg N/L in the plant data, while in the model results, it was calculated as 16.1±6.3 mg N/L (Figure 5.60c).

Figure 5.61 illustrates the concentration of TP in the effluent for the P3 plant. According to the plant data, the average TP concentration in the effluent was calculated to be 0.9±1.6 mg P/L, whereas the model results estimated the average to be 1.3±2.1 mg P/L. The high values of TP seen in the graph can be attributed to the biomass escaping in the final sedimentation tanks.

The parameters used in the model calibration of the P3 plant model are listed in Table 5.10, along with the default values employed in the model. The simulation results reveal that the maximum specific nitrifier growth rate for the P3 plant are lower in comparison to the literature (Henze et al., 2000, Melcer et al., 2003, Wichern et al., 2003). While, P3 plant has the highest maximum hydrolysis rate among the other plants, correction factor for anaerobic hydrolysis value is still 35% of the default value of the model.

Figure 5.62 presents the biogas flowrates and simulation results for the P3 plant. The average biogas flow rate of the P3 plant was calculated at around 9,000 m^3/day, and this value is far lower than the design biogas flow rate (İnsel et al., 2020). The 35% reduction of the correction factor indicates that the biogas yield is low due to the slow anaerobic hydrolysis rate in the anaerobic digestion process. It should be noted that the plant has two different stages: high-rate activated sludge system and BNR system. Model simulations were performed considering the influent and operational data of both plants while examining these values.

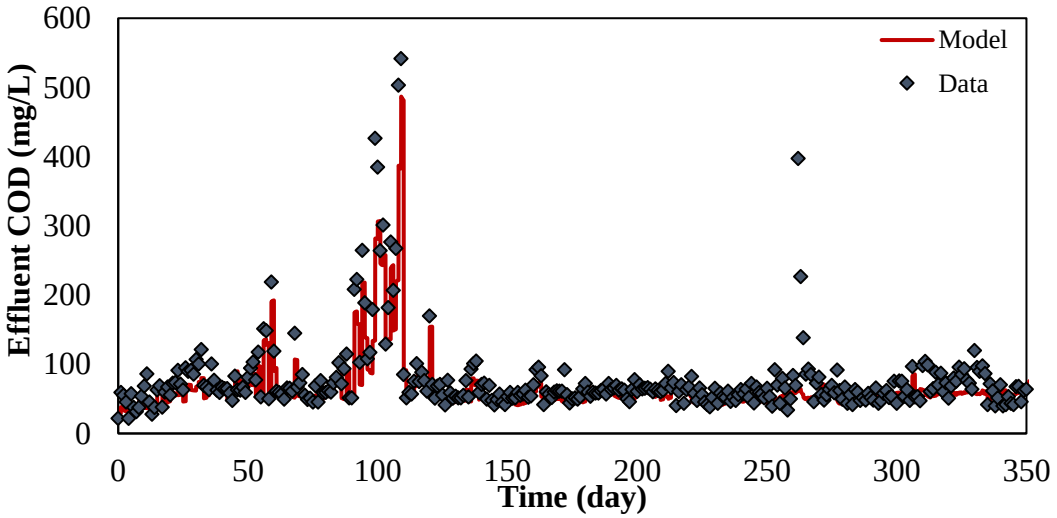

Figure 5.59 : Effluent COD concentrations and simulation results for P3.

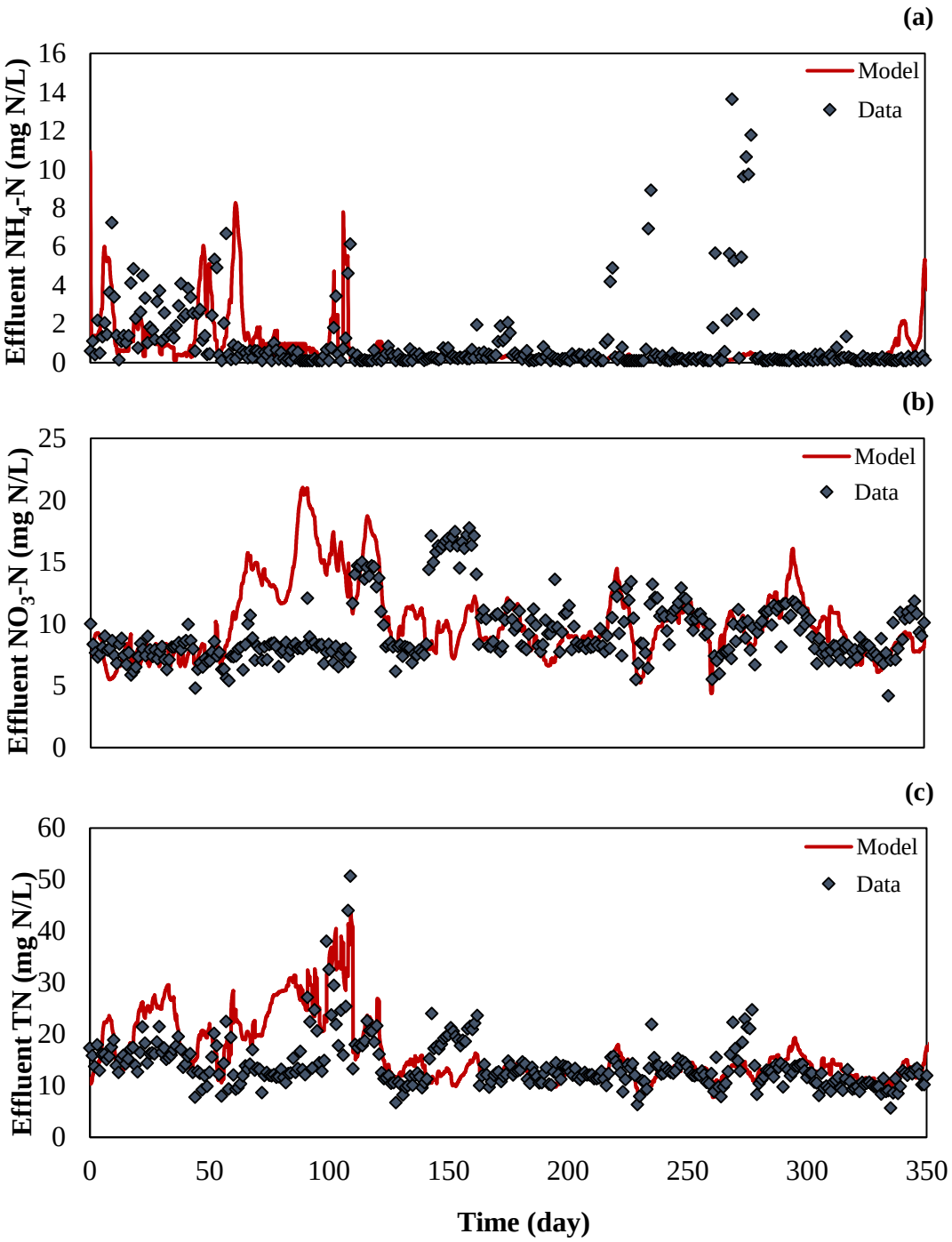

Figure 5.60 : Effluent NH_4-N (a), NO_X-N (b), and TN (c) concentrations and simulation results for P3.

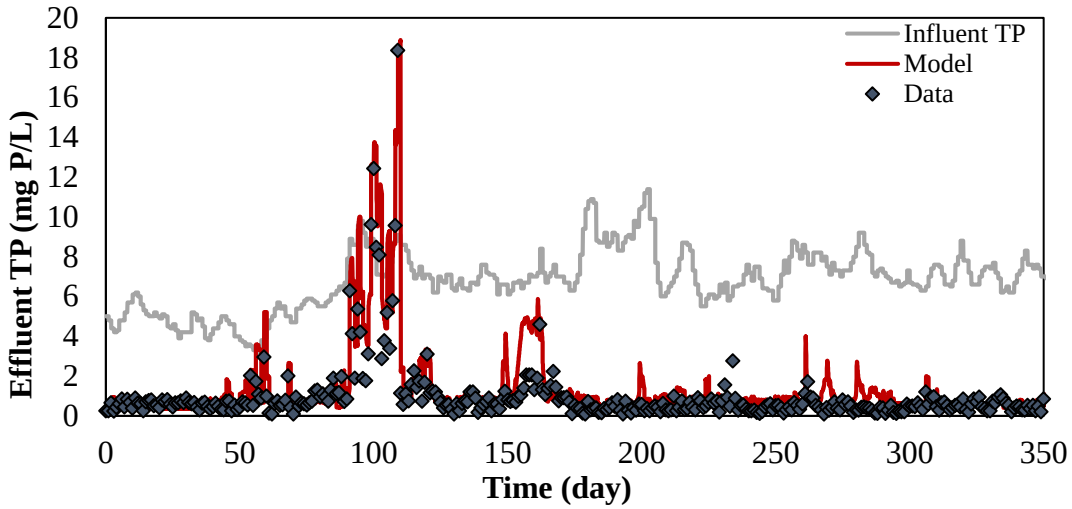

Figure 5.61 : Effluent TP concentrations and simulation results for P3.

Table 5.10 : Model kinetic parameters for P3 (20°C).

Parameter	Symbol	Info	Unit	P3	Default
Max. specific growth rate for NITO	μ_{NITO}	Exp.	day^{-1}	0.60	0.90
Half saturation of NH_x for NITO	$K_{O2,NITO,AS}$	Calibr.	g N/m^3	1.0	0.7
Max. specific growth rate for OHO	μ_{OHO}	Exp.	day^{-1}	3.5	4.0
Decay rate for OHO	b_{OHO}	Exp.	day^{-1}	0.4	0.62
Maximum hydrolysis rate	q_{HYD}	Exp.	day^{-1}	1.8	2.00
Half saturation for hydrolysis	$K_{HYD,AS}$	Exp.	g COD/g COD	0.06	0.05
Correction for anaerobic hydrolysis	$\eta_{HYD,ana}$	Calibr.	-	0.18	0.50
COD of volatile organics	$i_{CV,X}$	Meas.	g COD/g VSS	1.65	1.80
Maximum growth rate of AMETO	μ_{AMETO}	Exp.	day^{-1}	0.6	0.3
Half saturation of VFA for AMETO	K_{VFA}	Exp.	mg COD/L	550	400

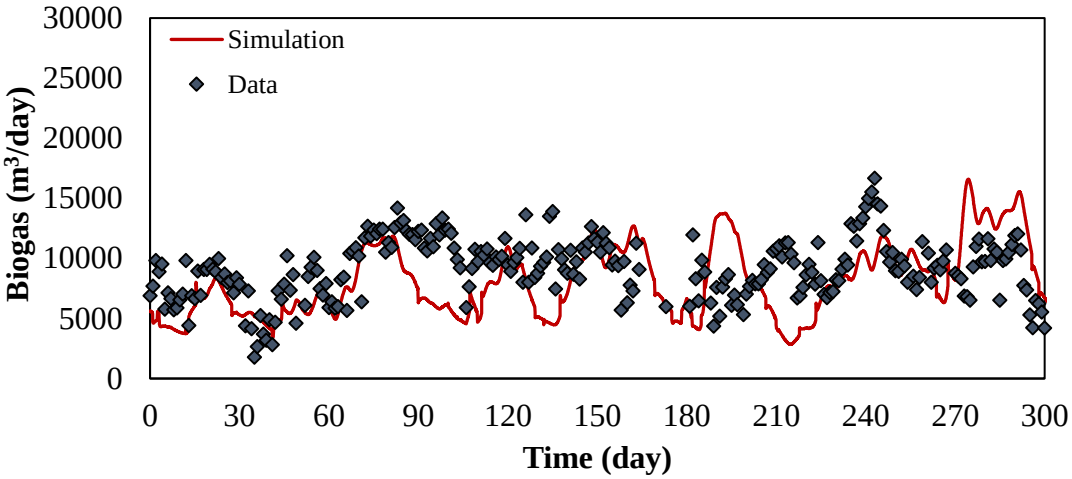

Figure 5.62 : Biogas flowrates for P3.

5.4.4 Dynamic estimation of hydrolysis rate for primary sludge

The main objective for the dynamic process simulation was to identify the representative anaerobic hydrolysis rates by evaluating the different sludge feeding

compositions (primary to secondary) versus biogas production. This would exhibit the different anaerobic hydrolysis rates for primary and secondary sludges.

As mentioned in the previous sections, dynamic modeling studies were carried out with an anaerobic digester system with only primary sludge feeding (P4) to see the effect of primary sludge mass fraction (PSMF) on the hydrolysis rate. At this point in the study, the treatment units of the plant were not included in the study since the focus was on the anaerobic hydrolysis rate, and the effects on the anaerobic digester were examined and calibration of the model was done on biogas flowrate by including the influent wastewater characterization and primary sedimentation unit removal efficiencies. Figure 5.63 depicts the simulation layout for P4.

The P4 plant receives an average flow rate of 150,000 m^3/day. The influent concentrations of COD, TKN, and TP are 1200 mg/L, 85 mg N/L, and 9.5 mg P/L, respectively. The plant has primary sedimentation tanks, a selector tank, Bio-P tanks, anoxic and aerobic activated sludge basins, and followed by final clarifiers. Only primary sludge is thickened and sent to the MAD. The average biogas production from the digester is reported to be 9,500 m^3/day.

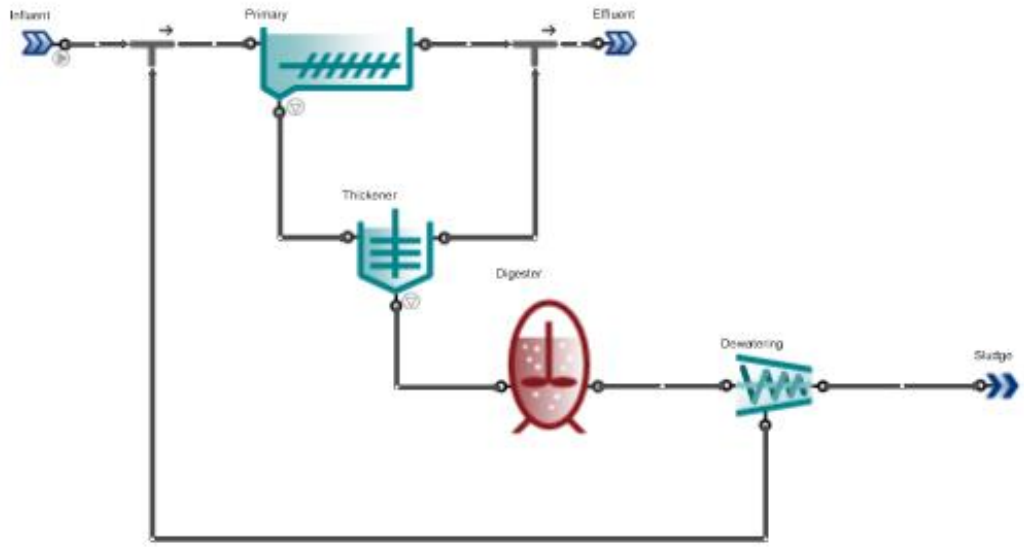

Figure 5.63 : Simulation layout for P4 (Sumo).

The dynamic simulation studies for the P4 plant yielded biogas quantities as shown in Figure 5.64. The modeling studies found the value of $\eta_{HYD,ana} \cdot q_{HYD}$ as 0.15 for the P4 plant (PSMF=100%).

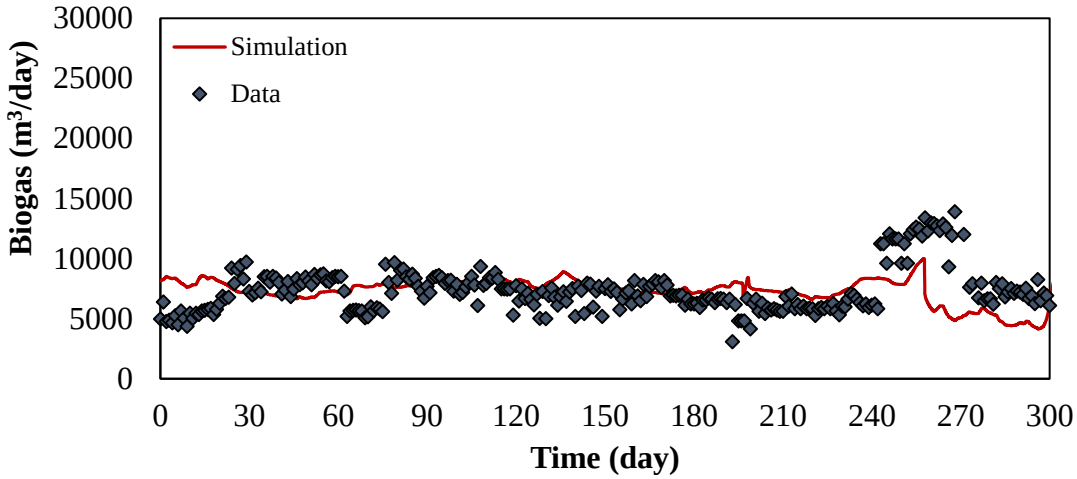

Figure 5.64 : Biogas flowrates for P4.

5.5 Biogas Simulations of WWTPs at Different Primary Sludge Mass Fractions

Plant-wide simulation and model calibration of big data belong to the WWTPs (P1, P2, P3 and P4) exhibited the relationship between the PSMF and the maximum hydrolysis rate term ($\eta_{HYD,ana} \cdot q_{HYD}$). Figure 5.65 reflects a linear correlation (R^2=0.98) between PSMF and $\eta_{HYD,ana} \cdot q_{HYD}$. The validity of this relation has been tested with the simulation results of P5, P6 and P7 as shown on Figure 5.65. The analysis of seven full-scale MADs feeding with different primary sludge mass fractions (PSMF 0 to 100%) have great importance for the resolution of the anaerobic hydrolysis kinetics. The two critical findings; the value of $\eta_{HYD,ana} \cdot q_{HYD}$ for primary sludge (0.15 for P4; PSMF=100%) and secondary sludge (0.40 for P2; PSMF=0%), revealed that $\eta_{HYD,ana} \cdot q_{HYD}$ value has to be in the range of 0.15-0.40 depending on the PSMF fraction fed to MAD (Figure 5.65). Therefore, re-adjustment of $\eta_{HYD,ana}$ for each plant is required to estimate the daily produced biogas at different PSMFs when using the default model.

In addition, the maximum anaerobic hydrolysis rates ($\eta_{HYD,ana} \cdot q_{HYD}$) used in simulations ($\eta_{HYD,ana} \cdot q_{HYD}$) exhibited parallel results with the maximum biogas production rates (R_m) for P1, P2, and P3, obtained via Modified-Gompertz model from SMA and BMP tests. For instance, P3 has the highest $\eta_{HYD,ana} \cdot q_{HYD}$ model parameter of 0.32 day^{-1} that corresponds to the maximum y_m value of 50 L/kg/day in the Modified-Gompertz model.

One should consider that, the most sensitive parameters in the simulations are the hydrolysis and decay rate that directly influence the biogas production in anaerobic digester. Other kinetic parameters can be regarded as non-sensitive parameters with their statistical ranges provided in Table 5.11. Kinetic parameters and standard deviations were estimated from batch tests by means of parameter estimation tool of AQUASIM software. Briefly, the standard deviations of the kinetic parameters were calculated by taking the inverse of Fisher Information Matrix (FIM) known as the summary of all parameter sensitivities (Reichert, 1998). The simulations also indicated that changing the estimated value of parameters (p) with their respective standard deviations (σ), changes the biogas flowrate less than 10%. Hence, the uncertainty on biogas estimation due to parameter errors (σ) could be neglected in comparison to the biogas yields obtained as a function of primary sludge mass (PSM).

Table 5.11 : Model kinetic parameters for P1, P2 and P3 (20°C).

Symbol	Info	Unit	P1	P2	P3	σ/p	Default
μ_{NITO}	Exp.	day^{-1}	0.65	0.55	0.60	0.05	0.90
$K_{O2,NITO,AS}$	Calibr.	g N/m^3	0.4	0.7	1.0	-	0.7
μ_{OHO}	Exp.	day^{-1}	4.0	4.0	3.5	0.04	4.0
b_{OHO}	Exp.	day^{-1}	0.4	0.4	0.4	0.15	0.62
q_{HYD}	Exp.	day^{-1}	1.1	1.4	1.8	0.06	2.00
$K_{HYD,AS}$	Exp.	g COD/g COD	0.06	0.06	0.06	0.02	0.05
$\eta_{HYD,ana}$	Calibr.	-	0.23	0.11	0.18	-	0.50
$\eta_{OHO,anpx}$	Exp.	-	0.60	0.40	0.40	-	0.60
$i_{CV,X}$	Meas.	g COD/g VSS	1.45	1.50	1.65	0.05	1.80
μ_{AMETO}	Exp.	day^{-1}	0.5	0.5	0.6	-	0.3
$K_{VFA,AMETO,AS}$	Exp.	mg COD/L	350	650	550	-	400

Figure 5.66 summarizes the simulation results of recalibrated model (Sumo1) considering the respective $\eta_{HYD,ana}$ values of each plant with different PSMF, compared to actual plant data. Accordingly, biogas production for each treatment plant was successfully estimated by re-adjusting $\eta_{HYD,ana}$ parameter. The error bars given in Figure 5.66 reflect the standard deviations (±σ) of the measured biogas flowrates in WWTPs. It should be noted that the maximum hydrolysis rates in plants P4, P5, P6, and P7 were assumed to be the average of the P1, P2, and P3 plants (q_{HYD}=1.3 day^{-1}) that were previously determined with batch tests.

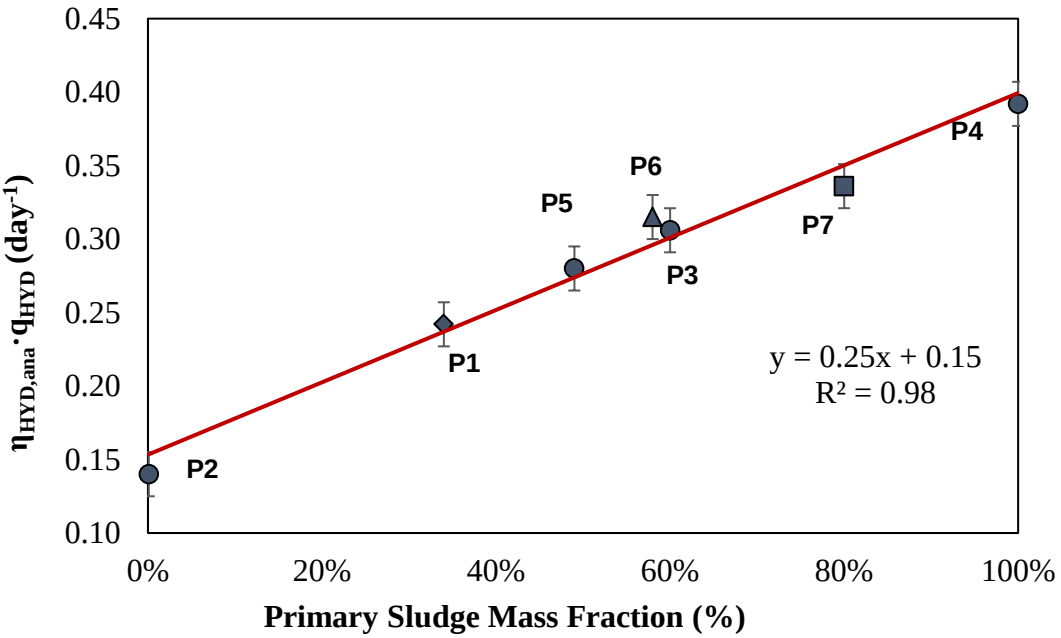

Figure 5.65 : Hydrolysis rates for different primary sludge mass fractions.

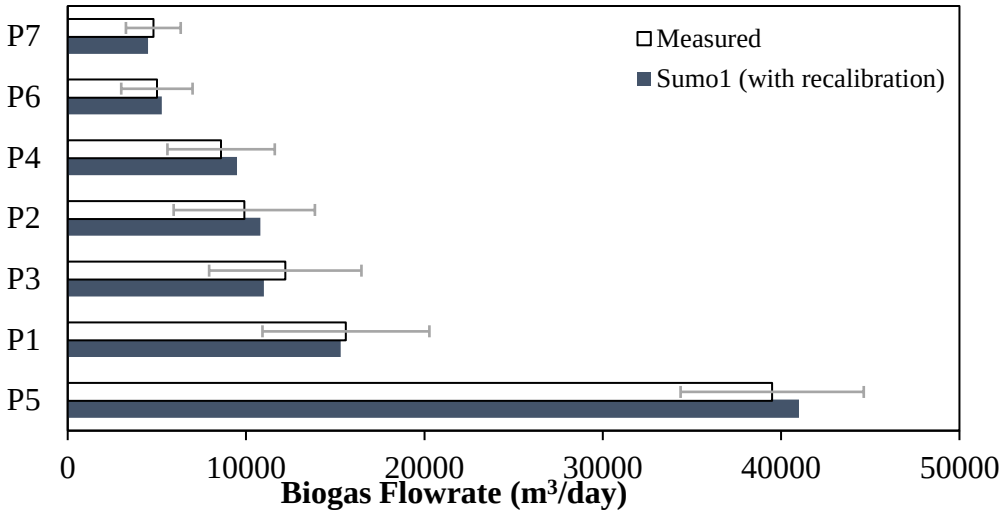

Figure 5.66 : Average biogas flowrates with recalibrated Sumo1 model.

5.6 Modification of Activated Sludge Model with Segregated Hydrolysis Kinetics

According to the death-regeneration model, endogenous microbial products (X_E) and slowly biodegradable organic matter (X_B) are regenerated as a result of biomass decay. In current plant-wide models (GPS-X, Biowin, Sumo, etc.), it is assumed that the particulate organic matter originated from biomass decay (secondary sludge) and from the influent wastewater (captured in primary sludge) have the same degradation

pathway and particulate organic matter conversion is achieved with a single hydrolysable COD component (X_B). Practically, the decay rates under anaerobic conditions are adjusted by the reduction factor for anaerobic hydrolysis ($\eta_{HYD,ana}$) with reference to the aerobic hydrolysis rate.

This study showed that hydrolysis of secondary sludge was found to have much lower degradation rate than primary sludge, indicating the different hydrolysis rate of influent originated (X_B) and decay oriented particular organics ($X_{B,E}$), contrary to the commonly accepted model structure. Obviously, hydrolysis rate for particulate organics significantly differs depending on the source, X_B or $X_{B,E}$, and current model structure (Sumo1 or other plant-wide models) does not consider this differentiation. Besides, in the decay-hydrolysis reaction chain, biomass decay is the rate limiting step therefore hydrolysis of $X_{B,E}$ is first controlled by the decay rate. Inherently, there is a certain balance between decay and hydrolysis rate. Hence, a slight accumulation of $X_{B,E}$ will occur when the hydrolysis rate of $X_{B,E}$ converges to the decay rate and eventually affects the biogas production in anaerobic digesters.

The attempts on the model calibration of long-term data belong to P1, P2, P3, and P4 showed that applying one single hydrolysis reaction kinetics for both X_B and $X_{B,E}$ does not satisfy the biogas production profile in every change in the primary sludge mass fraction. Hence, when studying with the current plant-wide models, model recalibration of biogas is required for any change in PSMF in terms of $\eta_{ana,HYD}$. Whereas, the robustness of the model is its ability to predict process performance without requiring recalibration, even if operational conditions are changed. Therefore, the structure of the death-regeneration model is modified as Sumo1H and tested for the estimation of biogas flowrates without any recalibration.

The Sumo1H model relies on the separation of the hydrolysis rates of particulate organic matter in the influent wastewater (X_B) and organic matter produced from biomass decay ($X_{B,E}$) by having different degradation kinetics for primary and secondary sludges (Figure 5.67). $X_{B,E}$ is formed through the active biomass decay and undergoes hydrolysis reaction according to the new model (Figure 5.67). In the model, anaerobic degradation rates are regulated with different $\eta_{HYD,ana}$ for X_B and $X_{B,E}$ to predict the biogas flowrates of all WWTPs, accurately.

Sumo1H eliminates the requirement for model recalibration of biogas as a function of biological sludge fraction fed to anaerobic digester, by modifying the model. Using this approach, simulations of the biogas flow rates given in Figure 5.66 were reproduced by adjusting the parameter $\eta_{HYD,ana}$ for X_B and $X_{B,E}$ components to 0.30 and 0.11, respectively (Figure 5.68).

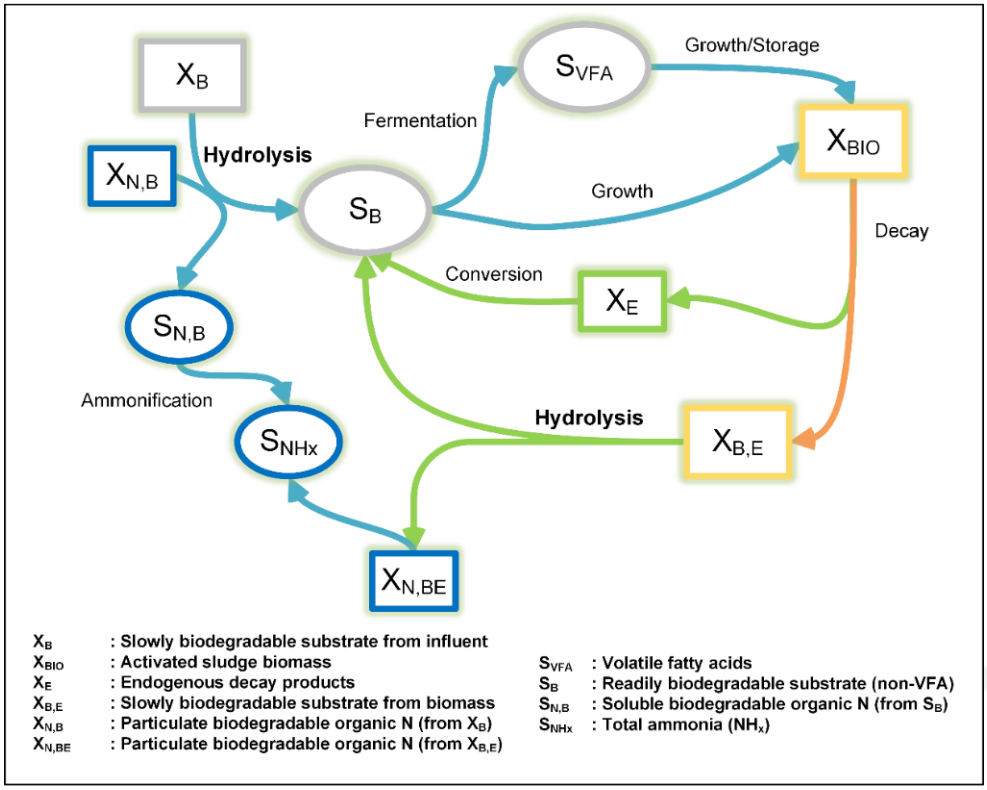

Figure 5.67 : Proposed model structure for biodegradable organics and active biomass (Sumo1H).

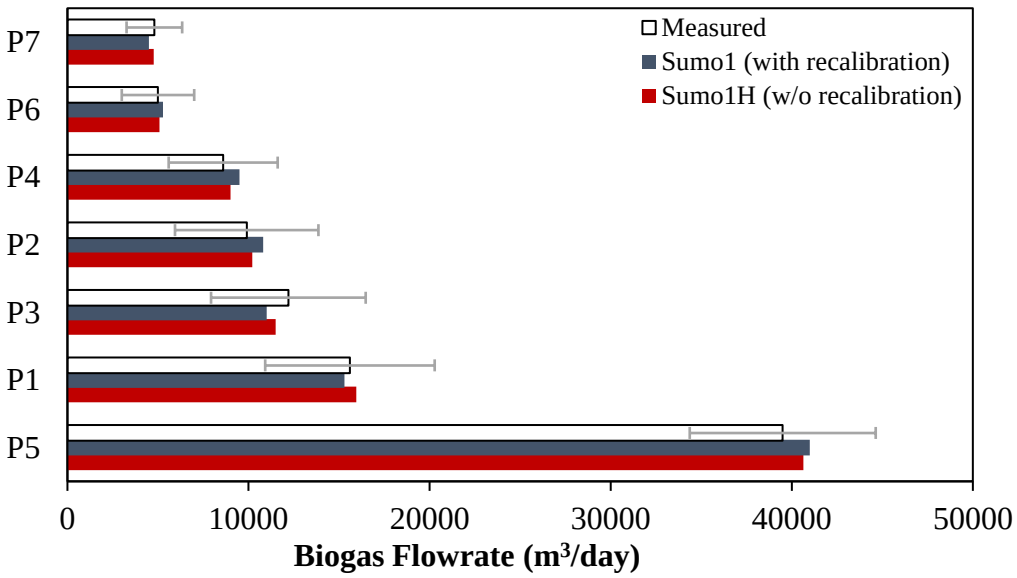

Figure 5.68 : Average biogas flowrates with Sumo1H model.

As a result, the biogas measurements in the plants (P1-P7) can be successfully predicted using the new model (Sumo1H), effectively eliminating the previous need for frequent model recalibration. This improvement not only streamlines the modeling process but also enhances the reliability of the predictions. The effluent parameters, which represent the average performance of the plants, have been both calculated and measured, and their details are provided in Table 5.12.

It is important to note that the performance of plant P4 is not included in these results since only primary sludge is fed to the digester, differing from the other plants. Furthermore, the plants coded as P1, P2, P3, and P6 are designed as BNR systems, whereas P5 operates as a high-rate activated sludge system, emphasizing the rapid processing of wastewater. P7, on the other hand, is specifically designed for nitrogen removal.

The strong correlation between the modeled and actual data underscores the effectiveness of Sumo1H in accurately simulating plant performance. This validation provides confidence in the model's use for predicting biogas production together with overall plant efficiency, making it a valuable tool for optimizing wastewater treatment operations and planning future upgrades.

Table 5.12 : Effluent performance analysis of plants conducted with Sumo1H model.

Effluent Parameters	Unit	WWTPs											
		P1		P2		P3		P5		P6		P7	
		Data	Model	Data	Model	Data	Model	Data	Model	Data	Model	Data	Model
Total COD	mg O_2/L	43	44	50	52	80	70	45	40	37	40	33	37
Total Nitrogen	mg N/L	7.0	8.0	9.8	10	10	9.8	NA	30	5.1	5.7	8.5	9.0
Ammonia Nitrogen	mg N/L	1.4	1.2	5.4	4.5	0.9	1.2	NA	27	<1	0.5	<0.5	0.1
Total Phosphorus	mg P/L	0.8	0.6	1.0	0.9	0.9	0.7	NA	5.2	0.90	0.95	NA	5.5

6. CONCLUSION AND RECOMMENDATIONS

The paradigm within which wastewater treatment plants are conceptualized and designed has evolved significantly, transitioning from methodologies predominantly grounded in standardized designs to those that prioritize an experimental, evidence-based framework. This contemporary methodology is characterized by its interdisciplinary approach, encapsulating principles and techniques from chemistry, microbiology, bioprocess engineering, and control engineering. This comprehensive approach facilitates the extensive application of wastewater and biomass characterization techniques, thereby enabling the acquisition of critical data reflective of local conditions. Such data facilitates informed decision-making processes, ensuring engineering practices adhere to established safety thresholds. Furthermore, model-based experimental characterization is indispensable in delineating the operational boundaries of wastewater treatment facilities and in critically evaluating potential upgrades to existing systems.

The selection of appropriate wastewater and sludge treatment methodologies is contingent upon specific considerations, including the fractionation of influent COD and the kinetic parameters particular to the biomass in question. Consequently, the integration of experimental endeavors with sophisticated full-scale plant-wide modeling tools emerges as a formidable strategy for the selection of suitable treatment systems and the execution of robust process calculations.

In practical use, plant-wide models apply one single hydrolysis kinetics for influent-originated (X_B) and decay-oriented particulate organics ($X_{B,E}$). Contrary to traditional assumptions in wastewater treatment modeling, it was observed that secondary sludge undergoes hydrolysis at a much slower kinetics compared to primary sludge. This discrepancy suggests that current models like Sumo1 and other comprehensive wastewater treatment models fail to account for the variance in hydrolysis rates between different types of particulate organics. Typically, model recalibration is a critical process in wastewater treatment modeling to ensure accurate predictions of system behavior, particularly in the production of biogas from anaerobic digesters.

Recalibration is often necessary when different sludge types are treated, affecting the efficiency of the model in predicting biogas flowrates. Traditional models, such as Sumo1, require frequent recalibration to adapt to the variations in sludge composition and operational conditions in different treatment facilities. This recalibration process can be time-consuming and resource-intensive, as it involves extensive data collection and analysis to adjust model parameters to match observed plant performance accurately.

The Sumo1H model significantly reduces the necessity for such recalibrations by incorporating adjustable parameters for hydrolysis rates that are specific to the origin of the particulate organics—X_B and $X_{B,E}$. By fitting the kinetics of parameters to reflect the inherent differences in hydrolysis rates of primary and secondary sludges, Sumo1H allows for more stable and consistent model performance across various conditions without the continuous need for recalibration. This approach not only enhances the predictability and reliability of the model but also optimizes the operational efficiency of biogas production processes in wastewater treatment plants.

A pivotal discovery within the scope of the current study is the observation that hydrolysis kinetics deviate significantly from values previously accepted within the scholarly literature. This revelation underscores the importance of a deep understanding of the individual kinetics of processes. Overlooking such critical knowledge can precipitate significant design inefficiencies and failures. As such, this study makes a seminal contribution by providing a comprehensive database on plant-specific process kinetics derived from full-scale operations. It unequivocally demonstrates that a tailored approach to kinetic characterization is crucial for developing more precise full-scale wastewater treatment plant designs, particularly in municipal wastewater with significant industrial contributions.

The pursuit of compliance with discharge standards and energy generation via biogas through anaerobic sludge digestion necessitates an intricate calculation of organic matter transformations within wastewater treatment facilities. Within the activated sludge process framework, the slow biodegradability of organic matter, whether inherent in the influent or resultant from biomass decay, constitutes a significant reserve for nutrient removal and energy production. Contemporary process models attribute the degradation of this organic matter to the rate-limiting hydrolysis process,

conceptualizing the organic matter cycle through a singular particulate biodegradable COD component.

This investigation facilitated the experimental determination of COD fractionation and specific process kinetics alongside the evaluation of full-scale plant performances. Biogas production metrics were substantiated through plant-wide dynamic simulations. These simulations, applied to full-scale municipal WWTPs of varying configurations, indicated the necessity for model recalibration contingent upon the mass fractions of primary sludge directed towards digestion processes. The innovative model delineated the biodegradation kinetics of particulate organics derived from influent and those produced through biomass decay, revealing that particulate organic matter in primary sludge degrades thrice as fast as that originating from biomass decay. Consequently, this refined model accurately characterized the biogas production potential of seven full-scale municipal wastewater treatment plants, showcasing distinct degradation kinetics.

Moreover, this novel modeling approach promises to revolutionize the design criteria for BNR systems, including the precise sizing of Bio-P tanks and the optimization of anoxic zones for enhanced denitrification. It heralds a new concept of accurate assessment of biogas production capabilities and the design and optimization of sludge disintegration processes, such as thermal hydrolysis. Thus, the proposed model facilitates a comprehensive reevaluation of process performance and design methodologies for biological processes, including sludge fermentation and BNR processes. However, developing specific experimental procedures for determining novel model parameters, particularly concerning hydrolysis under anaerobic and anoxic conditions, remains imperative.

REFERENCES

Andrews J. F. (1974). Dynamic models and control strategies for waste-water treatment processes. *Water Research, 8* (5), 261–289. doi: 10.1016/0043-1354(74)90090-6.

Angelidaki, I., & Ahring, B. K. (1993). Thermophilic anaerobic digestion of livestock waste: the effect of ammonia. *Applied microbiology and biotechnology*, *38*, 560-564. doi: 10.1007/BF00242955.

Angelidaki, I., Ellegaard, L., & Ahring, B. K. (1999). A comprehensive model of anaerobic bioconversion of complex substrates to biogas. *Biotechnology and bioengineering*, *63*(3), 363-372. doi: 10.1002/(SICI)1097-0290(19990505)63:3<363::AID-BIT13>3.0.CO;2-Z.

APHA. (2012). Standard Methods for the Examination of Water and Wastewater. 22nd Edition, American Public Health Association, American Water Works Association, Water Environment Federation, Washington, DC, USA.

Appels, L., Baeyens, J., Degreve, J., & Dewil, R. (2008). Principles and potential of the anaerobicdigestion of waste-activated sludge. *Progress in Energy and Combustion Science*, *34*, 755-781. doi: 10.1016/j.pecs.2008.06.002.

Ariunbaatar, J., Panico, A., Esposito, G., Pirozzi, F., & Lens, P. N. L. (2014). Pretreatment methods to enhance anaerobic digestion of organic solid waste. *Applied Energy*, *123*, 143-156. doi: 10.1016/j.apenergy.2014.02.035.

Arshad, A., Hashmi, H.N., & Qureashi, I.A. (2011). Anaerobic digestion of Chlorphenolic Wastes. *Int J Environ Resources, 5* (1), 149–158.

Artan, N. (1987). *Aktif çamurda çözünmüş kalıcı ürün oluşumu modeli.* (Ph.D. Thesis). Istanbul Technical University, Graduate School, Istanbul.

ATV-131 (2000) *Dimensioning of Single Stage Activated Sludge Plants*. GFA Publishing Company of ATV-DVWK Water, Wastewater and Waste. Hennef, Germany. ISBN: 3-935669-82-8.

Barat, R., Serralta, J., Ruano, M. V., Jiménez, E., Ribes, J., Seco, A., & Ferrer, J. (2013). Biological Nutrient Removal Model No. 2 (BNRM2): a general model for wastewater treatment plants. *Water Science and Technology*, *67*(7), 1481-1489. doi: 10.2166/wst.2013.004.

Barker, P.S., & Dold, P.L. (1997). General model for biological nutrient removal activated-sludge systems: model presentation. *Water Env Res.*, *69* (5), 969-984. doi: 10.2175/106143097X125669.

Batstone, D. J. (2006). Mathematical modelling of anaerobic reactors treating domestic wastewater: Rational criteria for model use. *Reviews in Environmental Science and Bio/Technology*, *5*(1), 57-71. doi: 10.1007/s11157-005-7191-z.

Batstone, D.J., Keller, J., Angelidaki, I., Kalyuzhnyi, S.V., Pavlostathis, S.G., Rozzi, A., … & Vavilin, V.A. (2002). The IWA Anaerobic Digestion Model No 1 (ADM1), IWA Publishing, London.

Bidstrup, S.M., & Grady, Jr.C.P.L. (1987). A user's manual for SSSP simulation of single sludge processes for carbon oxidation, nitrification and denitrification. Environmental Systems Engineering, Clemson Univ., Clemson, SC, ABD.

Bougrier, C., Delgenes, J. P., & Carrère, H. (2007). Impacts of thermal pre-treatments on the semi-continuous anaerobic digestion of waste activated sludge. *Biochemical Engineering Journal*, *34*(1), 20-27. doi: 10.1016/j.bej.2006.11.013.

Brun, R., Kühni, M., Siegrist, H., Gujer, W., & Reichert, P. (2002). Practical identifiability of ASM2d parameters—systematic selection and tuning of parameter subsets. *Water research*, *36*(16), 4113-4127. doi: 10.1016/S0043-1354(02)00104-5.

Brun, R., Reichert, P., & Künsch, H. R. (2001). Practical identifiability analysis of large environmental simulation models. *Water Resources Research*, *37*(4), 1015-1030. doi: 10.1029/2000WR900350.

Cano, R., Pérez-Elvira, S. I., & Fdz-Polanco, F. (2015). Energy feasibility study of sludge pretreatments: A review. *Applied Energy*, *149*, 176-185. doi: 10.1016/j.apenergy.2015.03.132.

Chen, Y., Cheng, J. J., & Creamer, K. S. (2008). Inhibition of anaerobic digestion process: A review. *Bioresource Technology*, *99* (10), 4044-4064. doi: 10.1016/j.biortech.2007.01.057.

Çokgör, E.U. (1997). *Aerobik sistemlerde proses stokiometrisi ve kinetiğinin respirometrik olarak değerlendirilmesi.* (Ph.D. Thesis). Istanbul Technical University, Graduate School, Istanbul.

de la Rubia, M. A., Perez, M., Romero, L. I., & Sales, D. (2002). Anaerobic mesophilic and thermophilic municipal sludge digestion. *Chemical and biochemical engineering quarterly*, *16*(3), 119-124.

de Mes, T. Z. D., Stams, A. J. M., Reith, J. H., & Zeeman, G. (2003). Methane production by anaerobic digestion of wastewater and solid wastes. *Bio-methane & Bio-hydrogen*, *2003*, 58-102.

Dold, P. &Marais, G.v.R. (1986). Evaluation of the general activated sludge model proposed by the IAWPRC task group. *Water Science and Technology*., *18* (6), 63-89. doi: 10.2166/wst.1986.0061.

Dold, P.L, Ekama, G. A, & Marais, GvR. (1980). A general model for the activated sludge process. *Progress in Water Technology*, *12* (6), 47-54. doi: 10.1016/B978-1-4832-8438-5.50010-8.

Donoso-Bravo, A., Mailier, J., Martin, C., Rodríguez, J., Aceves-Lara, C. A., & Wouwer, A. V. (2011). Model selection, identification and validation in anaerobic digestion: a review. *Water research*, *45*(17), 5347-5364. doi: 10.1016/j.watres.2011.08.059.

Donoso-Bravo, A., Pérez-Elvira, S. I., & Fdz-Polanco, F. (2010). Application of simplified models for anaerobic biodegradability tests. Evaluation of pre-treatment processes. *Chemical Engineering Journal*, *160*(2), 607-614. doi: 10.1016/j.cej.2010.03.082.

Drewnowski, J. (2014). The impact of slowly biodegradable organic compounds on the oxygen uptake rate in activated sludge systems. *Water Science and Technology*, *69*(6), 1136-1144. doi: 10.2166/wst.2013.771.

Drewnowski, J., & Makinia, J. (2011). The role of colloidal and particulate organic compounds in denitrification and EBPR occurring in a full-scale activated sludge system. *Water Science and Technology*, *63*(2), 318-324. doi: 10.2166/wst.2011.056.

Droste, R. L. (1997). Theory and practice of water and wastewater treatment. John Wiley & Sons, New Jersey, USA.

Eastman, J. A., & Ferguson, J. F. (1981). Solubilization of particulate organic carbon during the acid phase of anaerobic digestion. *Journal Water Pollution Control Federation*, 352-366.

Ekama, G. A., & Wentzel, M. C. (1999). Difficulties and developments in biological nutrient removal technology and modelling. *Water Science and Technology*, *39*(6), 1-11. doi: 10.1016/S0273-1223(99)00117-1.

Ekama, G. A., Sötemann, S. W., & Wentzel, M. C. (2007). Biodegradability of activated sludge organics under anaerobic conditions. *Water research*, *41*(1), 244-252. doi: 10.1016/j.watres.2006.08.014.

Ekama, G.A. (2009). Using bioprocess stoichiometry to build a plant-wide mass balance based steady-state WWTP model. *Water Research*, *43*, 2101–2120. doi: 10.1016/j.watres.2009.01.036.

Ekama, G.A., Barnard, J.L., Gunthert, F.W., Krebs, P., McCorquodale, J.A., Parker, D.S., & Wahlberg, E.J. (1997). Secondary settling tanks: theory, modelling design and operation. IAWQ Scientific and Technical Report No. 6, IWA Publishing, London.

Ekama, G.A., Dold, P. L., & Marais, GvR. (1986). Procedures for determining influent COD fractions and the maximum specific growth rate of heterotrophs in activated sludge systems. *Water Science and Technology*, *18*, 91-114. doi: 10.2166/wst.1986.0062.

Elliott, A. & Mahmood, T. (2007). Pretreatment technologies for advancing anaerobic digestion of pulp and paper biotreatment residues. *Water Research*, *41* (19), 4273-86. doi: 10.1016/j.watres.2007.06.017.

EPA. (1994). Land Application of Sewage Sludge, A Guide for Land Appliers on the Requirements of the Federal Standards for the Use or Disposal of Sewage Sludge, 40 CFR Part 503. U.S. Environmental Protection Agency, EPA/831-B-93-002b.

Eskicioglu, C., Kennedy, K. J., & Droste, R. L. (2006). Characterization of soluble organic matter of waste activated sludge before and after thermal pretreatment. *Water research*, *40*(20), 3725-3736. doi: 10.1016/j.watres.2006.08.017.

Etuwe, C. N., Momoh, Y. O. L., & Iyagba, E. T. (2016). Development of mathematical models and application of the modified gompertz model for designing batch biogas reactors. *Waste and biomass valorization*, *7*, 543-550. doi: 10.1007/s12649-016-9482-8.

Fetting, C. (2020). The European Green Deal. ESDN Report, December 2020, ESDN Office, Vienna.

Filipe, C.D.M, & Daigger, G.T. (1998). Development of a revised metabolic model for the growth of phosphorus-accumulating organisms. *Wat. Env. Res*., *70* (1), 67-79. doi: doi.org/10.2175/106143098X126900.

Garret M.T., & Sawyer C. N. (1952). Kinetics of removal of soluble BOD by activated sludge. In Proc: 7th Annual Ind. Wastes Conf., Purdue University, Lafayette, IN, 7-9 May, 51-77.

Gavala, H.N., Angelidaki, I., & Ahring, B.K. (2003). Kinetics and modeling of anaerobic digestion process. *Biomethanation I*, *81*, 57-93. doi: 10.1007/3-540-45839-5_3.

Gerber, M., & Span, R. (2008). An analysis of available mathematical models for anaerobic digestion of organic substances for production of biogas. In: *International Gas Union Research Conference (IGRC), Paris*.

Gianico, A., Braguglia, C. M., Cesarini, R., & Mininni, G. (2013). Reduced temperature hydrolysis at 134°C before thermophilic anaerobic digestion of waste activated sludge at increasing organic load. *Bioresource Technology*, *143*, 96-103. doi: 10.1016/j.biortech.2013.05.069.

Goel, R., Mino, T., Satoh, H., & Matsuo, T. (1999). Modeling hydrolysis processes considering intracellular storage. *Water Science and Technology*, *39*(1), 97-105. doi: 10.1016/S0273-1223(98)00779-3.

Gossett, J. M., & Belser, R. L. (1982). Anaerobic digestion of waste activated sludge. *Journal of the Environmental Engineering Division*, *108*(6), 1101-1120. doi: 10.1061/JEEGAV.0001359.

Grau, P., De Gracia, M., Vanrolleghem, P. A., & Ayesa, E. (2007). A new plant-wide modelling methodology for WWTPs. *Water Research*, *41*(19), 4357-4372. doi: 10.1016/j.watres.2007.06.019.

Gujer, W., & Larsen, T. A. (1995). The implementation of biokinetics and conservation principles in ASIM. *Water Science and Technology*, *31* (2), 257-266. doi: 10.1016/0273-1223(95)00198-V.

Gujer, W., & Zehnder, A. J. (1983). Conversion processes in anaerobic digestion. *Water science and technology*, *15*(8-9), 127-167. doi: 10.2166/wst.1983.0164.

Gujer, W., Henze, M., Mino, T., & van Loosdrecht, M.C.M. (1999). Activated sludge model No 3., *Water Sci. Technol*., *39* (1), 183-193. doi: 10.1016/S0273-1223(98)00785-9.

Güneş, G., Hallaç, E., Özgan, M., Ertürk, A., Okutman Taş, D., Çokgor, E., ... & Insel, G. (2019). Enhancement of nutrient removal performance of activated sludge with a novel hybrid biofilm process. *Bioprocess and biosystems engineering*, *42*, 379-390. doi: 10.1007/s00449-018-2042-9.

Hellinga, C., Schellen, A.A.J.C., Mulder, J.W., van Loosdrecht, M.C.M., & Heijnen, J.J. (1998). The Sharon process: an innovative method for nitrogen removal from ammonium rich wastewater. *Water Science and Technology*, *34*, 135-142. doi: 10.1016/S0273-1223(98)00281-9.

Henze, M. (1992). Characterization of wastewater for modelling of activated sludge processes. *Water Science and Technology*, *25* (6), 1-15. doi: 10.2166/wst.1992.0110.

Henze, M. (2004). Modeling of aerobic wastewater treatment processes, *Environmental Biotechnology: Concepts and Applications*, pp. 121-134.

Henze, M., & Mladenovski, C. (1991). Hydrolysis of particulate substrate by activated sludge under aerobic, anoxic and anaerobic conditions. *Water research*, *25*(1), 61-64. doi: 10.1016/0043-1354(91)90099-C.

Henze, M., Grady, C.P.L.Jr, Gujer, W., Marais, G.v.R., & Matsuo, T. (1987). Activated sludge model No.1. IAWPRC Science and Technical Report No. 1, IAWPRC, London.

Henze, M., Gujer, W., Mino, T., & Van Loosedrecht, M. (2000). *Activated sludge models ASM1, ASM2, ASM2d and ASM3*. IWA Publishing. London, UK.

Henze, M., Gujer, W., Mino, T., Matsuo, T., Wentzel, M..C, & Marais, G.v.R. (1995). Activated sludge model No.2., IAWPRC Task Group on Mathematical Modelling for Design and Operation of Biological Treatment. IAWQ, London.

Henze, M., van Loosdrecht, M.C., Ekama, G.A. & Brdjanovic, D. (2008). *Biological wastewater treatment*. IWA publishing. London, UK.

Hiatt, W.C., & Grady, C.P.L. (2008). An updated process model for carbon oxidation, nitrification and denitrification. *Water Environ Res.*, *80* (11), 2145-2156. doi: 10.2175/106143008X304776.

Hungate, R. E. (1967). Hydrogen as an intermediate in the rumen fermentation. *Archiv für Mikrobiologie*, *59*, 158-164. doi: 10.1007/BF00406327.

Hvala, N., Vrečko, D., & Bordon, C. (2018). Plant-wide modelling for assessment and optimization of upgraded full-scale wastewater treatment plant performance. *Water Practice & Technology*, *13*(3), 566-582. doi: 10.2166/wpt.2018.070.

Ikumi, D. S., & Harding, T. H. (2020). Kinetics of biological and chemical processes in anoxic-aerobic digestion of phosphorus rich waste activated sludge. *Water Research*, *170*, 115333. doi: 10.1016/j.watres.2019.115333.

Ikumi, D. S., Harding, T. H., Brouckaert, C. J. & Ekama, G. A. (2011). Plant wide integrated biological, chemical and physical bioprocesses modeling of wastewater treatment plants in 3 phases (aqueous-gas-solid). Research Report W136, Dept of Civil Eng., Univ. of Cape Town, Rondebosch, Cape, RSA.

İnsel, G. (2004). *Model-based activated sludge systems analysis for carbon, nitrogen and phosphorus removal mechanisms.* (Ph.D. Thesis). Istanbul Technical University, Graduate School, Istanbul.

Insel, G., Guder, B., Gunes, G., & Cokgor, E. (2012). Are standard wastewater treatment plant design methods suitable for any municipal wastewater? *Water Sci Technol., 66* (2), 328-335. doi: 10.2166/wst.2012.176.

Insel, G., Orhon, D., & Vanrolleghem, P.A. (2003). Identification and modelling of aerobic hydrolysis–Application of optimal experimental design. *J Chem Technol Biotechnol., 78* (4), 437–445. doi: 10.1002/jctb.807.

Insel, G., Ozyildiz, G., Okutman-Tas, D., Guven, D., Zengin, G. E., Pala-Ozkok, I., ... & Cokgor, E. (2022). A comprehensive evaluation of process kinetics: A plant-wide approach for nutrient removal and biogas production. *Water Research*, *217*, 118410. doi: 10.1016/j.watres.2022.118410.

İnsel, H. G., Artan, N., Çokgör Ubay, E., Okutman Taş, D., Akça Güven, D., Zengin Balcı, G. E., and Özyıldız, G. (2022). Kentsel Atıksu Arıtma Tesisleri Proses Seçimi, Tasarımı Ve Modellenmesi El Kitabı. İstanbul. ISBN: 978-605-9507-56-1.

İnsel, H. G., Artan, N., Çokgör Ubay, E., Okutman Taş, D., Akça Güven, D., Zengin Balcı, G. E., Pala Özkök, İ., Özyıldız, G. (2020). İleri Biyolojik Atıksu Arıtma Tesisi Deneysel Karakterizasyon ve Dinamik Koşullarda Modellenmesi - Final Raporu. İstanbul.

Jenkins, D., & Wanner, J. (2014). *Activated sludge-100 years and counting*. IWA publishing.

Kazadi Mbamba, C., Flores-Alsina, X., Batstone, D. J., & Tait, S. (2016). Validation of a plant-wide phosphorus modelling approach with minerals precipitation in a full-scale WWTP. *Water Research*, *100*, 169-183. doi: 10.1016/j.watres.2016.05.003.

Kazadi Mbamba, C., Lindblom, E., Flores-Alsina, X., Tait, S., Anderson, S., Saagi, R., ... & Jeppsson, U. (2019). Plant-wide model-based analysis of iron dosage strategies for chemical phosphorus removal in wastewater treatment systems. *Water research*, *155*, 12-25. doi: 10.1016/j.watres.2019.01.048.

Khanal, S. K. (2008). Microbiology and Biochemistry of Anaerobic Biotechnology. S. K. Khanal. In *Anaerobic Biotechnology for Bioenergy Production Principles and Application* (pp. 29-41). Wiley - Blackwell.

Kor G. (2019) *Effect of Microwave Pretreatment on Fate of Antimicrobials and Conventional Pollutants During Anaerobic Sludge Digestion and Biosolids Quality for Land Application.* (Ph.D. Thesis). Istanbul Technical University, Graduate School, Istanbul.

Koupaie, E. H., & Eskicioglu, C. (2016). Conventional heating vs. microwave sludge pretreatment comparison under identical heating/cooling profiles for thermophilic advanced anaerobic digestion. *Waste management*, *53*, 182-195. doi: 10.1016/j.wasman.2016.04.014.

Krishna, C., & van Loosdrecht, M.C.M. (1999). Substrate flux into storage and growth in relation to activated sludge modeling. *Water Res., 33* (14), 3149-3161. doi: 10.1016/S0043-1354(99)00031-7.

Lay, J. J., Li, Y. Y., and Noike, T. (1997). Influences of pH and moisture content on the methane production in high-solids sludge digestion. *Water Research, 31*, 1518-1524. doi: 10.1016/S0043-1354(96)00413-7.

Li, H.L. & Wang, Y. (2011). Influence of total solid and stirring frequency on performance of dry anaerobic digestion treating cattle manure. In: Zhouzhou, Y., Luo, Q. (Eds.), Chemical, Mechanical and Materials Engineering. Stafa-Zurich: Trans Tech Publications Ltd.

Li, Y., & Noike, T. (1987). Characteristics of the degradation of excess activated sludge in anaerobic acidogenic phase. *Japan Journal of Water Pollution Research*, *10*(12), 729-740.

Lizarralde, I., Fernández-Arévalo, T., Brouckaert, C., Vanrolleghem, P., Ikumi, D. S., Ekama, G. A., ... & Grau, P. (2015). A new general methodology for incorporating physico-chemical transformations into multi-phase wastewater treatment process models. *Water Research*, *74*, 239-256. doi: 10.1016/j.watres.2015.01.031.

Lizarralde, I., Fernández-Arévalo, T., Manas, A., Ayesa, E., & Grau, P. (2019). Model-based opti mization of phosphorus management strategies in Sur WWTP, Madrid. *Water research*, *153*, 39-52. doi: 10.1016/j.watres.2018.12.056.

Lu, J. Q., Gavala, H. N., Skiadas, I. V., Mladenovska, Z., & Ahring, B. K. (2008). Improving anaerobic sewage sludge digestion by implementation of a hyper-thermophilic prehydrolysis step. *Journal of Environmental Management*, *88* (4), 881-889. doi: 10.1016/j.jenvman.2007.04.020.

Lyberatos, G., & Skiadas, I.V. (1999). Modelling of anaerobic digestion - a review. *Global Nest International Journal*, *1* (2), 63-76.

Mahmoud, A., Zaghloul, M. S., Hamza, R. A., & Elbeshbishy, E. (2023). Comparing VFA composition, biomethane potential, and methane production kinetics of different substrates for anaerobic fermentation and digestion. *Fermentation*, *9*(2), 138. doi: 10.3390/fermentation9020138.

Makinia, J., & Zaborowska, E. (2020). Mathematical modelling and computer simulation of activated sludge systems. IWA Publishing.

Mamais, D., Jenkins, D., & Pitt, P. (1993). A rapid physical-chemical method for the determination of readily biodegradable soluble COD in municipal wastewater. *Water Research, 27*(1), 195-197.

McCarty, P. L. (1964). Anaerobic waste treatment fundamentals. *Public works, 95* (9), 91 – 99.

McCarty, P. L., & Mosey, F. E. (1991). Modelling of anaerobic digestion processes (a discussion of concepts). *Water science and technology*, *24*(8), 17-33. doi: 10.2166/wst.1991.0216

McCarty, P.L. & Smith, D.P. (1986). Anaerobic wastewater treatment. *Environmental Science & Technology*, *20*, 1200-1206.

Melcer, M., Dold, P., Jones, R.M., Bye, C.M., Takacs, I., Stensel, H.D., … & Bury, S. (2003). Methods for wastewater characterization in activated sludge modeling. Water Environment Research Federation, International Water Association, Alexandria, ABD. ISBN: 1-893664-71-6.

Mendes, C., Esquerre, K., & Queiroz, L. M. (2015). Application of Anaerobic Digestion Model No. 1 for simulating anaerobic mesophilic sludge digestion. *Waste Management*, *35*, 89-95. doi: 10.1016/j.wasman.2014.10.013.

Metcalf & Eddy. (2014). AECOM-Wastewater Engineering: Treatment and Resource Recovery (5th Edition), McGraw-Hill Education, New York.

Mino, T., San Pedro, D. C., & Matsuo, T. (1995). Estimation of the rate of slowly biodegradable COD (SBCOD) hydrolysis under anaerobic, anoxic and aerobic conditions by experiments using starch as model substrate. *Water Science and Technology*, *31*(2), 95-103. doi: 10.1016/0273-1223(95)00183-N.

Murnleitner, E., Kuba, T., van Loosdrecht, M.C.M, & Heijnen, J.J. (1997). An integrated metabolic model for the aerobic and denitrifying biological phosphorus removal. *Biotechnol Bioeng.*, *54* (5), 434-450. doi: 10.1002/(SICI)1097-0290(19970605)54:5<434::AID-BIT4>3.0.CO;2-F.

Nguyen, T. K. L., Ngo, H. H., Guo, W. S., Chang, S. W., Nguyen, D. D., Nghiem, L. D., & Nguyen, T. V. (2020). A critical review on life cycle assessment and plant-wide models towards emission control strategies for greenhouse gas from wastewater treatment plants. *Journal of environmental management*, *264*, 110440. doi: 10.1016/j.jenvman.2020.110440.

Noike, T., Endo, G., Chang, J. E., Yaguchi, J. I., & Matsumoto, J. I. (1985). Characteristics of carbohydrate degradation and the rate-limiting step in anaerobic digestion. *Biotechnology and bioengineering*, *27*(10), 1482-1489. doi: 10.1002/bit.260271013.

Nopens, I, Batstone, D.J., Copp, J., & Jeppson, U. (2009). An ASM/ADM model interface for dynamic plant-wide simulation. *Water Res.*, *43* (7), 1913-1923. doi: 10.1016/j.watres.2009.01.012.

Novaes, R. F. (1986). Microbiology of anaerobic digestion. *Water Sci. Technol.*, **18** (12), 1-14. doi: 10.2166/wst.1986.0159.

Obileke, K., Nwokolo, N., Makaka, G., Mukumba, P., & Onyeaka, H. (2020). Anaerobic digestion: Technology for biogas production as a source of renewable energy—A review. *Energy & Environment*, *32* (2), 191 – 225. doi: 10.1177/0958305X20923117.

Olsson, G., Nielsen, N. K., Lynggaard-Jensen, A., & Steyer, J.P. (2005). Instrumentation, control and automation in wastewater systems. IWA Publishing, Scientific and Technical Report No: 15, London, UK.

Orhon, D. &Artan, N. (1994). *Modelling of Activated Sludge Systems*. Lanchester: Technomic Publishing Co., Inc.

Orhon, D., & Okutman, D. (2003). Respirometric assessment of residual organic matter for domestic sewage. *Enzyme and microbial technology*, *32*(5), 560-566. doi: 10.1016/S0141-0229(03)00023-1.

Orhon, D., Artan, N. & Cimşit, Y. (1989). The concept of soluble residual product formation in the modelling of activated sludge. *Water Science and Technology*, *21* (4-5), 339-350. doi: 10.2166/wst.1989.0236.

Orhon, D., Babuna, F.G. & Karahan, O. (2009). *Industrial wastewater treatment by activated sludge*. IWA Publishing.

Orhon, D., Karahan, Ö., & Sözen, S. (1999). The effect of residual microbial products on the experimental assessment of the particulate inert COD in wastewaters. *Water Research*, *33* (14), 3191-3203. doi: 10.1016/S0043-1354(99)00207-9.

Orhon, D., Sozen, S., & Artan, N. (1996). The effect of heterotrophic yield on the assessment of the correction factor for anoxic growth. *Water Sci Technol.*, *34* (5-6), 67-74. doi: /10.1016/0273-1223(96)00630-0.

Ortega-Martinez, E., Sapkaite, I., Fdz-Polanco, F., & Donoso-Bravo, A. (2016). From pre-treatment toward inter-treatment. Getting some clues from sewage sludge biomethanation. *Bioresource technology*, *212*, 227-235. doi: 10.1016/j.biortech.2016.04.049.

Otuzalti, M. M., & Perendeci, N. A. (2018). Modeling of real scale waste activated sludge anaerobic digestion process by Anaerobic Digestion Model 1 (ADM1). *International journal of green energy*, *15*(7), 454-464. doi: 10.1080/15435075.2018.1479265.

Owen, W.F., Stuckey, D.C., Healy, J.G.Jr., Young, L.Y., & McCarty, P.L. (1979). Bioassay for monitoring biochemical methane potention and anaerobic toxicity. *Water Research*, *13*, 485-492. doi: 10.1016/0043-1354(79)90043-5.

Pala-Özkök, İ. (2012). *Inhibitory impact of selected antibiotics on biodegradation characteristic and microbial population under aerobic conditions*. (Ph.D. Thesis). Istanbul Technical University, Graduate School of Science Engineering and Technology, Istanbul.

Parkin, G. F., & Owen, W. F. (1986). Fundamentals of anaerobic digestion of wastewater sludges. *Journal of Environmental Engineering*, *112* (5), 867-920. doi: 10.1061/(ASCE)0733-9372(1986)112:5(867).

Pavlostathis, S. G. (1985). *A kinetic model for anaerobic digestion of waste activated sludge*. (Ph.D. Thesis). Cornell University, Ithaca, New York.

Pavlostathis, S. G., & Giraldo-Gomez, E. (1991). Kinetics of anaerobic treatment: a critical review. *Critical Reviews in Environmental Science and Technology*, *21*(5-6), 411-490. doi: 10.1080/10643389109388424.

Pavlostathis, S. G., & Gossett, J. M. (1986). A kinetic model for anaerobic digestion of biological sludge. *Biotechnology and bioengineering*, *28*(10), 1519-1530. doi: 10.1002/bit.260281010.

Pavlostathis, S. G., Miller, T. L., & Wolin, M. J. (1988). Fermentation of insoluble cellulose by continuous cultures of Ruminococcus albus. *Applied and Environmental Microbiology*, *54*(11), 2655-2659. doi: 10.1128/aem.54.11.2655-2659.1988.

Pohland, F. G. (1992). Anaerobic Treatment: Fundamental concept, application, and new horizons. J. F. Malina, & F. G. Pohland. In *Design of Anaerobic Process for the Treatment of Industrial and Municipal Wastes* (s. 1-40). Lancaster, USA: Technomic Publishing Co. Inc.

Reichert, P. (1998). AQUASIM 2.0-User manual. Swiss Federal Institute for Environmental Science and Technology. Dubendorf, Switzerland.

Rieger, L., Gillot, S., Langergraber, G., Ohtsuki, T., Takács, I., Winkler, S., & Shaw A. T. (2012). Guidelines for Using Activated Sludge Models IWA Task Group on Good Modelling Practice. Scientific and Technical Report No 21, IWA Publishing, London, UK.

Rittmann, B. E. & McCarty, P. L. (2001). Environmental biotechnology: principles and applications. McGraw-Hill Education.

Rosenthal A. (2020) What did I just feed my digester? - A Practical Guide to Predictive Modeling of Multi-Feed Biogas Plants, inCTRL webinar series, Toronto, Canada, July 8-9.

Sarioglu, M., Sayi Ucar, N., Ubay Cokgor, E., Orhon, D., van Loosdrecht, M.C.M., & Insel, G. (2017). Dynamic modeling of nutrient removal by an MBR operated at elevated temperatures. *Water Res.*, *123*, 420-428. doi: 10.1016/j.watres.2017.07.001.

Seco, A., Ruano, M.V., Ruiz-Martinez, A., Robles, A., Barat, R., Serralta, J., & Ferrer, J. (2020). Plant-wide modelling in wastewater treatment: showcasing experiences using the Biological Nutrient Removal Model. *Water Sci Technol.*, *81* (8), 1700–1714. doi: 10.2166/wst.2020.056.

Siegrist, H., Vogt, D., Garcia-Heras, J., & Gujer, W. (2002). Mathematical Model for Meso- and Thermophilic Anaerobic Sewage Sludge Digestion, *Environ Sci Technol.*, *36*, 1113-1123. doi: 10.1021/es010139p.

Smolders, G.J.F., van der Meij, J., van Loosdrecht, M.C.M., & Heijnen, J.J. (1994). Stoichiometric model of the aerobic metabolism of the biological phosphorus removal process. *Biotech Bioeng.*, *44*, 837-848. doi: 10.1002/bit.260440709.

Solon, K., Flores-Alsina, X., Mbamba, C. K., Ikumi, D., Volcke, E. I. P., Vaneeckhaute, C., ... & Jeppsson, U. (2017). Plant-wide modelling of phosphorus transformations in wastewater treatment systems: Impacts of control and operational strategies. *Water Research*, *113*, 97-110. doi: 10.1016/j.watres.2017.02.007.

Sötemann, S.W., Rensburg, P., Ristow, N.E., Wentzel, M.C., Loewenthal, R.E., & Ekama, G.A. (2005). Integrated chemical/physical and biological processes modelling Part 2-Anaerobic digestion of sewage sludges. *Water SA, 31* (4), 378-4738. doi: 10.10520/EJC116284.

Sözen, S. (1995). *Nitrifikasyon-Denitrifikasyon Kinetiğinin Deneysel Karakterizasyonu*. (Ph.D. Thesis). Istanbul Technical University, Graduate School, Istanbul.

Sözen, S., Orhon, D., & San, H. A. (1996). A new approach for the evaluation of the maximum specific growth rate in nitrification. *Water Research, 30*(7), 1661-1669. doi: 10.1016/0043-1354(96)00031-0.

Sözen, S., Orhon, D., Ubay-Çokgör, E., Görgün E., Insel G., Karahan Ö., … & Ünal A. (2008). İSKİ Tuzla Biyolojik ve Paşaköy İleri Biyolojik Atıksu Arıtma Tesislerinin Tasarım Kriterlerinin İncelenmesi", Sonuç Raporu, İstanbul Teknik Üniversitesi, Çevre Mühendisliği Bölümü, Maslak.

Sözen, S., Ubay Cokgör, E., Orhon, D., & Henze, M. (1998). Respirometric analysis of activated sludge behaviour–II. Heterotrophic growth under aerobic and anoxic conditions. *Water Research, 32* (2), 476–488. doi: 10.1016/S0043-1354(97)00210-8.

Spanjers, H., & Vanrolleghem, P. (1995). Respirometry as a tool for rapid characterization of wastewater and activated sludge. *Water Science and Technology, 31*(2), 105-114. doi: 10.1016/0273-1223(95)00184-O.

Speece, R.E. (1988). A survey of municipal anaerobic sludge digesters and diagnostic activity assays. *Water Research, 22* (3), 365–372. doi: 10.1016/S0043-1354(88)90260-6.

Takács I. (2008). *Experiments in Activated Sludge Modelling*. (Ph.D. Thesis). Ghent University, Belgium.

Takács, I., Patry, G., & Nolasco, D. (1991). A dynamic model of the clarification-thickening process. *Water Res., 25* (10), 1263-1271. doi: 10.1016/0043-1354(91)90066-Y.

Tomei, M. C., Braguglia, C. M., Cento, G., & Mininni, G. (2009). Modeling of anaerobic digestion of sludge. *Critical Reviews in Environmental Science and Technology, 39*(12), 1003-1051. doi: 10.1080/10643380801977818.

Tyagi, V. K., & Lo, S.-L. (2013). Sludge: A waste or renewable source for energy and resources recovery? *Renewable and Sustainable Energy Reviews, 25*, 708-728. doi: 10.1016/j.rser.2013.05.029.

Tyagi, V., & Lo, S. L. (2011). Application of physico-chemical pretreatment methods to enhance the sludge disintegration and subsequent anaerobic digestion: an up to date review. *Reviews in Environmental Science and Biotechnology, 10* (3), 215-242. doi: 10.1007/s11157-011-9244-9.

Ubay Çokgör, E., Sözen, S., Orhon, D., Henze, M. (1998). Respirometric analysis of activated sludge behaviour-I. Assessment of readily biodegradable substrate. *Water Research, 32* (2), 461-475. doi: 10.1016/S0043-1354(97)00209-1.

Valentini, A., Garuti, G., Rozzi, A., & Tilche, A. (1997). Anaerobic degradation kinetics of particulate organic matter: a new approach. *Water science and technology*, *36*(6-7), 239-246. doi: 10.1016/S0273-1223(97)00528-3.

Van Haandel, A. C., Dold, P. L., & Marais, G. V. R. (1982). Optimization of nitrogen removal in the single sludge activated sludge process. *Water Science and Technology*, *14*(6-7), 443-461. doi: 10.2166/wst.1982.0118.

Vanrolleghem, P. A., Insel, G., Petersen, B., Sin, G., De Pauw, D., Nopens, I., ... & Gernaey, K. (2003). A comprehensive model calibration procedure for activated sludge models. In WEFTEC 2003 (pp. 210-237). Water Environment Federation.

Vanrolleghem, P. A., Rosén, C., Zaher, U., Copp, J., Benedetti, L., Ayesa, E., & Jeppsson, U. (2005). Continuity-based interfacing of models for wastewater systems described by Petersen matrices. *Water science and technology*, *52*(1-2), 493-500. doi: 10.2166/wst.2005.0558.

Vavilin, V. A., Rytov, S. V., & Lokshina, L. Y. (1996). A description of hydrolysis kinetics in anaerobic degradation of particulate organic matter. *Bioresource technology*, *56*(2-3), 229-237. doi: 10.1016/0960-8524(96)00034-X.

Verstraete, W., DeBaere, L., & Rozzi, A. (1981). Phase separation in anaerobic digestion: motives and methods. *Trib. CEBEDEAU*, *34*.

Vesilind, P.A. (1968). Design of prototype thickeners from batch settling tests. *Water Sewage Works*, *115* (7), 302–307.

Wentzel, M.C., Ekama, G.A., & Marais, G.v.R. (1992). Processes and modeling of nitrification denitrification biological excess phosphorus removal systems - a review. *Water Sci Technol.*, *25* (6), 59-82. doi: 10.2166/wst.1992.0114.

Wichern, M., Lübken, M., Blömer, R., & Rosenwinkel, K. H. (2003). Efficiency of the Activated Sludge Model no. 3 for German wastewater on six different WWTPs. *Water science and technology*, *47*(11), 211-218. doi: 10.2166/wst.2003.0607.

Wild, D., von Schulthess, R., & Gujer, W. (1995) Structured modelling of denitrification intermediates. *Water Sci. Technol*., *31* (2), 45-54. doi: 10.1016/0273-1223(95)00179-Q.

Yagci, N., Insel, G., Artan, N., & Orhon, D. (2004). Modeling and calibration of phosphate and glycogen accumulating organism competition for acetate uptake in sequencing batch reactor. *Water Sci Technol.*, 50 (6), 241-250. doi: 10.2166/wst.2004.0382.

Yuan, Y., Hu, X., Chen, H., Zhou, Y., Zhou, Y., & Wang, D. (2019). Advances in enhanced volatile fatty acid production from anaerobic fermentation of waste activated sludge. *Science of the total environment*, *694*, 133741. doi: 10.1016/j.scitotenv.2019.133741.

Zeikus, J. G. (1981). Microbial intermediary metabolism in anaerobic digestion. In *Anaerobic digestion 1981: proceedings of the Second International Symposium on Anaerobic Digestion held in Travemhunde, Federal Republic of Germany, on 6-11 September, 1981*.

Zhang, C., Su, H., Baeyens, J., & Tan, T. (2014). Reviewing the anaerobic digestion of food waste for biogas production. *Renewable and Sustainable Energy Reviews*, *38*, 383–392. doi: 10.1016/j.rser.2014.05.038.

Zhen, G., Lu, X., Kato, H., Zhao, Y., & Li, Y. Y. (2017). Overview of pretreatment strategies for enhancing sewage sludge disintegration and subsequent anaerobic digestion: Current advances, full-scale application and future perspectives. *Renewable and Sustainable Energy Reviews*, *69*, 559-577. doi: 10.1016/j.rser.2016.11.187.

URL-1 <*https://www.dynamita.com*>, date retrieved 27.03.2024, Dynamita.

APPENDICES

Appendix A: Components in Sumo Model Matrix

APPENDIX A: Components in Sumo Model Matrix

Table A.1: Components in Sumo model matrix (URL-1).

Symbol	Name	Model	Definition	Unit
S_{VFA}	Volatile fatty acids (VFA)	Sumo1 Sumo2 Sumo2C Sumo2S Sumo4N	A fermented product representing a combination of acetate and other volatile fatty acids produced in an anaerobic environment from S_B. It is available for biological removal by OHOs, CASTOs (PAOs, GAOs), and AMETOs and chemical removal during HFO reduction.	g COD·m^{-3}
S_B	Readily biodegradable substrate (non-VFA)	Mini_Sumo Sumo1 Sumo2 Sumo2S Sumo4N	Non-VFA organic material that can be fermented to VFA, it represents a group of readily biodegradable organic material present in wastewater.	g COD·m^{-3}
$S_{B,mono}$	Readily biodegradable substrate as monomers (non-VFA)	Sumo2C	Small molecular weight substrate mainly consumed by AHOs in 1st stage of high-rate process.	g COD·m^{-3}
$S_{B,poly}$	Readily biodegradable substrate as polymers	Sumo2C	Readily biodegradable substrate that is not degraded in 1st stage of a high-rate process. Consumed by OHOs in 2nd stage.	g COD·m^{-3}
S_{MEOL}	Methanol (MEOL)	Sumo1 Sumo2 Sumo2C Sumo2S Sumo4N	A methyl alcohol or the simplest alcohol. A commonly used external carbon source for denitrification.	g COD·m^{-3}
C_B	Colloidal biodegradable substrate	Sumo1 Sumo2 Sumo2C Sumo2S Sumo4N	A biodegradable organic component, flocculates to form XB. Analytically can be approximated by flocculation or filtration (larger than 0.1 micron but smaller than 1.2 micron)	g COD·m^{-3}
X_B	Slowly biodegradable substrate	Mini_Sumo Sumo1 Sumo2 Sumo2C Sumo2S Sumo4N	High molecular weight particulates that are hydrolyzed by extracellular enzymes to release S_B. They are introduced directly from the influent and released during the bacterial decay process in death-regeneration concept models.	g COD·m^{-3}
S_U	Soluble unbiodegradable organics	Mini_Sumo Sumo1 Sumo2 Sumo2C Sumo2S Sumo4N	A soluble organic material that is not degraded biologically or chemically in wastewater and leaves in the effluent. Typically, measured by performing a flocculated filtration test on the effluent of a nitrifying plant. It also has a nitrogen and phosphorus content. There is only one process, the Thermal Hydrolysis Process, which generates S_U from X_U in the model.	g COD·m^{-3}
C_U	Colloidal unbiodegradable organics	Sumo1 Sumo2 Sumo2C Sumo2S Sumo4N	A non-biodegradable organic material, flocculates to form X_U and leaves the plant in the WAS or cake. Analytically can be approximated by flocculation or filtration (larger than 0.1 micron but smaller than 1.2 micron)	g COD·m^{-3}

Table A.1 (continued): Components in Sumo model matrix.

Symbol	Name	Model	Definition	Unit
X_U	Particulate unbiodegradable organics	Mini_Sumo Sumo1 Sumo2 Sumo2C Sumo2S Sumo4N	A non-biodegradable organic material that is larger than 1.2 micron. It is not hydrolysed and remains untransformed due to biological and chemical reactions. The thermal hydrolysis process model is the only unit that converts a portion of X_U to S_U.	g COD·m^{-3}
X_{STO}	Storage product of AHOs	Sumo2C	An internal cell storage organic material stored by AHOs in low SRT systems using $S_{B,mono}$ and S_{VFA}. Its production doesn't involve any energy and growth.	g COD·m^{-3}
X_{PHA}	Stored polyhydroxyalkanoates (PHA)	Sumo1 Sumo2 Sumo2C Sumo2S Sumo4N	Polyhydroxyalkanoates considered as an internal organic cellular storage product of CASTOs (PAOs). The composition of alkanoates is represented as poly-β-hydroxybutyrate.	g COD·m^{-3}
X_{GLY}	Stored glycogen (GLY)	Sumo1 Sumo2 Sumo2C Sumo2S Sumo4N	Internal organic cellular storage product of CASTOs (GAOs).	g COD·m^{-3}
X_E	Endogenous decay products	Mini_Sumo Sumo1 Sumo2 Sumo2C Sumo2S Sumo4N	An organic material released during cell lysis under aerobic and anoxic environment, it has an extremely slow conversion rate of 0.07 per day and it converts to X_B while releasing S_{NHx} and S_{PO4}. The X_E builds in a system with increasing SRT.	g COD·m^{-3}
$X_{E,ana}$	Anaerobic endogenous decay products	Sumo1 Sumo2 Sumo2C Sumo2S Sumo4N	An organic material released on cell lysis under anaerobic environment and hydrolysed in aerobic environment to release S_B, S_{NHx}, and S_{PO4}. This component is responsible for the additional VS destruction observed in a post aerobic digestion process.	g COD·m^{-3}
X_{OHO}	Ordinary heterotrophic organisms (OHO)	Mini_Sumo Sumo1 Sumo2 Sumo2C Sumo2S Sumo4N	Generalist facultative ordinary hetrotrophic organisms that consume different soluble biodegradable organics including S_B, S_{VFA}, and X_{MEOL} and can perform biological removal under aerobic, anoxic, and anaerobic environments. They are also responsible for hydrolysis of the particulates. In MiniSumo and Sumo1, they perform one step denitrification, meaning from S_{NOx} to S_{N2}. In other models they follow two steps, S_{NO3} reduction to S_{NO2}, and S_{NO2} reduction to S_{N2}.	g COD·m^{-3}
X_{CASTO}	Carbon storing organisms (CASTO)	Sumo1 Sumo2 Sumo2C Sumo2S Sumo4N	A special group of carbon storing heterotrophic organisms representing a combination of both PAOs and GAOs. The process conditions dictate the ratio of PAO to GAO achieved in the process model. They are responsible for taking part in the EBPR process. They store PHA and/or GLY during the anaerobic conditions, and consume stored carbon during anoxic and aerobic environments to generate polyphosphate (X_{PP}). In Sumo1, they perform one step denitrification, meaning from S_{NOx} to S_{N2}. In other models they follow two steps, S_{NO3} reduction to S_{NO2}, and S_{NO2} reduction to S_{N2}.	g COD·m^{-3}

Table A.1 (continued): Components in Sumo model matrix.

Symbol	Name	Model	Definition	Unit
X_{MEOLO}	Anoxic methanol utilizers (MEOLO)	Sumo1 Sumo2 Sumo2C Sumo2S Sumo4N	Specialist heterotrophic organisms responsible for removal of X_{MEOL}. Only found in systems with methanol addition and compete with OHOs during denitrification process. In Sumo1, they perform one step denitrification, meaning from S_{NOx} to S_{N2}. In other models they follow two steps, S_{NO3} reduction to S_{NO2}, and S_{NO2} reduction to S_{N2}.	g COD·m^{-3}
X_{AHO}	Carbon adsorption heterotroph organisms (AHO)	Sumo2C	Heterotrophic organisms storing readily biodegradable small molecular weight components represented as $S_{B,mono}$ and volatile fatty acids (S_{VFA}) into X_{STO}. The growth rate of AHOs is higher than that of the OHOs and outgrow them in a short SRT system of <2 days. They only carry out aerobic consumption of the X_{STO} and are expected to be seeded from the influent.	g COD·m^{-3}
X_{NITO}	Aerobic nitrifying organisms (NITO)	Mini_Sumo Sumo1	Obligate aerobic autotrophic organism responsible for complete nitrification, from S_{NHx} to S_{NOx}. It represents a combination of AOBs and NOBs for simplification in the referred models.	g COD·m^{-3}
X_{AOB}	Aerobic ammonia oxidizers (AOB)	Sumo2 Sumo2C Sumo2S Sumo4N	Obligate aerobic autotrophic organism responsible for the first step in nitrification, from S_{NHx} to S_{NO2}.	g COD·m^{-3}
X_{NOB}	Nitrite oxidizers (NOB)	Sumo2 Sumo2C Sumo2S Sumo4N	Obligate aerobic autotrophic organism responsible for the second step in nitrification, from S_{NO2} to S_{NO3}.	g COD·m^{-3}
X_{AMX}	Anammox organisms (AMX)	Sumo2 Sumo2C Sumo2S Sumo4N	A chemoautotrophic anaerobic bacteria that oxidizes ammonium with nitrite as the electron acceptor and with CO2 as the main carbon source. They are slow growers and have a long doubling time.	g COD·m^{-3}
X_{AMETO}	Acidoclastic methanogens (AMETO)	Mini_Sumo Sumo1 Sumo2 Sumo2C Sumo2S Sumo4N	Anaerobic archea that consume S_{VFA} to produce S_{CH4} and S_{CO2} as a metabolic by-product and don't grow under aerobic conditions.	g COD·m^{-3}
X_{HMETO}	Hydrogenotrophic methanogens (HMETO)	Mini_Sumo Sumo1 Sumo2 Sumo2C Sumo2S Sumo4N	Anaerobic archea that consume S_{H2} and S_{CO2} to produce S_{CH4} as a metabolic by-product and don't grow under aerobic conditions.	g COD·m^{-3}
X_{ASRO}	Acidoclastic sulfate-reducing organisms (ASRO)	Sumo2S	A group of bacteria and archaea that perform anaerobic respiration utilizing S_{SO4} and S_{VFA}, reducing it to S_{H2S} and generating S_{CO2}. They compete with AMETOs for S_{VFA} and negatively impact performance of a digester.	g COD·m^{-3}

Table A.1 (continued): Components in Sumo model matrix.

Symbol	Name	Model	Definition	Unit
X_{HSRO}	Hydrogenotrophic sulfate-reducing organisms (HSRO)	Sumo2S	A group of bacteria and archaea that perform anaerobic respiration utilizing S_{SO4} and S_{H2}, reducing it to S_{H2S}. They compete with HMETOs for S_{H2} consumption and negatively impact performance of a digester.	g COD·m^{-3}
X_{SOO}	Sulfur-oxidizing organisms (SOO)	Sumo2S	They oxidize S_{H2S} in two steps under aerobic and anoxic environments, first from S_{H2S} to X_S (elemental sulfur) and second from X_S to S_{SO4}.	g COD·m^{-3}
X_{ALGAE}	Photosynthetic organisms (ALGAE)	Mini_Sumo Sumo1 Sumo2 Sumo2C Sumo2S Sumo4N	A group of photosynthetic organisms which grow, assimilate nutrients, S_{CO2} and generate S_{O2} in the presence of light. They consume S_{O2} through respiration.	g COD·m^{-3}
S_{NHx}	Total ammonia (NHx)	Mini_Sumo Sumo1 Sumo2 Sumo2C Sumo2S Sumo4N	Total ammonia nitrogen is a sum of ammonium and free ammonia. An essential nutrient for the biokinetic growth reactions.	g N·m^{-3}
S_{NH2OH}	Hydroxylamine (NH2OH)	Sumo4N	An intermediate product produced by AOB from S_{NHx}. It is then oxidized to S_{NO} under aerobic environments. It is also reduced to form S_{N2O} under anoxic environments.	g N·m^{-3}
S_{NOx}	Nitrate and nitrite (NOx)	Mini_Sumo Sumo1	A sum of nitrate and nitrite, and electron acceptor for anoxic reactions. In the referred Models it is considered nitrate for all COD conservation purposes.	g N·m^{-3}
S_{NO2}	Nitrite (NO2)	Sumo2 Sumo2C Sumo2S Sumo4N	A sum of nitrous acid and nitrate ion and electron acceptor for anoxic reactions.	g N·m^{-3}
S_{NO3}	Nitrate (NO3)	Sumo2 Sumo2C Sumo2S Sumo4N	An electron acceptor for anoxic reactions.	g N·m^{-3}
$S_{NO,AOB}$	Nitric oxide of AOB (NO)	Sumo4N	Nitric oxide generated by AOBs from S_{NH2OH} and either oxidized to S_{NO2} and reduced to S_{N2O}. It is considered as an internal product.	g N·m^{-3}
$S_{NO,OHO}$	Nitric oxide of OHO (NO)	Sumo4N	Nitric oxide generated by OHOs during S_{NO2} reduction. It is considered as an internal product.	g N·m^{-3}
S_{N2O}	Nitrous oxide (N_2O)	Sumo4N	Generated by OHOs from $S_{NO,OHO}$ and by AOBs from $S_{NO,AOB}$.	g N·m^{-3}
S_{N2}	Dissolved nitrogen (N_2)	Mini_Sumo Sumo1 Sumo2 Sumo2C Sumo2S Sumo4N	Only nitrogenous product of denitrification except for in Sumo4N model and is subject to gas transfer.	g N·m^{-3}

Table A.1 (continued): Components in Sumo model matrix.

Symbol	Name	Model	Definition	Unit
$S_{N,B}$	Soluble biodegradable organic N (from S_B)	Mini_Sumo Sumo1 Sumo2 Sumo2C Sumo2S Sumo4N	A nitrogen containing soluble organic material (urea, amino acids, amines, and others) that releases nitrogen as total ammonia on ammonification in wastewater treatment. In the model it doesn't have COD associated.	$g\ N \cdot m^{-3}$
$X_{N,B}$	Particulate biodegradable organic N (from X_B)	Mini_Sumo Sumo1 Sumo2 Sumo2C Sumo2S Sumo4N	A nitrogen containing particulate organic material (proteins and others) that releases $S_{N,B}$ on hydrolysis in wastewater treatment. In the model it doesn't have COD.	$g\ N \cdot m^{-3}$
$X_{N,U}$	Particulate unbiodegradable organic N	Sumo1 Sumo2 Sumo2C Sumo2S Sumo4N	A nitrogen containing particulate organic material that is not biologically or chemically degraded in the plant and leaves with the cake solids. The only process that degrades $X_{N,U}$ to S_{NHx} is the thermal hydrolysis process.	$g\ N \cdot m^{-3}$
S_{PO4}	Orthophosphate (PO_4)	Mini_Sumo Sumo1 Sumo2 Sumo2C Sumo2S Sumo4N	Soluble inorganic phosphorus, represents a combination of Phosphoric acid, Dihydrogen phosphate ion, Hydrogen phosphate ion, Phosphate ion. An essential nutrient for the biokinetic growth reactions.	$g\ N \cdot m^{-3}$
X_{PP}	Stored polyphosphate (PP)	Sumo1 Sumo2 Sumo2C Sumo2S Sumo4N	Poly-phosphate considered as an internal inorganic cellular storage product of CASTOs (PAOs). The composition of X_{PP} is $(Ca_{0.1}K_{0.1}Mg_{0.35}PO_3)_n$.	$g\ N \cdot m^{-3}$
$S_{P,B}$	Soluble biodegradable organic P (from S)	Sumo1 Sumo2 Sumo2C Sumo2S Sumo4N	A phosphorus containing soluble organic material that releases phosphorus as S_{PO4} in wastewater treatment. In the model it doesn't have COD.	$g\ P \cdot m^{-3}$
$X_{P,B}$	Particulate biodegradable organic P (from X_B)	Mini_Sumo Sumo1 Sumo2 Sumo2C Sumo2S Sumo4N	A phosphorus containing particulate organic material that releases $S_{P,B}$ on hydrolysis in wastewater treatment. In the model it doesn't have COD.	$g\ P \cdot m^{-3}$
$X_{P,U}$	Particulate unbiodegradable organic P	Sumo1 Sumo2 Sumo2C Sumo2S Sumo4N	A phosphorus containing particulate organic material that is not biologically or chemically degraded in the plant and leaves with the cake solids. The only process that degrades $X_{P,U}$ to S_{PO4} is the process model of thermal hydrolysis process.	$g\ P \cdot m^{-3}$
S_{O2}	Dissolved oxygen (O_2)	Mini_Sumo Sumo1 Sumo2 Sumo2C Sumo2S Sumo4N	Dissolved oxygen is major electron acceptor for aerobic system and is subjected to gas transfer.	$g\ P \cdot m^{-3}$

Table A.1 (continued): Components in Sumo model matrix.

Symbol	Name	Model	Definition	Unit
S_{CH4}	Dissolved methane (CH_4)	Mini_Sumo Sumo1 Sumo2 Sumo2C Sumo2S Sumo4N	Dissolved methane is the most reduced form of carbon and end product of methanogenesis. They are subjected to gas transfer.	g COD·m^{-3}
S_{H2}	Dissolved hydrogen (H_2)	Mini_Sumo Sumo1 Sumo2 Sumo2C Sumo2S Sumo4N	Dissolved hydrogen is generated during fermentation and transformed to S_{CH4} during methanogensis. They are subjected to gas transfer.	g COD·m^{-3}
S_{ALK}	Alkalinity (ALK)	MiniSumo	Assumed to be bicarbonate and used for appropriate conversion of electric charges in the biokinetic reactions.	eq ALK·L^{-1}
S_{CO2}	Total inorganic carbon (CO_2)	Sumo1 Sumo2 Sumo2C Sumo2S Sumo4N	A sum of carbonic acid, bicarbonate ion, carbonate ion. It is end product of many biological reactions. As bicarbonate it is a substrate for nitrification and also consumed during methanogenesis.	g TIC·m^{-3}
X_{INORG}	Inorganics in influent and biomass	Mini_Sumo Sumo1 Sumo2 Sumo2C Sumo2S Sumo4N	It represents the inorganic inerts present in influent and the biomass (0.11 g TSS·g COD^{-1}). It has a S_{Na}, S_{Cl}, S_{Ca} and S_{Mg} content.	g TSS·m^{-3}
S_{CAT}	Other strong cations (as Na^+)	Sumo1 Sumo2 Sumo2C Sumo2S Sumo4N	Represented as sodium and is an essential element for biomass. It participates in pH and precipitation reactions.	g Na·m^{-3}
S_{AN}	Other strong anions (as Cl^-)	Sumo1 Sumo2 Sumo2C Sumo2S Sumo4N	Represented as chloride and is an essential element for biomass. It participates in pH and precipitation reactions.	g Cl·m^{-3}
S_{Ca}	Calcium	Sumo1 Sumo2 Sumo2C Sumo2S Sumo4N	An essential element for biomass and X_{PP} and participates in pH and precipitation reactions.	g Ca·m^{-3}
S_{Mg}	Magnesium	Sumo1 Sumo2 Sumo2C Sumo2S Sumo4N	An essential element for biomass and X_{PP}. It participates in pH and precipitation reactions.	g Mg·m^{-3}
S_K	Potassium	Sumo1 Sumo2 Sumo2C Sumo2S Sumo4N	An essential element for biomass and X_{PP}. It participates in pH and precipitation reactions.	g K·m^{-3}
S_{H2S}	Hydrogen sulfide (H_2S)	Sumo2S	Dissolved hydrogen sulfide gas, its subjected to gas transfer, biological and chemical reactions.	g S·m^{-3}

Table A.1 (continued): Components in Sumo model matrix.

Symbol	Name	Model	Definition	Unit
S_{SO4}	Sulfate (SO_4)	Sumo2S	An end product of S_{H2S} oxidation. It participates in pH determination	g S·m^{-3}
X_S	Particulate elemental sulfur (S)	Sumo2S	An intermediary product of partial S_{H2S} oxidation.	g S·m^{-3}
X_{FeOH}	Ferric hydroxide compounds (FeOH)	MiniSumo	Phosphorus-binding capacity of ferric hydroxides	g Fe·m^{-3}
X_{FeP}	Ferric phosphate compounds (FeP)	MiniSumo	This component results from binding phosphorus to the X_{FeOH}.	g Fe·m^{-3}
X_{AlOH}	Aluminium hydroxide compounds (AlOH)	MiniSumo	It stands for phosphorus-binding capacity of possible Al hydroxides	g Al·m^{-3}
X_{AlP}	Aluminium phosphate compounds (AlP)	MiniSumo	This component results from binding phosphorus to the X_{AlOH}.	g Al·m^{-3}
S_{Fe2}	Ferrous ion (Fe2)	Sumo1 Sumo2 Sumo2C Sumo2S Sumo4N	Ferrous ion oxidized to ferric ion and then participates in X_{HFO} formation. It precipiates S_{H2S} to X_{FeS} and S_{PO4} to X_{Vivi} under anaerobic environments.	g Fe·m^{-3}
$X_{HFO,H}$	Active hydrous ferric oxide, high surface (HFO,H)	Sumo1 Sumo2 Sumo2C Sumo2S Sumo4N	A ferric hydroxide with high surface area and high capacity to bind S_{PO4}. Higher mixing condition results in more $X_{HFO,H}$ formation compared to $X_{HFO,L}$.	g Fe·m^{-3}
$X_{HFO,L}$	Active hydrous ferric oxide, low surface (HFO,L)	Sumo1 Sumo2 Sumo2C Sumo2S Sumo4N	A ferric hydroxide with low surface area and low capacity to bind S_{PO4}. Poor mixing condition results in more $X_{HFO,L}$ formation compared to $X_{HFO,H}$.	g Fe·m^{-3}
$X_{HFO,old}$	Aged unused hydrous ferric oxide (HFO,old)	Sumo1 Sumo2 Sumo2C Sumo2S Sumo4N	When there is excess ferric addition and not much S_{PO4} is available then $X_{HFO,H}$ and $X_{HFO,L}$ formed age into $X_{HFO,old}$. These are incapable of removing S_{PO4}.	g Fe·m^{-3}
$X_{HFO,H,P}$	P-bound hydrous ferric oxide, high surface (HFO,H,P)	Sumo1 Sumo2 Sumo2C Sumo2S Sumo4N	The Fe-S_{PO4} complex formed with $X_{HFO,H}$.	g Fe·m^{-3}
$X_{HFO,L,P}$	P-bound hydrous ferric oxide, low surface (HFO,L,P)	Sumo1 Sumo2 Sumo2C Sumo2S Sumo4N	The Fe-S_{PO4} complex formed with $X_{HFO,L}$.	g Fe·m^{-3}
$X_{HFO,H,P,old}$	Aged P-bound hydrous ferric oxide, high surface (HFO,H,P,old)	Sumo1 Sumo2 Sumo2C Sumo2S Sumo4N	Aged form of $X_{HFO,H,P}$.	g Fe·m^{-3}

Table A.1 (continued): Components in Sumo model matrix.

Symbol	Name	Model	Definition	Unit
$X_{HFO,L,P,old}$	Aged P-bound hydrous ferric oxide, low surface (HFO,L,P,old)	Sumo1 Sumo2 Sumo2C Sumo2S Sumo4N	Aged form of $X_{HFO,L,P}$.	g Fe·m^{-3}
$X_{HAO,H}$	Active hydrous aluminium oxide, high surface (HAO,H)	Sumo1 Sumo2 Sumo2C Sumo2S Sumo4N	Aluminium hydroxide with high surface area and high capacity to bind S_{PO4}. Higher mixing condition results in more $X_{HAO,H}$ formation compared to $X_{HAO,L}$.	g Al·m^{-3}
$X_{HAO,L}$	Active hydrous aluminium oxide, low surface (HAO,L)	Sumo1 Sumo2 Sumo2C Sumo2S Sumo4N	Aluminium hydroxide with low surface area and low capacity to bind S_{PO4}. Poor mixing condition results in more $X_{HAO,L}$ formation compared to $X_{HAO,H}$.	g Al·m^{-3}
$X_{HAO,old}$	Aged unused hydrous aluminium oxide (HAO,old)	Sumo1 Sumo2 Sumo2C Sumo2S Sumo4N	When there is excess X_{HAO} and not much S_{PO4} is available then XHAO and $X_{HAO,L}$ formed age into $X_{HAO,old}$. These are incapable of removing S_{PO4}.	g Al·m^{-3}
$X_{HAO,H,P}$	P-bound hydrous aluminium oxide, high surface (HAO,H,P)	Sumo1 Sumo2 Sumo2C Sumo2S Sumo4N	The Al-S_{PO4} complex formed with $X_{HAO,H}$.	g Al·m^{-3}
$X_{HAO,L,P}$	P-bound hydrous aluminium oxide, low surface (HAO,L,P)	Sumo1 Sumo2 Sumo2C Sumo2S Sumo4N	The Al-S_{PO4} complex formed with $X_{HAO,L}$.	g Al·m^{-3}
$X_{HAO,H,P,old}$	Aged P-bound hydrous aluminium oxide, high surface (HAO,H,P,old)	Sumo1 Sumo2 Sumo2C Sumo2S Sumo4N	Aged form of $X_{HAO,H,P}$.	g Al·m^{-3}
$X_{HAO,L,P,old}$	Aged P-bound hydrous aluminium oxide, low surface (HAO,L,P,old)	Sumo1 Sumo2 Sumo2C Sumo2S Sumo4N	Aged form of $X_{HAO,L,P}$.	g Al·m^{-3}
X_{CaCO3}	Calcium carbonate ($CaCO_3$)	Sumo1 Sumo2 Sumo2C Sumo2S Sumo4N	Essential chemical for pH control - a precipitate that forms readily	g TSS·m^{-3}
X_{ACP}	Amorphous calcium phosphate (ACP)	Sumo1 Sumo2 Sumo2C Sumo2S Sumo4N	Elemental composition of $Ca_3(PO_4)_2 \cdot 4H_2O$.	g TSS·m^{-3}

Table A.1 (continued): Components in Sumo model matrix.

Symbol	Name	Model	Definition	Unit
X_{BSH}	Brushite (BSH)	Sumo1 Sumo2 Sumo2C Sumo2S Sumo4N	Elemental composition of $CaHPO_4 \cdot 2H_2O$. Forms at lower pH values than Struvite	g TSS·m^{-3}
X_{STR}	Struvite (STR)	Sumo1, Sumo2, Sumo2C, Sumo2S, Sumo4N	Formed under anaerobic environments and has an elemental composition of $MgNH_4PO_4 \cdot 6H_2O$.	g TSS·m^{-3}
X_{Vivi}	Vivianite (Vivi)	Sumo1 Sumo2 Sumo2C Sumo2S Sumo4N	Formed under anaerobic environments and has an elemental composition of $Fe_3(PO_4)_2 \cdot 8H_2O$.	g TSS·m^{-3}
X_{FeS}	Iron sulfide (FeS)	Sumo2S	Formed under anaerobic environments and is a precursor for pyrite formation.	g TSS·m^{-3}
H	Enthalpy	Mini_Sumo Sumo1 Sumo2 Sumo2C Sumo2S Sumo4N	An energy-like property that is used to calculate temperature of a system. It flows from the influent unit to the plant.	MJ·m^{-3}
S_{ALPHA}	Alpha indicator	Mini_Sumo Sumo1 Sumo2 Sumo2C Sumo2S Sumo4N	A surrogate representing the surfactant composition in the wastewater.	unitless
$S_{ORPswitch}$	ORP driver for CASTO activity switches	Sumo1 Sumo2 Sumo2C Sumo2S Sumo4N	A surrogate switch to calculate the activity of CASTOs.	unitless
G_{CO2}	Carbon dioxide gas (CO_2)	Sumo1 Sumo2 Sumo2C Sumo2S Sumo4N	Gaseous form represented in bubbles of wastewater system.	g TIC·m^{-3}
G_{CH4}	Methane gas (CH_4)	Mini_Sumo Sumo1 Sumo2 Sumo2C Sumo2S Sumo4N	Gaseous form represented in bubbles of wastewater system.	g COD·m^{-3}

Table A.1 (continued): Components in Sumo model matrix.

Symbol	Name	Model	Definition	Unit
G_{H2}	Hydrogen gas (H_2)	Mini_Sumo Sumo1 Sumo2 Sumo2C Sumo2S Sumo4N	Gaseous form represented in bubbles of wastewater system.	g COD·m^{-3}
G_{O2}	Oxygen gas (O_2)	Mini_Sumo Sumo1 Sumo2 Sumo2C Sumo2S Sumo4N	Gaseous form represented in bubbles of wastewater system.	g O_2·m^{-3}
G_{NH3}	Ammonia gas (NH_3)	Sumo1 Sumo2 Sumo2C Sumo2S Sumo4N	Gaseous form represented in bubbles of wastewater system.	g N·m^{-3}
G_{N2}	Nitrogen gas (N_2)	Mini_Sumo Sumo1 Sumo2 Sumo2C Sumo2S Sumo4N	Gaseous form represented in bubbles of wastewater system.	g N·m^{-3}
G_{NO}	Nitric oxide gas (NO)	Sumo4N	Gaseous form represented in bubbles of wastewater system.	g N·m^{-3}
G_{N2O}	Nitrous oxide gas (N_2O)	Sumo4N	Gaseous form represented in bubbles of wastewater system.	g N·m^{-3}
G_{H2S}	Hydrogen sulfide gas (H_2S)	Sumo2S	Gaseous form represented in bubbles of wastewater system.	g S·m^{-3}
$G_{CO2,atm}$	Carbon dioxide gas (CO_2)	Sumo1 Sumo2 Sumo2C Sumo2S Sumo4N	Gaseous form represented in the atmosphere around wastewater systems.	%v/v
$G_{CH4,atm}$	Methane gas (CH_4)	Mini_Sumo Sumo1 Sumo2 Sumo2C Sumo2S Sumo4N	Gaseous form represented in the atmosphere around wastewater systems.	%v/v
$G_{H2,atm}$	Hydrogen gas (H_2)	Mini_Sumo Sumo1 Sumo2 Sumo2C Sumo2S Sumo4N	Gaseous form represented in the atmosphere around wastewater systems.	%v/v

Table A.1 (continued): Components in Sumo model matrix.

Symbol	Name	Model	Definition	Unit
$G_{O2,atm}$	Oxygen gas (O_2)	Mini_Sumo Sumo1 Sumo2 Sumo2C Sumo2S Sumo4N	Gaseous form represented in the atmosphere around wastewater systems.	%v/v
$G_{NH3,atm}$	Ammonia gas (NH_3)	Sumo1 Sumo2 Sumo2C Sumo2S Sumo4N	Gaseous form represented in the atmosphere around wastewater systems.	%v/v
$G_{N2,atm}$	Nitrogen gas (N_2)	Mini_Sumo Sumo1 Sumo2 Sumo2C Sumo2S Sumo4N	Gaseous form represented in the atmosphere around wastewater systems.	%v/v
$G_{NO,atm}$	Nitric oxide gas (NO)	Sumo4N	Gaseous form represented in the atmosphere around wastewater systems.	%v/v
$G_{N2O,atm}$	Nitrous oxide gas (N_2O)	Sumo4N	Gaseous form represented in the atmosphere around wastewater systems.	%v/v
$G_{H2S,atm}$	Hydrogen sulfide gas (H_2S)	Sumo2S	Gaseous form represented in the atmosphere around wastewater systems.	%v/v
$S_{MM,index}$	Methyl mercaptan production index	Sumo2S	A surrogate for indicating the potential for odor generation at a wastewater facility.	Unitless

CURRICULUM VITAE

Name Surname **:** Gökşin ÖZYILDIZ

EDUCATION

B.Sc.: Istanbul Technical University, Environmental Engineering, 2012

B.Sc.: Istanbul Technical University, Civil Engineering, 2013

M.Sc.: Istanbul Technical UniversityEnvironmental Sciences and Engineering, 2018

PROFESSIONAL EXPERIENCE:

- ***April '17 - …*** Research Assistant
  Istanbul Technical University, Environmental Engineering Department
- ***January '14 – April '15*** Purchasing Manager
  Mutluhan Construction Industry Company Limited
- ***March '13 – December '13*** Purchasing Engineer
  Mutluhan Construction Industry Company Limited

PUBLICATIONS AND PRESENTATIONS FROM THE THESIS:

- ***Ozyildiz, G.***, Zengin, G.E., Guven, D., Cokgor, E., Ozdemir, O., Hauduc, H., ... & Insel, G. (2023). Restructuring anaerobic hydrolysis kinetics in plant-wide models for accurate prediction of biogas production. *Water Research, 245*, 120620. doi: 10.1016/j.watres.2023.120620.
- Insel, G., ***Ozyildiz, G.***, Okutman-Tas, D., Guven, D., Zengin, G. E., Pala-Ozkok, I., ... & Cokgor, E. (2022). A comprehensive evaluation of process kinetics: A plant-wide approach for nutrient removal and biogas production. *Water Research, 217*, 118410. doi: 10.1016/j.watres.2022.118410.
- ***Ozyildiz, G.***, Okutman-Tas, D., Zengin, G.E., Guven, D., Sagir Kurt, E., Atli, E., ... & Insel, G. (2021). Kinetic evaluation of organic carbon degradation in large-scale wastewater treatment plants with low biogas yield. 4th IWA Resource Recovery Conference, 5-8 September, Turkey.

- ***Ozyildiz, G.***, Okutman-Tas, D, Guven, D., Zengin, G.E., Cokgor, E., Insel, G. (2022). A model based evaluation of anaerobic conversion kinetics on full-scale municipal sludge digesters. 9th International Conference on Sustainable Solid Waste Management, 15-18 June 2022, Corfu, Greece.

OTHER PUBLICATIONS AND PRESENTATIONS:

- Bodur, M., Ergin, S., Alkay, T., Kahraman, S., Selvi, E., ***Ozyildiz, G.***, ... & Insel, G. (2024). Simulation assisted process simplification and energy recovery from a cryptic biological nutrient removal plant. *Journal of Water Process Engineering*, *58*, 104760. doi: 10.1016/j.jwpe.2023.104760.
- ***Ozyildiz, G.***, Bodur, M., Dilsizoglu-Akyol, N., Kilicarpa, A., Olmez-Hanci, T., Cokgor, E., ... & Insel, G. (2023). Simulating the impact of ozonation on biodegradation characteristics of industrial wastewater concentrated with membrane filtration. *Journal of Environmental Chemical Engineering*, *11* (2), 109286. doi: 10.1016/j.jece.2023.109286.
- Duba, S., Sözen, S., Dogruel, S., Olmez-Hanci, T., ***Ozyildiz, G.***, Cokgor, E., & Orhon, D. (2023). Anatomy of chemically enhanced sewage settling by particle size distribution analysis. *Journal of Chemical Technology & Biotechnology*, *98* (3), 679-690. doi: 10.1002/jctb.7273.
- Gunes, G., Guven, D., Cokgor, E., Balci, G. Z., ***Ozyildiz, G.***, Erdincler, A., ... & Insel, G. (2023). Efficient organic carbon utilization for combined nutrient removal and biogas production in hybrid biofilm activated sludge system. *Biochemical Engineering Journal*, *193*, 108862. doi: 10.1016/j.bej.2023.108862.
- Demirkaya, E., Ciftcioglu, B., ***Ozyildiz, G.***, Zengin, G. E., Pala-Ozkok, I., Cokgor, E., & Tas, D. O. (2022). Comprehensive evaluation of starter culture impact on the bioreactor performance and microbial kinetics. *Biochemical Engineering Journal*, *177*, 108233. doi: 10.1016/j.bej.2021.108233.
- Ciftcioglu, B., Demirkaya, E., Salih, E., Soylu, D., ***Ozyildiz, G.***, Zengin, G. E., ... & Tas, D. O. (2021). Insights into the acute effect of anti-inflammatory drugs on activated sludge systems with high solids retention time. *Environmental Technology*, *42*(25), 3920-3931. doi: 10.1080/09593330.2020.1761456.
- Guventurk, A., Ozturk, D., ***Ozyildiz, G.***, Ayisigi, E., Guven, D., Zengin, G. E., ... & Cokgor, E. (2020). Determination of the potential of pickle wastewater as

feedstock for biopolymer production. *Water Science and Technology*, *81*(1), 21-28. doi: 10.2166/wst.2020.060.

- ***Ozyildiz, G.***, Olmez-Hanci, T., & Arslan-Alaton, I. (2019). Effect of nano-scale, reduced graphene oxide on the degradation of bisphenol A in real tertiary treated wastewater with the persulfate/UV-C process. *Applied Catalysis B: Environmental*, *254*, 135-144. doi: 10.1016/j.apcatb.2019.04.092.
- Insel, G., Karagunduz, A., Aksel, M., Cokgor, E., Kor-Bicakci, G., ***Ozyildiz, G.***, ... & Keskinler, B. (2018). Membrane integrated process for advanced treatment of high strength Opium Alkaloid wastewaters. *Water Science and Technology*, *77*(7), 1899-1908. doi: 10.2166/wst.2018.065.
- Guventurk, A., Ozturk, D., ***Ozyildiz, G.***, Guven, D., Zengin Balci, G. E., Okutman Tas, D., Olmez-Hanci, T., Pala-Ozkok, I., Yagci, N., Insel, G., Cokgor, E. (2019). Determination of the potential of pickle wastewater as feedstock for biopolymer production. 10th IWA International Symposium on Waste Management problems in Agro-Industries, Rhodos, Greece, 19 - 21 June 2019.
- Ciftcioglu, B., Demirkaya, E., Salih, E., Soylu D., ***Ozyildiz, G.***, Zengin Balci, G. E., Guven, D., Pala-Ozkok, I., Cokgor, E., Okutman Tas, D. (2019). Acute effect of micropollutants on an activated sludge system with high sludge retention time operated as a sequencing batch reactor. 10th IWA International Symposium on Waste Management problems in Agro-Industries, Rhodos, Greece, 19 - 21 June 2019.
- Demirkaya, E., Unver, H., Cifcioğlu, B., ***Ozyildiz, G.***, Zengin Balci, G.E., Pala-Ozkok, I., Cokgor, E., Okutman Tas, D. (2018). Effect of Seed Biomass on Wastewater Treatment Performance. 4th International Conference on Recycling and Reuse, Istanbul University, Istanbul, Turkey.
- Gumuslu, E., Insel, G., Olmez-Hanci, T., Germirli-Babuna, F., Okutman-Tas, D., Cokgor, E., Sayi-Ucar, N., ***Ozyildiz, G.***, Yuksek, G., Dizge, N. Firat-Ertem, D., Yıldırım, O., Erturan, O., Kirci, B. (2016). Wastewater Reuse Potential of Paint Operations in an Oven Manufacturing Plant. 3rd International Conference on Recycling and Reuse, Istanbul University, Istanbul, Turkey.

SCHOLARSHIP:

- Vehbi Koç Foundation – Undergraduate Merit-Based Scholarship